J-PARC 10-05

MLF Annual Report 2009

J-PARC

Foreword to the MLF Annual Report 2009

It is our great pleasure to issue the Materials and Life Science Experimental Facility (MLF) annual report. This is the first issue since J-PARC started construction in 2001. The first neutrons were successfully produced in the mercury target in May 2008 with accelerators power of 4 kW, followed by the first muon production in September. The user programme was started in December 2008 with 20kW. However, we found a problem in the RFQ of the LINAC just after starting the routine operation in January 2009. After improvements on the evacuating systems and conditioning the RFQ, 120kW operation was started in November 2009. Although we have had other problems in the hydrogen circulation system for moderators, we have been achieving very reliable operation of over 93% since then.

Now, 18 neutron instruments have been funded. Eight of them and two muon ports are available for user programs. Three are in the commissioning phase and five are under construction. We have tested neutronic performances of each beam port and confirmed that the neutronic characteristics reasonably agreed with what we designed. Neutron flux from coupled moderators is really high, and time structures from the poisoned decouple moderator are very sharp as we estimated. The muon flux has already achieved the world's highest flux even with 120 kW due to advantages in the proton energy and target performance.

We have called for proposals worldwide twice a year, collected about 250 proposals in total, and the number is gradually but steadily increasing year by year. We have strengthened programmes for industrial use of neutrons, and as a result the fraction of proposals from industries has exceeded more than 30%.

We are planning to ramp up the accelerator power to 200 kW in 2010. In parallel, developments to mitigate the pitting problem on the target container will be extensively advanced by putting microbubbles of helium gas in the mercury flow. Scintillation detector systems are also well underway as helium-3 alternatives. All of those are conducted with international partners.

Year 2009 gave us very fruitful experiences and stimulated us to seek further developments in the future.

MLF Division Director
Masatoshi Arai

Contents

Muon Science

Facility Status

Publication List

TOPICS

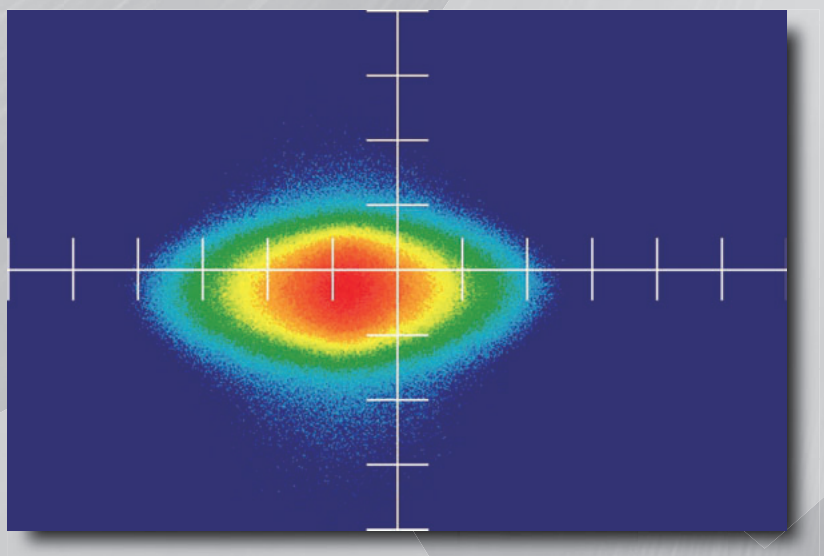

The First Pulse Neutron Production at J-PARC/MLF, Exciting Milestone

Y. Ikeda

J-PARC Center
2-4 Shirakata Shirane, Tokai-mura, Ibaraki-ken 319-1195

The two years of 2008 and 2009 have been the most exciting and critical period of the J-PARC project history summarizing the past nine years since the project start in 2001. Three accelerators consecutively achieved their beam injections, and three user facilities started beam operation for the first time, demonstrating the production of the secondary particles of interest, e.g., neutron, muon, Kaon, and neutrino. At the Materials and Life science Experimental Facility (MLF), we always recall the deeply memorable day of May 30, 2008, when the first shot of proton beam from 3 GeV synchrotron (RCS) was injected to the mercury neutron production target, and the extracted neutron pulse was observed for the first time. September 26, 2008 was the other exciting day for the MLF with the first muon beam extraction. These two events were co-memorial achievements for all MLF team members.

To share the excitement of the first beam at the MLF for the neutron, I like to refer to a note of the newsletter sent out right after the event, as follows; "*30th of May is the Memorial Day for JSNS. At 10:15 AM, 3GeV proton beam transport facility (3NBT) succeeded in transporting the proton beam extracted from 3GeV rapid cycling synchrotron (RCS) to the mercury target in MLF which was located about 300m from 3GeV RCS. The beam transport was confirmed with nine current transformers (beam intensity monitors) installed in the 3NBT line. At 2:25 PM, the first neutron by the proton-beam induced spallation reaction was produced successfully at a spallation neutron source in the Materials and Life Science Experimental Facility (MLF). Several trillions of protons were accelerated up to about 97 % of the velocity of light by the 3 GeV Synchrotron, and a bunch of the high-energy protons was introduced in the MLF for the first time. The protons induced the spallation reactions with mercury at the center of the neutron target. Finally, success of the first neutron production was confirmed by observing several tens of thousands of neutrons per 1 cm^2 in an experimental room 14 m apart from the center of the neutron source.*"

It is notable that the current time of flight (CTOF) measurement enabled direct observation of neutron spectrum with just a single pulse, in which Li-glass scintillation is applied to detect slow neutrons. When it was ready for the first beam, we counted down for the time of the first proton pulse injection to the mercury neutron production target from RCS. Suddenly a great cheer arose when we looked at the spectrum on a TV monitor screen! Figure 1, is the historical record of the spectrum showing clear Maxwellian shape distribution with a peak at 12 meV, corresponding to the para-hydrogen energy gap. This figure will be used for a long time.

The control room of MLF was crowded with many people gathered to participate in this most exciting instance being a witness to MLF history. The control room was filled with enthusiasm. Occasionally, JAEA president, T.

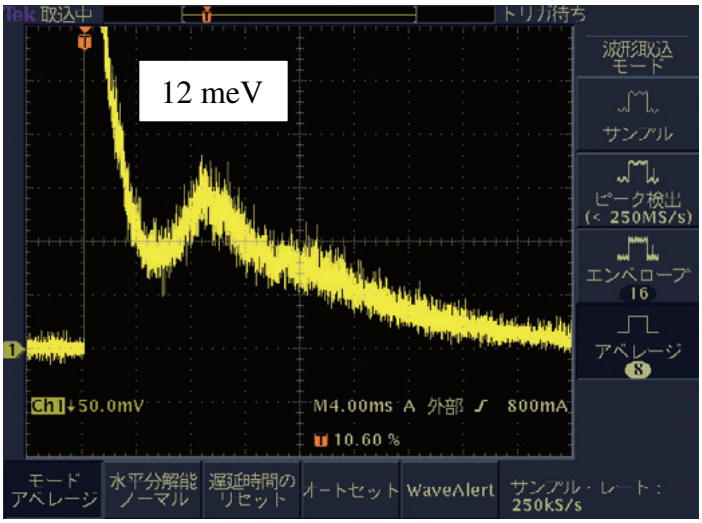

Fig.1 The current TOF output spectrum of a Digital Oscilloscope corresponding to the first shot of pulse neutron production.

Fig.2 People celebrating the first pulse neutron production at the MLF control room on May 30, 2008.

Okazaki chanced to visit to celebrate that particular achievement. From both KEK and JAEA, important executives gave very warm words to the MLF team. I wish to express my appreciation to all of them again. Figure 2 is a picture of the gathered people taken at the moment of celebration for the success.

Of course you can't see now where you'll end up, but you have to start somewhere. The longest journey begins with a single step. I believe that this event was such a turning point, and the most important proof of the great victory of the MLF construction team's teamwork. Always it is true that every completion is a beginning into a new era.

As this issue of the first annual report is very special and a co-memorial for the MLF construction in the J-PARC project, I believe that this will remain in the mind of all who participated and shared this invaluable experience in J-PARC history.

I would sincerely like to convey my gratitude to all my colleagues of MLF who I fully respect and am proud of their accomplishments.

Prof. Noboru Watanabe, a pioneer of the spllation neutron source in Japan, receiving flower bouquet at the last lecture of the spllation neutron source in J-PARC, 30th March 2005

First muon beam and world's strongest pulsed muon production at J-PARC MUSE

Y. Miyake[a,b], K. Shimomura[a,b], N. Kawamura[a,b], P. Strasser[a,b], A. Koda[a,b], H. Fujimori[a,b], S. Makimura[a,b], K. Nakahara[a,b], M. Kato[a,b], S. Takeshita[a,b], K. Nishiyama[a,b] , R. Kadono[a,b], W. Higemoto[b,c], T. Ito[b,c], K. Ninomiya[b,c], K. Kubo[d], and M. Doyama[e]

[a] Muon Science Laboratory, High Energy Accelerator Research Organization (KEK), Ibaraki 319-1106, Japan
[b] Muon Section, Materials and Life Science Division, J-PARC Center, Ibaraki 319-1195, Japan
[c] Japan Atomic Energy Agency (JAEA), Ibaraki 319-1195, Japan
[d] International Christian University, Tokyo 181-8585, Japan
[e] Teikyo University of Science and Technology, Yamanashi 405-0018, Japan

The muon science facility (MUSE, abbreviation of MUon Science Establishment) is locates in the Materials and Life Science Facility (MLF) of the Japan Proton Accelerator Research Complex (J-PARC) in Tokai. The MUSE facility is currently the only muon source in Asia, which has already delivered the world strongest pulsed muon beam in the world. We are still aiming to increase intensity of the beam tenfold in the near future. Here we report on the first muon beam of the MUSE facility.

The muon production target of MUSE is a 20 mm thick graphite placed 33 m upstream of the proton beam line from the neutron production target in MLF. The graphite target generates both positively charged pions (π^+) and negatively charged pions (π^-) through the nuclear reactions between the 3 GeV accelerated proton and the carbon nucleus. Figure 1 shows the 20 mm-thick edge-cooled non-rotating graphite muon target, and the muon target chamber. On September 19th, 2008, the muon target was placed into the 3GeV proton beam line, for the first time at MLF.

For the construction state phase 1, the MUSE team managed to design, build and install one superconducting decay/surface muon beamline, so called D-Line, with a modest-acceptance (about 45 mSr) of the pion injector, where either surface muons or decay muons can be extracted. The former are obtained from the decay of π^+ stopped near the surface of the graphite target in the proton beam line, and the latter are obtained through the in-flight decay of π^+/π^- confined by a strong longitudinal magnetic field of several T from a superconducting solenoid magnet. Figure 2 show a picture of the D-line.

For the first beam delivery, we tried to extract surface muons (μ^+), which have a momentum of 30 MeV/c. At the beginning, we commissioned the D-line optics by tuning the superconducting magnet, the quadrupole and bending magnets, and the DC separator in order to optimize the transportation of the surface muon beam and to eliminate the e^+ contamination. At 12:10 on September 26th, 2008, we managed to deliver the first surface muon beam to the D1

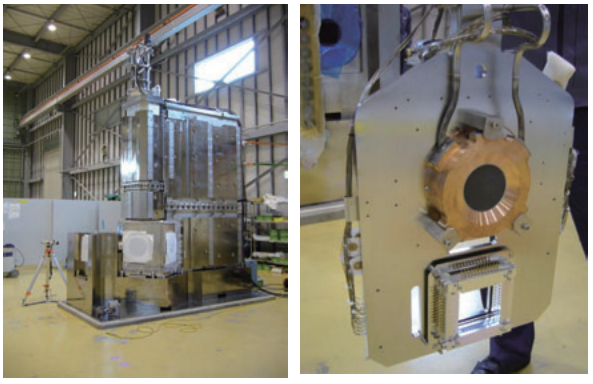

Fig.1 Pictures of the muon target chamber (left figure) and the 20 mm thick graphite muon production target (right figure).

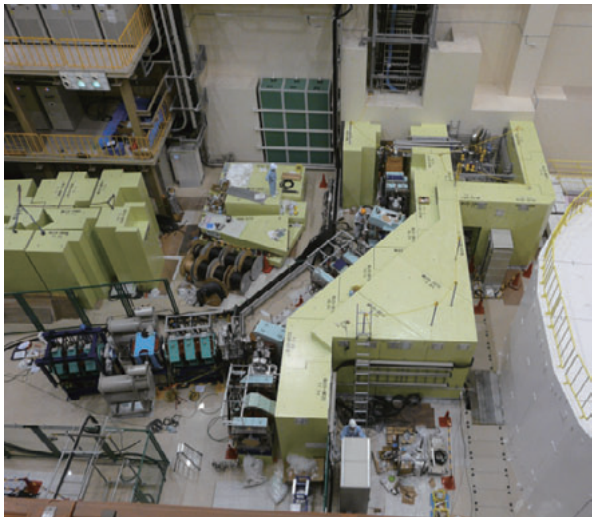

Fig.2 Construction of the D-Line secondary muon beamline.

muon experimental area [1]. In front of a live audience of about 100 people who gathered to celebrate the first muon extraction at MLF, we demonstrated a muon spin rotation (μSR) measurement of an aluminum plate under a magnetic field applied perpendicular to the muon spin polarization. The decay positrons were detected by the general-purpose μSR spectrometer (DΩ1) equipped with 128×2 channels of positron counters. The resulting muon spin precession due to the applied magnetic field was clearly observed by the spectrometer. Figure 3 shows the μSR spectrum witnessed by the audience. The profile of the muon beam was also measured by a profile monitor and an imaging plate (IP). Figure 4 shows a picture of the profile of the muon beam measured by an imaging plate (IP). For the IP measurement, a thick plate with a character set written as "J-PARC MUSE" was placed in front of the imaging plate. Figure 5 shows a picture celebrating the first muon beam production at J-PARC MUSE.

Extraction of the negative muons (μ^-) requires full excitation of the superconducting solenoid magnet, because they are only available by in-flight decay of pions. On December 25th, 2008, we finally succeeded in the extraction of negative muons, after fixing the refrigerator system of the solenoid. As a demonstration of

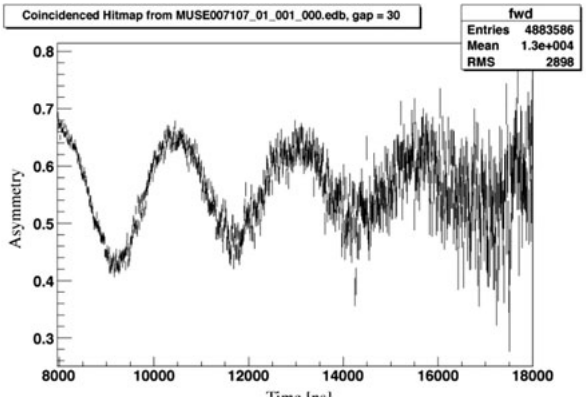

Fig.3 The first μSR asymmetry spectrum of an aluminum target.

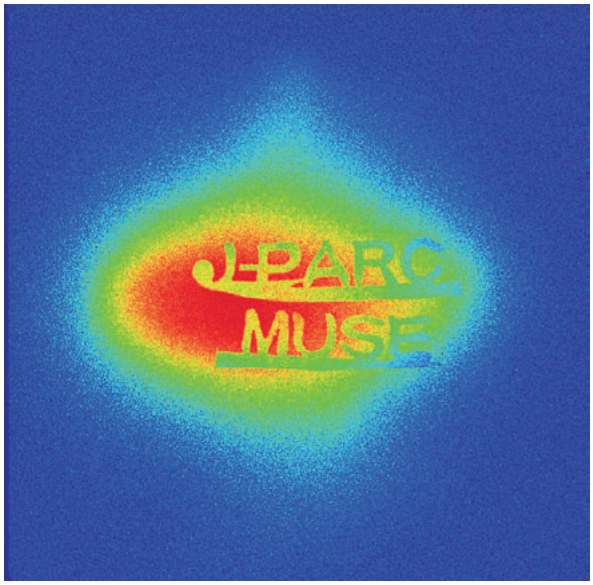

Fig.4 Muon beam profile measured by an imaging plate.

Fig.5 A picture of the people who gathered to celebrate the first muon beam production at J-PARC MUSE.

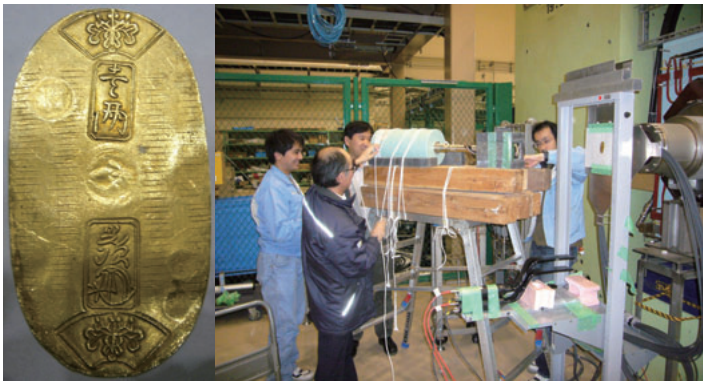

Fig.6 Muonic X-ray measurement system at the D2 area. Tempo-Koban (supplied by Prof. S. Saito) was placed in front of the Ge-detector.

the negative muon beam extraction, we tried to measure the characteristic X-rays from the Tempo-Koban [2], as is shown in Fig. 6.

In November 2009, by undergoing iterative beam tuning and by developing the beam line elements such as separator, the surface muons (μ^+) extraction rate was significantly increased up to 1.8×10^6/s with use of a 120 kW proton beam from the RCS. The achieved intensity is equivalent or even larger than that at the RIKEN-RAL muon facility [3]. This is the reason why that the world's strongest pulsed muon source was claimed to be achieved at MUSE, even if we use a 120 kW proton beam intensity. Moreover, in December, 2009, we could obtain almost 2.5 times more surface muons by obtaining a 300 kW proton beam from the RCS. This intensity will correspond to 1.5×10^7/s surface muons when in the future proton beam will reach a power of 1MW.

With use of the world's strongest pulsed muon beam at MUSE, Takeshita *et al*. have already published a paper demonstrating the presence of a macroscopic phase separation between the superconducting and magnetic phases in co-doped iron pnictide $CaFe_{1-x}Co_xAsF$ [4].

Summary

Construction of the D-Line at MUSE was completed in the summer of 2008, as scheduled. And we succeeded in the extraction of a "surface muon (μ^+)" beam on September 26th, 2008 and "decay muon (μ^+/μ^-)" beam on December 25th, 2008. Finally, we achieved the world's strongest pulsed muon source at MUSE in November 2009 with the use of a 120 kW proton beam.

References

[1] P. Strasser et al., J. Phys.: Conf. Ser. 225 (2010) 012050.

[2] K. Ninomiya et al., J. Phys.: Conf. Ser. 225 (2010) 012040.

[3] K. Nagamine et al. Hyp. Interact. 101/102 (1996) 521.

[4] S. Takeshita et al., PRL 103 (2009) 027002.

Neutron Source

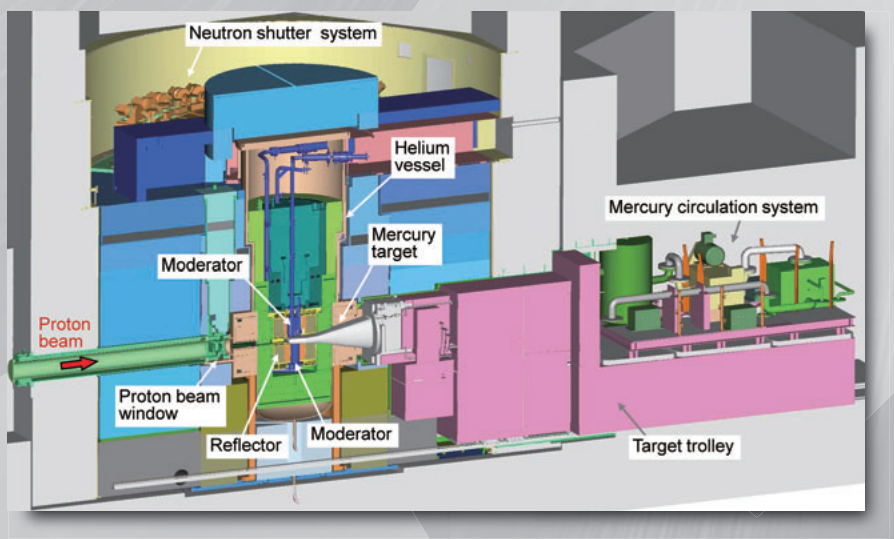

Status of the Japan Spallation Neutron Source (JSNS)

M. Futakawa, H. Takada, F. Maekawa, S. Sakamoto, K. Haga, S. Meigo, K. Sakai, Y. Kasugai, M. Teshigawara, T. Aso, H. Kinoshita, K. Oikawa, M. Harada, S. Hasegawa, H. Kogawa, T. Wakui, T. Kai, M. Seki, A. Watanabe, K. Ohtsu, T. Uehara, K. Ikezaki, T. Haraguchi, K. Hanano, H. Tatsumoto, M. Ohi, Y. Kawakami, M. Ito, H. Sakurayama, T. Naoe, A. Akutsu and T. Suzuki

Neutron source section, Materials and life science division, J-PARC center
Japan Atomic Energy Agency, Tokai-mura, Ibaraki, 319-1195

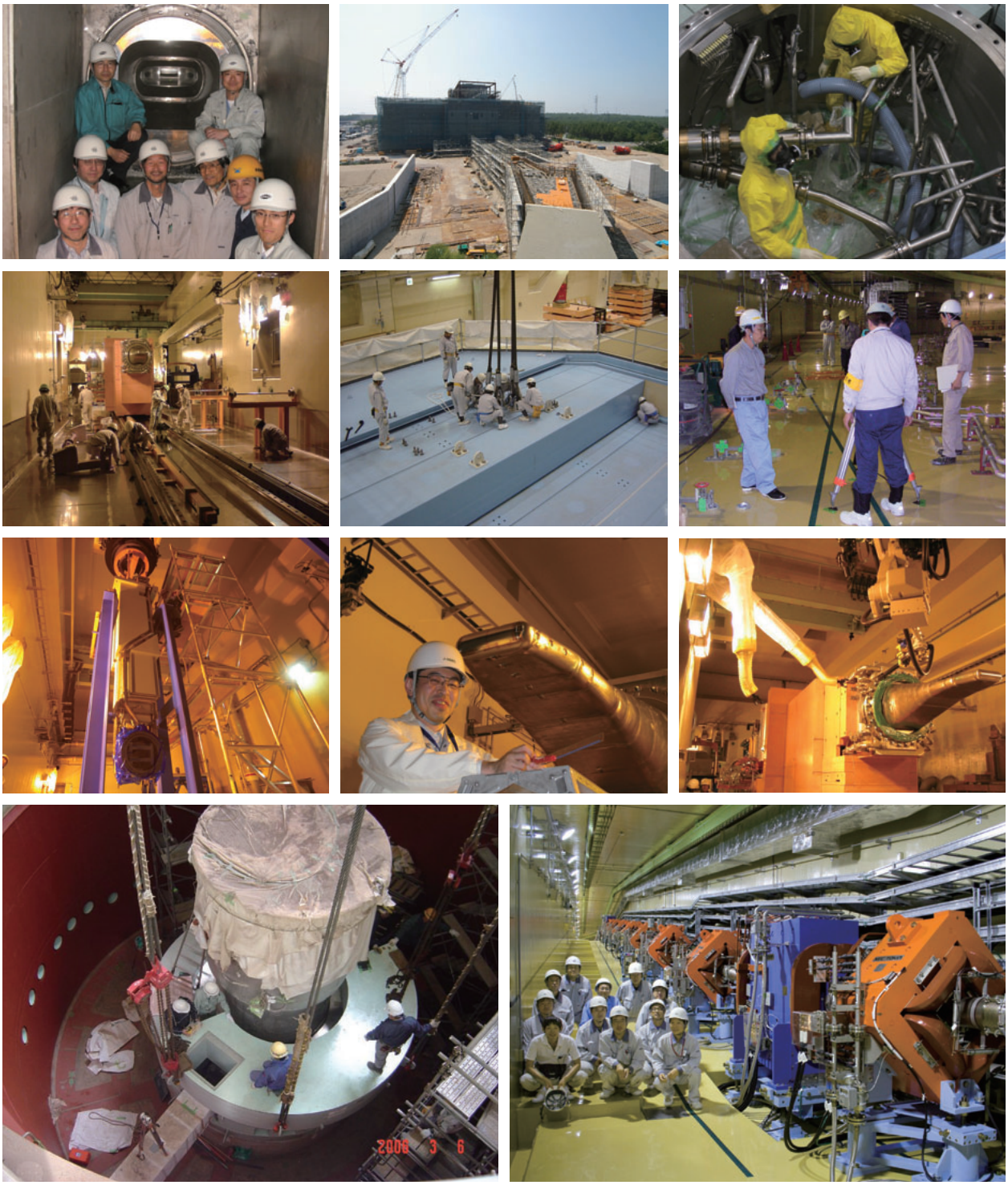

3-GeV Proton Beam Transport to Muon and Neutron Targets

The Japan Spallation Neutron Source (JSNS), and the Muon Science facility (MUSE) in the materials and life science experimental facility (MLF) are shown in Fig. 1. For both sources, 3 GeV proton beam is delivered from a rapid cycling synchrotron (RCS) to the targets. Before the injection to the RCS, the proton beam is accelerated up to 181 MeV by a LINAC. The beam is accumulated in short bunches such as 150 ns duration and accelerated up to 3 GeV in the RCS. After extraction, the beam is transferred to the muon production target and the spallation neutron source. The 3 GeV proton beam is introduced to the mercury target for a neutron source and to a carbon graphite target of 2 cm thickness for a muon source. In order to utilize the proton beam efficiently for particle production both targets are aligned in a cascade scheme, where the carbon graphite target is located 30 m upstream of the neutron target. On May 30th 2008, the first beam could be delivered to the neutron target without significant beam loss. After that, we succeeded in providing a stable 120-kW proton-beam with availability larger than 90 %.

Design of beam optics, magnet and monitor

In the design of beam transport system, first of all, we carefully designed beam optics from the extraction septum magnet at the RCS to the muon and neutron targets. The beam optics is shown in Fig. 2. When we started to design, an intensity of 1-MW beam was extremely high and no one had any experience of the design. [1, 2] By choosing the cascade scheme, it is more difficult because we easily understood by a simple calculation that the amount of beam loss caused at the muon target was equivalent to total beam produced at ISIS which was the most intense pulse spallation neutron source in the world when we designed. By a precious design of beam optics, it was found that the beam loss can be minimized by focusing at the muon production target. By focusing at the muon target of carbon, it makes large angular divergence of the beam, which leads to small angular expansion due to the scattering at the target. Even minimizing the loss, about 8% beam loss around at the muon target exists. Therefore, we carefully designed the quadrupole and steering magnets around the muon target especially for the radiation resistance cooperated with the MUSE team. As a halo conductor of the coil, a mineral insulator cable (MIC) is chosen having extreme high radiation resistance more than 1MGy. We discussed many times about the way of alignment of the magnet, which is one of the important issues. We determined that the position and height of the magnet are given by the base plate and pins below the magnet. By using a laser tracker, all magnets except around the muon target were aligned precisely. All components were aligned to the designated position within accuracy of 0.1 mm.

Except close to the targets, in order to allow maintenance by human hands, acceptable beam

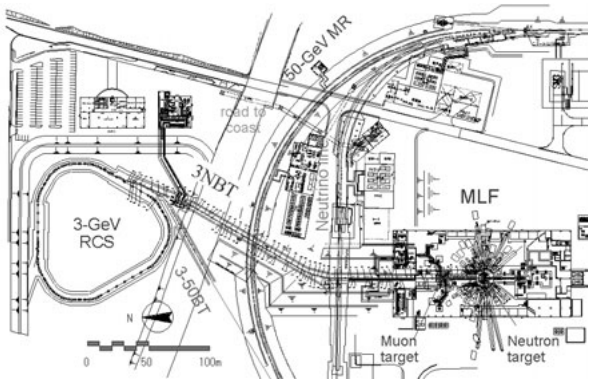

Fig.1 The side view of the SANS instrument TAIKAN in J-PARC.

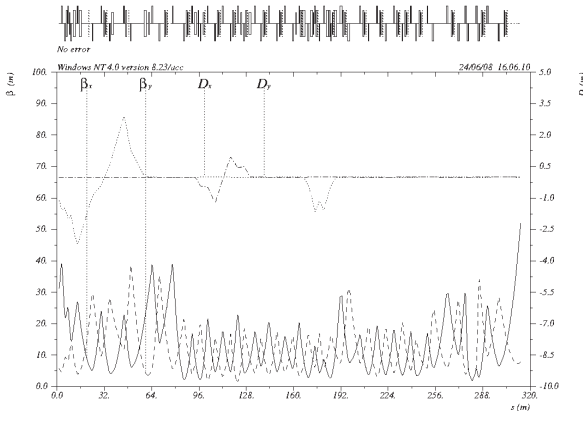

Fig.2 Beam optics from the RCS to the JSNS

loss is limited to 1 W/m. In the design, we determined the acceptance of the beam larger than 324 π mm mrad which is physical aperture at the RCS. During acceleration in the RCS, the beam emittance shrinks to 54 π mm mrad by the adiabatic dumping for 181-MeV proton injection. However a small fraction of beam exists having an emittance of up to 324 π mm mrad due to blow up by space charge. Therefore we decided to have an aperture larger than 324 π mm mrad along the entire beam line. In Fig. 2, Dx and Dy represent the dispersion function for horizontal and vertical directions, respectively. In the design, an achromatic beam transport line was aimed at to suppress the expansion of the beam due to momentum spread.

It has been reported that the damage is proportional to the fourth power of the peak current density of the beam [3]. In order to comprehend the damage to the target, the beam profile monitoring plays important roles. It is necessary to know the characteristics of the projectile on the target. In order to measure the beam position and shape, 15 Multi-Wire Profile Monitors (MWPMs) are installed in the beam line. Silicon Carbide (SiC) is used as sensor wires due to their small interaction with the primary beam. [1, 5] Rutherford scattering cross section is proportional to the square of the atomic number of the wire material, a low atomic number material has been selected to minimize beam scattering. To recognize performance of the present MWPMs, we carried out examination by irradiation of 500-MeV proton beam at KEK in 1999. It was found that a reliable profile can be obtained by the SiC wires.

The wire frame of the MWPM can be moved out so that the beam can pass without interaction when no measurement is performed. In order to watch the profile of the incident beam on the beam dump and the target continuously, a stationary type of beam profile monitor was located at the entrance of the beam dump and the neutron target. The proton beam window is located at 1.8 m upstream of the neutron target, which consists of aluminum alloy (AlMg3) having thickness of 5 mm. At the proton beam window, we placed the MWPM shown in Fig. 3 to watch continuously the beam status at the target. For observation of the beam center position without interaction, we installed 14

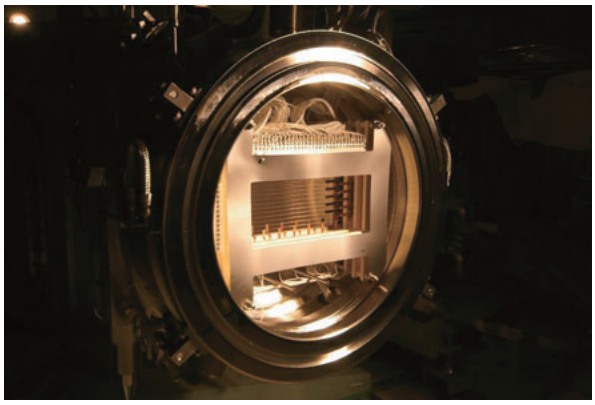

Fig.3 Multi Wire Profile Monitor (MWPM) at Proton Beam Window which is located 1.8 m front of the mercury target.

pieces of Beam Position Monitors (BPMs) along the beam transport line.

For the measurement of the beam intensity, current transformers (CTs) are installed in the beam line. Inside of the current transformers, a titanium duct is attached for connecting to other vacuum equipment. Data of the monitors are acquired by a network-based CAMAC controller via the Experimental Physics and Industrial Control System (EPICS) standard.

During beam operation, it is important to know the status of the beam loss. If the amount of beam loss exceeds the allowable value of 1 W/m, the beam should be stopped immediately. Loss monitors are located at the front of all quadrupole magnets where the beam diameter becomes relatively large.

Earliest beam commissioning to the target

At the end of May 2008, we had begun beam commissioning in the MLF. By only one-shot of the beam, we succeeded in delivering the 3-GeV proton beam to the neutron target. From the experience during beam dump operation, we learned many things about tuning of the beam and monitors. The experience of beam dump leads us to succeed in delivering the beam to the target. Figure 4 shows the beam monitor signals from the first beam on the target.

Without significant beam loss, the first beam was able to be introduced to the MLF on 30 May 2008. The intensity of the first proton beam was approximately 4×10^{11} ppp and the transmission efficiency larger than 90%. After fine tuning of the beam orbit and beam monitor system, the beam profile was measured by the MWPM located at the proton beam window. As

for the first neutron beam measurement at the JSNS, it was planned to carry out measurement employing the Current mode Time-Of-Flight (CTOF)[4] technique because of its reliability and convenience. In Fig. 5, the neutron TOF spectrum is shown, which can be obtained for only one shot. By the comparison with the calculation, it was found that the calculation showed good agreement with the experimental result.

Since the proton beam profile on the spallation neutron target is very important, we tried to obtain the beam profile on the target. In order to achieve good performance of the neutron source, there was not enough left around the target to place any devices for the beam profile measurement. To fit the requirement with the tiny space around the target, we adopted an activation technique, which required only small space for thin foil. Placing a sheet of aluminum foil (0.3 mm in thickness) on the target, the beam profile was obtained from the residual dose distribution on the foil. After irradiation, the foil was removed from the target and attached to the imaging plate (Fuji Film BAS-SR 2040) to read the dose distribution. Figure 6 shows the observed result. It was found that the beam shape had been Gaussian with FWHM of 42.5 and 18.8 mm in horizontal and vertical directions, respectively. These widths show quite good agreement with the data obtained by the β function of optics and the beam emittance obtained by the SIMPSONS including the scattering on the proton beam window. The center position of the beam is continuously observed by BPM. It was found that the stability of beam position was good and the deviation of the center position was typically 0.6 mm at BPM position.

In Fig. 6, it was also found that beam was not skewed in real space. Figure 7 shows the comparison of the vertical profile results obtained by activation technique and MWPM, the latter of which gives the beam profile projected on the horizontal and vertical axis, placed at proton beam window. It was found that

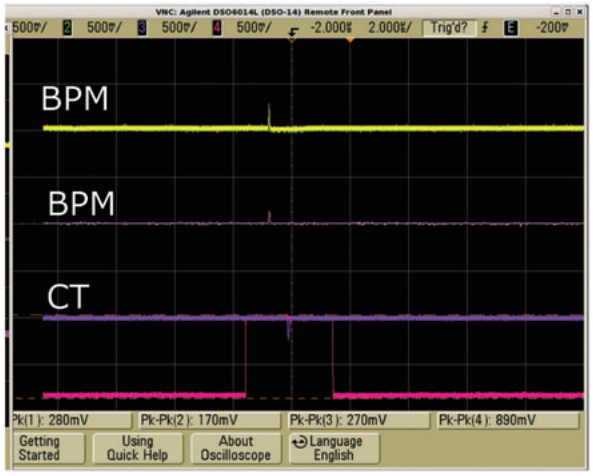

Fig.4 For the first beam to deliver to mercury target, signals of beam position monitors (BPMs) and CT.

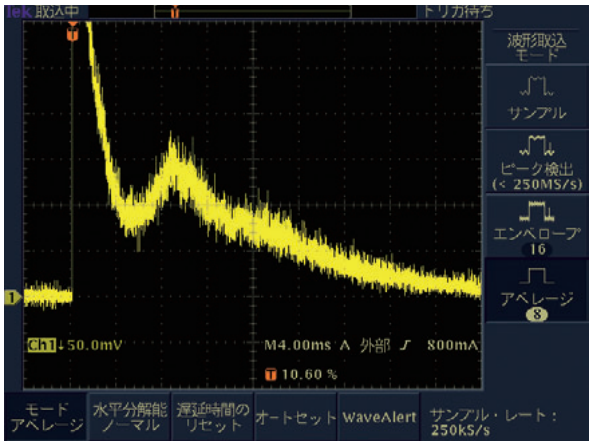

Fig.5 Time-of-flight spectrum for the first neutron beam measured by the current mode time-of-flight (CTOF) technique

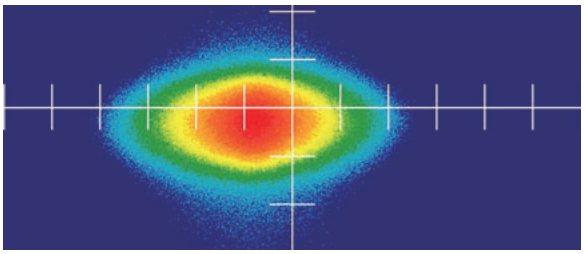

Fig.6 Beam profile observed by the activation of the aluminum foil(0.3mm-t) located on the spallation neutron target (one division in figure is 10 mm)

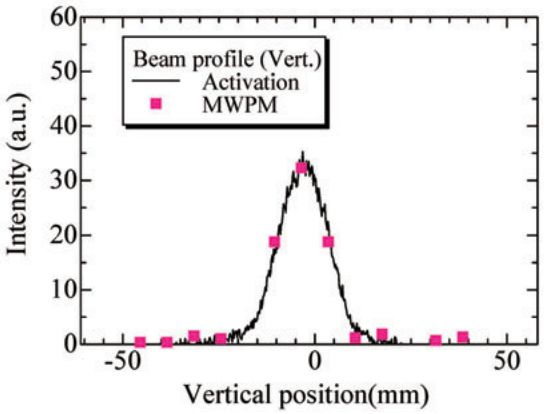

Fig.7 Comparison of results of vertical beam profile obtained by activation technique and multi-wire- profile-monitor (MWPM).

both results showed remarkably good agreement. Therefore it was concluded that the beam current density could be derived from the result of the MWPM.

Beam commissioning in JFY 2009

In December 2008, user beam providing begun. Besides providing user beam some beam studies were performed to achieve high power operation. Response of steering magnet on the beam position is important to correct beam orbit as intended. The result of the beam center orbit distribution along the beam line was measured by giving the kick angle of the most upstream horizontal steering magnet by 1 mrad. Although the original design showed good agreement in general, the considerable disagreement was found in the downstream section. To fit the orbit to the experimental result, it was calculated by changing quadrupole magnet field equally. Consequently, the calculation by decreasing Bρ by 2% reproduced the experiment in the whole beamline very well. This fact indicated that the fields of the quadrupole magnets are 2% smaller than design value, although the magnetic field for each quadrupole magnet was measured. In the magnetic field measurement, a hall prove sensor was used. The response of the hall prove might cause 2% disagreement. In Fig. 8, the original design calculation is compared with the experimental result when the magnetic fields of all the quadrupole magnets were increased by 2%. It shows the remarkable good agreement between experiment and design calculation. It is demonstrated that the beam optics behave as designed.

In November 2009, a clear pitting damaged was found at the target vessel of SNS so that the profile became more important. We have developed new technique to observe proton beam profile on the target. In order to perform beam profile measurement by activation, access to the target is necessary after beam irradiation. After early beam commissioning, the radiation around the target is extremely high such as several Sv/h therefore a remote handling technique is required. We have developed an activation technique by utilizing an Imaging Plate (IP). By remote handling technique, the IP (Fuji Film BAS-SR 2040) is attached to the target vessel shown in Fig. 9. The IP contained in holder was attached to the hook of in-cell crane by human hands. At the entrance of hot cell, radiation was several tenths of μSv/h so that humans can access. The IP approached to the target by the crane and contacted with the target by help of the master slave manipulator as shown in Fig. 9. Typical duration of exposure time was five minutes. After the exposure, the image of radiation was read out by the reader of the IP.

In Fig. 10, the beam profile result obtained by the IP after 120 kW beam irradiation in December 2009 is shown. In the distribution, it was recognized that a clear Gaussian peak exists without tilting, which showed the similar result by foil activation technique. Figure 10 also shows the horizontal distribution obtained by the IP. The distribution can be well described by the

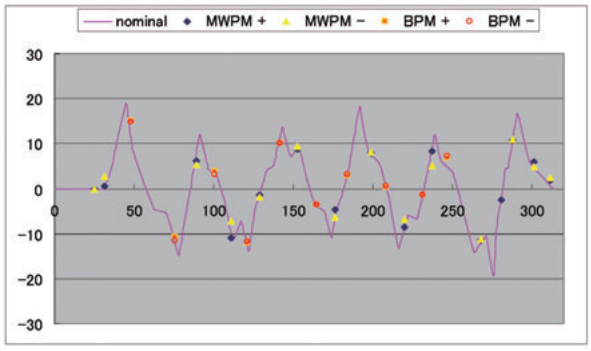

Fig.8 Comparison of original calculation with experimental result, when the magnet fields of all the magnets were increased by 2%

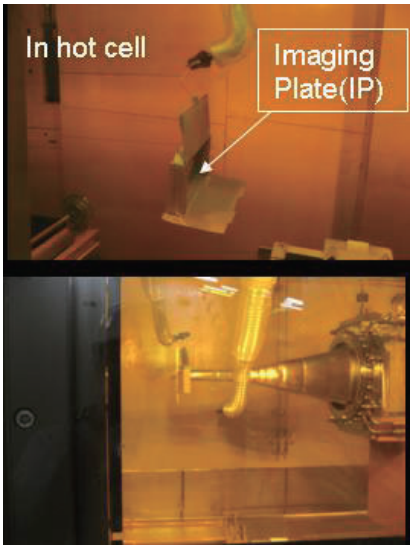

Fig.9 Beam profile measurement using the IP placed on the mercury target vessel by remote handling technique performed after beam irradiation at hot cell. The IP placed in a holder (above) was contacted with the target by help of the master slave manipulator (bottom).

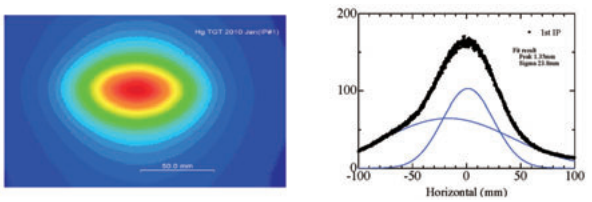

Fig.10 Result of beam profile obtained by the IP. 2D profile (left) and profile on the horizontal axis with the Gaussian fitting curves (right).

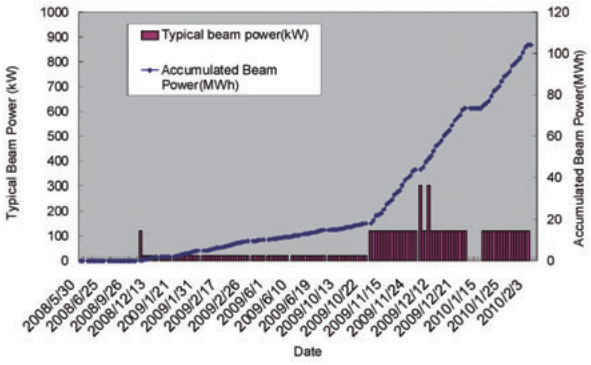

Fig.11 Typical beam power to deliver to spallation neutron source (vertical bar, left axis), accumulated beam power (diamonds, right axis)

combinations of two Gaussian functions having small and large widths. The shorter one was thought to be the initial protons. The longer was thought to be the secondary particles.

During beam operation, beam profile was continuously measured by the MWPM located on the proton beam window. For each pulse, Gaussian function fitting was performed to obtain peak heat density. Beam profile on the target is slightly different from the profile on the MWPM, because of the beam divergence. In order to obtain the beam profile on the target, the beam width is expanded about 20% on the MWPM to correct the width for the divergence of the beam. As the beam power increased, we expanded gradually the beam size. In each run, it was found that the results obtained by the IP and the MWPM showed good agreement. Therefore, we can obtain a reliable beam profile on the mercury target from the MWPM.

Trend of proton beam power is shown in Fig. 11. After early stage of beam commissioning, it was confirmed that the critical issue did not exist and we have been ramping up the beam power since then.

In December 2008, a short duration of 100 kW operation was demonstrated and continuous 20-kw operation began. In November 2009, we started delivering beam of 120 kW with remarkably good availability as 90%. For short duration of one hour, we demonstrated 300-kW beam operation to the spllation neutron source. It was shown that the beam loss was very small and the beam status was very stable. Even after beam operation at 300 kW, the residual dose in the beam transport system was as small as background level.

It should be noted that the beam has not been stopped for long duration due to the beam transport system since user program has started. During beam tuning, some troubles happened on the power supplies of magnet, however, troubles did not occur for the user beam time period. In JFY 2010, we plan to increase beam power above 200 kW.

References

1) S. Meigo et al., Nucl. Instr. Meth A 562 (2006) 569
2) S. Sakamoto et al., Nucl. Instr. Meth A 562 (2006) 638
3) M. Futakawa et al., J. Nucl. Matterial, Proceedings of IWSMT-6 to be published.
4) S. Meigo et al., J. Nucl. Sci. and Technol. Suppl. 1 (2000) 789.
5) S. Meigo, et al., Nucl. Instrum. Meth. A 600, (2009) 41.

R&D for the mercury target system

Figure 1 shows the bird's eye view of the mercury target system which consists of a target vessel, a mercury circulation system and a target trolley. The target vessel, where neutrons are generated by spallation reactions between mercury nuclei and injected protons, is installed at the front end of the target trolley and mercury is circulated through the target vessel by the mercury circulation system. Because the target vessel and the surrounding components are highly radio-activated, all maintenance operations of the mercury target system components have to be done by remote handling in the hot cell [1].

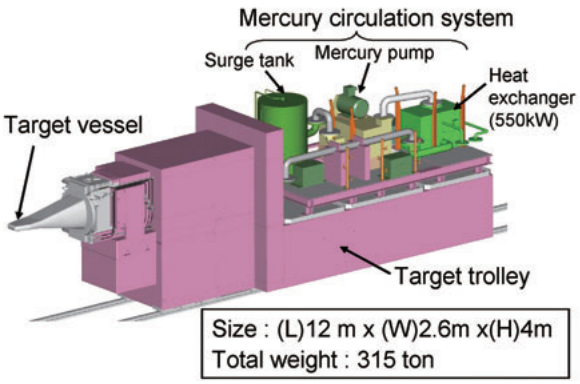

Fig.1 Bird's eye view of mercury target system

The target vessel is one of the most important components in the mercury target system. Because the structure of the target vessel, which is triple-walled, is very complicated and all parts have to be assembled by welding with precise tolerance of dimension, a lot of welding tests were carried out to optimize the welding technique and conditions. Especially welding of the forefront wall of the target vessel, where proton beams are injected through, was carried out with special care to reduce the residual stress as low as possible. The residual stresses on mock-up models welded by TIG welding were measured by the strain gauge method and numerical analyses were also carried out to investigate the effects of the welding methods. Based on those test results, the first target vessel was fabricated as shown in Fig. 2.

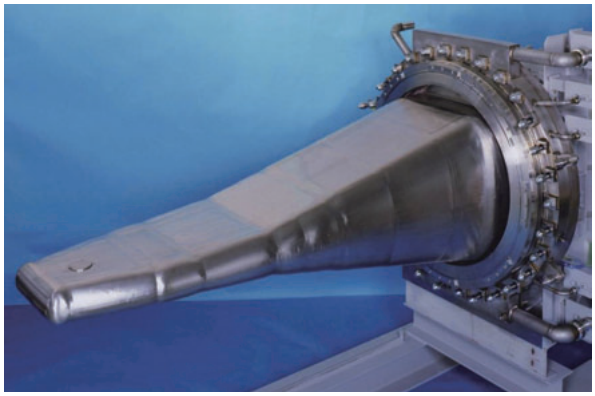

Fig.2 Target vessel

A permanent magnet rotating type induction pump, which is called PM pump and shown in Fig. 3, is the key component in the mercury circulation system. Because the driving force is given to mercury by Lorentz force generated by rotating magnetic field, the mercury channel can be completely enclosed by duct walls and the possibility of radio-active mercury leak is almost nothing, which is the great merit of the PM pump. The numerical simulations were performed for detailed design of the PM pump. The stress in the duct could be reduced by installation of ribs around the duct without increasing heat loss. Coupled analyses of magnetic field and hydro-dynamics were also carried out to check the flow pattern in the mercury channel caused by the Lorentz force and the channel size was optimized to achieve high pump efficiency [2].

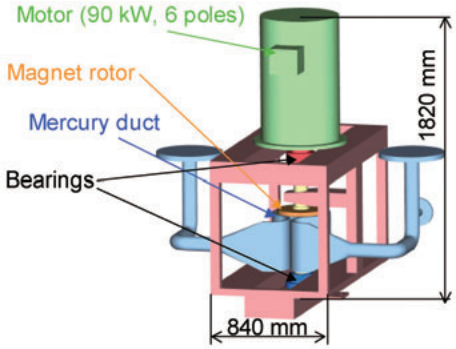

Fig.3 Schematic drawing of PM pump

Off-beam commissioning

Remote handling tests of the target system components were carried out during the off-

beam commissioning successfully. The target vessel, whose lifetime is estimated to be half a year in 1 MW operation, was detached from and attached to the forefront of the target trolley with precise positioning tolerance by remote handling operation according to the designed procedure. All components of the mercury circulation system could be handled also by remote handling using the crane and the manipulators installed in the hot cell, and the operation procedure was revised based on the test results to achieve the smooth operation.

Characteristics of the mercury circulation system were also measured during the off-beam commissioning. Figure 4 shows the characteristics of the PM pump. The estimated performance curve agreed well with measured one and it was confirmed that the discharged pressure of 0.1 MPa is required to operate the mercury circulation system in 41 m^3/h, which is the design flow rate of the mercury.

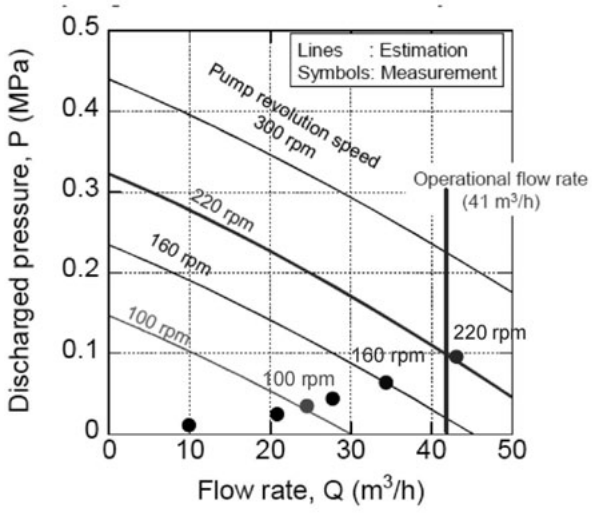

Fig.4 Characteristics of PM pump

On-beam commissioning

On Day1, the mercury target system received the first proton beam. Strain measurements were carried out to verify the numerical model which was used to access the structural integrity of the target vessel for pressure waves. The results showed good agreement between numerical and measured strains as well as other verification test using the proton beam at WNR in LANL.

Development on pressure wave mitigation

In the mercury target, the pressure waves caused by thermal shock due to the pulsed proton injection will degrade the target vessel and this degradation will extremely shorten the lifetime of the target. We found that microbubbles in mercury will mitigate considerably the pressure wave. Techniques to mitigate pressure waves have been developed, in which microbubbles of helium are injected and distributed in the mercury [3]. We found by numerical analyses that microbubbles of less than 50 m in diameter are required with volume fraction of more than 0.05% for compressive pressure mitigation. Thus, the development of a bubble generator, which is called a bubbler, was started.

The bubblers are being developed taking account of the condition of the mercury circulation system. A flow resistance of the bubble generator should be less than 0.2 MPa at 41 m^3/h of the mercury flow based on the pump ability. In R&D activity, three types of bubblers were examined: needle type, venturi type and swirl type bubblers. It was found that the swirl type was the most promising candidate because the other two types of bubblers could not generate microbubbles which meet our requirements.

Figure5 (a) shows a schematic drawing of a swirl type bubbler. It consists of a swirler and Venturi. The swirler comprises guide vanes fastened on inside of the pipe to make swirl flow in the mercury. The venturi makes swirl velocity higher and makes pressure distribution at outlet of the venturi suitable for the microbubble generation. Gas is injected from the center of the swirler to make a gas column at the center of the swirl type bubbler. The gas column is bent at the outlet of the venturi by Coanda effect. The bended column is fractured into microbubbles due to the strong pressure change and the high swirl velocity at the outlet of the venturi.

The flow resistance of the bubbler and the suppression of the swirl at the downstream of the bubbler are concerns to install the swirl bubbler into the target.

When the swirl type bubbler is installed into the pipe such as the target inlet, swirl flow remains in the downstream of the bubbler, which gathers the generated microbubbles at the center of the swirl and makes a gas column again. The outer view of the swirl type bubbler is cylindrical, but the cross section of the mercury target inlet is almost rectangular as shown in

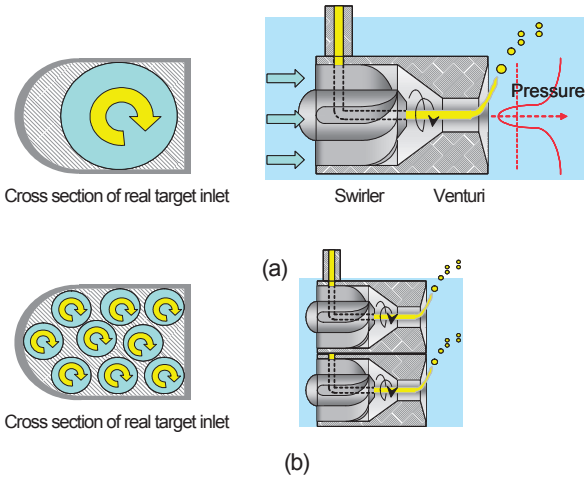

Fig.5 Schematic drawings of (a) single and (b) multi type swirl bubblers

Fig.5. If a large single bubbler is installed as shown in Fig. 5(a), the cross section of the flow channel of mercury reduces in the bubbler and the flow resistance increases. The cross section of the flow channel can be increased by arraying a lot of small bubblers as shown in Fig. 5(b), which is called the multi-type swirl bubbler. Reduction of the bubbler diameter enables short length bubbler, which reduces the flow resistance in all the bubblers. Furthermore, the swirl flows interfere with each other at the outlet of the bubblers, which suppress the swirl flow remaining in the downstream.

The performance of the multi-type swirl bubbler was verified at the real size mercury loop, which is the Target Test Facility (TTF) in Oak Ridge National Laboratory (ORNL), in summer 2009. The multi-type swirl bubbler made microbubbles of applicable size for the pressure wave mitigation. The flow resistance could be reduced to 1/3 of the single bubbler which could make the same size of microbubbles as the multi type swirl bubbler. The volume fraction of the microbubbles at the front end of the target was estimated based on the results of the TTF test, and we had the prospect that proper amount of microbubbles can be distributed by arranging the bubbler installation position.

The development of the gas supply system

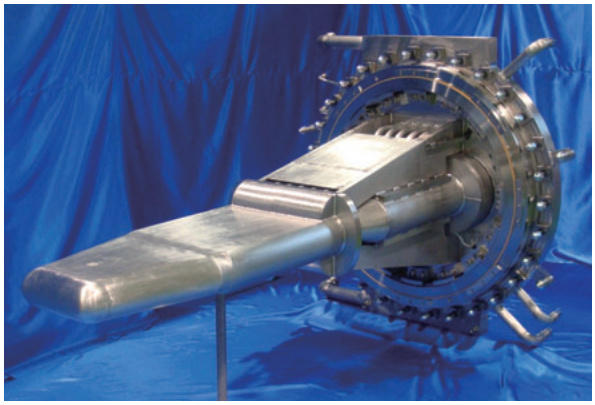

Fig.6 Photograph of #2 target

to the bubbler has been carried out. The accumulation of the injected gas in the mercury loop and its effect on the system operation were studied, and we could get prospect that both the mercury loop and the gas supply system will be operated stably. The multi-type swirl bubbler and gas supplying system will be installed in summer 2011.

Preparation of #2 target vessel

In order to replace the target vessel in case of an unexpected trouble, the #2 target vessel and its storage container have been prepared. In the design of the #2 target vessel, issues on the fabrication of the first target vessel were scrutinized and the structure was redesigned. Figure 6 shows the photograph of the #2 target vessel. Typical difference between the first shown in Fig. 2 and #2 target vessel is the structure of the rear part. The outer shroud in the rear part of the #2 target was eliminated and the inner mercury vessel was substituted by thick pipes in order to reduce the fabrication cost without sacrificing safety.

References

[1] K. Haga et al., Proc. of ICONE 12-49518 (2004).
[2] H. Kogawa et al., Nucl. Instrum. Meth. A 600 (2009) 97.
[3] M.Futakawa et al., J. Nucl. Sci. Technol., 45, 10 (2008) 1041.

Cryogenic Hydrogen System

Introduction

Cryogenic hydrogen system of the JSNS provides supercritical hydrogen with temperature of 18 K and pressure of 1.5 MPa to three moderators and absorbs nuclear heating of about 3.8 kW produced in these moderators for 1 MW beam. This system consists of a helium refrigerator system and a hydrogen circulation system as shown in Fig.1. [1][2] Since this was the first time that supercritical hydrogen with such high pressure was generated in Japan, precious preparations with and without the proton beam were necessary to our system.

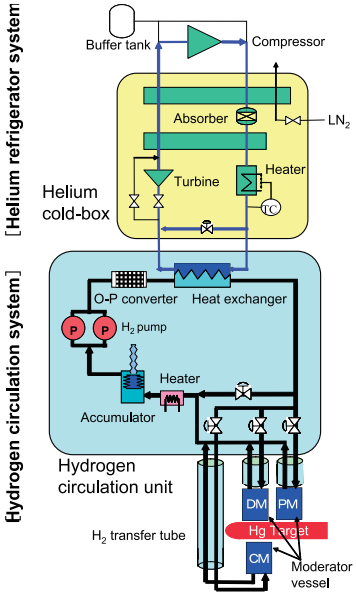

Fig.1 Schematic flow diagram of the cryogenic hydrogen system

Outline until 2007

The design of cryogenic hydrogen system was started in FY2003 as shown in Fig. 2. We entered into a contract with Taiyo Nippon Sanso Co. in autumn 2004, and each component for the system was manufactured in two years. Under the high pressure gas regulation in Japan, the installation was allowed by government in August 2006 and finished in December 2007. A cryogenic test as a trial was performed with other equipment such as a cooling water system except for the three moderator lines in winter 2007. The final inspection was received and the refrigerating was permitted by the Governor of Ibaraki in March 2007.

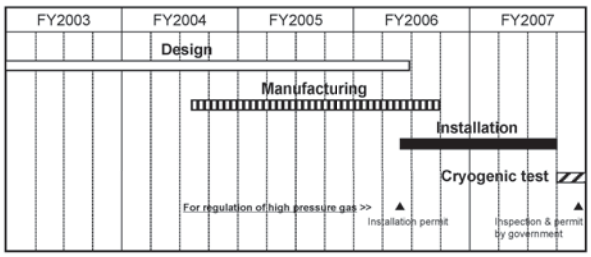

Fig.2 Construction history of the cryogenic system.

Spring 2008

Figure 3 shows the operation history of FY2008. In April 2008, we carried out the integrated test where supercritical hydrogen was circulated through three moderators for the first time. It was confirmed that the cryogenic hydrogen system operation successful and was examined step by step such as a cool-down step, rated operation of supercritical hydrogen and a warm-up step.

From May 22 to June 2, the cryogenic system was operated for the first beam operation. It achieved the rated operation of supercritical condition on May 29, and maintained this condition for three days. On Day-1, the first proton beam of 4 kW was received to the MLF target and the first cold neutron beam was provided at 14:25 on May 30. We succeeded in cooling the spallation neutron and sending as cold neutron beam to neutron users of the lead of the beam line. [3]

As the next RUN #17, the cryogenic system was operated for 15 days from June 13 to 27. The MLF beam operation was scheduled from June 16 to 26. However, the operation was

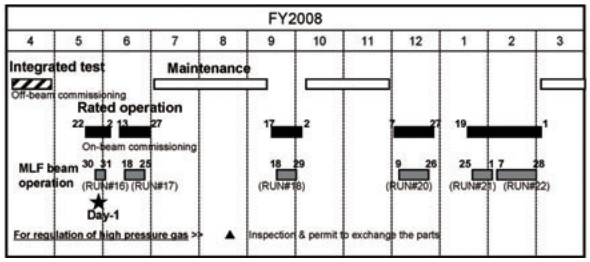

Fig.3 Cryogenic system operation in FY2008

stopped early for one day, because the temperature rise of helium at the heat exchanger was found and it caused instability in the helium refrigerator.

Summer 2008

During summer from July for about 2.5 months, we investigated the cause of temperature rise of helium in the helium refrigerator. It was found that the temperature rise was due to leak of the liquid nitrogen supply valve, which was repaired immediately. Because leak due to corrosion was found in the flexible piping between the outside and inside building for the hydrogen supply, the flexible piping was exchanged for a new one. After exchanging, the system was inspected and permitted by the Governor of Ibaraki under the regulation of high pressure gas in August. In the hydrogen pump system, an issue of severe temperature reduction was observed at the pump flange, which was fixed by improvement of the seal performance.

From the middle of September, the cryogenic system was operated for 16 days as the RUN #18 without any problem. The MLF beam operation was until 18 from September 29.

Autumn 2008

RUN #19 was canceled due to RFQ troubles in the LINAC. In October, the helium leak was found in the blanket. In November, the helium blanket structure for safety of hydrogen explosion was repaired.

Winter 2008-2009

In RUN #20, the cryogenic system was operated for 21 days in December. In the first half of this RUN, the on-beam commissioning was carried out at 20-kW proton beam. The MLF target received proton beam at 100 kW for the first time on December 9. In order to suppress large pressure change caused by beam injection from the accelerator, the cryogenic system has a pressure control system which is composed by an accumulator as a passive volume control and a heater as an active control for thermal compensation. We confirmed the performance that pressure fluctuation caused by 100 kW proton beam injection can be absorbed by the pressure control system. [4] Figure 4 shows the result of pressure control at 100-kW beam

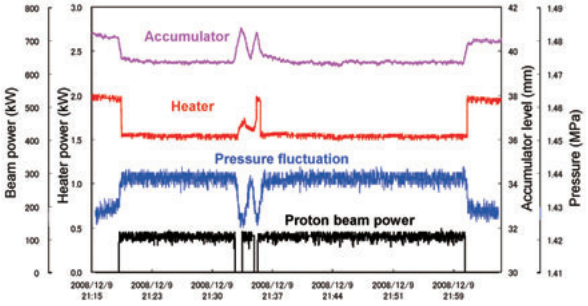

Fig.4 Result of pressure control at 100kW beam injection.

injection, which demonstrates that the pressure can be controlled as designed.

In RUNs #21 and #22, the cryogenic system was continuously operated for 42 days in January and February with the beam power of 20 kW. The cryogenic system had two pumps, i.e. pump-A and B. At the end of RUN #21 on February 2009, pump-B was stopped by an interlock because the vibration of the rotor shaft exceeded an allowable value of 20 m during 0.1 s, which was a threshold periodic time that we called "delay time". After this trip, the alternative pump-A was completely dedicated to circulate the liquid hydrogen until the end of RUN #22.

After inspection of the pump, no damage was found in pump-B, which is observed in March 2009. In order to investigate the reason of failure, the off-normal detection system by FFT analysis was installed in the vibration sensor, which helped us to understand the status of the pump described below.

Spring 2009

At the end of RUN #22 on March 2009, pump-A was stopped during the cryogenic system warm-up by the interlock for an inverter over current. Pump-A was taken away from the system and was inspected. It was found that the impeller was damaged. It seemed that debris like a piece of metal remained and hit where the impeller turned with high speed of 40,000 rpm. Pump-A was repaired and the hydrogen loop was cleaned by flushing with pressurized nitrogen gas in April and May. After the thorough flushing, the pumps were not stopped due to the impeller damage again.

Figure 5 shows the operation history of FY2009. The hydrogen pump was repaired in April and May. A sampling system for ortho-para hydrogen ratio measurement, which is

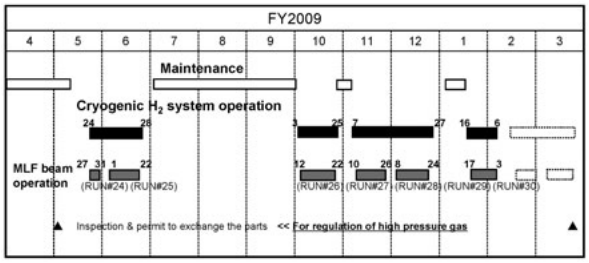

Fig.5 Operation history of FY2009

important to understand neutronic performance in the moderators, and the differential pressure sensor were installed in the cryogenic system. On May 1st, the cryogenic system was inspected and permitted by the government of Ibaraki under the high-pressure gas safety law.

From May 24 to the end of June, the cryogenic system was operated for RUNs #24 and #25 at the beam power of 20 kW. During operation period, the hydrogen pumps were stopped 15 times because of interlocking caused by the excess vibration at the rotor shaft. After the pump trip, we confirmed that the system status especially for the pump was ready to operate. The pump system can be restarted normally. By the FFT analysis, it was found that the rotor vibration was dumped less than 0.7 s when serious mechanical damage of the pump did not appear. In order to decrease the unnecessary trips, we extended the delay time from 0.1 s to 0.5 s. After modification, the pumps did not trip again in this RUN. At the end of RUN #25, we carried out the pump test by changing the rotation speed and the pump head. We could not clear the cause of the phenomenon, which might be one of the characteristics of the hydrogen pump of a gas bearing type. It has been under investigation.

Summer 2009

In the summer maintenance period, the hydrogen pumps, the helium leak detectors, the moisture and oxygen sensors for hydrogen and the cooling tower for the compressor were maintained. For the whole cryogenic hydrogen system, inspection based on the Japanese regulation was also carried out. In order to understand the behavior of the hydrogen pump, we placed more thermo sensors around the impeller in the safety box, which were located at the vacuum area.

Autumn 2009

In RUN #26, the cryogenic system was operated for 23 days in October. During operation, the hydrogen pump-A tripped due to interlocking by excess vibration of the rotor shaft, however no evidence was found on the pump. Therefore, we decided that the delay time expanded more from 0.5 to 0.9 s. After changing the time, the pumps have never tripped again due to the vibration so far.

After one week operation of "stand-by mode", which is economical operation mode without liquid nitrogen, it was found that the outlet temperature at the heat exchanger of the refrigerator rose gradually. Furthermore, in additional one week, the hydrogen temperature and pressure also rose in the hydrogen loop. We considered that thermal conduction lost in the heat exchangers due to the impurities in the helium gas. After the warm-up of RUN #26, the moisture contamination was measured. It was found that the amount of moisture was too high such as 160 ppm around the heat exchangers. Therefore, helium gas in the cold box was purified by pursing and evacuating repeatedly for three weeks. As a result, the temperature rise could be significantly suppressed less than 2 K during RUN #27 as shown in Fig. 6.

The cryogenic system was continuously operated from November to December as RUNs #27 and #28. The MLF target has received 120 kW of proton beam since this RUN. On December 9, the MLF target received proton beam with the power of 300 kW for the first time. We also confirmed the performance that the pressure fluctuation caused by 300-kW proton beam injection can be absorbed by the

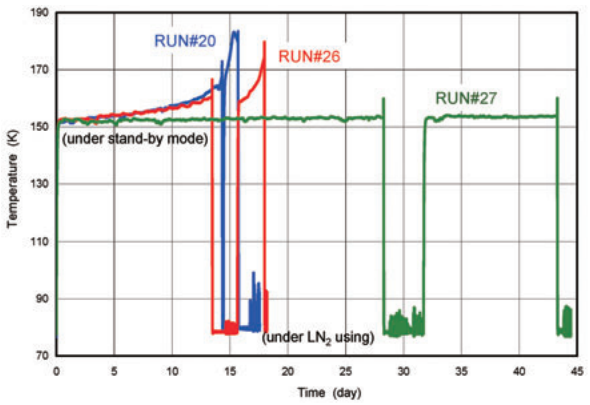

Fig.6 Result of improved behavior in the cold box (Temperature trends around the heat exchanger in the cold box).

pressure control system in the same way as the 100 kW injection of last year. Figure 7 shows the behavior of pressure control at 300 kW beam injection. It was demonstrated that the pressure fluctuation caused by a 300-kW proton beam injection could be absorbed by the system within about 15 kPa as designed. It can be expected that the pressure fluctuation at the 1-MW beam injection will be controlled within 50 kPa as shown in Fig. 8. [5]

Winter 2009-2010

Before RUN #29, in order to decrease the moisture contamination of helium gas in the cold box, we purified it by pursing and evacuating repeatedly for about one week. However, because the amount of nitrogen in the helium gas increased, it took time to conduct purifying work so the start of RUN #29 was delayed for two days. For RUN #29, the cryogenic system was operated for 22 days without any problem in January and February 2010.

During preparation of the cryogenic system operation at the beginning of February for RUN #30, a leakage from the helium area to the hydrogen area in the accumulator was found. Therefore, we could not fill up hydrogen and pressurized it in the hydrogen loop, and could not start operation and RUN #30 and #31 were

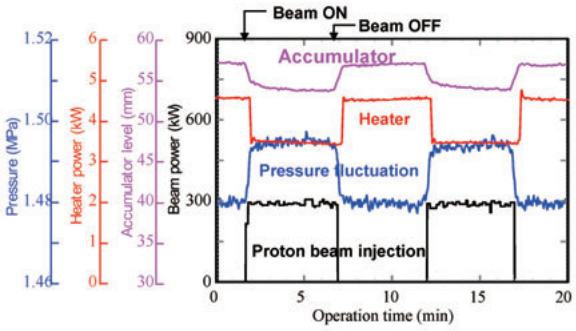

Fig.7 Result of pressure control at 300 kW beam injection

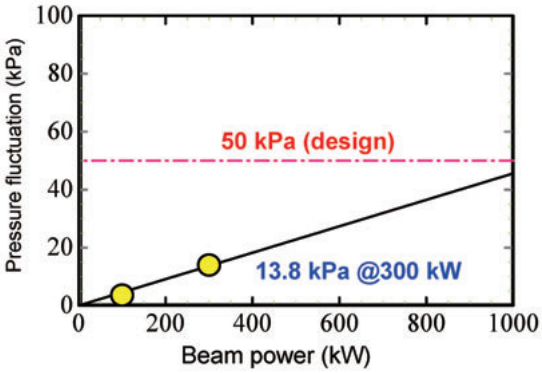

Fig.8 Measured pressure fluctuation and estimation for proton beam power.

cancelled. It is necessary for a long time to re-manufacture the accumulator and re-install. The earliest recovery way, which operates without the accumulator function filling it with hydrogen, will permit us beam operation with the beam power less than 120 kW. Finally, the operation without the accumulator function was chosen and the recovery was finished in March. The on-beam commissioning will be carried out in FY2010 April, and the user operation will begin as RUN #33 in May, without the accumulator.

References

[1] T. Aso, et al., Advances in Cryogenic Engineering, 51A 763-770 (2005).

[2] T. Kato, et al., Journal of the Cryogenic Society of Japan, Vol.42 No.8 277-264 (2007).

[3] H.Tatsumoto, et al., Advances in Cryogenic Engineering, “Development of the cryogenic hydrogen system for spallation neutron source”, accepted and printing now.

[4] H.Tatsumoto, et al., Advances in Cryogenic Engineering, “Pressure fluctuation behavior in the cryogenic hydrogen system by 100kW proton beam injection”, accepted and printing now.

[5] H.Tatsumoto, et al., Journal of the Cryogenic Society of Japan, Vol.45 No.4 181-190 (2010).

Completion of Off-beam Commissioning

To be ready to accept the first proton beam to the target station, much effort was devoted to demonstrate maintainability of the core components of the target station, such as the moderators, reflector, core-vessel inserts and neutron beam shutters. Although we encountered many troubles during the off-beam commissioning period, all planned commissioning work was completed by the first beam acceptance.

The moderators, reflector and proton beam window are planned to be replaced periodically mainly due to radiation damage. As the off-beam commissioning, those components with plugs at their operating positions were pulled up into a transfer cask, moved horizontally in the high-bay area on the 3rd floor, and put into the hot-cell. The components were handled remotely in the hot-cell by using the power manipulator and master-slave manipulators to demonstrate their replacement work (Fig.1). Finally the components were taken back to the operating positions with the reverse procedure.

Shutter inserts such as a neutron guide tube and a steel collimator for several neutron beam lines were inserted into the shutter blocks during the off-beam commissioning period. Although the inserts and the shutter blocks had not been activated at that time, the operation was conducted using shielded handling devices to confirm maintainability of radioactive shutter inserts after the beam acceptance.

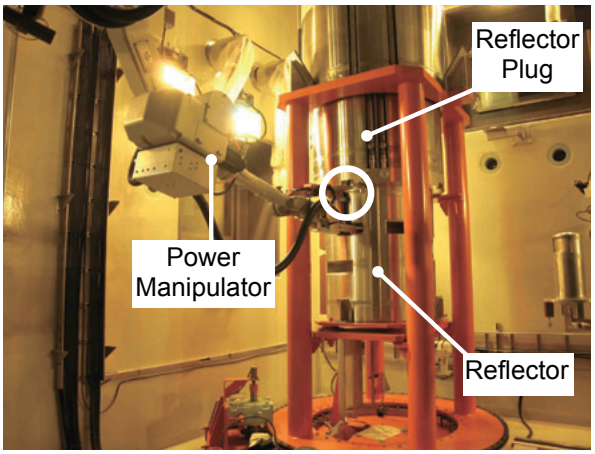

Fig.1 A scene of remote-handling operation. The power manipulator is turning a bolt to join the reflector to the reflector plug at the position shown with a white circle.

Fig.2 Core-vessel insert handling devise in testing in the HENDEL building

An operation test of the core-vessel insert handling device, which was a remote-handling device to replace core-vessel inserts, was conducted successfully in the HENDEL building (Fig.2).

On-beam operation

All the components in the target station were made ready by Day-1, and the first proton beam was accepted successfully. In most cases, all the components of the target station functioned adequately during JFY 2008 and 2009. Cooling water circulated with the rated flow rates in the moderators, reflector, reflector plugs, helium - vessel (He-vessel) and water-cooled shield. The moderators were cooled down to 20 K, and cryogenic hydrogen circulated with the rated flow rates in them. Helium gas was charged successfully in the He-vessel. Vacuum in the core-vessel inserts and the shutter inserts were maintained without any troubles for all the neutron beam lines.

However, one trouble happened in the

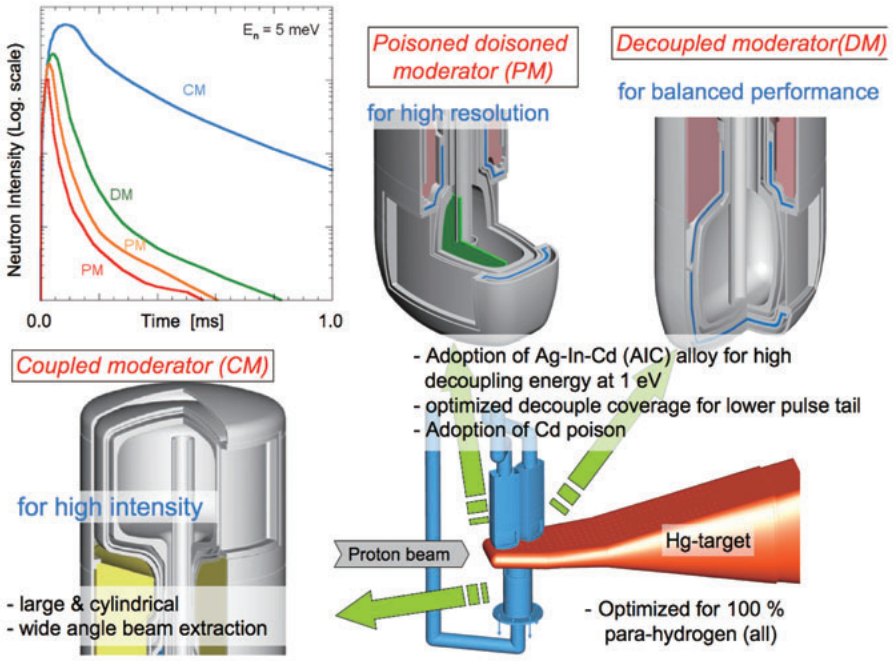

Fig.3 Three distinctive hydrogen moderators with their pulse shapes

shutter system. In September 2008, a servomotor-driven neutron beam shutter of one of the neutron instruments became non-operational when users wanted to open the shutter. After that, similar troubles happened sometimes in shutters even for other neutron instruments. The failed shutter could be recovered by resetting the local controller, but the MLF shift leader had to go to the local control panel for resetting while losing 20-30 minutes of user's beam time. Possible causes were investigated extensively to fix the trouble such as electric noise, mechanical structure and sequence of the shutter operation. After several months' investigations, a cause was finally found in the firmware of servo-amps. The servo-amps for all the 23 shutters were replaced with new ones to fix the trouble in March 2009.

Confirmation of expected performance

The most important performance for the neutron target station is neutronic performance of the three distinctive hydrogen moderators (Fig.3). We need to know whether the users can utilize the neutron beams as designed or not. We also need to confirm adequacy of the neutronics design of the neutron source itself because the source receives the high power beam of 1 MW and the design is very severe. Accordingly, we constructed a neutron instrument, "NeutrOn Beam-line for Observation and Research Use"

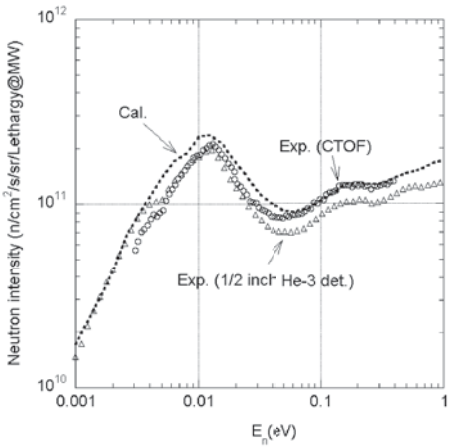

Fig.4 Comparison of measured and calculated absolute neutron spectral intensity

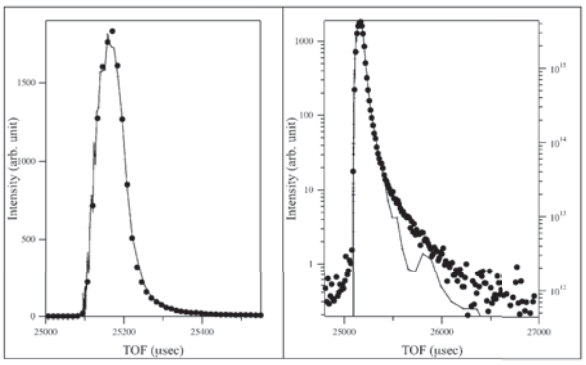

Fig.5 Observed (symbols) and calculated (lines) pulse shapes at E=1.86meV measured with a Mica sample on NOBORU in the linear scale (left) and the logarithmic scale (right).

(NOBORU) [1,2], at beam-line No.10 of MLF.

Neutron spectral intensity, time structure of neutron pulses, intensity distributions of

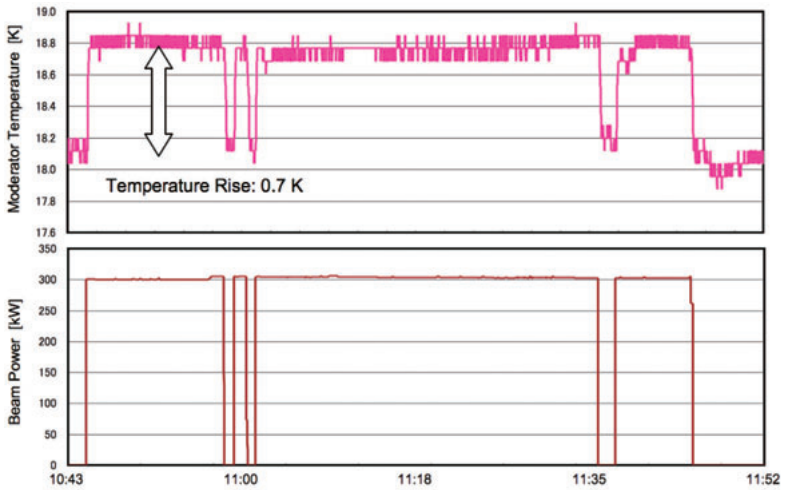

Fig.6 Records of proton beam power (lower) and hydrogen temperature (upper) during 300 kW operation.

the neutron beam cross-section, a luminosity distribution on a viewed surface of the moderator and so on were measured at 14 m from the decoupled moderator. Figures 4 and 5 compare absolute spectral intensity and pulse shape, respectively, between measured and calculated values. The measured spectral shape and pulse shape are reproduced very accurately by the calculation. The calculated spectral intensity agrees within ±30% with the measured one. [3]

On December 10th, 2009, a high-power operation at 300 kW was conducted. The hydrogen temperature rise of 0.7 K due to nuclear heating was observed in the cryogenic hydrogen system during the high-power operation as shown in Fig. 6. Estimation of the nuclear heating value in the hydrogen moderators may involve large uncertainty because the estimated value for 1 MW proton beam power is only 3.75 kW (0.375%). Nevertheless, the measured temperature rise is very close to its design value.

Judging from the measured and operational data so far acquired, although they are very limited, we can say that we are delivering neutron beams to users as designed, and the design of the J-PARC neutron source is adequate.

References

1) K. Oikawa, et al., Nucl. Instr. Meth. A **589** (2008) 310.
2) F. Maekawa, et al., Nucl. Instr. Meth. A **600** (2009) 335.
3) F. Maekawa, et al., Nucl. Instr. Meth. A **620** (2010) 159.

The final version of the documents for the first application for radiological license of MLF was submitted to MEXT (Ministry of Education, Culture, Sports, Science and Technology) in March 2008 after the review by the advisory committee[1] which started in October 2007. The documents consisted of the followings: (1) Two kinds of official forms of (1a) Usage of radioactive isotopes and (1b) Operation of radiation generators including muon and neutron target system, a proton beam transport line, muon beam lines and neutron beam lines, (2) An additional document and (3) Two references on (3a) Handling of radioactive products and (3b) Risk assessment of leakage of radioactive products to environment.

The license was issued in April 2008, and it permitted the followings: (1) Operation of the neutron and muon targets with 4 kW proton beam, (2) Usage of seven neutron beam lines of BL1, 3, 4, 8, 10, 19 and 20 and two muon beam lines of D1 and D2, (3) Use of the radioactive isotopes of ^{252}Cf and minor actinides, such as ^{244}Cm, etc., to be used for cross section measurements at BL4.

On May 13, the radiation controlled area was set at the 1st and 2nd experimental halls and the utility areas in the MLF. It was determined that the experimental halls were controlled as non-contaminated area, called "second-class controlled area", during the commissioning period and the early stage of common use.[2]

The license has been updated twice a year along with power-up of the proton beam intensity and installation of new beam lines. The updated items of each license and the licensing dates are tabulated in Table 1.

Table 1 Updated items, licensing dates of each license

No.	Date[1)] Month/Year	Beam Power [kW]	New Beam Lines[2)]
1	Apr./08	4	[N]: BL1, 3, 4, 8, 10, 19, 20 [M]: D1, D2
2	Oct./08	100	[N]: BL5, 12, 14, 16, 21
3	Apr./09	250	*
4	Oct./09	250	*
5	Apr./10	250	*

1) Licensing date
2) [N]: Neutron beam line, [M]: Muon beam line
*: Minor changes of the shielding configuration were applied.

The governmental checks were carried out for each license on the shield structures and dose rates in the controlled area and on its boundary. No significant dose has been measured at the checking positions in the governmental check, and we passed all checks perfectly.

Two kinds of radiological issues, which had not been predicted in the design stage, arose after beginning of the proton beam operation: one is "Hot-cell dose" issue [1] and, the other is the issue on "Tritium behavior in the mercury".

The "Hot-cell dose" issue came up in July 2008 after the first series of the beam commissioning. An unexpected phenomenon was found when we measured the dose rates around the mercury-circulation pipes on the target trolley; the dose rates increased after draining the mercury to the drain tanks under the target trolley. The typical measurement positions and the results are shown in Fig.1. We supposed that the dose rates in the hot-cell where the target trolley was installed drastically decreased after mercury drain since the drain tanks were shielded by thick steel, and we estimated that the dose rates went down lower enough to perform hands-on maintenance in the cell [2]. In order to find the reason, the gamma-ray spectroscopy measurement was carried out in the cell using an HPGe detector in October and November 2008. The position of the detector from the target trolley is shown in Fig.2. The followings were concluded from the measurement:

・Some of the spallation products selectively

[1] In the advisory committee, the issue of cavitations damage for the mercury target was also discussed, and the committee recommended that this issue should be reviewed again before the upgrade of proton beam intensity at which the damage become crucial for the operation.

[2] The experimental halls were designed and constructed as contaminated areas, called "first-class controlled areas". In the second-class controlled area, from the viewpoint of prevention of radioactive contamination, powder samples needed to be contained in airtight containers such as vanadium tubes, etc.

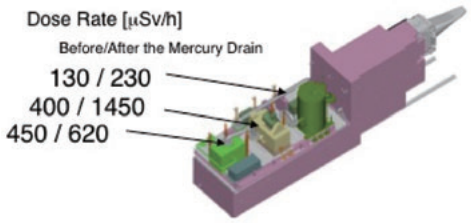

Fig.1 Typical positions and the results of the dose-rate measurements around the mercury-circulation pipes before and after the mercury drain. The measurement was carried out after the first series of the beam commissioning on July 2008. The integrated beam power of the first series was 17 kWh.

adhered to the inner walls of the mercury pipes. Before the mercury drain, the mercury worked as a shield of the adhered radioactive products.

- The radioactive products of ^{188}Ir dominated to the gamma dose in the hot cell. The measurement also showed that ^{118}Ir decayed with 10 days half-life, since the physical half-life of ^{188}Ir is 1.7 days. This means that ^{188}Pt, which is a parent nuclide of ^{188}Ir and has the half-life of 10.2 days, was stuck on the piping walls.
- Our estimation on the hot-cell dose was much underestimated. By extrapolating the current measurement results to 1 MW, the dose rate at the distance of 10 meters from the back-end of the trolley would be 10 mSv/h. For the hands-on work in the cell, a temporal shield is required to be set behind the trolley.

In April 2009, the design work of the temporal shield started, and the conceptual specification was determined as follows:

- The shield material is steel, and the thickness is 150 mm.
- In order to shield gamma rays scattered by walls of the cell, the shield needs to cover the whole region of the inner section of the hot cell. Therefore, considering the setting process of the shield, it consists of three parts of the iron blocks and their mounting.
- Setting of the shield in the hot cell is carried out using the overhead travelling crane of the high bay.

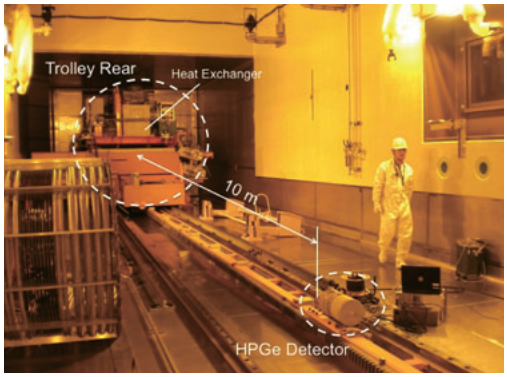

Fig.2 A photo of the gamma-ray spectroscopy measurement in the hot cell. An HPGe detector was set at a distance of 10 m from the back-end of the target trolley.

The procurement of the shield proceeded as scheduled, and it was delivered to the MLF in February 2010. The setting test in the hot cell was successfully performed.

The issue on "tritium behavior" is related to the process of the off-gas generated in the mercury. We estimated that considerable amounts of tritium were generated in the mercury via spallation reactions. If we supposed that all amount of tritium vaporized to the gas phase in the surge tank in the mercury circulation system, the tritium process was required to release them to environment in conformity with the regulation on radioactive concentration in exhaust air. We prepared the off-gas process system to remove the tritium from such kinds of radioactive gaseous waste. In order to check whether the gas process was needed or not, the helium gas in the gas phase was sampled and the radioactivity was measured in September 2008. As a result, we found that the amount of tritium in the gas phase was much less than the total amount, which was estimated with calculation, by a factor of 10^4. This meant that the almost all tritium remained in the mercury, but we are not sure this is true. This question, which we call "Tritium missing problem", should be solved by investigation of the chemical behavior of tritium in mercury for future use of the mercury target system with 1 MW.

References

1) Y. Kasugai et al., "Gamma Dose Measurements and Spectroscopy Analysis for Spallation Products in JSNS Mercury Circulation System", The fifth International Symposium on Radiation Safety and Detection Technology (ISORD-5), July 15-17 2009, Kitakyushu, Japan, to be published in J. Nucl. Sci. Techonol. (Supplement).

2) T. Kai et al., "Radioactivity Estimation at J-PARC Spallation Neutron Source by Using the DCHAIN-SP 2001 and PHITS Code", Proceedings of 1st Workshop on Accelerator Radiation Induced Activation (ARIA '08), Oct. 13-17 2008, Paul Scherrer Institut, Switzerland, 182-187 (2009).

Neutron Science

January 2007

October 2010

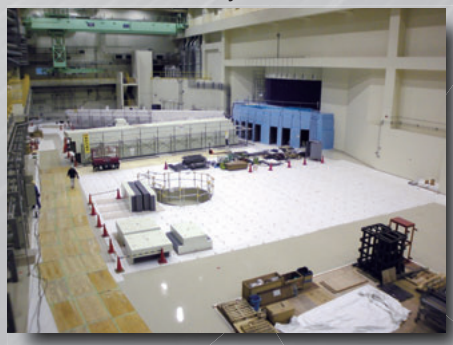

1st experimental hall

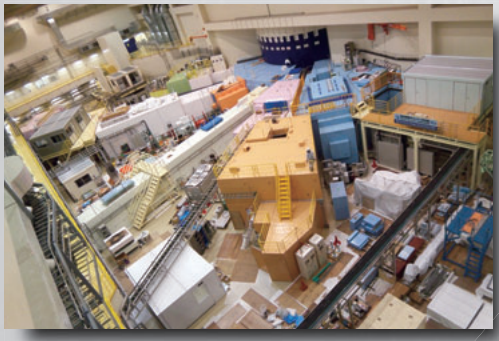

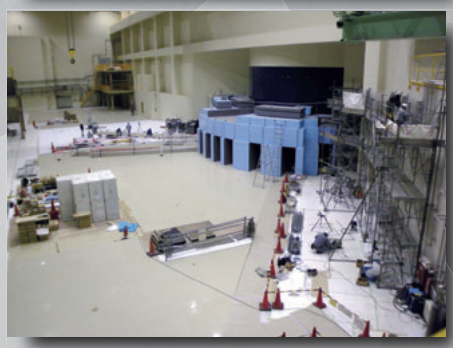

2nd experimental hall

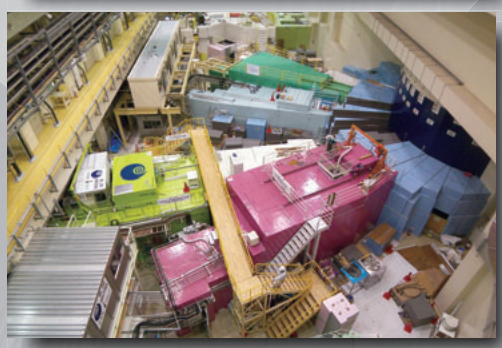

Intensive construction, day one and beginning of user program

Since 2001, researchers, engineers and other members in the MLF (Materials and Life Science) division have not only intensively constructed instruments, but they have also been involved in facility management, including process control of beamline construction, safety, maintenance, user support, beamtime management, outreach, and development of the proposal system. Although the beam power achieved by the end of 2009 was only 1/10 of the designed value, it has reached 40 times the power of KENS's beam. The repetition rate of 25 Hz, which is much smaller than that of the first target station at ISIS (50 Hz) and SNS (60 Hz), brightens the uniqueness of the neutron instruments at J-PARC, where a wide dynamical range is attained with limited loss of neutrons.

Since the construction of the MLF building was completed in April 2007, over 10 instruments have been installed in the MLF experimental halls, enabling the first beam experiment to be scheduled for the end of May 2008. At 14:25 on May 30th, 2008, the first neutron was detected by Li-glass scintillation detectors by the CTOF technique at one of five day-one instruments, NOBORU (BL10). Soon after this memorial event, the other four day-one instruments started: iBIX (BL03), ANNRI (BL04), SuperHRPD (BL08), and iMATERIA (BL20). All these day-one instruments measured the spatial distribution of the neutron beam with imaging plates and neutron spectra using Li-glass detectors by the CTOF technique. The first powder diffraction pattern of an iron steel block (both α-Fe and γ-Fe are included) was recorded on May 31st at SuperHRPD. In June, we measured the first Laue spot of KBr at iBIX, and the resonant absorption spectra of Au thin films at ANNRI.

In July 2008, we called for the first J-PARC general user proposals (2008B term) for the experimental period between December 23rd, 2008, and March 2009. For each of the six instruments, a total of 23 days of experiments were successfully carried out in the first MLF user program. Most recently, J-PARC general user proposals for nine instruments, 4SEASONS (BL01), iBIX, SuperHRPD, NOBORU, AMATERAS (BL14), ARISA-II (BL16), TAKUMI (BL19), iMATERIA, and NOVA (BL21), and the Ibaraki Prefecture general user proposals for industrial use on iBIX and iMATERIA were called for in the 2010B (60 days) term. In order to promote internationalization, all academic proposals were requested to be written in English; subsequently, the MLF proposal-reviewing process was also to be in English. The submitted proposals were reviewed by the Neutron Science Proposal Review Committee (NSPRC) including overseas committee members.

Now, in addition to the above 10 instruments, HRC (BL12) and NOP (BL05) are being used by project teams, and we are constructing the following six instruments: DNA (BL02), SPICA (BL09), PLANET (BL11), TAIKAN (BL15), VNR (BL17), and SENJU (BL18). All instruments in operation and under construction are shown in Fig. 1 and Fig. 2, and are listed in Table 1.

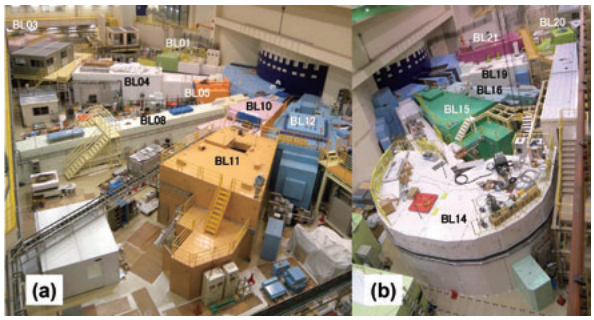

Fig.1 Overhead photo of neutron beamlines and instruments at MLF experimental halls in September 2010: 1st (a) and 2nd (b) experimental halls.

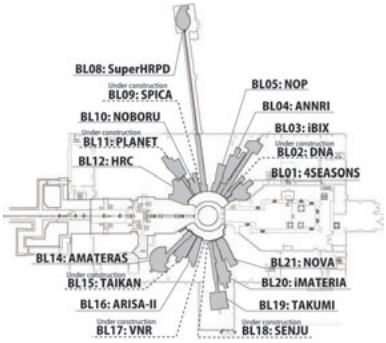

Fig.2 Layout and status of neutron instruments at MLF as of September 2010.

Table 1 Instrument specifications of instruments currently scheduled and under construction*.

Instrument	Beamline Number/ moderator**	Target	Specifications
4D Space Access Neutron Spectrometer (4SEASONS)	BL01 / C	Lattice and spin dynamics in high-T_c superconductors, etc.	$5 < E_i < 300$ meV, $\Delta E/E_i > 5\%$
Biomolecular Dynamics Spectrometer (DNA)	BL02 / C	Dynamics of biomolecules and soft materials.	Scan energy: $-25 < E <$ 45μeV, (Si analyzer (111): resolution ~1.2μeV)
IBARAKI Biological Crystal Diffractometer (iBIX)	BL03 / C	Biological neutron crystallography.	Maximum lattice constant ~150Å
Accurate Neutron-Nucleus Reaction Measurement Instrument (ANNRI)	BL04 / C	Neutron capture cross sections of minor actinides and long-lived fission products.	Two spectrometers. Ge detectors array (L_1=21.5m), NaI(Tl) detectors (L_2=27.9m)
Neutron Optics and Fundamental Physics Beam Line (NOP)	BL05 / C	Fundamental physics. Neutron β decay measurement etc.	Three (small divergence, high intensity, high polarization) beamlines
Super High Resolution Powder Diffractometer (SuperHRPD)	BL08 / DCP	Analysis of complicated and hierarchical structures.	d=0.3~45Å, Δd/d=0.1~3.0% (best 0.035% at 2θ=175°)
Special Environment Neutron Diffractometer (SPICA)	BL09 / DCP	Materials Science for batteries.	d=0.1~125Å, Δd/d>0.08%
NeutrOn Beam-line for Observation & Research Use (NOBORU)	BL10 / DC	Neutronics research, R&D.	L_1=14m, maximum beam size 100mm × 100mm, band width ~9Å
High Pressure Neutron Diffractometer (PLANET)	BL11 / DC	Neutron diffraction under high pressure.	d=0.21~4.1Å, Δd/d~0.5% Pressure and temperature: 0~20GPa, 10K-2000K
High Resolution Chopper Spectrometer (HRC)	BL12 / DC	Phonon vibration and dispersion, elemental spin and orbital excitation in magnetic	$1 < E_i < 2000$ meV, $\Delta E/E_i \geq$ 2.5% (1% in the future)
Cold-neutron Disk-chopper Spectrometer (AMATERAS)	BL14 / C	Quasielastic & Inelastic scattering for dynamical properties in atomic, molecular	$1 < E_i < 80$ meV, $\Delta E/E_i > 1\%$
Smaller-Angle Neutron Scattering Instrument (TAIKAN)	BL15 / C	Analysis of nanostructures and microstructures in hard, soft, biological materials.	Q=0.003~13Å^{-1}, Q_{min}=0.0005 Å^{-1} (in focusing mode)
High Performance Neutron Reflectometer with a Horizontal Sample Geometry (ARISA-II)	BL16 / C	Surface and interfaces structure in softmatter materials.	Q=0.005~0.4Å^{-1}, $\Delta Q/Q$ >1 %,
Polarized Neutron Reflectometer with a Vertical Sample Geometry (VNR)	BL17 / C	Magnetic structures in thin films and multilayers	Q=0.005~1.2Å^{-1}, $\Delta Q/Q$ >2 %,
Single Crystal Neutron Diffractometer under Extreme Condition (SENJU)	BL18 / DCP	Structure of functional materials under controlled environmental conditions.	Maximum lattice constant ~50 Å
Engineering Materials Diffractometer (TAKUMI)	BL19 / DCP	Stress/strain measurements in materials science and mechanical engineering.	d=0.5~2.7Å, Δd/d=0.4% (best Δd/d=0.2%)
IBARAKI Materials Design Diffractometer (iMATERIA)	BL20 / DCP	Structural and chemical analysis for materials	d=0.09~58Å, Δd/d=0.16% (at d=0.18~2.5Å)
High Intensity Total Diffractometer (NOVA)	BL21 / DC	Structures of hydrogen-storage materials and disordered materials.	Q=0.01~100Å^{-1}, $\Delta Q/Q$=7~0.3%

* See J-PARC/MLF website http://j-parc.jp/MatLife/en/instrumentation/ns_spec.html for further details.
** C: coupled H_2 moderator, DC: decoupled H_2 moderator, DCP: decoupled-poisoned H_2 moderator

Instruments strategy and first data
single-crystal diffractometers

There are two single-crystal diffractometers: the scheduled instrument iBIX (BL03) is for biological crystallography and small molecules (organic compounds) [1], and the diffractometer SENJU (BL18), is currently under construction, for materials science. In order to achieve its characteristics, in iBIX, a new compact detector system with a short time resolution composed of scintillator sheets of ZnS:Ag/$^{10}B_2O_3$ and wavelength-shifting-fiber (WLSF) arrays in the X-Y axes was adopted. SENJU will provide various combined sample environments, such as high-magnetic field and low temperature, to expand the range of materials and engineering sciences.

Powder diffractometers and total scattering instrument

There are three general purpose diffractometers with different intensity and resolution, and three dedicated diffractometers for different objectives. This is a natural

consequence of high-achievable performances of diffractometers with sharp pulsed sources for JSNS decoupled/decoupled-poisoned moderators. In the decoupled moderator, the tails of pulse peaks are removed by the decoupler. The S/N above 100 meV must be better than 1.5 - 2 in order to lead to the preferred decoupling energy of 1 eV with Ag-In-Cd (AIC). The designed performance of AIC was verified at NOBORU by examining the profile shape, as shown in Fig. 3. On the other hand, the decoupled-poisoned moderator was designed so as to achieve the designed resolution within a 100 m flight path in SuperHRPD (BL08), which is a powder diffractometer having the highest resolution [2]. Figure 4 shows the comparison of a Bragg reflection measured by SuperHRPD as well as Sirius, a high resolution powder diffractometer of KENS; the FWHM is three time improved in SuperHRPD and the tail of each Bragg peak observed in Sirius is absent in SuperHRPD resulting in 10 times improvement in 1/10-width [3]. An example obtained by SuperHRPD is shown in Fig. 5 where satisfactory Rietveld analyses were obtained with Z-Rietveld, a Rietveld analysis software developed for J-PARC powder diffractometers.

TAKUMI (BL19) is a dedicated engineering neutron diffractometer to promote scientific and industrial studies [3]. A typical result obtained using TAKUMI in the project "Stress/Strain Studies in Superconducting Composite" is shown in Fig. 6 [4]. iMATERIA (BL20) is a versatile neutron diffractometer funded by the local government, Ibaraki Prefecture, to promote industrial applications of neutron beams at J-PARC [5]. Currently, it takes about 30 minutes to obtain 'Rietveld-quality' powder diffraction data for X-ray laboratory-sized standard oxide samples measured at an accelerator power of 120 kW of the accelerator power. NOVA (BL21) is a very high-intensity diffractometer (total scattering instrument) that allows us to obtain a global description of the structure of crystals and disordered materials (amorphous solids, glasses, and liquids) by the Fourier transform of the normalized measured scattering intensity $S(Q)$ over a wide range of momentum transfer Q [6]. Figure 7 shows $S(Q)$ of vanadium hydride VD_2 up to 50 $Å^{-1}$. PLANET (BL11) is a dedicated high-pressure powder diffractometer, and SPICA (BL09) is a special-environment powder diffractometer for battery research. Both SPICA and PLANET are currently under construction.

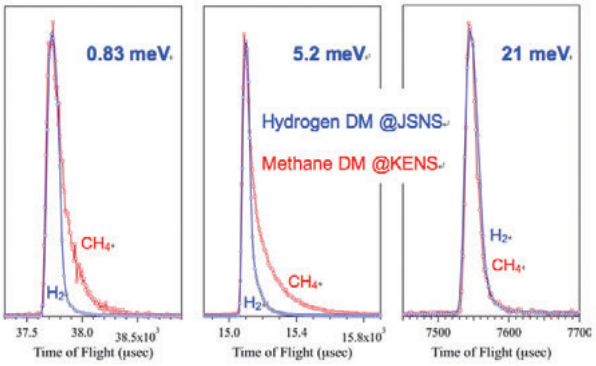

Fig. 3 Neutron pulse shapes at J-PARC JSNS (Japan Spallation Neutron Source)'s hydrogen decoupled moderator (DM), measured on NOBORU, and KENS/KEK's methane DM on a linear scale.

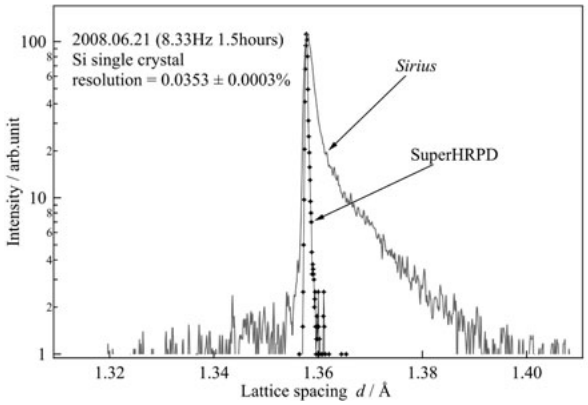

Fig. 4 Bragg reflection of Si (400) at d = 1.36 Å shows the best resolution with $\Delta d/d$ = 0.0353(3) % [3]. In comparison, the same Bragg reflection obtained by the previous high resolution powder diffractometer Sirius at KENS is shown.

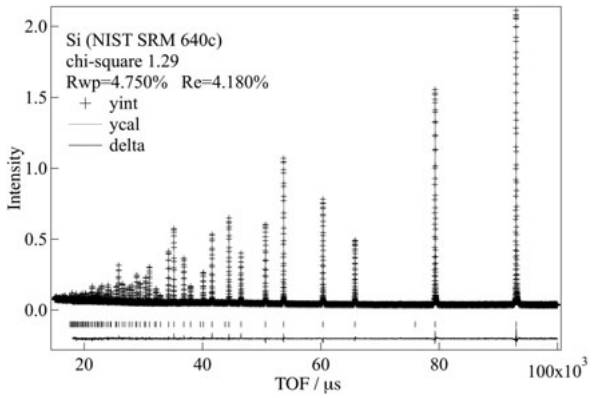

Fig. 5 Rietveld analysis result of L-Alanine_R using Z-Rietveld.

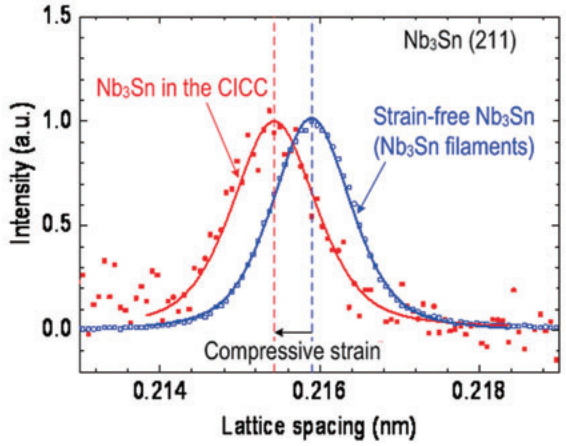

Fig. 6 Difference in lattice spacing of Nb_3Sn in International Thermonuclear Experimental Reactor (ITER) Toroidal Field (TF) conductor and the strain-free Nb_3Sn filaments extracted from the Nb_3Sn strands [4]. The ITER TF conductor is a Cable-In-Conduit Conductor (CICC) composed of 900 Nb_3Sn strands, 522 copper strands, a central spiral and a SUS316LN circular jacket.

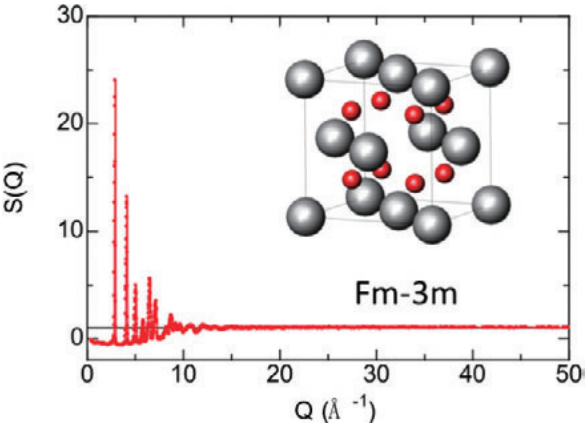

Fig. 7 Static structure factor *S(Q)* for vanadium hydride VD_2 measured by NOVA.

Inelastic scattering instruments

There are four spectrometers with a different range of Q-ω space: two Fermi-chopper spectrometers with different resolutions, 4SEASONS (BL01) and HRC (BL12): one disk chopper spectrometer, AMATERAS (BL14); and one backscattering spectrometer, DNA (BL02). 4SEASONS is a high-intensity Fermi-chopper spectrometer, which was installed at the coupled moderator port, with medium energy resolution > 5% (E_i = 5~300 meV) [7]. HRC is a high-resolution Fermi-chopper spectrometer with the best energy resolution of 1% (E_i = 1~2000 meV). AMATERAS is a high-resolution disk-chopper spectrometer using cold neutrons [8]. By combining the high peak intensity from a coupled moderator and the newly developed high-speed disk-choppers (maximum revolution: 350 Hz; minimum burst time: 7.6 μs) for pulse shaping and monochromating, the spectrometer realizes both high resolution and high intensity in the range of E_i = 1-20 meV, and can show sufficient performance up to E_i < 80 meV. DNA is a crystal analyzer backscattering spectrometer with a pulse shaping disk-chopper to realize 1 μeV even with a 40 m flight path [9].

Results obtained using 4SEASONS are shown in Fig. 8: the first inelastic measurement on single crystals of $CuGeO_3$ with accelerator power of only ~18 kW [10]. This might be the first demonstration of the repetition rate multiplication (RRM) technique using Fermi-chopper spectrometer [11]. Similar "multi E_i" results of inelastic measurement on silica (SiO_2) glass using AMATERAS are shown in Fig. 9, demonstrating that the RRM technique is a powerful method for studying phonon dynamics in non-crystalline materials [12]. The RRM technique is achieved with a new data acquisition scheme at J-PARC, called event recording. It is not necessary to define time bins beforehand for the time axis, and we merely measure scattered neutrons, each of which is tagged with a time stamp and stored over the source period event by event. We can define time bins afterward to make them match a required energy resolution. It is a very useful scheme for all kinds of instruments and experiments especially for time-resolved measurements under various sample environments.

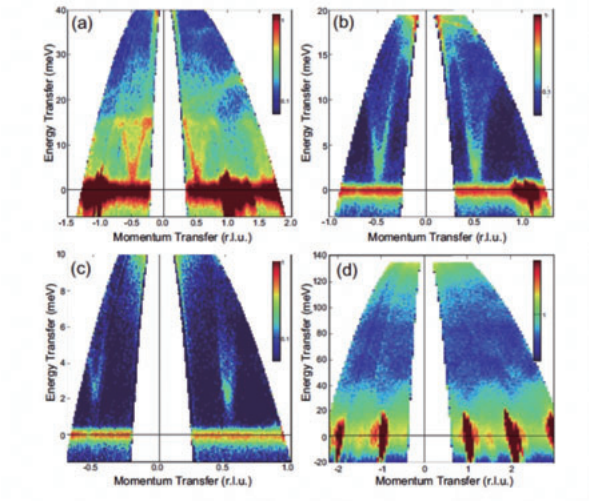

Fig. 8 First inelastic scattering measurements on 4SEASONS. Magnetic scattering spectra of $CuGeO_3$ below the spin-Peierls transition temperature, where data with (a) E_i = 45.4meV, (b) 21.5 meV, (c) 12.6 meV, and (d) 150.7 meV were obtained simultaneously [11].

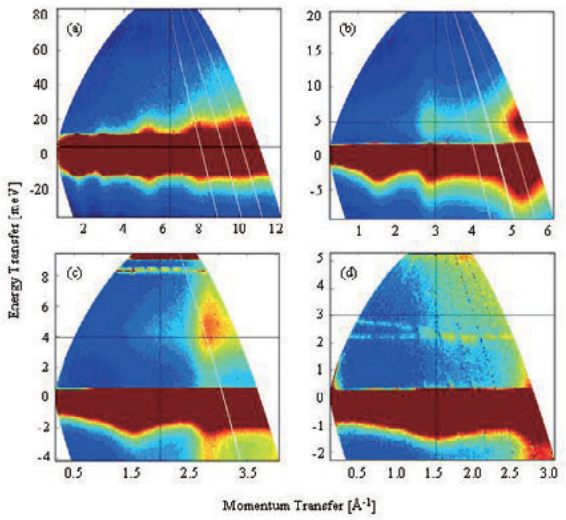

Fig. 9 Inelastic scattering measurements on AMATERAS. Simultaneous observation of multiple two-dimensional *S(Q,E)* maps for SiO_2 glass by one measurement [12]. The horizontal axis shows the momentum transfer and the vertical axis shows the energy transfer. The incident energies were (a) 94.1, (b) 23.6, (c) 10.5, and (d) 5.9 meV. The signal lines around 8 meV in (c) and around 2-3 meV in (d) are noise due to the experimental background.

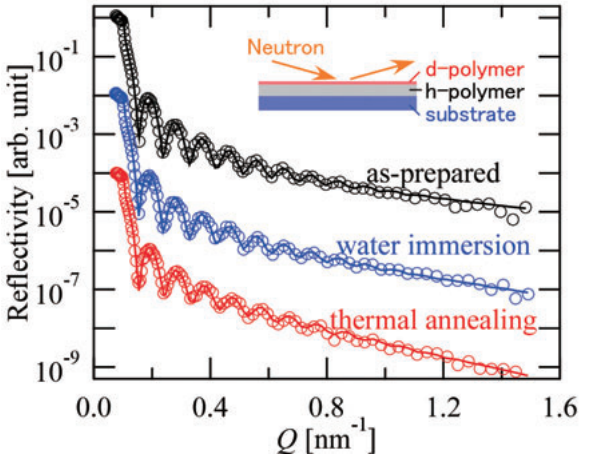

Fig.10 Reflectivity measurement of polymer bilayers as prepared, after water immersion, and after thermal annealing, on ARISA-II.

Reflectometers and smaller-angle scattering instrument

There are one SANS and two reflectometers with different sample geometries. TAIKAN (BL15) is a small-angle scattering instrument covering a wide Q-range (Q = 0.003-13 $Å^{-1}$) beyond those covered by traditional SANS instruments [13]. TAIKAN is under construction, and will be provided with a polarized or focused neutron beam. ARISA-II (BL16) is a neutron reflectometer with horizontal sample geometry, and permits routine measurement of reflectivities as low as 10^{-6} in typical run times of several hours at an accelerator power of 120 kW. Figure 10 shows the example of the reflectivity data taken by ARISA-II. A deutrated polymer (poly(methyl methacrylate); PMMA) layer was put on a normal polymer film, and compared the structural change of the surface polymer layer after water immersion and thermal annealing. Another reflectometer, VNR (BL17), also under construction, is a polarized neutron reflectometer for vertical sample geometry.

Other instruments and beamlines in operation

NOP (BL05) is a beamline for fundamental physics experiments using novel techniques of neutron optics. ANNRI (BL04) is an instrument for accurate measurement of neutron-capture cross sections, mainly for detailed engineering designs and safety evaluations of innovative nuclear reactor systems. Figure 11 shows neutron-capture gamma-ray yields for ^{244}Cm obtained using ANNRI. Resonance peaks of ^{244}Cm are clearly observed at 7.67, 16.77, 22.85, 34.99, and 96.12 eV. This is the first experimental result of ^{244}Cm (n, γ) cross-section measurement performed with an accelerator facility, in the world. NOBORU (BL10) is a beamline for studying the neutronic performance of JSNS, as shown in Fig. 3, and the test beamport for R&D activities of innovative devices and for testing new ideas of future instruments at MLF, among other things [14]. At NOBORU, pulse shape measurements and various important test experiments have been performed, such as R&D on energy-selective imaging, and test experiments of the MIEZE-type spin echo technique and of neutron magnetic scattering using a high-magnetic-field apparatus (~ 40 Tesla).

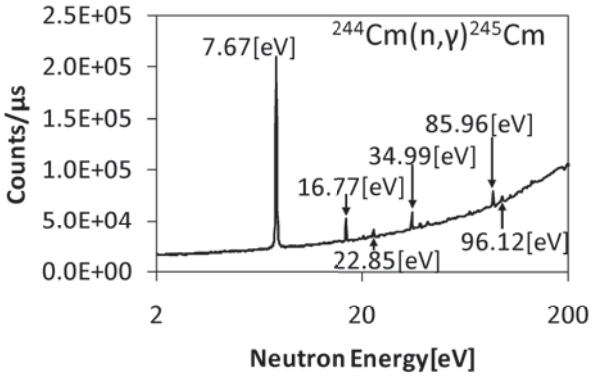

Fig.11 Neutron-capture γ-ray yields of ^{244}Cm sample measured on ANNRI.

References

[1] I. Tanaka, K. Kusaka, K. Tomoyori, N. Niimura, T. Ohhara, K. Kurihara, T. Hosoya and T. Ozeki, Nucl. Instr. Meth. **A 600**, (2009) 161-163.

[2] T. Kamiyama and K. Oikawa, ICANS-XVI (2003) 309-314.

[3] S. Harjo, A. Moriai, S. Torii, H. Suzuki, K. Suzuya, Y. Morii, M. Arai, Y. Tomota, K. Akita and Y. Akiniwa, Mater. Sci. Forum **524-525**, (2006) 199-204.

[4] K. Osamura et al., J. Cryo. Soc. Jpn. **45**, (2010) 135-147.

[5] T. Ishigaki et al., Nucl. Instr. & Meth. **A 600**, (2009) 189-191.

[6] T. Otomo and K. Suzuya, J. Cryst. Soc. Jpn. **50**, (2008) 13-17.

[7] R. Kajimoto, T. Yokoo, K. Nakajima, M. Nakamura, K. Soyama, T. Ino, S. Shamoto, M. Fujita, K. Ohyama, H. Hiraka, K. Yamada and M. Arai, J. Neutron Res. **15**, (2007) 5-12

[8] K. Nakajima, M. Nakamura, R. Kajimoto, T. Osakabe, K. Kakurai, M. Matsuda, M. Metoki, S. Wakimoto, T. J. Sato, S. Itoh, M. Arai, K. Yoshida and K. Niita, J. Neutron Res. **15**, (2007) 13-21.

[9] N. Takahashi, K. Shibata, T. Sato and M. Arai, J. Neutron Res. **15**, (2007) 61-67.

[10] R. Kajimoto, M. Nakamura and M. Arai. Neutron News **21**(1), (2010) 55-56: M. Nakamura, R. Kajimoto, Y. Inamura, F. Mizuno, M. Fujita, T. Yokoo and M. Arai, J. Phys. Soc. Jpn. **78**, (2009) 093002

[11] K. Nakayoshi, Y. Yasu, E. Inoue, H. Sendai, M. Tanaka, S. Satoh, S. Muto, N. Kaneko, T. Otomo, T. Nakatani, and T. Uchida, Nucl. Instr. & Meth. **A 600**, (2009) 111-113.

[12] M. Nakamura, K. Nakajima, Y. Inamura, S. Ohira-Kawamura, T. Kikuchi, T. Otomo and M. Arai, J. Atom Indonesia, **36**, (2010) 116-120.

[13] T. Shinohara, S. Takata, J. Suzuki, T. Oku, K. Suzuya, K. Aizawa, M. Arai, T. Otomo, and M. Sugiyama, Nucl. Instr. & Meth. **A 600**, (2009) 111-113.

[14] F. Maekawa, K. Oikawa, M. Harada, T. Kai, S. Meigo, Y. Kasugai, M. Ooi, K. Sakai, M. Teshigawara, S. Hasegawa, Y. Ikeda and N. Watanabe, Nucl. Instr. & Meth. **A 600**, (2009) 335-337.

T. Kamiyama and K. Suzuya

Neutron Science Section, Materials and Life Science Division, J-PARC Center Tokai, Ibaraki, 319-1195 Japan

Huge vacuum chamber installed in High Resolution Chopper spectrometer (HRC, BL12).

BL 01: Recent Progress in BL01, 4SEASONS

The **4**D **S**pace **A**cces**s** Neutr**on** **S**pectrometer 4SEASONS, also called 四 季*(SIKI)* in Japanese, is a high-intensity Fermi-chopper spectrometer. It is intended to provide high counting rate up to 300 meV neutron energy with medium resolution ($\Delta E/E_i \sim 6\%$ at $E = 0$) to efficiently collect weak inelastic signals from novel spin and lattice dynamics especially in high-T_c superconductors and related materials. For this purpose, the instrument is equipped with advanced instrumental design. This includes an elliptic-shaped converging neutron guide coated with high critical-angle (m = 3–4) super-mirrors, and long-length (2.5 m) ^{3}He position sensitive detectors (PSDs) arranged cylindrically inside the vacuum scattering chamber. Furthermore, the spectrometer makes active use of multiple-incident-energy measurements by the repetition rate multiplication (RRM) technique, which greatly improves the measurement efficiency. The major specifications of the instrument are summarized in Table 1.

In fiscal 2008, the construction of the instrument progressed significantly. For example, 160 PSDs (Fig. 1) and the guide tube were installed in this year. Finally, the spectrometer accepted the first neutron beam on September 19, 2008 (Fig. 2), and started the commissioning with neutron beam.

Table 1 Specifications of 4SEASONS.

Beamline	BL01
Moderator	Coupled
Neutron guides	Elliptically converging shape with m=3-4 super-mirrors
Incident energy	10-300 meV
Energy Resolution	$\Delta\hbar\omega/E_i = 6$ % FWHM at $\hbar\omega = 0$ when $\Delta t_{chopper} = \Delta t_{moderator}$
Flight paths	Moderator-sample = 18.03 m, Sample-detector = 2.5 m
Fermi chopper	At 1.71m upstream the sample, rotating in 25-600 Hz at 25 Hz interval
Band definition	Two disk choppers at 9 m and 12 m, rotating at 25 or 12.5 Hz
Background (T0) chopper	At 8.5 m, rotating at 25 or 50 Hz
Detectors	2.5 m from the sample position Horizontal coverage: −35° to 55° (−35° to 130° in the future) Vertical coverage: −25° to 27° Position sensitive ^{3}He tubes. 16 atm partial pressure, 19 mm dia. × 2.5 m × 191 pcs. (351 pcs. in the future)

Unfortunately, due to the delay in development of the Fermi chopper, we could not perform inelastic scattering measurements in this year. Nevertheless, we did several important tests and tuning of the instrument using neutron beams, such as calibration of the detectors, study on background scattering, and many bug fixes and updates of the software.

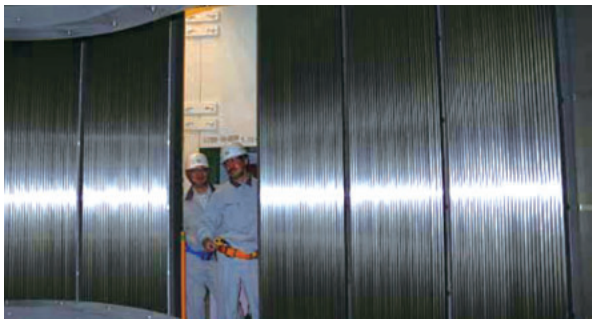

Fig.1 ^{3}He position sensitive detectors.

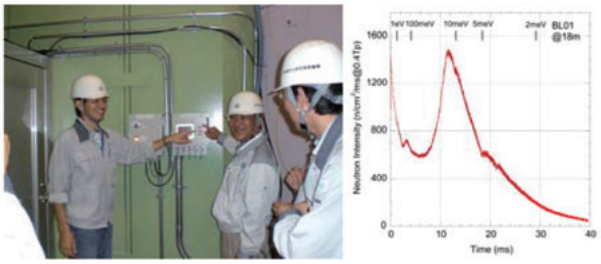

Fig.2 First neutron beam on 4SEASONS. (Left) Dr. Kajimoto and Dr. Arai are opening the shutter to introduce the beam into the instrument. (Right) The time-of-flight spectrum measured by C-TOF.

The construction of 4SEASONS continued in fiscal 2009. We installed additional 31 PSDs. We setup the vacuum system for the vacuum scattering chamber, which is a combination of a screw pump, a turbo molecular pump, and a cryo pump, and can evacuate the chamber to ~10^{-6} Torr. We also prepared a 4K cryostat as a standard sample environment device. The most notable progress was the installation of the Fermi chopper, by which the instrument finally became a spectrometer. The first inelastic scattering measurement was done in June 2009. It is to measure magnetic excitations in single crystals of the spin-Peierls compound $CuGeO_3$. In spite of the fact that the beam power of the accelerator was only ~18 kW at that time, we could roughly map the overall feature of the magnetic excitations in this one-dimensional quantum anti-

ferromagnet by just a 5.5 hour measurement on a 25 g sample. More noteworthy in this measurement is that we could obtain multiple data with different incident energies (E_i's) simultaneously (multi-E_i measurement) (Fig. 3) by RRM with the monochromating chopper. This might be the first demonstration of the RRM technique by a Fermi chopper spectrometer, and proved its high potential in inelastic scattering measurements. The result was published as the honorable first paper with neutron scattering data in MLF [1]. In addition, we performed several test measurements, and started user program. These include measurements on copper oxide and iron-based superconductors. After these accomplishments, we held a ceremony on December 25, 2009 with about 60 participants to celebrate the completion of the construction of 4SEASONS (Fig. 4).

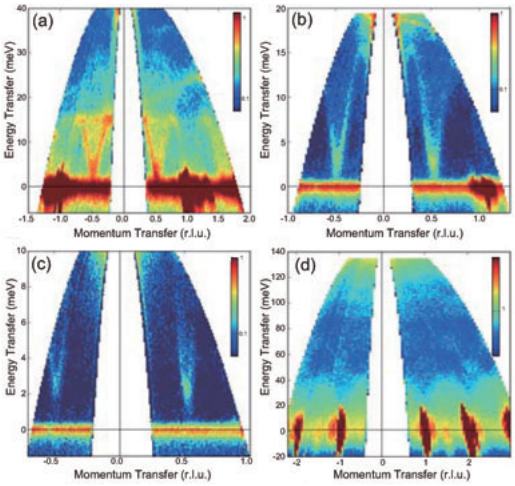

Fig.3 Result of the fist inelastic scattering measurement on 4SEASONS [1]. Magnetic scattering spectra of $CuGeO_3$ below the spin-Peierls transition temperature, where data with (a) E_i = 45.4 meV, (b) 21.5 meV, (c) 12.6 meV, and (d) 150.7 meV are obtained simultaneously.

Although we held the completion ceremony, we still have many things to do before the instrument achieves its perfect condition. One of the most important, but difficult tasks is to reduce background scattering [2]. The most important measure for this purpose is to suppress high-energy neutrons and derived background by utilizing a so-called T0 chopper. We could perform the first on-line test in January 2010, half a year later than the starting of inelastic scattering measurements, and found that the powerful effect of the T0 chopper. Figure 5 shows time spectra measuring a vanadium sample with and without the T0 chopper rotating in 25 Hz. It shows that the background is dramatically decreased by the T0 chopper e.g. by a factor of 10^{-2}–10^{-3} at E_i ~ 300 meV. Unfortunately, however, the T0 chopper malfunctioned soon after this test measurement. It will be reinstalled on October 2010 after fixing the problem.

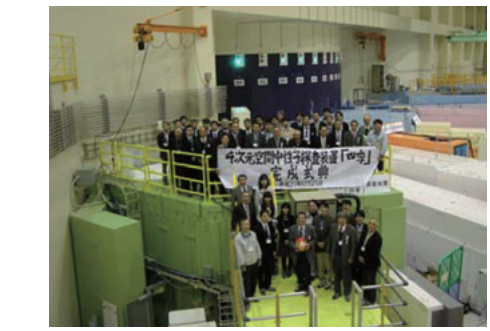

Fig.4 Completion ceremony.

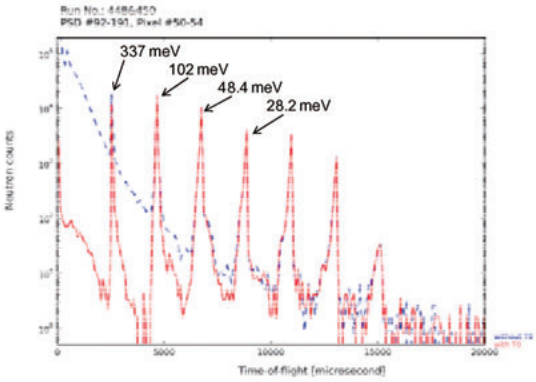

Fig.5 Time spectra measuring a vanadium sample with (solid line) and without (dashed line) the T0 chopper. The Fermi-chopper was rotated at 300 Hz [2].

To summarize, in fiscal 2008 and 2009, the construction of 4SEASONS progressed significantly. We started inelastic scattering experiments and succeeded in performing the multi-E_i measurements. Although there are still remaining issues such as suppressing background scattering, we are continuing further upgrading of the instrument. The construction of 4SEASONS is supported by Grant-in-Aid for Specially Promoted Research from MEXT (No.17001001) and is being conducted in collaboration with KEK and Tohoku University.

References

1) M. Nakamura et al., J. Phys. Soc. Jpn. **78** (2009) 093002.
2) R. Kajimoto et al., Proceedings of ICANS-XIX.

R. Kajimoto and M. Nakamura Materials and Life Science Division, J-PARC Center, Tokai, Ibaraki 319-1195

BL 02: The Si Crystal Analyzer Backscattering Spectrometer DNA at BL02 - Instrumental Specification and Construction Schedule -

A Si-crystal analyzer backscattering spectrometer DNA [1] is planned to be installed at the pulsed neutron source of the Material and Life Science Facility (MLF), J-PARC, and the construction was partially begun in the summer of 2010. It is a unique spectrometer to cover the area of the micro-eV energy range, among the several spectrometers which are installed or planned to be constructed at MLF.

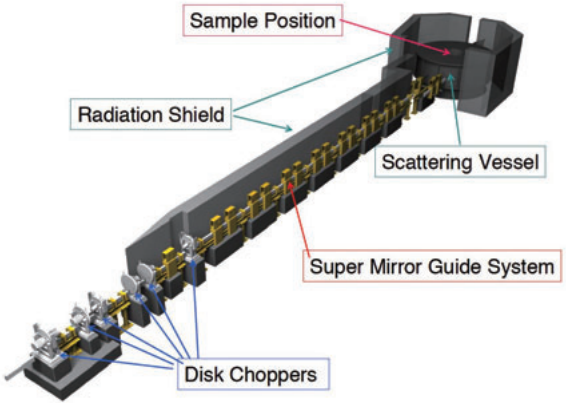

Fig.1 Overview of DNA Spectrometer

In order to determine the instrumental specifications of DNA the international advisory committee on DNA (IAC-DNA) has been held twice, in Feb. 2008 and in Nov. 2008 [2]. The IAC members are Dr. Dan Neumann: chairman (NIST, USA), Prof. Ferenc Mezei (ISSP, Hungary), Dr. Hannu Mutuka (ILL, France), Dr. Philip Tregenna-Piggott (PSI, Switzerland). The instrumental specifications proposed by DNA construction team were deeply discussed, and they were finally approved with minor revisions.

Fig.2 The advisory committee members and DNA construction team members at the MLF tour of the 1st IAC-DNA.

The instrumental specifications are shown in Table 1. It is designed to use the coupled moderator at MLF as a pulsed neutron source and to utilize a pulse shaping disc chopper, which has two counter rotating discs in the speed of up to 300 Hz, on the beam line setting near the bulk shield wall of the source. The pulse shaped neutron beam is guided to the sample position in the vacuum chamber by the super-mirror guide tube which is the parallel (partly ballistic-shaped at the pulse shaping chopper) curved shape with a radius of curvature: 2200 m in horizontal cross section. In the center of the vacuum chamber, a sample position is located at 42 m away form the coupled moderator. The analyzer banks of Si(111) and Si(311) single crystal wafers which are pasted on the spherical surface, are mounted at the right and left side each in the vacuum chamber. The Bragg angle of those analyzer crystals is about 87.5 deg on the average and the distance between the sample position and the analyzer crystal is about 2.3 m. The analyzed neutron beams are detected by the ^{3}He gas position sensitive detector located at around the sample position. The expected energy resolution and the dynamic range of the Si(111) crystal analyzer are about 1.2 micro-eV and from -25 to +45 micro-eV, respectively.

Table 1 Instrumental specifications of DNA

Items	Specification
Neutron source	Coupled Liquid H_2 Moderator (BL02)
L_1 (source-sample)	42 [m]
L_2 (sample-analyzer)	~ 2.3 [m]
L_3 (analyzer-detector)	~2.0 [m]
Crystal Analyzer	
Crystal and reflection index	Si(111) Si(311)
Bragg angle of analyzers	~87.5 [deg.]
Energy resolution	~1.2 [μeV]: Si(111) ~5 [μeV]: Si(311)
Momentum range	$0.07 < Q < 1.98$ [A^{-1}]: Si(111) $0.60 < Q < 3.80$ [A^{-1}]: Si(311)
Scan energy range	$-25 < E < 45$ [μeV]: Single pulse scan around E_f $-300 < E < 5100$ [μeV]: RRM scan in second frame

Fig.3 BL02 construction area in MLF No.1 experimental hall (on 28 July, 2010) .The blue stands are columns of the neutron guide system.

The construction of DNA will be completed in the middle of JFY2011, and then commissioning will be conducted for about six months.

The field of expected scientific research on the DNA spectrometer is very wide including the soft matter dynamics, the bio-molecular dynamics, the chemical molecular dynamics, the characterizations of the functional materials and the spin dynamics in the magnetism.

References

1) N. Takahashi, et al., Journal of Physics and Chemistry of Solids 68, 2199-2203(2007).
2) M. Arai, et al., JAEA-Review 2008-036 (2008): M. Arai, et al., JAEA-Review 2009-014 (2009)

K. Shibata[1)], N. Takahashi[1)], Y. Kawakita[1)], K. Nakajima[1)], W. Kambara[1)], M. Arai[1)], T.J. Sato[1),2)], H. Nakagawa[3)] and S. Fujiwara[3)]

[1)] MLF Division, J-PARC Center, Japan Atomic Energy Agency, Tokai, Ibaraki 319-1195, Japan
[2)] ISSP-NSL, University of Tokyo, Tokai, Ibaraki 319-1106, Japan
[3)] Neutron Materials Research Center, Quantum Beam Science Directorate, JAEA, Tokai, Ibaraki 319-1195, Japan

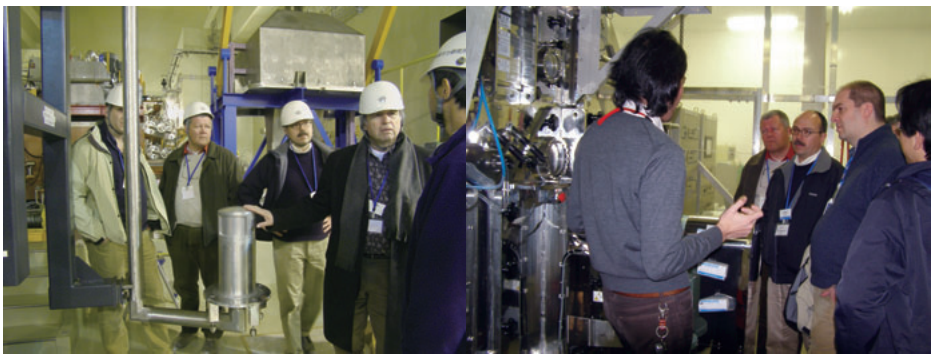

The DNA advisory committee members, D. Neumann (NIST), H. Mutka (ILL), F. Mezei (ESS Hungary), P. Tregenna-Piggott (PSI), visiting laboratories of neutron source (left) and of film deposition for optical devices (right).

BL 03: IBARAKI Biological Crystal Diffractometer iBIX

iBIX is located at BL03 in the 1st experimental room of MLF in J-PARC. A diffractometer room is shielded biologically, and contains detectors and a goniometer at the end of a guide tube. Data collection is controlled from an air-conditioned cabin on a mezzanine floor, which also contains the data acquisition electronics. Basic design requirements for iBIX were that 1 it should allow data collection from samples with a maximum unit cell dimension of 135 Å, that 2 it should allow data collection up to 1.2 Å biological macromolecules and 0.7 Å organic compounds resolution, and that 3 it should be possible to collect a full data set in three to four days for a crystal of 2 mm^3 in volume, and/or in about one month for a crystal of 0.1 mm^3 in volume of biological macromolecules[1].

To realize this performance, a coupled moderator intense neutrons, but a broad pulse in time resolution was selected. This is because biological neutron crystallography is an intensity limited technique and the pulse repetition rate of 25 Hz of J-PARC provides an advantage of a high resolution measurement in time, which compensates for the broad pulse shape of the coupled moderator. To retain the time resolution, iBIX has a flight path length of 40 m L1; distance between a neutron moderator and the sample. The beam divergence was designed to be less than 0.20° at the sample position by the combination of specially designed guide tubes composed of super-mirrors with different reflectivity, which have a total length of 25m, in order to meet the requirements of crystal cell dimensions and the observable minimum d-spacing[2].

iBIX detector system has to have a high spatial resolution less than around 1mm for each detector at a distance of 0.49 m L2 from the sample position, a smaller non-sensitive area that allows the detectors to cover a large solid angle subtended by a sample, higher counting rate, low γ-ray sensitivity and so on. In order to meet these conditions, iBIX adopted a new compact two-dimensional detector system with a short time-resolution composed of scintillator sheets of ZnS: Ag/$^{10}B_2O_3$ to convert Bragg reflections of thermal neutron into light and wavelength-shifting-fiber WLSF arrays in X-Y axes to receive the scintillation light two-dimensionally and to transmit to the light guide [3]. At present, 14 detector units, each with a 133 mm x 133 mm sensitive area, have been installed to make measurements more efficient Fig.1. The current parameters of the detectors are efficiency: 20 - 50%, spatial resolution: about 1 mm, counting rate: about 500 kcps, and γ/neutron ratio: 10^{-5}.

Data reduction software "STARGazer", modified from ISAW developed at Argonne National Laboratory, USA, is used [4]. STARGazer is composed of a data processing part and a data visualization part. In recent experiments, it has been demonstrated that "STARGazer" can be used to index a lysozyme crystal in tetragonal form, with a maximum cell edge of 80 Å.

Cryogenic equipment is available for blowing low temperature gas He 20 K - and N2 90 K - Fig.1 for low temperature data collection experiments. N_2 can be supplied from air by compressing it, so 90 K temperature is kept without using N_2 cylinders, and 20 K temperature is kept by changing a He cylinder.

Since the end of December 2008, iBIX has been available to users and several proteins and

Table 1 iBIX specifications.

Item	iBIX BL03
Moderator	Coupled H_2 para 100×100 mm^2
Measurement region in d-spacing	0.35 Å < d < 50 Å Maximum unit cell length~150 Å
Neutron wavelength and flux	0.5 Å < λ < 8 Å or more than that $7x10^7$ n/sec/cm^2 *1
Standard size of sample	1 mm^3, minimum 0.1 mm^3 when 1 MW
Special sample environment	He 20K-, N_2 90K-
Standard	0.5 days organic compounds
measurement time	3 days biological macromolecules*2
State of operating	Open use program was started in December 2008

*1 Estimation between 0.5 Å < λ < 3.9 Å when 1 MW
*2 When sample volume 2 mm^3, 30 detectors and 1 MW

organic compounds have been tested while the accelerator power was under 20kW. Diffraction data were obtained from organic compound sample crystals. One of them, ammonium hydrogen tartarate crystallized in heavy water and provided a full data set under cryo-conditions 110K. The crystal volume was 21.6 mm^3 and the unit cell parameters were a=7.65 Å, b=7.79 Å, c=11.04 Å in orthorhombic form, respectively. The exposure time was 12 hours per setting, and the total measurement time was 11 days at about 20 kW accelerator power. A 2*Fo-Fc* nuclear density map of a preliminary structure analysis of ammonium hydrogen tartarate is shown in Fig.2. Another organic compound, glutamic acid in α phase was also analyzed using a full data set collected on iBIX at room temperature. The crystal volume was 11.5 mm^3 and the unit cell parameters were a=7.07 Å, b=8.76 Å, c=10.28 Å in orthorhombic form, respectively. The exposure time was four hours per setting, and the total measurement time was about three days at about 120 kW accelerator power. The final R factor was 8.89 % for 1673 reflections with intensities greater than 4 σ after application of an extinction correction in GSAS General Structure Analysis System.

A full data set of an RNaseA protein crystal treated in heavy water has been collected at room temperature using iBIX. This protein will act as standard sample for neutron protein crystallography, and has already been thoroughly analyzed. The crystal volume was 4.7 mm^3 and the unit cell parameters were a=30.4 Å, b=38.6 Å, c=53.4 Å, β=105.8° in monoclinic form, respectively. The exposure time was five hours per setting, and the scheduled total measurement time was about 17 days at 120kW accelerator power. From these data, some diffraction spots of 1.4 Å in resolution could be observed after indexing.

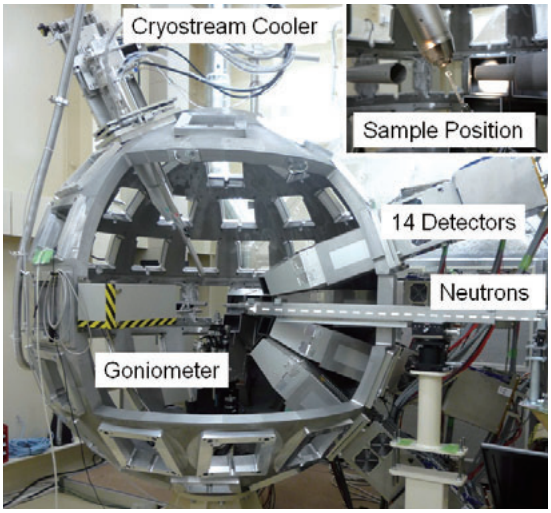

Fig.1 iBIX sample position with detectors and cryogenic equipment.

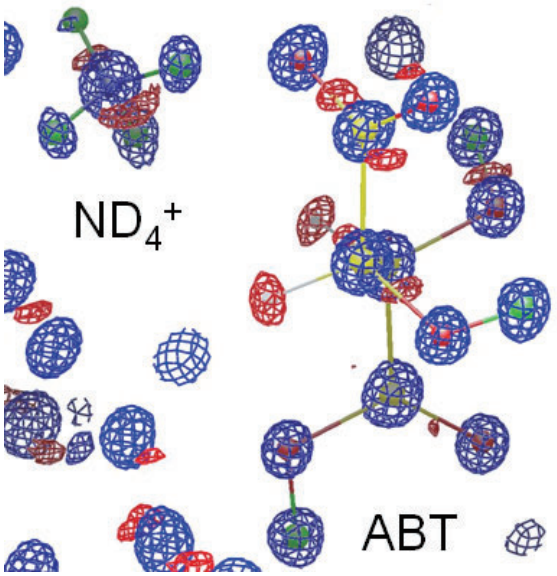

Fig.2 A 2*Fo-Fc* nuclear density map of ammonium hydrogen tartarate ammonium bitartrate; ABT and ammonium ion ND_4^+. Blue and red contours show 3σ and -3σ levels, respectively.

According to the preliminary results presented here, the performance of iBIX at 120kW accelerator power is very good. Because the planned final accelerator power at J-PARC is 1MW and the number of detectors will double in a couple of years, these results are very encouraging and suggest that we might expect nearly 20 times higher efficiency than the present one when the iBIX reaches its final conditions.

References

1) I. Tanaka, *et al.*, Nucl. Instr. Meth. A, **600** 2009 161.
2) K. Kusaka *et al.*, Physica B **385-386**, 2006 1062.
3) T. Hosoya *et al.*, Nucl. Instr. Meth. A, **600** 2009 217.
4) T. Ohhara *et al.*, Nucl. Instr. Meth. A, **600** 2009 195.

I. Tanaka[a], K. Kusaka[a], T. Hosoya[a], N. Niimura[a], T. Ohhara[b], K. Kurihara[b], T. Yamada[a], Y. Ohnishi[a], K. Tomoyori[a] and T. Yokoyama[a]

[a]Frontier Research Center for Applied Atomic Sciences, Ibaraki University, 162-1, Shirakata, Tokai, Ibaraki 319-1106, Japan,
[b]Quantum Beam Science Directorate, Japan Atomic Energy Agency (JAEA), 2-4, Shirakata-Shirane, Tokai, Ibaraki, 319-1195, Japan

BL 04: Status of BL04

Introduction

Accurate data of neutron-capture cross sections are important in detailed engineering designs and safety evaluations of innovative nuclear reactor systems. Especially, neutron-capture cross sections of minor actinides (MAs) and long-lived fission products (LLFPs) have attracted attention recently in the field of nuclear systems proposed for transmutation of radioactive waste and various innovative reactor systems proposed for the Generation-IV. However, accurate measurements of these cross sections are very difficult due to high specific radioactivity of these samples. Therefore, we have constructed an accurate neutron-nucleus reaction measurement instrument (ANNRI). The ANNRI is located on the Beam line No. 04 of the materials and life science experimental facility (MLF) in the Japan Proton Accelerator Research Complex (J-PARC). We have performed measurements of MAs and LLFPs and obtained preliminary neutron-capture cross sections.

Outline of the ANNRI

Fig. 1 shows side and top views of the ANNRI and Fig. 2 shows photographs of the ANNRI and a large Ge-detector array "4π Ge spectrometer". The neutron beam is provided to the experimental area 1 and 2 through a T0 chopper at L = 12 m, neutron filter at L = 13 m, and double disk chopper instruments at L = 14 m. Measurements of neutron capture cross sections are performed by using the "4π Ge spectrometer" set at L = 21.5 m and a NaI(Tl) spectrometer set at L = 27.9 m.

The "4π Ge spectrometer" is the main detector of the ANNRI and is located in the experimental area 1. The "4π Ge spectrometer" consists of two cluster -Ge detectors and eight coaxial Ge detectors with BGO-Compton-suppression shields. To reduce background, all detectors are surrounded by a shield made of borax-containing resin, lead, and iron. A ^{6}LiH shield is placed in front of each germanium detector to protect germanium crystals against damage caused by scattered neutrons. The peak efficiency of the "4π Ge spectrometer" is 3.6 ± 0.1 % for 1.33 MeV γ rays. A typical energy resolution is 9.8 keV at beam-on condition and 2.4 keV at beam-off condition in FWHM for 1.33 MeV γ rays [1].

In the ANNRI, there are five collimators between the moderator to the sample position of the "4π Ge spectrometer". The most downstream collimator in these five ones is called "rotary collimator" and defines the spatial distributions of the beams at the sample position of the "4π Ge spectrometer". The diameter of the neutron beam-holes of the "rotary collimator" is variable as 22 mm, 7 mm, and 3 mm.

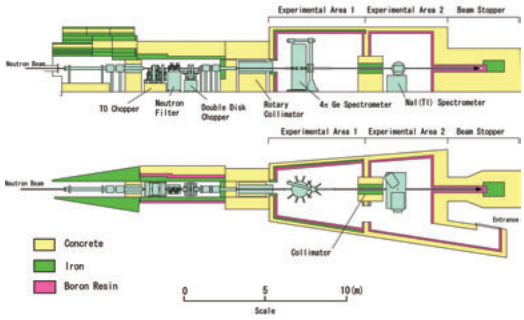

Fig.1 Side and top views of the ANNRI.

Fig.2 Photographs of the J-PARC/MLF/ANNRI (left), and "4π Ge spectrometer" (right).

Energy-integrated neutron intensities at the L=21.5 m sample position are 7.5×10^{5} n/s/cm^{2} in the neutron energy range of 1.5-25 meV, and 1.1×10^{5} n/s/cm^{2} in 0.9-1.1 keV at a proton energy of 3 GeV, an average beam power of 17.5 kW, and a repetition rate of 25 Hz. In future, these intensities are expected to be increased to 4.3×10^{7}, and 6.3×10^{6} n/s/cm^{2} at 1-MW operation [2]

A data acquisition (DAQ) system for the "4π Ge spectrometer" is required to deal with a large amount of signals from the spectrometer in a short time. In order to handle high event rates, a high performance DAQ system based on a digital data processing technique was developed.[3] The

data were measured with event-by-event mode (list mode) storing the information of γ-ray pulse height, TOF and time-interval between coincidence signals. The time resolution of the DAQ is 10 ns. The dead time of this system is only 3.3 μs per event at 50k events/s and the maximum event rate is more than 200k events/s.

The NaI(Tl) spectrometer is located in the experimental area 2 and provides data in high neutron-energy regions and supplemental data of the "4π Ge spectrometer". Fig. 3 shows a photograph of the NaI(Tl) spectrometer. The NaI(Tl) spectrometer is composed of two NaI(Tl) detectors. One NaI(Tl) detector has a size of 330 mm in diameter and 203 mm in length and is placed at 90 degrees with respect to the neutron beam. The other one has a size of 203 mm in diameter and 203 mm in length and is placed at 125 degrees. Both of the detectors have NaI(Tl) anti-Compton suppressors and shields against scattered neutrons and external γ rays.

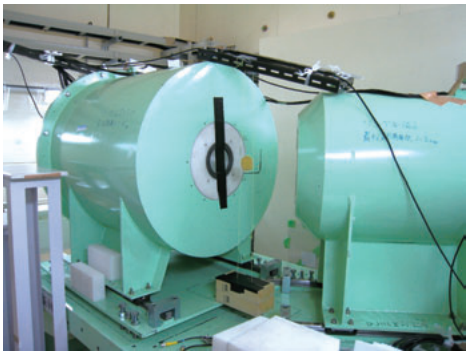

Fig.3 A photograph of the NaI(Tl) spectrometer.

An example of experiments

As an example of neutron-capture cross-section measurements, experiment of ^{244}Cm with the "4π Ge spectrometer" is shown in this report.

A ^{244}Cm sample was made of 0.6 mg curium oxide and its activity was 1.8 GBq. The ^{244}Cm sample was sealed in aluminum capsules 9 mm in outer-diameter and 0.5 mm thick walls. The isotopic abundances of curium oxide in the ^{244}Cm sample are 89.67 ± 1.78% of ^{244}Cm, 2.66 ± 0.34% of ^{245}Cm, and 7.08 ± 0.33% of ^{246}Cm. The measurement time for the ^{244}Cm sample was about 33 hours

Fig. 4 shows neutron-capture gamma-ray yields for the ^{244}Cm. In this experiment, neutron energies were calibrated with resonances in ^{197}Au (n, γ) reaction. Resonance peaks of ^{244}Cm are clearly observed at 7.67, 16.77, 22.85, 34.99, 96.12 eV.

This is the first experimental result of ^{244}Cm (n, γ) cross-section measurement performed with an accelerator facility in the world. The result also shows that neutron-capture cross sections can be measured using a small amount (less than 1 mg) of a high radioactive sample at the ANNRI.

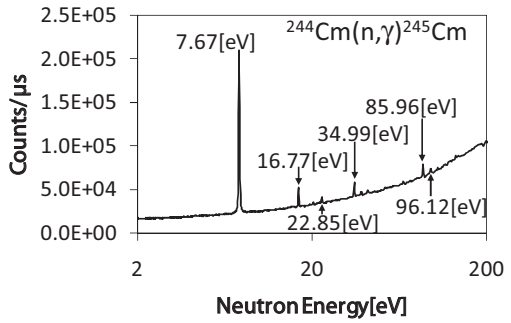

Fig.4 Neutron-capture γ-ray yields of the ^{244}Cm sample.

Summary

The new experimental instrument ANNRI including the "4π Ge spectrometer" and the NaI(Tl) spectrometer has been build at beamline No.4. Neutron-capture cross-section measurements have been started. In near future, the spectrometers will be used not only for nuclear data but also nuclear astrophysics and quantitative analysises.

Acknowledgements

Present study is the result of "Study on nuclear data by using a high intensity pulsed neutron source for advanced nuclear system" entrusted to Hokkaido University by the Ministry of Education, Culture, Sports, Science and Technology of Japan (MEXT).

References

1) T. Kin *et. al.*, the 2009 NSS-MIC Conf. Rec., **N24-2** (2009).
2) Y. Kiyanagi, *et. al.*, Conf. Rec. of the ND2010, 1303 (2010).
3) A. Kimura, *et. al.*, AIP Conference Proceedings, **769**, 784 (2005).

A. Kimura, T. Fujii[1], S. Fukutani[1], K. Furutaka, S. Goko[*], H. Harada, J. Hori[1], M. Igashira[2], T. Kamiyama[3], T. Katabuchi[2], T. Kin, K. Kino[3**], F. Kitatani, Y. Kiyanagi[3], M. Koizumi, M. Mizumoto[2], S. Nakamura, M. Ohta[***], M. Oshima, K. Takamiya[1] and Y. Toh

Energy Agency 2-4 Shirakata Shirane, Tokai, Naka, Ibaraki Japan
[1]Research Reactor Institute, Kyoto University
[2]Research Laboratory for Nuclear Reactors, Tokyo Institute of Technology
[3]Graduate School of Engineering, Hokkaido University
*Present address: Graduate School of Engineering, Hokkaido University
**Present address: High Energy Accelerator Research Organization
***Present address: Center of Atomic and Molecular Technology, Osaka University

BL 05: Neutron Optics and Physics (NOP)

A beamline "Neutron Optics and Physics (NOP)" facility is under construction at the port BL05 for the study of neutron optics and fundamental physics. The BL05 beamline views the coupled moderator. A shutter and a biological shield are in the regions of L = 2.3-4.3 m and L = 4.3-7.2 m, respectively, where L is the distance from the moderator. Supermirrors of m=2 with a cross section of 100 mm × 110 mm are installed in the shutter and biological shields are for transporting neutrons with a high divergence angle. A pre-position shield covers the region of L = 7.2-12m. The beam benders are installed in the void space inside the pre-position shield having height and width of 2 m and 1 m, respectively. The benders with the curvature radii of approximately 100m distribute cold neutrons into three beam branches: low-divergence beam branch, unpolarized beam branch and polarized beam branch. The interriors of beam benders are filled with helium gas. Fast neutrons are absorbed in the beam dump placed in the region of L = 12-16 m. The bent neutrons are transported into beam holes penetrating the beam dump and measuring approximately 15cm × 15cm. The configuration of the NOP beamline is shown in Fig.1.

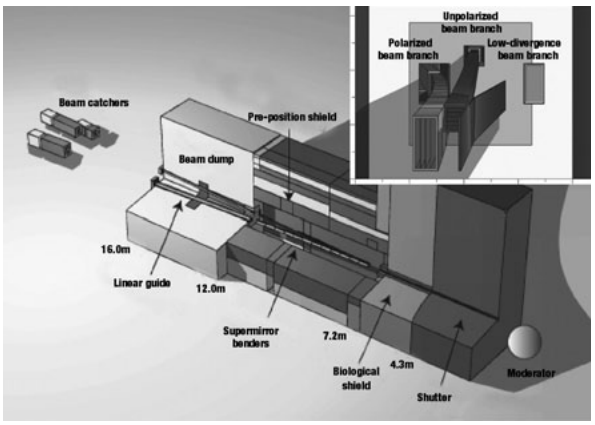

Fig. 1 Schematic view of the configuration of the NOP beamline for the study of neutron optics and fundamental physics at the beam port BL05.

The low-divergence beam branch is designed for multilayer neutron interferometry. Two supermirrors of m = 3 are installed to transport neutrons slower than 1.2×10^{3} m s^{-1} with the density of 1.8×10^{6} cm^{-2} μsr^{-1} s^{-1} MW^{-1}. The multilayer interferometer for the pulsed beam is under development. The beam branch is currently applied as the test port for the MIEZE-type spin echo and also for the study of specularity of the neutron reflection on the material surface.

Fig. 2 Installation of a spin flip chopper for the measurement of neutron lifetime at the polarized beam branch of the NOP beamline.

The polarized beam branch is designed for the study of the neutron decay. A multichannel magnetic supermirror bender with m = 2.8 is installed to provide polarized neutrons. The length of the bender is 4.5 m and the cross section is 10 cm×4 cm. The bent neutrons are designed to be transported by a m = 2 straight guide in the region of L = 12-16 m, which has not been installed yet. After the completion of the additional guide installation and alignment, the flux of 4.0×10^{8} cm^{-2} s^{-1} MW^{-1} and polarization of 99.8% can be obtained for the neutron energy of larger than 1.5 meV. Currently a measurement of the neutron lifetime is under development. We measure both incident neutrons and decayed electrons using a time projection chamber (TPC). To reduce the background events efficiently, we have developed a spin flip chopper (SFC). The Fig.2 shows the experimental setup at the beginning of the R&D phase of the SFC and TPC. The developed SFC and a prototype TPC are currently at the commissioning phase.

The unpolarized beam branch is designed as a versatile beam branch. A measurement of angular distribution of scattering cross section is planned for the search of new medium range interactions between neutrons and neutral atoms. A five channel supermirror bender is installed to bend neutrons upward with a curvature radius of 100 m. The length of the bender is 4 m and the cross section is 5 cm × 4cm. The bent neutrons are designed to be transported by a m = 2 straight guide in the region of L = 12-16 m, which has not been installed yet. A neutron flux of 1.2×10^{9} cm^{-2} s^{-1} MW^{-1} is expected after the completion of the additional guide installation and alignment. Currently, a principle-proof experiment of the time-focusing of ultracold neutrons (UCNs) is in preparation at the unpolarized beam branch. The time-focusing can be applied as an efficient transport of pulse UCN source, which is proposed for the measurement of neutron electric dipole moment at J-PARC. We have successfully produced ultra cold neutrons (UCN) for the principle-proof experiment. The very cold neutrons contained in the cold neutron beam are converted to UCN by the Doppler shift on the reflection of a moving mirror. The Doppler shifter is shown in Fig.3. It is designed to decelerate the v~140m/s neutrons to UCNs with the multilayer mirror, which has the m-value of m = 10.

Fig.3 Doppler shifter installed at the unpolarized beam branch of the NOP beamline for the study of neutron optics and fundamental physics at the beam port BL05. A moving multilayer mirror of m=10 is installed to convert very cold neutrons (v~140m/s) to ultracold neutrons by the Doppler shift.

References

1) K. Mishima et al., Nucl. Instrum. Methods Phys. Res. **A600** (2009) 342.

H. M. Shimizu, T. Ino, S. Muto, K. Mishima, T. Yoshioka, K. Taketani and Y. Arimoto

Neutron Science Division, High Energy Accelerator Research Organization (KEK), 1-1 Oho, Tsukuba, Ibaraki, 305-0801, Japan

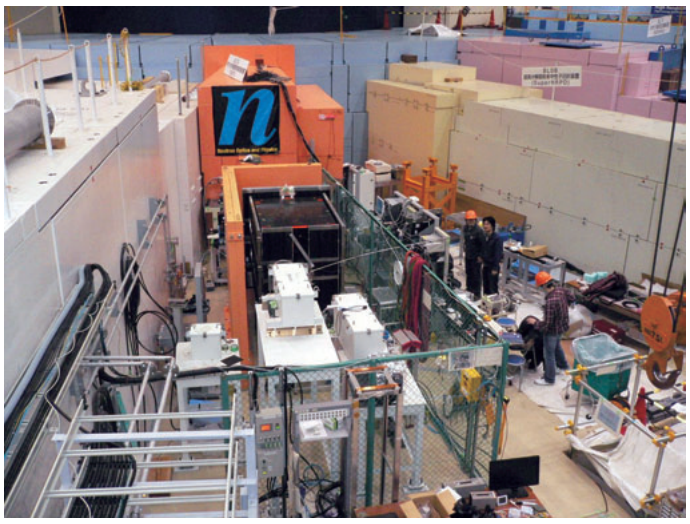

BL05 NOP under commissioning.

BL 08: Status of SuperHRPD

The repetition rate of 25 Hz lower than that of ISIS TS-I and SNS is advantageous for neutron powder diffractometers (NPD) at J-PARC where a wide dynamical range is attainable with limited loss of neutrons. To widen further the wavelength range of SuperHRPD, the super high resolution powder diffractometer at BL08, the flight path should be shorter than 100 m, which requires development of a high resolution moderator [1]. The high resolution moderator is also requested to satisfy, for accurate crystal structure analyses, the symmetrical pulses with less tails.

We have chosen a decoupled poisoned hydrogen moderator; hydrogen moderator is better than water moderator in the energy region lower than 100 meV because narrow and symmetrical pulse region (slowing down region) extends to longer wavelength range. Demands on S/N above 100 meV to be better than 1.5-2 order lead to the preferred decoupling energy of 1 eV with AIC [1, 2, 3]. As for the poisoning material, on the other hand, the choice of Cd results in the shift of symmetrical region to the shorter wavelength region, and narrower and more symmetrical Δt at $\lambda > 1$ Å will be attained by selecting 20 mm depth on average (25mm at the deepest). Although poisoning energy is larger in Cd, peak intensity is not so different. Compared with decoupled non-poisoned moderator, integrated intensity decreases by 2/3 ($\lambda = 1$ Å) to 1/4 ($\lambda = 8$ Å), but peak intensity does not so decrease: 4/5 (1 Å) to 1/2 (8 Å). Detailed comparison between designed performance and experimental results is being examined.

SuperHRPD consists of tapered iron collimators in biological shields, 82.6 m guide tube with m = 3 starting at 7.145 m, disk choppers, beamline monitors, slits, a sample chamber with the sample position at 94.2 m, detectors, various neutron shields and beamstop. To install this long flight path instrument, the construction of a beamline building with 4 m (H) x 3 m (W) x 50 m (L) and a SuperHRPD experimental hall with 7 m (H) x 10 m (W) x 13 m (L) were started in July and completed by the end of December, 2007.

The design, installation and alignment of the guide tube system were carefully executed because of an expected ground settlement and earthquake. It is noted elliptical guide was examined but not adopted because the unequal sinking might deteriorate neutron transmission.

The guide tube is composed of a 31.245 m curved guide part (5.55m, 1.695m plus 32.0 m with 0.11 m gap for the second disk chopper at 12.75 m) with a cross section of 25 mm (W) x 75 mm (H), and 51.4 m straight guide part with a cross section of 25 mm (W) x 55 mm (H) between the instrument and the moderator. The radius of curvature of the curved part is 5 km. Here, the guide tube cross sections are different to minimize the effect of unequal subsidence of the MLF main building and that of the beamline building: with the present guide tube design, 10 % loss of intensity at most by the 1 cm difference in height due to subsidence [4]. We also envisioned that unequal floor sinking might complicate the guide-tube re-alignment. Then we minimized the number of pedestals connecting guide tubes and the floor; three units of guide tubes (typically one unit is 2 m) were located inside a metal jacket of 6 m length, which is placed on a long steel rail. The rail is connected to the floor with small number of pedestals. In principle, we only have to adjust four pedestals in 80 m guide tube when conducting re-alignment.

Two disk choppers were planned to prevent frame overlap and to utilize a wide wavelength; one is a single disk at 7.1 m with an opening angle of 26.5°, and the other one is a counter-rotating double disk chopper at 12.75 m with 47°.

We proceeded with the construction project of SuperHRPD in two phases in order to accept neutron beam and start the general user program as early as possible. In the "Phase-I", we concentrated on beamline components including guide tubes, shielding, choppers, *etc.* and started up quickly by using the existing *Sirius* chamber and detectors. In the "Phase-II", after the careful R&D studies on windows and chamber designing, we constructed a new SuperHRPD chamber and replaced the *Sirius* chamber with

the new one in summer of 2009. In the later stage, we will install high-resolution detectors. The installation of guide tube, all the shielding and the re-cycled Sirius chamber was ended just before the first neutron production on May 30th, 2008.

Fig.1 The east building for BL08 (SuperHRPD).

The first powder diffraction pattern of an iron steel block (both α-Fe and γ-Fe is included, the specimen is kindly supplied by Y. Tomota) was recorded on May 31st with 500 shots of neutrons (0.2kW, 25 min.).

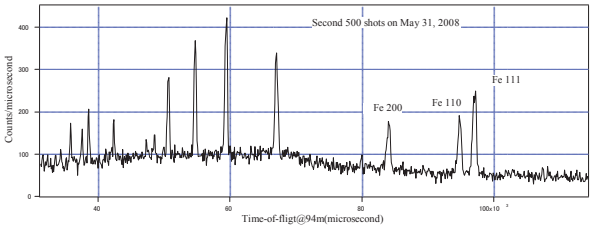

Fig.2 The first diffraction pattern of J-PARC/MLF: iron steel block.

On June 21st, 2008, we succeeded in achieving the best resolution among all the neutron powder diffractometers in the world, and a part of detector had achieved $\Delta d/d$ = 0.035 %. Fig.3 shows a comparison of two Bragg peaks measured by SuperHRPD and the *Sirius* diffractometer at KENS; the FWHM shows a threefold improvement in SuperHRPD and the tails of the Bragg peaks observed in *Sirius* were not observed in SuperHRPD, resulting in a 10-fold improvement in the 1/10-width with very symmetrical peak profile. This success was achieved by the long-term R&D work for the high resolution decoupled poisoned moderator by the moderator group to attain the desired resolution within the 100 m flight path. This characteristic is very effective for both precise crystal structure analyses of complicated materials with large unit cells and the detection of tiny structural distortions. It is emphasized that development of the high resolution moderator with less tails in profile is successful.

We measured some sealed standard samples filled with powder to check the "time focusing" procedure, as well as to verify the capability of SuperHRPD as a high-resolution powder diffractometer. In Fig. 4, the diffraction pattern of Si powder (NIST SRM 640c) and its Rietveld analysis result with Z-Rietveld [5] is shown. Z-Rietveld is a Rietveld analysis software and one of the powder diffraction data analysis software suit, Z-Code, which had been developed by our group. As a result, an excellent fitting was obtained, and the chi-square value of the fitting was as low as 1.29.

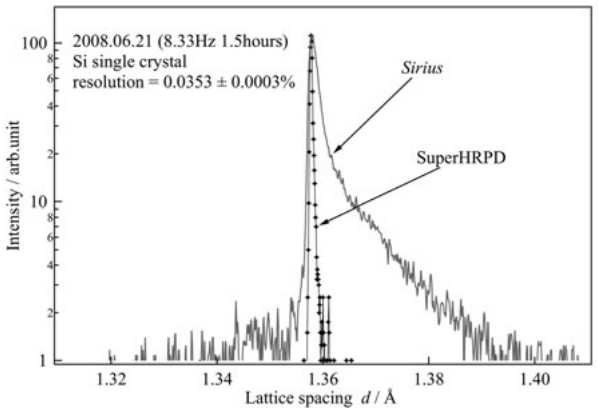

Fig.3 Si (400) reflection peak measured by SuperHRPD. For accurate crystal structure analyses, the symmetrical pulses with less tails are quite important

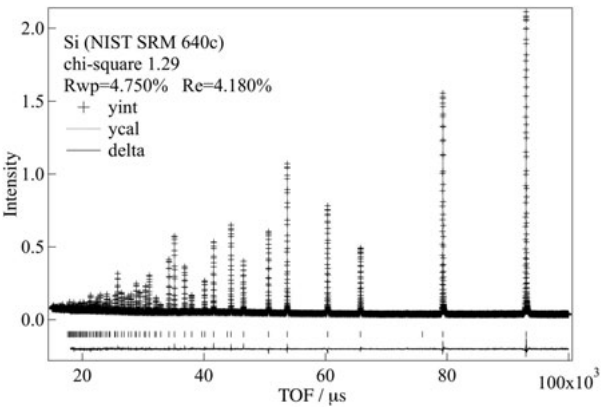

Fig.4 Rietveld analysis result of Si powder using Z-Code.

In the "Phase-II" started in the summer of 2009, we installed a new SuperHRPD chamber (Fig. 5). The new chamber was developed so as to improve *S/N* and to achieve better resolution as well as intensity. It was manufactured by a small and medium-sized enterprise group, JSS (the J-PARC Support Study Group), in Ibaraki Prefecture. The new chamber consists of a vacuum sample chamber with capacity of about 1 m^3, and gas-filled scattering banks around it. In the design concept of a new chamber, the detector solid angle was increased, d-range / *Q*-range was expanded, and also choices of high-intensity mode and high-resolution mode were implemented by varying incident collimations. To cover this large detector solid angle, about 1500 one-dimensional ^{3}He position-sensitive detectors (PSDs) of 1/2 inch in diameter can be installed in the backward bank, 90 degrees bank, and low-angle bank; at present, 320, 192 and 192 PSD(s) are installed, respectively. In future, high resolution detector will replace parts of detectors in the backward bank. The 'on-beam commissioning' of all detectors at the new SuperHRPD was completed in autumn 2009, and the general user program restarted with this new chamber.

Fig. 5 A new SuperHRPD chamber was installed in summer of 2009.

Although we are still using old PSDs with the 1cm pixel size, it is worth evaluating the present resolution in the high-resolution mode with the diamond powder sample. Fig. 6 shows a detector range dependence of the resolution. It was shown that the resolution $\Delta d/d$ better than 0.06 % was realizable by limiting the detector range as well as using sample holder of diameter 3 mm.

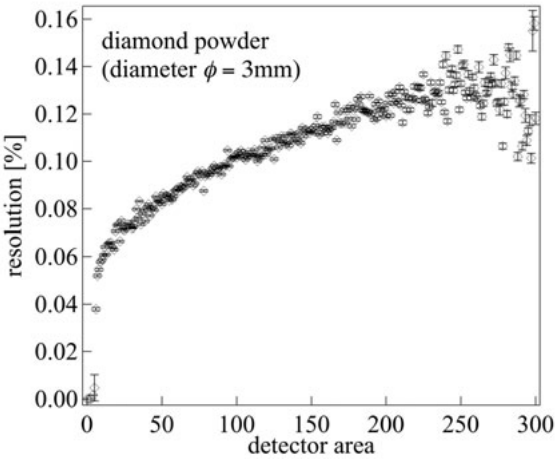

Fig.6 A detector range dependency of the resolution.

References

1) T. Kamiyama and K. Oikawa, "Two Powder Diffractometers at J-PARC", Proc. of ICANS-XVI, Deusseldorf-Neuss, Germany, May 12-15 (2003) 309-314.
2) M. Harada, M. Teshigawara, N. Watanabe, T. Kai and Y. Ikeda, "Optimization of Poisoned and Unpoisoned Decoupled Moderators in JSNS", Proc. ICANS-XVI. **2** (2003) 697-706.
3) M. Harada, S. Saito, M. Teshigawara, M. Kawai, K. Kikuchi, N. Watanabe, Y. Ikeda, "Silver-Indium-Cadmium Decoupler and Liner", Proc. ICANS-XVI. **2** (2003) 677-687.
4) K. Oikawa, F. Maekawa, M. Tamura, M. Harada,T. Kato, Y. Ikeda, K. Niita, "Preliminary investigation on the satellite building of MLF; beamline shielding analysis", Proc. of ICANS-XVII, **1** (2006) 139-145.
5) R. Oishi *et al.*, "Rietveld analysis software for J-PARC", Nucl. Instr. and Meth., **600(1)** (2009) 94-96.

S. Torii, J. Zhang, T. Panca, M. Ping, [1]T. Muroya, M. Yonemura, [2]R. Tomiyasu, [3]Y. Noda and T. Kamiyama

High Energy Accelerator Research Organization, Tokai Campus, Tokai, Ibaraki 319-1106

[1]Nippon Advanced Technology Corporation

[2]High Energy Accelerator Research Organization, Tsukuba Campus, Tsukuba, Ibaraki 305-0801

[3]Institute of Multidisciplinary Research for Advanced Materials, Tohoku University, Sendai 980-8577

BL 10: NOBORU

Overview of NOBORU

The NOBORU, "NeutrOn Beamline for Observation and Research Use" [1, 2] was the first neutron instrument in MLF/J-PARC completed in 2007. NOBORU has been constructed and managed by the Neutron Source Section of MLF Division, which also constructed the neutron source JSNS. Hence the prime mission of NOBORU is to study neutronic performance of JSNS. The NOBORU has another aspect to be served as a test beam port for R&D activities of innovative devices, for testing new ideas of future instruments at MLF, etc. Overview and specifications of NOBORU are illustrated in Fig. 1. Note that the instrument was named in deference to Prof. Noboru Watanabe for his great contributions in the construction of JSNS.

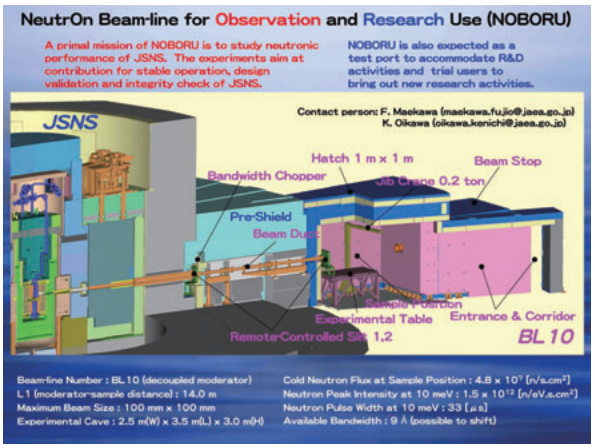

Fig.1 Overview and specifications of NOBORU.

Observation of the First Neutron Pulse on Day-1

NOBORU was accorded the honor of receiving the first pulsed neutron generated at MLF. To surely catch the first pulsed neutrons, the current mode time-of-flight (C-TOF) detector system [3] that was composed of a ^{6}Li-glass scintillation detector coupled with a photomultiplier tube and a digital oscilloscope for data taking was arranged.

After confirming proper proton beam transport from the 3 GeV RCS to JSNS, a neutron beam shutter of NOBORU was opened, and a 3 GeV proton beam containing 4x10^{11} protons was injected to the mercury target at 14:25 on 30th of May 2008. Soon after that, a TOF spectrum appeared on the display of the oscilloscope as shown in Fig. 2. Accordingly, the first memorial neutron pulse by the spallation reaction at JSNS was confirmed successfully. [4-6]

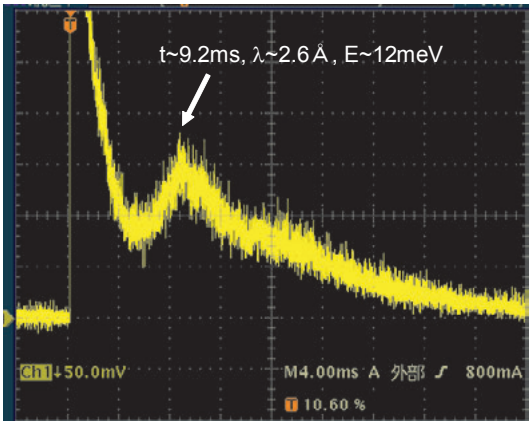

Fig.2 The time-of-flight spectrum for the first pulsed neutrons in J-PARC.

Neutron Source Characterization

Since the production of the first pulsed neutrons, we have made an effort to characterize the neutronic performance of JSNS by measuring the neutron beam with several experimental techniques. The TOF method with a calibrated ^{3}He detector and the gold foil activation method were employed for the flux intensity measurement. Figure 3 compares the measured and calculated neutron spectral intensities that show very good agreement between them. While considering also the gold foil measurement, we confirmed that the measured neutron flux intensities below 0.4 eV agreed within ±20% with the calculated values. [4-6]

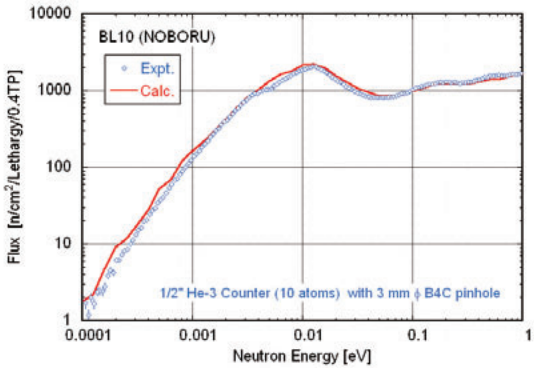

Fig.3 Comparison of measured and calculated absolute neutron spectral intensity.

Figure 4 compares neutron pulse shapes measured at the JSNS's hydrogen decoupled moderator (DM) and the KENS/KEK's methane DM. In the energy region below 10 meV, it is clearly observed that pulse tails of the JSNS's hydrogen moderator are much shorter than those of the KENS's methane moderator. This suitable feature is attributed to the small cross-section of the para-hydrogen below ~10meV and the advanced design for JSNS's DM.

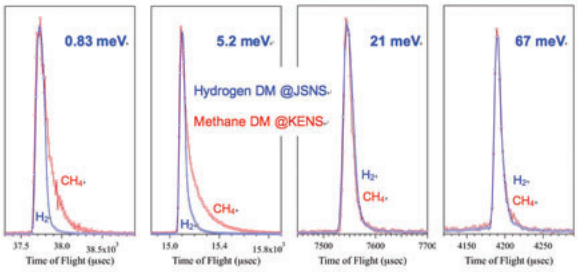

Fig.4 Neutron pulse shapes at JSNS's hydrogen DM and KENS/KEK's methane DM in the linear scale.

Test Port Use with Some Topics

As project use and general use of NOBORU, a variety of experiments were conducted in JFY 2008 and 2009: (i) R&D on energy-selective imaging, (ii) R&D on neutron detectors and optical devices, (iii) prompt gamma-ray analysis with TOF, (iv) neutron diffraction experiment under high magnetic fields, (v) demonstration experiment of MIEZE-type spin echo technique, (vi) study on single event upset in semiconductor devices, (vii) establishment of a calibration field with high-energy neutrons, etc. Two highlights are exhibited here.

High magnetic field Instruments for NeuTron Scattering (HINTS) have been developed by Prof. H. Nojiri of Tohoku Univ. [7]. Neutron diffraction at 40 Tesla was already achieved by the group as shown in Fig. 5. The system is now ready for determination of the magnetic structure of various compounds in high magnetic fields.

As one of applications of the energy-selective imaging, demonstration experiments for the resonance absorption imaging were conducted. As shown in Fig. 6, images of gold and indium samples were obtained by a 2-D Li-glass scintillation detector at TOF of 455 and 835 s, respectively, when the materials have large resonance peaks at the corresponding energies. This technique enables us to see through object with distinguishing materials inside.

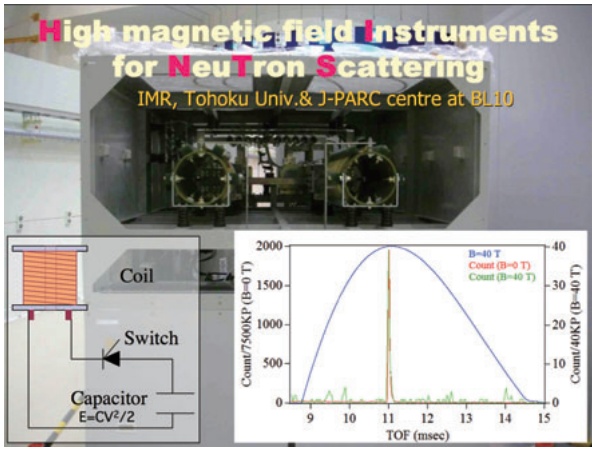

Fig.5 High magnetic field instruments "HINTS". (Photo of the 250 kJ capacitor bank, electric circuit and the pulsed magnetic field up to 40 T in coincident with a diffraction peak of a sample.)

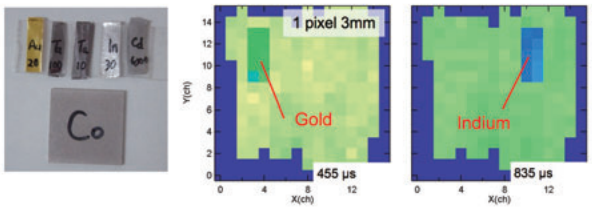

Fig.6 Example of 2-D images obtained with the resonance absorption imaging technique.

References

1) K. Oikawa, et al., Nucl. Instr. Meth., A 589 (2008) 310.
2) F. Maekawa, Nucl. Instr. Meth., A 600 (2009) 335.
3) S. Meigo, et al., J. Nucl. Sci. Technol., Supplement 1 (2000) 789.
4) M. Arai and F. Maekawa, Nucl. Phys. News, 19 (2009) 34.
5) F. Maekawa, et al., Nucl. Instr. Meth. A 620 (2010) 159.
6) F. Maekawa, et al., "Distinctive Features in Neutronic Performance of JSNS", Proc. of ICANS XIX, 19th meeting on Collaboration of Advanced Neutron Sources, March 8-12, 2010 Grindelwald, Switzerland, to be published.
7) H. Nojiri, et al., High Magnetic Field Spin Science News No.11, http://spin100.imr. tohoku.ac.jp/.

F. Maekawa and K. Oikawa Neutron Source Section, MLF Division, J-PARC Center

BL 11: High Pressure Neutron Diffractometer (PLANET)

The high-pressure science community in Japan has started the construction of the powder diffractometer dedicated to high-pressure experiments (PLANET) on BL-11 at MLF/J-PARC. The beamline realizes the measurement of diffraction and radiography for powder and liquid/glass samples at high pressures up to 20 GPa and 2000 K. The beamline aims to study crystal structure of hydrogen-bearing materials including hydrous minerals of the Earth's deep interior and structure of magma and light element liquids. For this purpose, our beamline is suited for *in-situ* measurements of neutron diffraction not only at high pressure but also at high temperature with stable and uniform heating condition. In order to achieve our goal, the beamline has two characteristics: One is the installation of a large-sized hydraulic press [1] and the other is using focusing guides [2,3].

The performance for the instrument required by users varies according to their research fields such as earth and space science, material science, and high-pressure physics and chemistry. Therefore, the instrumental design should incorporate wide Q range and have the flexibility for intensity-resolution optimization to improve versatility and efficiency in structure analysis of crystal and liquid at high pressure. Instrumental design was optimized based on the following concepts: (i) coverage of d-spacing from 0.2 Å to 4 Å in the first frame, (ii) worst acceptable instrumental resolution of 0.5% in $\Delta d/d$ at 90° bank; (iii) effective focus of neutrons with wavelengths less than 1 Å using a non-parallel guide, (iv) trade of resolution for intensity using slits and replaceable focusing devices.

Figure 1 shows the design of the instrument. The instrument views a decoupled liquid H_2 moderator with a cross section of 100 × 100 mm^2. The primary and secondary fight paths are 25 m and 1.5 m, respectively. The 11.5-m-long guide with elliptical shape starts at a distance of 11.5 m from the moderator. The guide has a rectangular cross-section and consists of four walls coated with material. Sample is placed at 2 m from the guide exit. The 90° detectors will be installed at 1.5 m from the sample position. Bandwidth of $\Delta\lambda$=5.8 Å is available using 25-Hz pulsed source. This allows diffraction data to be collected for d-spicing up to 4.1 Å. Accessible maximum Q value is 30 Å-1 using T0 chopper with 50 Hz drive.

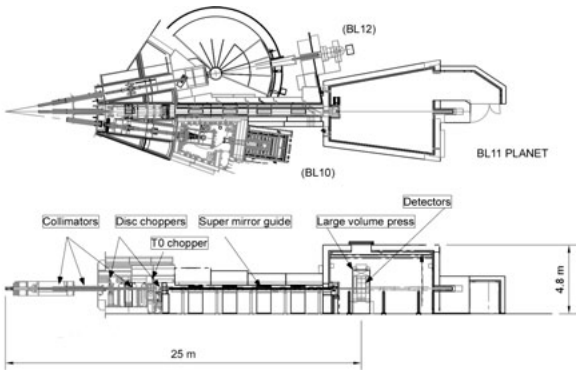

Fig.1 Layout of High Pressure Neutron Diffractometer (PLANET) on BL-11.

Figure 2 shows the geometry of a multi anvil press. For the powder diffraction measurements using multi-anvil press, an incident neutron beam passes through the vertical anvil gaps and irradiates the sample in the pressure medium. Diffracted neutrons go through the other anvil gaps at a 90° angle. Accordingly, 90° detectors are well compatible with a multi-anvil press. We are planning to install pinhole collimator and/or compact focusing device near the sample in order to produce a beam spot below the sample size of a few square millimeters. In addition, radial collimators will be placed between the sample and the detectors to restrict the field of view of the detectors to the sample volume and eliminate background scattering from thesurrounding materials right next to the sample.

Figure 3 shows the simulated incident neutron fluxes on the sample position in several configurations. Here, widths of the slit at guide exit in high-resolution mode and high-intensity mode are 5 mm and 21 mm, respectively. In the first frame (0.3-5.8 Å), the incident neutron fluxes are 9.6×10^7 n/s/cm^2 in high-intensity mode and 2.0×10^7 n/s/cm^2 in high-resolution mode when the neutron source operates at 1 MW. The high resolution mode achieves resolution 0.3%

in Δd/d. In the high intensity mode, resolution calculated from a simulated profile is 0.5% in Δd/d. Specification beamline parameters are summarized in Table 1.

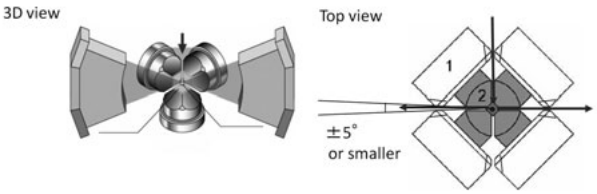

Fig.2 Geometry of a multi anvil press.

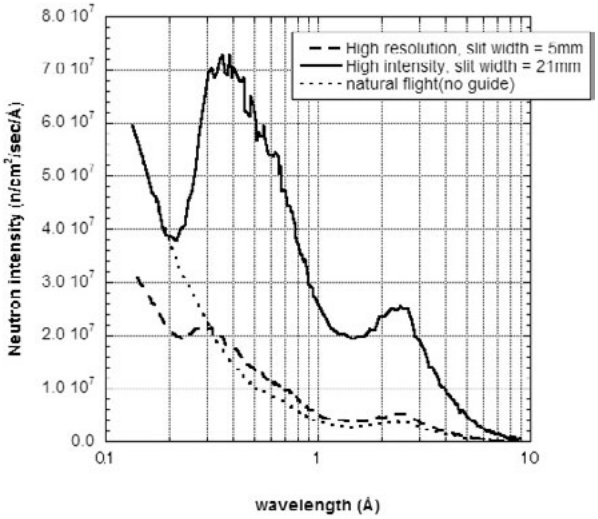

Fig.3 The incident neutron fluxes on the sample position in several configurations.

Table 1 Specification parameters

Moderator	Liquid H_2 decoupled (BL11)
Flight Path	
Source to Sample (L_1)	25 m
Sample to Detector (L_2)	1.5 m
Wavelength Range	0.29-5.76 Å
Detectors	^{3}He PSD
Angular Coverage	Horizontal ±11°, vertical ±35°
Resolution at 90°	$\Delta d/d < 0.005$

The highlight of this beamline is developing original high-pressure devices. The design of the high-pressure devices is proceeding in two categories. The first is the large-sized hydraulic press which can apply forces of 1500 tons to the sample. Such presses have produced many successful results on high-temperature experiments at synchrotron facilities. It has an advantage for stable high-pressure (up to 20 GPa) and high-temperature (up to 2000K) generation. The second is a new opposed-anvil cell with nano-polycrystalline diamond (NPD) [4], which is intend to generate pressures of more than 50 GPa for sample with volume of 1 mm^3.

The construction of this beamline is in progress and we are planning to start its commissioning from the spring season of 2011.
This project is made by the supports of Grant-in-Aid for Creative Scientific Research (19GS0205) from the Japan Society for Promotion of Science and Grant-in-Aid for Scientific Research on Innovative Areas (No. 20103001) from the Ministry of Education, Culture, Sports, Science and Technology (MEXT) of Japan.

References

1) W. Utsumi, H. Kagi, K. Komatsu, H. Arima, T. Nagai, T. Okuchi, T. Kamiyama, Y. Uwatoko, K. Matsubayashi and T. Yagi, Nucl. Instr. and Meth. A, **600** (2009) 50.
2) H. Arima, K. Komatsu, K. Ikeda, K. Hirota and H. Kagi, Nucl. Instr. and Meth. A, **600** (2009) 71.
3) H. Arima, T. Hattori, K. Komatsu, J. Abe, W. Utsumi, H. Kagi, A. Suzuki, K. Suzuya, T. Kamiyama, M. Arai and T. Yagi: J. Phys.: Conf. Ser., **215** (2010) 012025.
4) T. Okuchi, S. Sasaki, T. Osakabe, Y. Ohno, S. Odake and H. Kagi: J. Phys.: Conf. Ser., **215** (2010) 012188.

T. Hattori[1,2], H. Arima[2], A. Sano[1,2], W. Utsumi[1,2], H. Kagi[1,3] and T. Yagi[4]
[1] Quantum Beam Science Directorate, JAEA, Tokai, Ibaraki, 319-1195, Japan
[2] J-PARC Center, JAEA, Tokai, Ibaraki, 319-1195, Japan
[3] Graduate School of Science, The University of Tokyo, Tokyo, 113-0033, Japan
[4] The Institute of Solid State Physics, The University of Tokyo, Chiba, 277-8581, Japan

BL 12: Construction of High Resolution Chopper Spectrometer

High Resolution Chopper Spectrometer (HRC) was installed at the 12th beam line (BL12) at Material and Life Science Facility (MLF), J-PARC, for a wide range of dynamic studies of materials with high resolution and with relatively high energy neutrons. Originally, HRC was proposed as a project of High Energy Accelerator Research Organization (KEK). Also, Versatile Inelastic Neutron Spectrometer (VINS) was proposed by the University of Tokyo. KEK started the construction of HRC at BL12 with a small budget in 2004. Some parts were manufactured, but they could not be installed at J-PARC and just were stored at the Tsukuba campus of KEK. The construction of VINS at BL23 was approved by the committee of the instrumentation at J-PARC, but, it was not funded. In 2008, both institutes proposed to merge these projects to construct one chopper spectrometer, and the budget was concentrated to complete HRC at BL12, as a joint project between KEK and the University of Tokyo. KEK mainly built the shielding and the vacuum scattering chamber, the University of Tokyo mainly prepared the position sensitive He-3 detectors, as shown in Fig. 1. Devices such as a Fermi chopper, a T0 chopper, a guide tube, detector electronics, a cabin and a deck were also installed or delivered by the end of March 2010. It is possible to install detectors from -31° to 124° of scattering angles, but, owing to the recent situation of the limited supply of He-3 gas, the detectors were installed at the limited scattering angles from -10° to 40°, which corresponds to only 30% of the whole detector area. HRC was almost completed, except for the partial installation of the detectors. KEK and the University of Tokyo executed the announcement ceremony of the completion of the construction of HRC on 26 March 2010 (see Fig. 2).

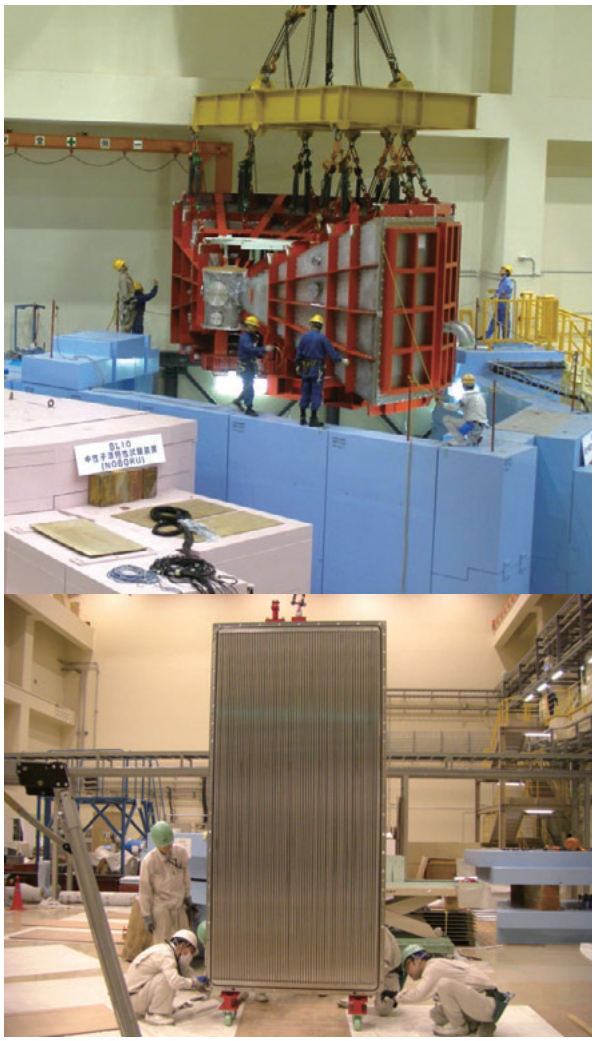

Fig.1 Construction of HRC. Upper: the shielding and the vacuum scattering chamber. Lower: an array of 64 pieces of the position sensitive He-3 detectors.

Fig.2 The announcement ceremony of the completion of the construction of HRC.

S. Itoh, T. Yokoo, S. Satoh, S. Yano* and T. J. Sato**
Neutron Science Division, Institute of Materials Structure Science, High Energy Accelerator Research Organization, Tsukuba, 305-0801
*College of Science and Engineering, Aoyama Gakuin University, Sagamihara, 252-5258
**Neutron Science Laboratory, Institute for Solid State Physics, The University of Tokyo, Tokai, 319-1106

BL 14: AMATERAS

AMATERAS is a cold-neutron disk-chopper spectrometer in the Materials and Life Science Experimental Facility (MLF) in J-PARC. By combination of high-peak intensity from a H_2-coupled moderator source and newly developed high-speed disk-choppers (the maximum revolution: 350Hz, the minimum burst time: 7.6 μsec.) for pulse shaping and monochromating, the spectrometer realizes both high-resolution ($\Delta E/E_i$<1%) and high-intensity (one order of magnitude higher than the present state-of-the-art chopper spectrometers) in the range of E_i = 1~20 meV, and can show sufficient performance up to E_i < 80 meV. [1, 2] Characteristic parameters are listed in Table 1.

AMATERAS was funded as a three-year term project of JAEA, which has been started from 2006 and construction of main part has been completed in spring of 2009. Shielding, a full set of disk-choppers (including three sets of fast disk choppers and two slow disk-choppers), DAQ electronics and 32 tubes of position sensitive detectors (number of detectors was increased up to 266 in the summer of 2009), a scattering chamber, a beam transport (neutron guide system) and related auxiliary systems were installed by then. At RUN#23/24, on 27 May, 2009, the first neutron beam was delivered to AMATERAS (Fig. 1).

Soon after that, we started the commissioning work on AMATERAS. In the course of the commissioning, we have measured the tunneling excitations in powder sample of γ-Picoline-N-Oxide. The excitations in low energy region ΔE < 240 μeV were clearly observed. Also, we have confirmed the $\Delta E/E_i$ ~ 1% resolution in the range of $E_i \leq 3$ meV in the same experiment.

Table 1 Characteristic parameters of AMATERAS.

Moderator	Coupled H_2 (BL14)
Flight Path	$L_{modrator\text{-}sample}$=30 m $L_{sample\text{-}detector}$=4 m
Incident Energy	1~80 meV (at its best @ 1~20 meV)
Energy Resolution	$\Delta E/E_i \geq 1\%$ @ E_i=20 meV
Scattering Angle	Horizontal: -5°~+112°(-40°~+140° when detectors are fully installed.) Vertical: -16°~ 22°
Fast Disk-Choppers	Radius: R=300 mm (center-to-center of slit) Revolution: $f \leq$350 Hzf No. 1 ($L_{modrator\text{-}chopper}$=7.1 m) 2 disks (Counter-Rotating) Slit width: 30 mm No. 2 ($L_{modrator\text{-}chopper}$=28.4 m) 2 disks (Counter-Rotating) Slit width: 10 & 30 mm No. 3 ($L_{modrator\text{-}chopper}$=14.2 m) 1 disk Slit width: 30 mm
Slow Disk-Choppers	Radius: R=300 mm Revolution: f=12.5 & 25 Hz Opening angle 0~175° (variable) $L_{modrator\text{-}chopper}$=9 m & 13.7 m
Beam Transport	$3Q_c$ & $3.8Q_c$ Curved Section: L=19.6 m, R=2 km
Detector System	^{3}He 1D-PSD 266 tubes (448 tubes at the full installation) ϕ=1 inch, L=3 m, p=10 atm

Problems also have been found in the commissioning. The most serious problem is in the neutron flux. We have measured the flux by activation measurements of Au foil and flux measurements by using a C-TOF and a standard ^{3}He-monitor. We have found that the flux at the sample position is 1/3 that of expected value. We have investigated the source of the problem and

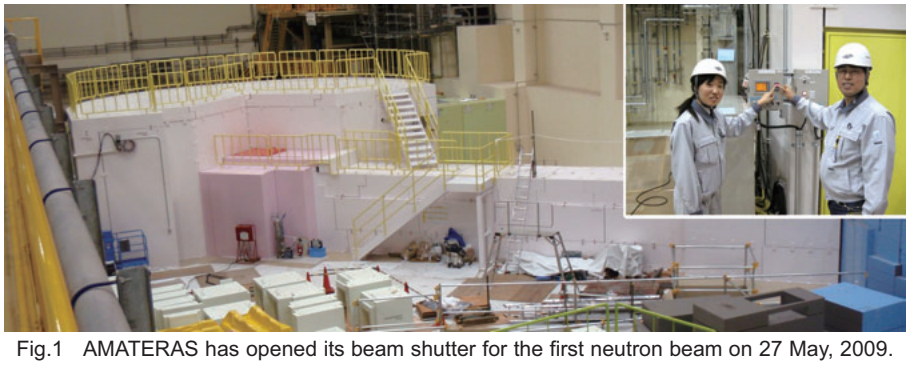

Fig.1 AMATERAS has opened its beam shutter for the first neutron beam on 27 May, 2009.

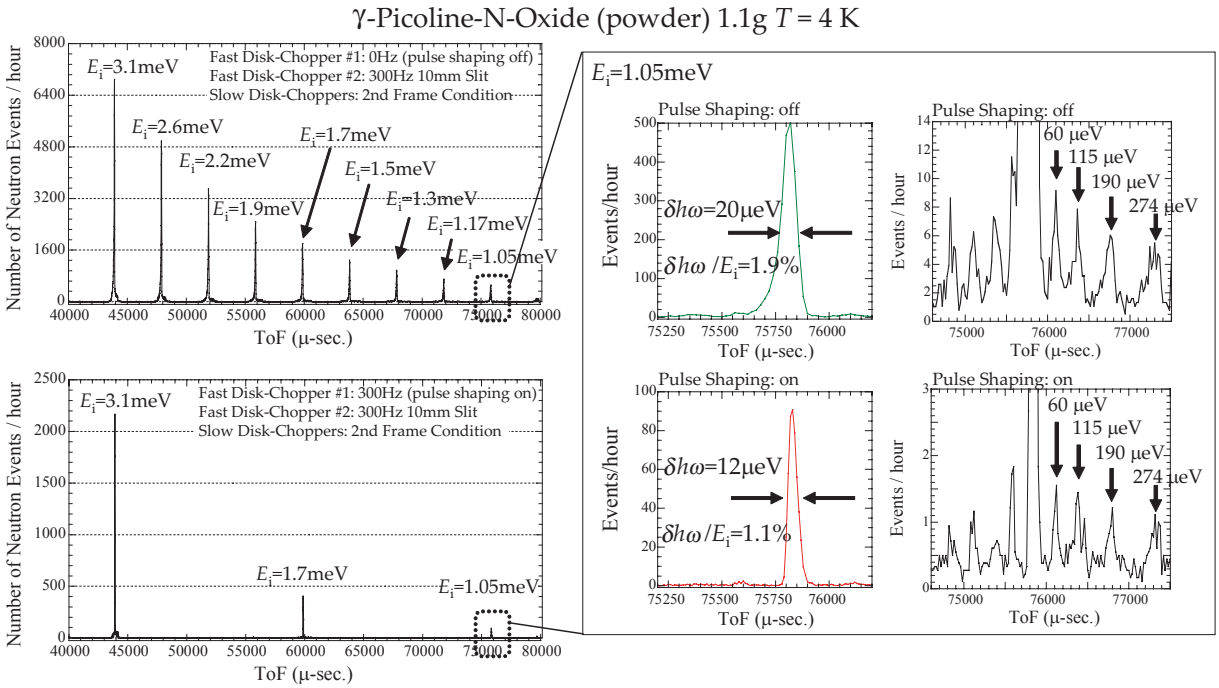

Fig.2 Spectrum from γ-Picoline-N-Oxide powder measured on AMATERAS at 100 kW operation.

finally found miss-alignment in guide mirrors. Resuming the intensity is highly desirable and we are now studying how to fix this problem.

In parallel to the commissioning works, we have started the user program on AMATERAS. The first call for proposals for AMATERAS has been started from Round 2009A. Three general-use and two project-use proposals were accepted for Round 2009A, and four general-use were accepted for Round 2009B. The first general-use experiment was carried out in December 2009.

The proposed researches were put on the various research fields: dynamics in proteins, magnetic materials, superconductors, and so on. Effect of hydration on protein dynamics was investigated by ToF-elastic resolution spectroscopy, with the advantage of the variation of the chopper condition of AMATERAS. Also, the dynamical effect on hydration onto the surface of fiber was studied by incoherent inelastic neutron scattering. This study is expected to contribute to the development of comfortable clothing materials. As a study on the magnetic material, a newly synthesized molecule-based spin system was measured. This system has anti-ferromagnetically coupled triangular units in the three-dimensional crystal. Magnetic dynamics in a powder sample of the system was investigated. The project-use proposal allocated in FY2009 was research on high-T_c superconductors. A related material to $La_{2-x}Sr_xCuO_4$ was measured, and magnetic excitations were clearly observed.

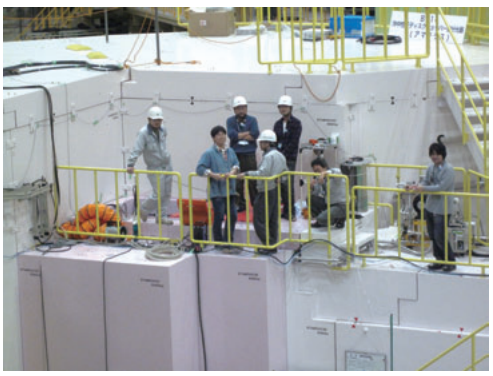

Fig.3 Member of user group and AMATERAS team are waiting for a crane to set a furnace on AMATERAS.

We note that one proposal was canceled due to the fault of an user-carry-in device. Also, experiments of three general-use proposals were not carried out due to the accidental shutdown of MLF at the end of JFY 2009. Two proposals were preformed in May of 2010. The remaining proposals also will be carried out in JFY2010.

References

1) K. Nakajima *et al.*, J. Neutron Res. **15** (2007) 13-21.
2) K. Nakajima and S. Ohira-Kawamura, Hamon, **20** (2010) 49-53. (in Japanese)

K. Nakajima and S. Ohira-Kawamura Neutron Science Section, MLF Division, J-PARC Center

BL 15: Development of the Smaller-Angle Neutron Scattering Instrument TAIKAN

The small-angle neutron scattering (SANS) technique has been indispensable in research of microstructures, higher-order structures, and hierarchical structures in materials science and life science. However, recent progress in nanotechnology and research of complex multi-component or multi-phase systems and non-equilibrium systems has required the SANS instrument to have the capability to measure structural information more efficiently with higher structural and time resolution.

In order to meet such requirements the smaller-angle neutron scattering instrument TAIKAN has been constructed at the BL15 in J-PARC since JFY2009 on the basis of the previous consideration [1][2]. TAIKAN is designed to cover a wide q-range ($q = 3 \times 10^{-3}$~$13 Å^{-1}$) simultaneously by using neutrons in broad wavelength bandwidth of about 0.4~8 Å produced at a spallation neutron source (1 MW) of the Materials and Life Science Experimental Facility (MLF).

The design concepts are shown as the following, 1) the utilization of intense neutron beam by choosing a coupled supercritical hydrogen moderator, 2) the usage of neutrons in broad wavelength bandwidth of about 0.4~8 Å in the first frame by deciding the maximum total flight path of about 20 m, 3) the optimization of instrument performance by considering the typical sample size of 12 mm in diameter and 1 mm in thickness, 4) the detector geometry to cover the wide solid angle with the good connectivity of the scattering angle 2θ, 5) the usage of polarized neutrons in broad wavelength bandwidth of about 2~8 Å, and 6) the improvement of q resolution in low q region by developing and adopting the advanced neutron focusing devices [3].

Figure 1 shows the side view of TAIKAN. In the upper stream, three low-speed disk choppers for the frame definition and a T_0 chopper for the elimination of fast neutrons and γ-rays are installed. Optical devices such as slits, two types of collimator (fine and coarse types), a quadrupole permanent magnet to produce polarized neutrons with higher polarization than 99.9%, and sextupole permanent magnets as magnetic neutron lens are also installed in three vacuum chambers. The combination of these devices can be changed by remote control to the normal beam mode with pinhole collimations and the polarizing or focusing beam mode according to the experimental conditions. The detector system is composed of small-, medium-, high-angle detector banks and a backward detector bank with arrays of one dimensional ^{3}He position sensitive detectors and a high-resolution area detector with spatial resolution of about 0.5 mm, which is used with a focusing system, at an ultra-small-angle detector bank. The scattering angle 2θ can be covered up to 50° with the small- and medium-detector banks. The accessible q range becomes then $q = 3 \times 10^{-3}$~$13 Å^{-1}$ with the normal beam mode. The can be reduced to the order of $10^{-4} Å^{-1}$ by selecting the focusing beam mode. Although the total number of detectors is about 2,400, 35% of them will be installed at a first step. The sample position is located at 14.35 m from the neutron moderator and a large space is prepared for research subjects in various scientific fields. A goniometer with the load capacity of 750 kgf, an automatic sample changer with temperature control system, a high-temperature furnace with thermal dilatometer, and a cryomagnet *etc*. will be installed and used in the space.

After the installation of these devices, beam commissioning will start at the end of JFY2010 with samples such as metal particles, magnetic materials, and biopolymers.

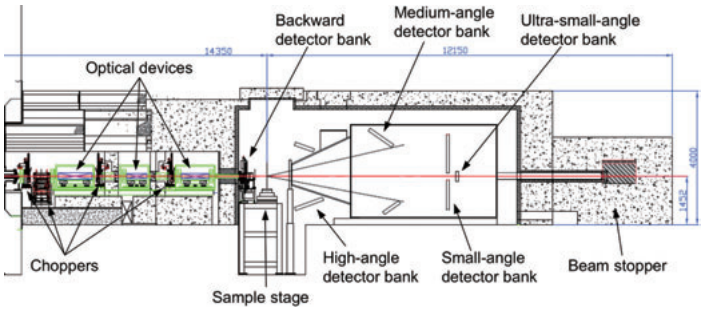

Fig.1 The side view of the SANS instrument TAIKAN in J-PARC.

References

[1] J. Suzuki, *et al.*, In the Proceedings of the 17th meeting of the ICANS, Santa Fe, 2005 pp.786-790.

[2] T. Shinohara, *et al.*, Nucl. Instr. and Methods, Phys. Res. A600 (2009) 111-113.

[3] T. Oku, *et al.*, J. Appl. Cryst. 40 (2007) s408-s413.

J. Suzuki[1], S. Takata[1], T. Shinohara[1], T. Oku[1], H, Kira[1], T. Nakatani[1], Y. Inamura[1], T. Ito[1], K. Suzuya[1], K. Aizawa[1], M. Arai[1], T. Otomo[2], M. Sugiyama[3]

1) MLF Division, J-PARC Center, Japan Atomic Energy Agency, Tokai, Ibaraki 319-1195, Japan
2) MLF Division, J-PARC Center, High Energy Accelerator Research Organization, Tsukuba, Ibaraki 305-0801, Japan
3) Research Reactor Institute, Kyoto University, Kumatori, Osaka 590-0494, Japan

BL 16: Horizontal-type Neutron Reflectometer ARISA-II

Neutron reflectometry is a powerful tool for investigating surface and interfacial structures of materials in the spatial range from nm to sub-μm. Because hydrogen and deuterium atoms have different scattering length for neutrons, this method can distinguish deuterated materials in the mixture of soft-condensed matters, such as polymer blends, bio-mimic membranes, and so on. Furthermore, high transmissivity of neutrons to materials enables us to probe deeply-buried interfaces such as solid/liquid interfaces in a non-destructive way.

ARISA-II is a horizontal-type neutron reflectometer at BL16 viewing a coupled liquid-hydrogen moderator, in MLF, J-PARC. In order to realize neutron reflectivity measurement with high flux neutron beam at MLF as early as possible, we decided to relocate old ARISA reflectometer, which worked at KENS facility in KEK until 2006, to BL16, and started to accept the neutron beam in 2008. In spite of the benefit of the beam flux, the relocated reflectometer, ARISA-II, didn't have enough ability to perform ordinary reflectivity measurement because background was high because only minimum components, that is, slits, sample stage, and detector, had been installed at this time.

In 2009, a disk chopper was installed so as to suppress the background due to frame-overlapping, that is, slow neutrons generated at earlier pulses. To check the effect of this chopper, the reflection from a standard Ni mirror with known film thickness was observed. As shown in Fig. 1, the background is drastically suppressed by this chopper especially for short wavelength. Also, additional shields were installed, and the observable reflectivity reached less than 10^{-6} thanks to this background suppression (These upgrades were supported by a Grant-in-Aid for Creative Scientific Research (16GS0417) from the Ministry of Education, Culture, Sports, Science and Technology of Japan).

After this upgrade, ARISA-II was open for users and four research groups measured neutron reflectivity of their samples until May 2010. At this time, the power of proton beam was 120 kW, and typical duration time was several hours for full Q-range measurement or less than twenty minutes for low-Q measurement. Figure 2 shows the example of the reflectivity data taken by

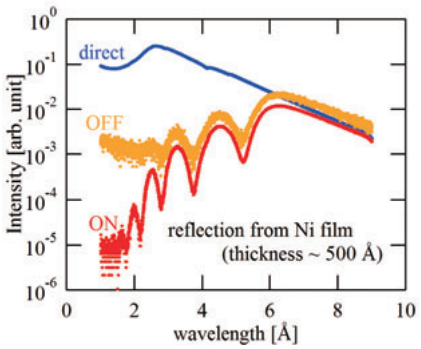

Fig.1 TOF profiles of direct beam and reflection beam with and without disk chopper at θ = 0.6 deg.

ARISA-II. A deutrated polymer (poly(methyl methacrylate); PMMA) layer was put on a normal polymer film, and compared the structural change of the surface polymer layer after water immersion and thermal annealing. By analyzing these data, it was shown that the annealing effect of these two treatments were almost the same (Fig. 3), even though water is a non-solvent for PMMA[1].

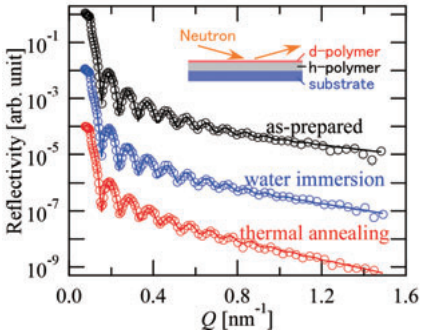

Fig.2 Reflectivity of polymer bilayers as prepared, after water immersion, and after thermal annealing

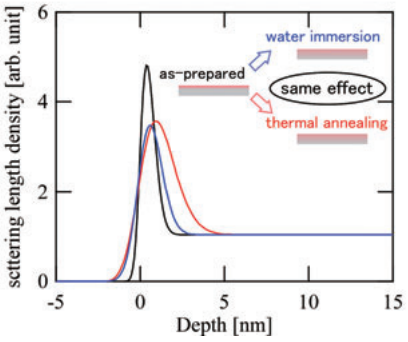

Fig.3 Scattering length density profile at the surfaces of polymer bilayers evaluated by reflectivity analysis

Next, we tried to upgrade ARISA-II for advanced surface analysis. Since $\boldsymbol{Q}$ vector is completely perpendicular to the surface when incident and reflection angles are the same (specular condition), we can evaluate the depth profile of the scattering length density from the

specular reflection as shown in Fig. 3. On the other hand, ***Q*** vector for off-specular condition includes the element which is parallel to the surface. This means that off-specular reflection includes the information about in-plane structure. Therefore, a position sensitive detector is strongly required to observe off-specular reflection for in-plane structure measurement.

For this purpose, we installed a two-dimensional position sensitive detector consisting of ^{6}LiF/ZnS scintillator (OHYO KOKEN KOGYO) and position sensitive photomultiplier tube (HAMAMATSU) was installed. Figure 4 shows the result of imaging test. Characters "BL16 ARISA II" made by Cd mask were observed. The spatial resolution was about 1 mm around the detector center. The efficiency of the detector comparing with ^{3}He gas detector (10 atm) was about 18% at 1.8 Å and 51% at 9 Å (Fig. 5).

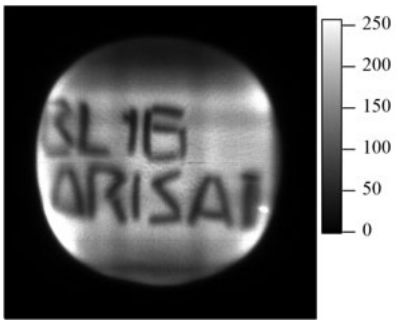

Fig.4 Image of shadow of Cd mask taken by new two-dimensional detector

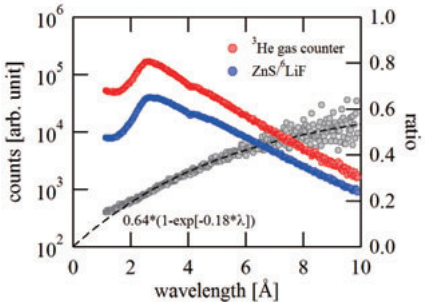

Fig.5 Comparison of efficiency between 3He gas counter and new scintillation counter.

Thanks to the two-dimensional detector, step scans for detector alignment are not needed now. Also, this enables us to measure off-specular reflection for in-plane structure analysis. To check the capability for this measurement, reflection from deutrated phospholipids (dipalmitoyl-phosphatidyl-choline) stacking on Si substrate was measured. According to a previous study with off-specular neutron reflectometry[2], phospholipid bilayers spontaneously aligned to be parallel to the surface of the substrate and off-specular reflection due to their undulation motion were observed.

Figure 6 shows the reflection intensity map depending on Q_z (perpendicular to the substrate) and Q_x (parallel to the substrate). Since the stacking of bilayers was periodically aligned, Bragg peaks were observed around Q_z =0.1 and Q_z =0.2 Å^{-1} along the specular reflection ridge with Q_x=0 μm . The orange lines in the figure mean the limit of specular reflection which comes from the beam divergence. Outside this limit, strong streaks from the Bragg peaks were observed. This off-specular reflection comes from the undulation motion as the previous study showed.

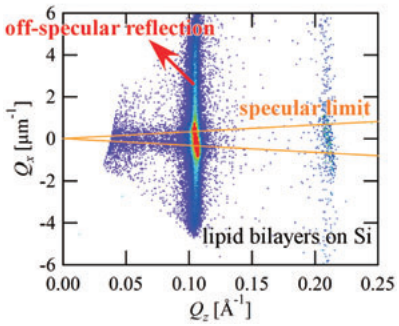

Fig.6 Reflectivity map of phospholipid bilayers on Si substrate

In summary, we successfully re-installed the old horizontal-type ARISA reflectometer as ARISA-II at MLF, J-PARC. Specular reflection down to 10^{-6} could be taken within several hours when beam power was 120 kW. Also, the detector was replaced to a two-dimensional detector with ^{6}LiF/ZnS scintillator. This enables us to measure specular and off-specular reflection at the same time. In the near future, T0 chopper will be installed and the old ARISA reflectometer will be replaced by a brand-new reflectometer supported by JST/ERATO TAKAHARA soft interface project.

References

1) A. Horinouchi, Y. Fujii, N. L. Yamada, K. Tanaka, *"Surface reorganization of thin poly(methyl methacrylate) films induced by water", Chem. Lett.* **39** (2010) 810-811.
2) T. Salditt, C. Münster, U. Mennicke, C. Ollinger, and G. Fragneto, *"Thermal Fluctuations of Oriented Lipid Membranes by Nonspecular Neutron Reflectometry", Langmuir* **19** (2003) 7703-7711.

N. L. Yamada, N. Torikai*, H. Sagehashi, S. Sato, Y. Fujii**, K. Tanaka**, K. Mitamura**, A. Takahara** and H. Seto
High Energy Accelerator Research Organization, Tsukuba, Ibaraki, 305-0801
* Mie University, 1577 Kurima-machiyacho, Tsu, Mie, 514-8507
**Kyushu University, 744 Motooka, Nishi-ku, Fukuoka 819-0395

BL 19: TAKUMI

Instrumentation

TAKUMI is a dedicated neutron diffractometer for promoting scientific and industrial studies in areas of materials science and engineering and mechanical engineering, i.e. engineering diffractometer. The idea to build an engineering diffractometer at J-PARC was been discussed in a workshop in late 2000. The desired performances, basic design [1,2] and the Letter of Intent for the engineering diffractometer at MLF/J-PARC were been approved in 2004, and then the detailed design was fixed at the end of 2006 after an advisory meeting held on October 2006. This instrument was funded for construction in 2006, followed by the construction started from March 2007. This instrument was then named "The Engineering Materials Diffractometer" officially with "TAKUMI" as the nickname.

This instrument is designed to place on beamline port 19 of the MLF and to view a decoupled-poisoned liquid H_2 moderator which is newly developed specially for J-PARC and can provide slow neutrons providing good symmetrical diffraction peak profiles throughout the acceptable wavelengths. The primary and the secondary flight paths are 40 m and 2 m, respectively.

TAKUMI was officially completed in March 2009 (end of 2008 FY), while the commissioning was started from September 2008 being parallel with the final stage of the construction. Status of TAKUMI on March 2009 is shown in Fig. 1.

TAKUMI started commissioning in September 2008 with only two detector modules, one at the north detector bank and the other at the south. After checking the validity and the stability of the detectors and the data acquisition system, powder diffraction data of an austenitic steel alloy with 10 mm diameter without beam collimation (high intensity mode) was measured, and the resolution (w = $\Delta d/d$) of 0.4% was confirmed, as designed. In the commissioning, the resolution $\Delta d/d$ of less than 0.2% was confirmed to be achieved from diffraction measurements using 2 mm diameter of annealed piano wire, with combination of beam collimation (high resolution mode). The *d*-range measured by TAKUMI with single pulse frame, i.e. standard operation, was confirmed to be 0.05 nm to 0.27 nm, showing the optimum range for studies of materials covered by this machine. TAKUMI adopted an event mode data recording method. TAKUMI run several user programs from end of 2008 FY to 2009 FY. It was found that the recording method is very useful for manipulating data as we like, for instance, detector range, time of flight binning width and time resolved data, even if the experiment is has been finished.

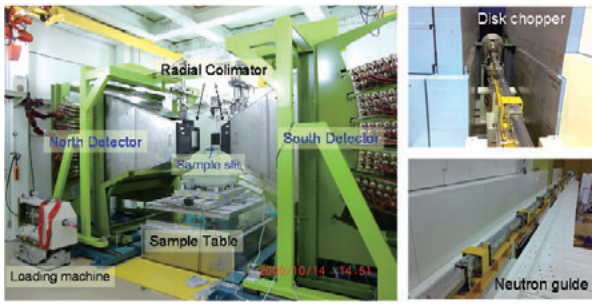

Fig.1 Status of TAKUMI on March 2009

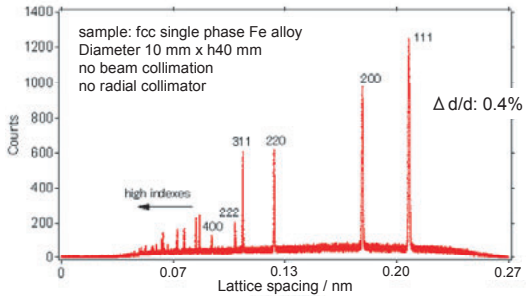

Fig.2 Diffraction pattern of an fcc Fe alloy measured at high intensity mode

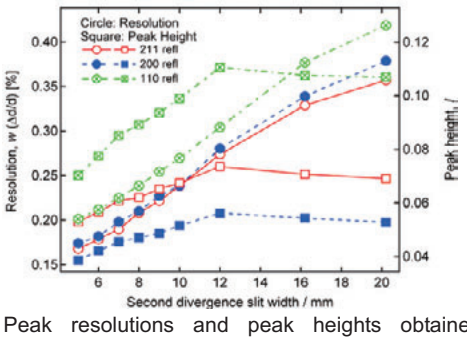

Fig.3 Peak resolutions and peak heights obtained by changing the divergence slit width

User programs

TAKUMI is one of the instruments at MLF that have many users. Many proposals have been

applied to TAKUMI since the user program at MLF/J-PARC was started. Two general uses and two project uses were conducted during 2008 FY. Proposals approved to be conducted during 2009 FY are shown in Table 1. As is shown in the table, even though there were only 16 proposals for general uses, six of them were proposed by users from industrial companies. Since commissioning of TAKUMI is still in progress, beam time allocation for instrumentation use was still high. However, the beam time for instrumentation use (commissioning) will be reduced gradually year by year and beam time for general uses will be increased until it becomes the majority.

Table 1 User programs during 2009 FY at TAKUMI

Proposal type	Number
Instrumentation use (IG)	1
Project uses (PG)	2
PG1 Stress/strain studies in superconducting composites	
PG2 High pressure neutron diffraction studies	
General uses	16
from universities: 10	
from industrial companies: 6	

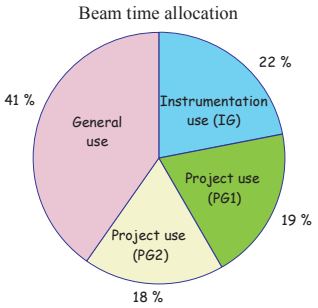

Fig.4 Beam allocation during 2009 FY at TAKUMI

Typical results from project use "Stress/Strain Studies in Superconducting Composites" will be shown briefly. This research project aimed to clarify internal strain behaviors in industrial superconducting composites generated due to their processes and/or during uses (at high magnetic field, high current density), and to understand the relation between the internal strains and their superconducting properties. This project was a collaboration research among scientists from several universities and institutes, who work on industrial superconducting composites including Nb_3Sn, Nb_3Al, $Bi_2Sr_2Ca_2Cu_3O_{10}$ (BSCCO) and $YBa_2Cu_3O_7$ (YBCO) wires or tapes. Results from this project have been reported briefly as a review in Ref. [3].

Residual strain measurements in

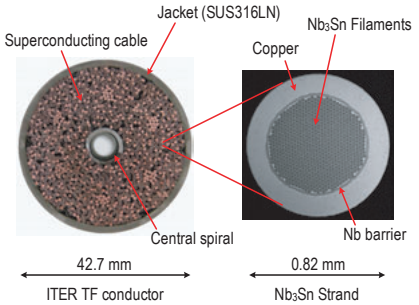

Fig.5 Cross sectional views of ITER TF conductor and Nb^3Sn strand

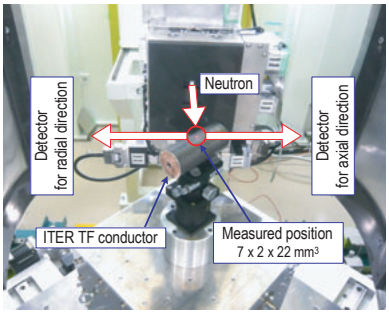

Fig.6 Experimental set-up of strain measurement in ITER TF conductor

International Thermonuclear Experimental Reactor (ITER) Toroidal Field (TF) conductor (Fig. 5) are briefly explained. The ITER TF conductor is composed of 900 Nb_3Sn strands, 522 copper strands, a central spiral and a $SUS_3$16LN circular jacket. Although it is well known that the superconducting properties of Nb_3Sn strands vary significantly depending on the presence of internal strain, the internal strain of strands in the conductor has not been measured so far because of the cabling configuration, their location in a jacket and the low volume fraction of Nb_3Sn. Neutron diffraction using TAKUMI was applied to the measurement of internal strain in Nb_3Sn of ITER TF conductor.

Figure 6 shows a sample arrangement for the strain measurement at TAKUMI. The gauge volume used in the measurement was 7×2×22 mm^3 and the measured position is shown by a circle. The total neutron path is approximately 60 mm. Since the volume fraction of Nb_3Sn in ITER TF conductor is only about 6% and no texture is found in Nb_3Sn wire, diffraction peaks from Nb_3Sn phase were very weak (Fig. 7). The peak height of the strongest peak from Nb_3Sn phase was only 1.4% in comparison to the 111 peak from Cu phase in TF coil. These may be reasons for the difficulties in measuring residual strains in Nb_3Sn wires in the ITER TF conductor. These difficulties can be overcome by using

TAKUMI due to its high intensity and low background. Peaks from Nb_3Sn phase were subsequently fitted to determine peak positions, and then reliable residual strains could be evaluated when Nb_3Sn filament dissolved from the ITER TF conductor was used as the d0 sample (Fig. 8). Further results have been reported in Ref. [4]. Data from neutron diffraction experiments herewith can be anticipated to help clarify strain states in coils for 100 kA class fusion reactors.

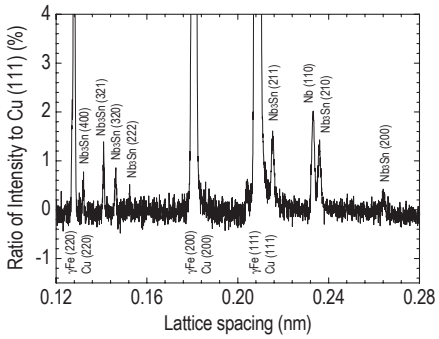

Fig.7 Diffraction pattern of ITER TF conductor for axial direction

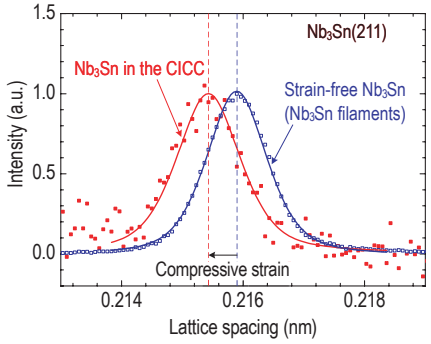

Fig. 8 Difference in lattice spacing of the Nb_3Sn in ITER TF conductor and the strain-free Nb_3Sn filaments extracted from the Nb_3Sn strands

To conduct experiments in various applications, developments of sample environmental (SE) devices are less than necessary. SE devices equipped at the present are a screw-typed loading machine with load capacity up to 50 kN, and a user-in dilatometer that can be used up to 1273 K. The loading machine is used to do insitu neutron diffraction measurements during tensile or compressive deformations with load or cross-head displacement controlled. Cyclic deformations with cross-head displacement speeds of less than 100 mm/min can be also conducted. We have developed a furnace that can be optionally installed to the loading machine enabling us to do deformation experiments at high temperatures up to 1273 K in vacuum, gas flow or air. Other SE devices are now under development. They are a Eurelian cradle (12kg capacity) for arbitrary sample rotation and a cryogenic load frame which is developed in the collaboration with users.

Preliminary test of high temperature tensile deformation was performed using a steel (S45C) specimen with the parallel shape of 6 mm diameter and 15 mm length. The incident slit was 5 mm width, no radial collimators were used. The tensile test was performed at 873K. The test condition is shown in Fig. 9. Diffraction patterns obtained were sliced every 10 s after the measurement finished and are plotted in Fig. 10, which is enlarged to show only 110 peaks. Peak positions are almost unchanged, while peak shapes become sharp during plastic deformation at 873 K.

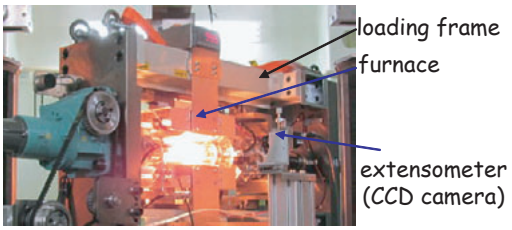

Fig.9 Deformation test at high temperature

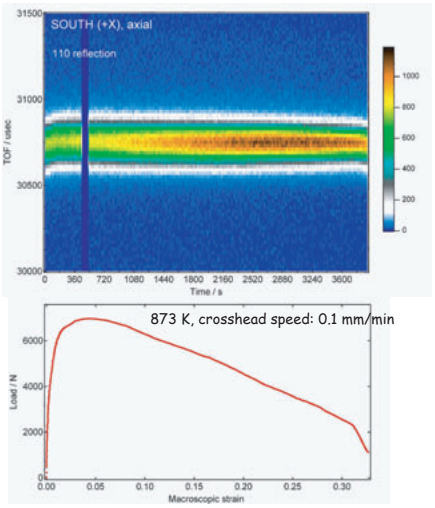

Fig.10 Diffraction profiles of 110 of S45C steel during tensile deformation at 873 K

References

1) A. Moriai, et al., Physica B385-386 (2006) 1043.
2) S. Harjo, et al., Mater. Sci. Forum 524-525 (2006) 199.
3) K. Osamura, S. Harjo, et al., J. Cryo. Soc. Jpn. 45 (2010) 135.
4) T. Hemmi, et al., submitted to IEEE Trans. Appl. Supercond.

K. Aizawa, S. Harjo, T. Ito, H. Arima, J. Abe*, T. Iwahashi and A. Moriai
Neutron Science Section, J-PARC Center, Tokai, Naka, Ibaraki
*Quantum Beam Science Directorate, JAEA, Tokai, Naka, Ibaraki

BL 20: The current status of versatile neutron diffractometer, iMATERIA

Ibaraki Prefecture, the local government of the area where J-PARC is situated in Japan, has decided to build a versatile neutron diffractometer (IBARAKI Materials Design Diffractometer, iMATERIA [1]) to promote industrial applications for neutron beam in J-PARC. iMATERIA is planned to be a high throughput diffractometer so that materials engineers and scientists can use this diffractometer like the chemical analytical instruments in their materials development process.

The roles for neutron diffraction in materials science are (1) to do structural analyses of newly developed materials, (2) to clarify the correlation between structures and properties (functions), and (3) to clarify the relation between structural changes and improvements of functions especially for the practical materials. To carry out such purposes, a diffractometer with super high resolution is not required. The matching among intermediate resolution around $\Delta d/d$ = 0.15%, high intensity and wide d coverage is more necessary.

This diffractometer is designed to look at a decoupled-poisoned liquid hydrogen moderator (36 mm, off-centered) (BL20), and to have the incident flight path (L1) of 26.5 m with three wavelength selection disk-choppers and straight neutron guides with the total length of 14.0 m. The instrumental parameters are listed in Table 1. There are four detector banks including a low angle and a small angle scattering detector bank. The angular coverage of each detector bank is also shown in Table 1. The rotation speeds for the disk-choppers are the same with the pulse repetition rate 25Hz for the most applications (normal mode). In this case, the diffractometer covers 0.18 < d (Å) < 2.5 with $\Delta d/d$ = 0.16% and covers 2.5 < d (Å) < 800 at three detector banks of 90 degree, low angle and small angle with gradually changing resolution. When the speed for wavelength selection disk-choppers is reduced to 12.5 Hz (wide-d mode), we can access a wider d-range, 0.18 < d (Å) < 5 with $\Delta d/d$ = 0.16%, and 5 < d Å) < 800 with gradually changing resolution.

Currently, it takes about 30 minutes to one hour to obtain 'Rietveld-quality' data for the X-ray sized sample measured at 120kW for standard oxide samples.

To promote industrial applications, a utilization system of this diffractometer is required. Since several tens to thousands of experiments will be carried out in one year, we have prepared an automatic sample exchange system [2] and large numbers of sample holders. The sample exchange system can store more than 600 samples at the same time at room temperature and watch sample is identified by an RFID tag on the top of the holder cap.

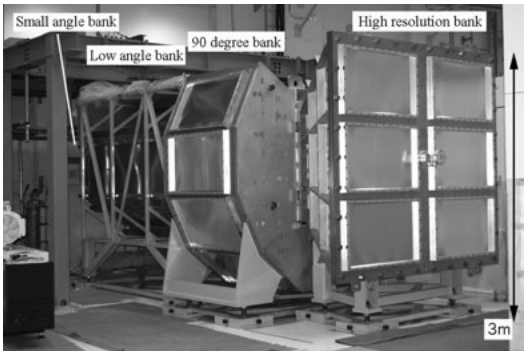

Fig.1 IBARAKI Materials Design Diffractometer, iMATERIA without detector for each bank and instrument shielding. High-resolution bank, special environment bank (90 degree bank), low angle bank, can be seen from right to left. Small angle detector banks, which are not shown in picture, are situated in the low angle vacuum chamber (left hand of the picture).

Table 1 Instrumental parameters of iMATERIA. L2 is the scattered flight path. The d-range for each bank is maximum value for two measurement mode.

L1		26.5 m
Guide length		Total 14 m (3 section)
Position of Disk choppers		7.5 m (double) 11.25 m (single) 18.75 m (single)
High Resolution Bank	2θ L2 d-range	$150° \leq 2\theta \leq 175$ 2.0 - 2.3m $0.09 \leq d(A°) \leq 5.0°$
Special Environment Bank	2θ L2 d-range	$80° \leq 2\theta \leq 100°$ 1.5m $0.127 \leq d(A°) \leq 7.2$
Low Angle Bank	2θ L2 d-range	$10° \leq 2\theta \leq 40°$ 1.2 - 4.5 m $0.37 \leq d(A°) \leq 58$
Small Angle Bank	2θ L2 d-range	$0.7° \leq 2\theta \leq 5°$ 4.5 m $0.37 \leq d(A°) \leq 58$

The high resolution bank is already operational for user experiments. Figure 2 shows a diffraction pattern obtained from Si powder sample at room temperature by the high resolution bank. The peak shape of iMATERIA is more symmetrical than that of Sirius diffractometer. Figure 3 plots the measured resolution $\Delta d/d$ for high resolution bank by using Si data. The average resolution $\Delta d/d$ =0.158% is in agreement with design value. The highest resolution is $\Delta d/d$ = 0.15% @ d = 0.9 Å.

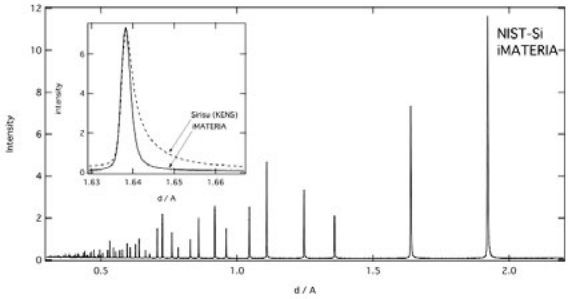

Fig.2 Neutron diffraction pattern for Si powder measured by iMATERIA. The inset in the figure shows the comparison for iMATERIA and Sirius data.

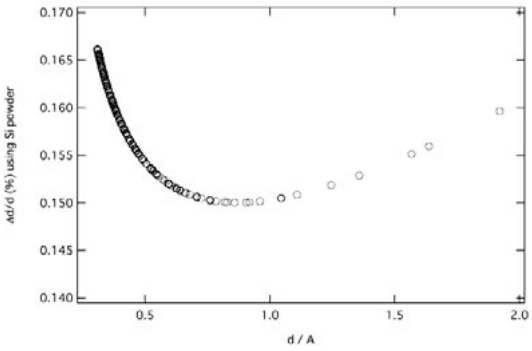

Fig.3 Measured resolution $\Delta d/d$ for high resolution bank as a function of d from Si data.

Figure 4 and 5 are Rietveld refinement patterns for Al_2O_3 and $YBa_2Cu_3O_{7-\delta}$ samples at the high resolution bank by Z-Rietveld[3]. It takes 19 min for Al_2O_3 and 26 min for $YBa_2Cu3O_{7-\delta}$ to collect Rietveld available data. The χ^2 vale for each refinement was 1.47 (Al_2O_3) and 2.48 (YBCO).

Figure 5 shows temporarily making diffraction pattern for low angle bank data of YBCO with high resolution bank data. Low angle bank covers wide scattering angle, 2θ, therefore, d-range and resolution for each detector are gradually changing. In Fig.5, we divide low angle bank data into 3 groups (35°, 25° and 15°). We are now considering how to divide each detector data into grouping.

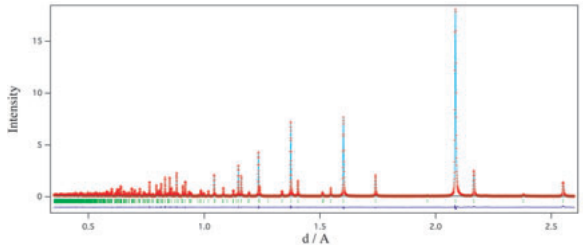

Fig. 4 Rietveld refinement pattern for Al_2O_3

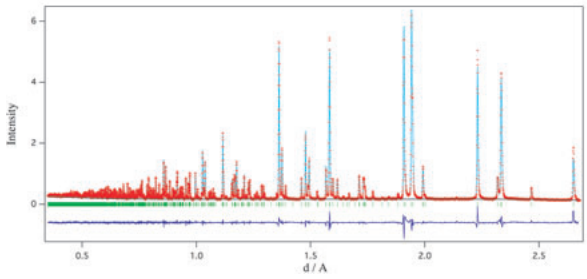

Fig.4 Rietveld refinement pattern for YBCO

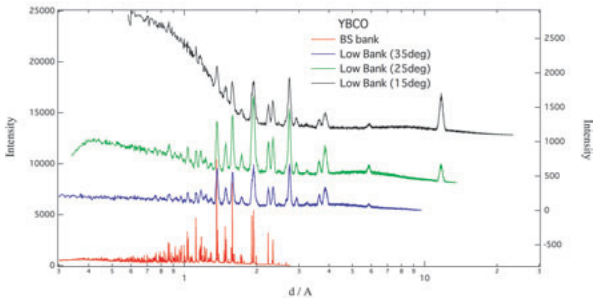

Fig.5 Data of low angle bank for YBCO

The low angle and 90 degree data will be open for users during FY2010. The small angle bank is under commissioning.

References

1) T. Ishigaki et. al., "IBARAKI materials design diffractometer (iMATERIA)-Versatile neutron diffractometer at J-PARC", Nucl. Instr. Meth. Phys. Res. A, 600, 189-191 (2009).
2) A. Hoshikawa et. al., "Development of an automatic sample changer for iMATERIA", Nucl. Instr. Meth. Phys. Res. A, 600, 203-206 (2009).
3) R. Oishi, et. al., "Rietveld analysis software for J-PARC", Nuclear Instruments and Methods A600, 94-96 (2009).

T. Ishigaki[1], A. Hoshikawa[1], M. Yonemura[2], K. Iwase[1], D.S. Adipranoto[1], H. Oguro[1] and T. Kamiyama[2]
[1]Frontier Research Center for Applied Nuclear Sciences, Ibaraki University, Tokai, Naka, Ibaraki, 319-1106, JAPAN.
[2]Neutron Science Laboratory, KEK, Tsukuba, Ibaraki, JAPAN.

BL 21: Commissioning of High Intensity Total Diffractometer (NOVA)

Construction of High Intensity Total Diffractometer (NOVA) at BL21 was almost completed in FY2009. Biological shields and vacuum tank were installed on 1st May 2008 and 6th March 2009. Main components are shown in Fig. 1.

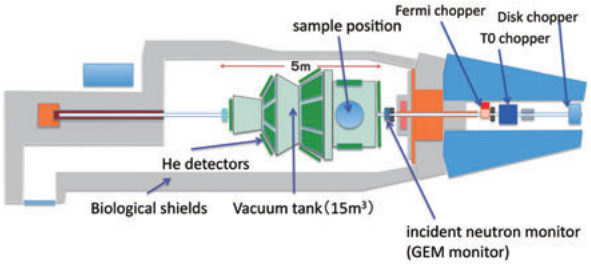

Fig.1 Main components of NOVA. Fermi chopper and T0 chopper will be installed in FY2010

Corrections of neutron wavelength-dependency are the key of the total scattering technique. One of the important wavelength-dependent factors is the incident neutron flux ($I_0(\lambda)$). Since the neutron flux of NOVA at sample position is estimated as 5 x 10^8 neutron/sec, very high-counting rate and high-efficiency neutron monitor are necessary to monitor the incident flux. Gas Electron Multiplier (GEM) monitor has been developed for NOVA [1]. Its counting-rate is about 1 MHz and efficiency is about 0.1%. In 2008, the commissioning of the GEM monitor was conducted. Through the commissioning, electronics, packages and cabling were improved and the stability GEM monitor was preliminarily confirmed. Also, ^{3}He detector system was tested at BL21 and expected performance was confirmed. After the installation of the vacuum tank, ^{3}He detectors were installed.

The first neutron diffraction was measured on 28th May 2009. As the first sample, diamond powder was chosen and clear Bragg peaks were observed by the very first measurement (Fig.2). Just after the first diffraction measurement, the ceremony of the completion of the construction of NOVA was held on 2nd June 2009 at Ibaraki Quantum Beam Research Center and MLF.

Until the end of March 2010, about 900 of ^{3}He position sensitive detectors (gas pressure: 20 atom, size: 1/2 inch diameter and 800 mm effective length) were installed to cover a large range of wave-vector change Q (0.01 Å^{-1}< Q < 100 Å^{-1}). Commissioning of hardware and software were progressed and the performance, especially data acquisition system consists of "NeuNET", "Si-TCP" and "DAQ-middleware", were confirmed. Figure 3 shows photos of installed NeuNET modules and computers for NOVA.

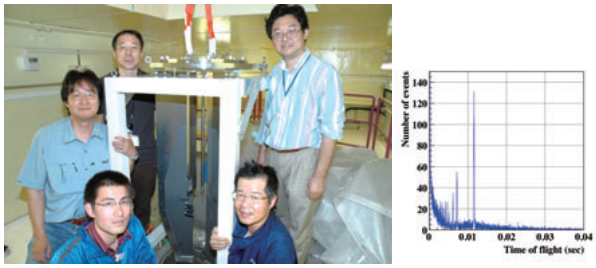

Fig.2 First diffraction measurement at NOVA (left) and observed Bragg peaks of diamond powder (right).

Standard samples such as silicon powder, silica glass, H_2O/D_2O liquids, mesoporous-silica (MCM-41), etc. were measured and confirmed that intrinsic back ground level of NOVA is reasonably low and obtained static structure factor, $S(Q)$, are consistent in absolute scale with those previously measured $S(Q)$ by another total diffractometer HIT-II at KENS.

Fig.3 NEUNET modules (right) and computers (left) of NOVA.

As one of the standard samples, deuterated vanadium was measured. Preliminary $S(Q)$ is shown in Fig. 2. Pair distribution function, $G(r)$, was obtained by the Fourier transformation of $S(Q)$ and is depicted as Fig.3. Because the

coherent neutron cross-section of vanadium is about 0.3% of deuterium, deuterium-deuterium (H-H) correlation mainly observed. It is confirmed that the obtained $G(r)$ is consistent with the previously reported structure parameters. Sample environment equipments have been fabricated: 1) Sample exchanger that can load 10-samples, 2) in-situ experiment in H_2/D_2 gas atmosphere (max pressure is 10 MPa and temperature range is 50K ~ 473K), 3) furnace of vanadium foil heater (room temperature to 1373 K). It is expected that full-scale research of hydrogen storage materials will be started soon.

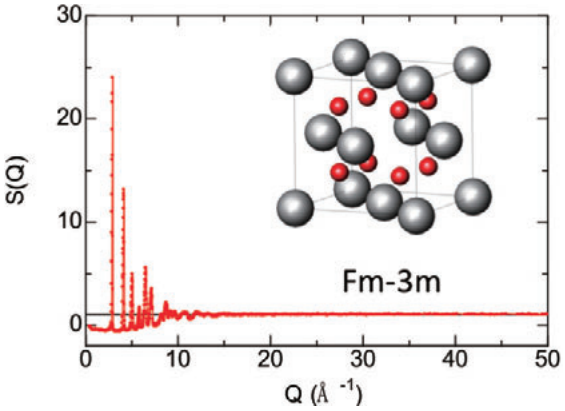

Fig.2 Static structure factor S(Q) deuterated vanadium measured by NOVA.

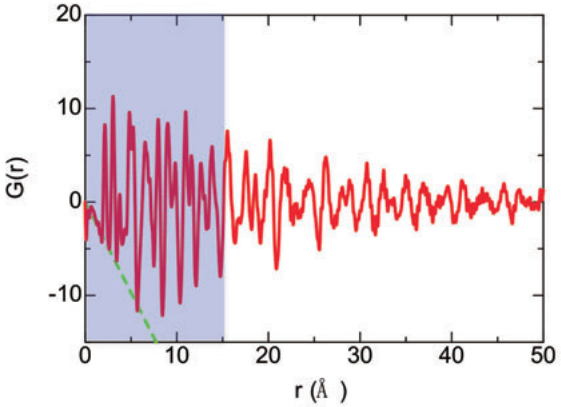

Fig.3 Pair distribution function $G(r)$ obtained by Fourier transformation of $S(Q)$. $G(r)$ is consistent with previously reported ones.

This research is supported by NEDO (New Energy and Industrial Technology Department Organization) under "Advanced Fundamental Research Project on Hydrogen Storage Materials"

Table 1 Resolution of each detector bank of NOVA.

Detector bank	2θ [deg]	L2 [m]	Δ Q/Q [%] (min, max)	Q range[nm^{-1}] (d range [nm])
small-angle	0.7~ 9	4	7 (4~50)	0.1 ~ 80 (0.08 ~ 62.8)
20-deg	12.6~ 28	2.8 ~3.0	2.5 (1.7~3.9)	2 ~ 260 (0.02 ~ 3.1)
45-deg	33~ 57	1.7~ 1.9	1.2 (0.9~1.5)	4 ~ 500 (0.01 ~ 1.6)
90-deg	72~ 108	1.2~ 1.3	0.6 (0.5~0.7)	10 ~ 820 (0.008 ~ 0.63)
back-scattering	135~ 170	1.0~ 1.4	0.3 (0.3~0.35)	14 ~ 1000 (0.006 ~ 0.45)

References

1) Ohshita, H., et al., *"Development of a neutron detector with a GEM"* NIM A (2010) in press.

NOVA group with Prof. Masakatsu Misawa (KEK) who was a pioneer in pulsed neutron total scattering.

T. Otomo[1], K. Suzuya[2], M. Misawa[1], N. Kaneko[1], H. Ohshita[1], T. Fukunaga[3], K. Itoh[3], K. Mori[3], M. Sugiyama[3], Y. Kameda[4], T. Yamaguchi[5], K. Yoshida[5], Y. Kawakita[6], K. Maruyama[7], S. Shinichi[2], S. Takata[2], S. Satoh[1], S. Muto[1], J. Suzuki[1], T. Ino[1], H. Shimizu[1], T. Kamiyama[1], S. Ikeda[1], Y. Yasu[1], K. Nakayoshi[1], H. Sendai[1], S. Uno[1] and M. Tanaka

[1]KEK, Tsukuba, Japan
[2]JAEA, Tokai, Japan
[3]KURRI, Kyoto Univ., Kumatori, Japan
[4]Yamagata Univ., Yamagata, Japan
[5]Fukuoka Univ., Fukuoka, Japan
[6]Kyushu Univ., Fukuoka, Japan
[7]Niigata Univ., Niigata, Japan

R&D of ^{3}He PSD for Neutron Spectrometers

Neutron detectors and data acquisition system are essential items for neutron experiments. Several types of detectors have been developed for various demands of detecting efficiency, counting rate, area coverage, position resolution, n/γ ratio and so on. Gas detectors are one of the most conventional detectors and have been used for research of high-energy physics. It is also effectively used in neutron science, in particular ^{3}He gas detector shows the best performance for thermal neutron detection. Position sensitive detectors (PSD) with ^{3}He gas are currently the most popularly installed neutron detectors. The PSD detects neutrons simply by the nuclear reaction of ^{3}He+n→ T+p+0.765MeV, and ionization. Incoming neutron position is defined by charge division providing the reasonable position resolution about 5mm for 1/2" diameter tube.

In the intense pulsed neutron facility, a recent trend is wide detector coverage placing many of one-dimensional PSDs, making a two-dimensional area detector. Direct geometry inelastic spectrometers (chopper spectrometers) mostly require large area coverage. For these kinds of spectrometers, a long PSD is quite useful. In J-PARC/MLF, there are several demands for PSD type in order to achieve required instrumental performance. Here we report the PSD required in MLF spectrometers and neutron irradiation tests results of brand new PSD. The PSD are originally provided by GE Reuter-Stokes and Toshiba Electron Tubes & Devices according to our demands.

Short PSD

The PSD with 1/2" (or 1") in diameter, 600 mm, and 10 atm ^{3}He partial pressure has been used for conventional PSD in Japanese neutron facility. Intense neutron, however, needs much faster counting rate even for the same dimension. Since much higher neutron energy is utilized in the pulsed neutron, high neutron efficiency is required as well. Thus, we tested several PSD based on the specification of 1/2", 1m and 20atm, which is newly developed PSD. Almost all the tests are performed at MUSASHI port in JRR-3. High-counting model shows 100 kcps of counting time, which is quite good performance that we expected, however it needs high applied voltage over 2300 V. This is not good (up to 2000 V is normal use) to use with current read-out circuit.

8mm PSD

Normally, the above mentioned 1/2"-1m-20atm PSD shows almost reasonable specifications. For particular use, however, much severe conditions are required. Obtaining high spatial resolution, we introduced slender 8mm diameter tube (600mm). Fine neutron beam makes intensity peak as shown in Fig. 1 (top). Obtained position resolution of FWHM= 4.5 mm is sufficient even for high resolution instruments. Linearity is less than 1 mm in the whole PSD.

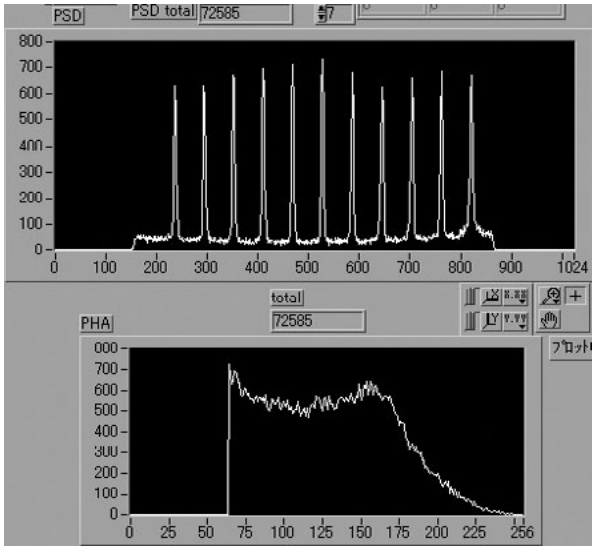

Fig.1 top : neutron peaks along PSD (abscissa). (bottom) Pulse height distribution

Long PSD

As mentioned above, a long tube PSD is utilized in chopper spectrometers. In MLF/J-PARC, three chopper instruments are currently under operation, namely, 4SEASONS, HRC and AMATERAS. The lengths of these detectors are 2.5 m, 2.8 m and 3 m, respectively, to minimize gaps between detectors. They will be accommodated in the scattering chamber under the high vacuum condition (~10^{-6} Torr) to reduce

the background. Therefore, new long PSDs were equipped with newly designed vacuum couplings with SHV connectors at the ends (SKYN^2-type) (Fig. 2). The linearity of the position sensitivity was confirmed within the error of 3 mm for all tested detectors. The resolution was less than 19 mm in FWHM. These performances were almost equivalent to those of conventional short PSD commonly used at KENS. We have found slight differences in the performance between the detectors provided by different venders, which were, however, completely acceptable to us.

Fig.2 A 2.5m length PSD on the testing stand at the test port (left). A newly designed vacuum coupling end SKYN^2 (right)

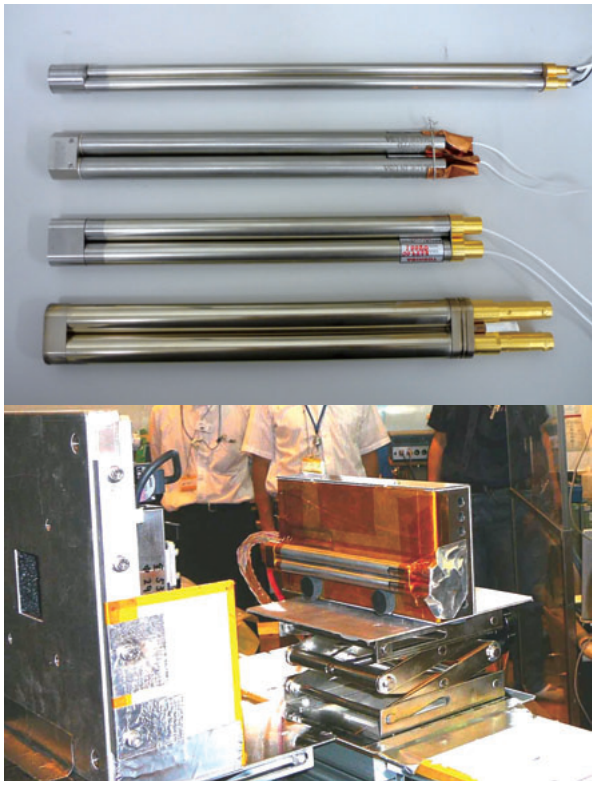

Fig.3 A prototype *Nunchaku* PSD and its experimental setup

Nunchaku PSD

The other type was the Nunchaku-type (U-type) PSD, shown in Fig. 3. It comprised sequentially coupled detectors. Since the connector was shared by two pieces, we can reduce the installing space. Such type of detectors will be installed for a backscattering spectrometer, DNA. We have tested several detectors from different benders and have obtained enough performance at the final moment.

Moreover, we designed and tested PSD with oval shaped tube and PSD with Al tube instead of stainless tube. Thus, there are many demands for a PSD used at new neutron source. However, recent big issue of ^{3}He crisis (a severe depletion of the existing ^{3}He stockpile and the present shortage of ^{3}He) prevents R&D and use of gas counters.

T. Yokoo, S. Satoh, K. Nakajima, M. Nakamura, R. Kajimoto, N. Takahashi and N. Kaneko
Neutron Science Section, MLF Division, J-PARC Center

Development of a neutron beam monitor with a GEM

We are developing a neutron beam monitor with a gas electron multiplier (GEM) [1] for the high-intensity total diffractometer (NOVA). Since a GEM is a gaseous detector with a high count rate capability (more than 10^6 Hz/cm^2) [2], the GEM-based detector is suitable for the neutron beam monitor of the NOVA.

The detector system was made by the assist of the KEK detector technology project [3]. A schematic cross-sectional view of the neutron detector is shown in Fig.1. Neutrons are detected by the ^{10}B(n,α)^{7}Li reaction. For approximately 0.1% neutron detection efficiency, a 0.02-μm-thick layer of ^{10}B was deposited on the Al plate. The chamber gas is a mixture of Ar and CO_2 (70:30). For gas amplification, two GEMs whose foil thickness was 50 μm were used. The gas gain is approximately 400.

Signals from the detector are inputted to an Application Specific Integrated Circuit (ASIC) called "FE2007" [4]. FE2007 is an amp-shaper-discriminator (ASD). The output digital signals from FE2007 are gathered into a field programmable gate array (FPGA), and then only interested events are selected. A hardware-based TCP Processor called "SiTCP" [5] is loaded in the same FPGA. The data transfer rate of the system reaches over 1 MHz with 10-byte data. FE2007 and SiTCP help to downsize the detector system. DAQ middleware [6] is a software framework of network-distributed DAQ system. The DAQ system of the detector is constructed by DAQ middleware. DAQ middleware is also available as an online monitor. The specifications of the detector system are shown in Table 1.

The plateau curve as a function of input high voltage is shown in Fig.2. The detector has plateau region between 2.7 kV and 2.85 kV. Over 2.9 kV, a discharge event occurred. For stable operation, we decided operating the detector at 2.75 kV. The typical wavelength-spectrum distribution is shown in Fig.3. The histogram represents the measurement, and the graph with a "+" symbol represents the calculation. The result of the calculation was derived from the estimation of the neutron reaction rate. Since the difference between the measurement and the calculation is small, we found that the wavelength-spectrum distribution is consistent. Beam profiles were measured by changing the detector position. The upper three figures in Fig.4 represent the measurement. The lower three figures in Fig.4 represent a Monte Carlo (MC) simulation. In the MC simulation, only the geometrical conditions were considered. The beam size and the beam pattern are explained as geometrical characteristics. The beam profiles agree with the MC simulation. We

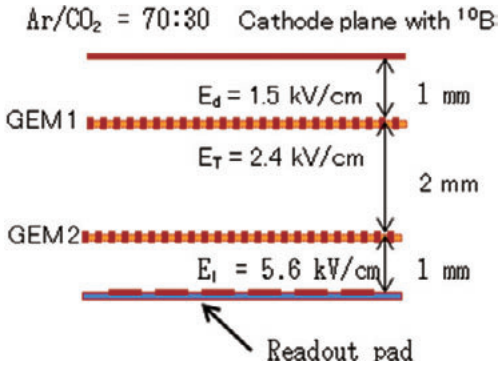

Fig.1 A schematic cross-sectional view of the detector.

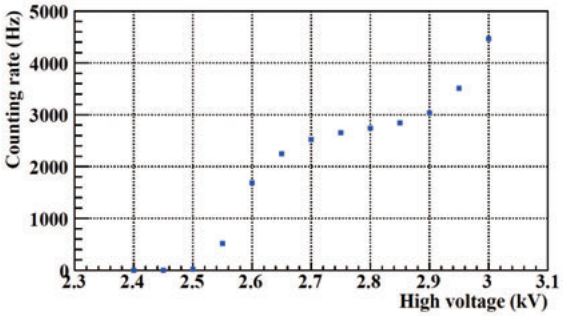

Fig.2 The plateau curve as a function of input high voltage

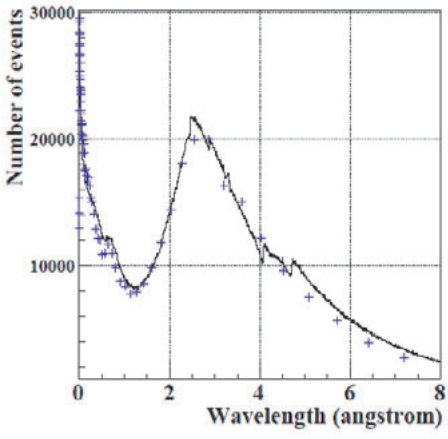

Fig.3 The typical wavelength-spectrum distribution

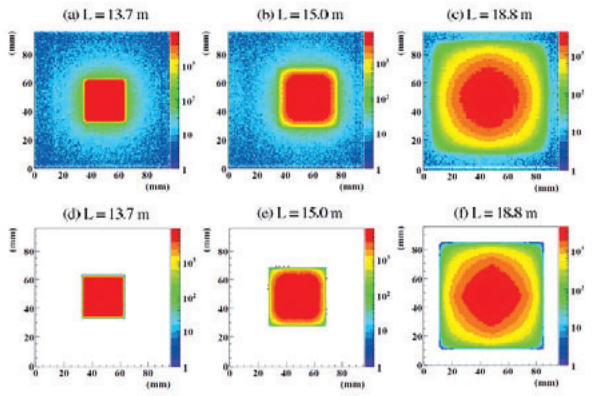

Fig.4 The beam profiles.

Table 1 Specifications of the detector

Detector size: 660 mm × 350 mm × 170 mm
Active area: 100 mm × 100 mm
Readout channel: 120 ch × 120 ch with 0.8 mm pitch
Input for the T0 timing is equipped.

found that the GEM-based detector has a good performance as the neutron beam monitor.

References

[1] F. Sauli, Nucl. Instr. and Meth. A 386 (1997) 531
[2] A. Bressan, Nucl. Instr. and Meth. A 425 (1999) 262
[3] Web site of the KEK detector technology project, http://rd.kek.jp.
[4] Y. Fujita, et al., "Performance of multi-channel and low power front-end ASIC for MPGD μ-PIC readout", presented at the IEEE NSS 2007
[5] T. Uchida, et al., IEEE Trans. Nucl. Sci. NS-55 (2008) 2698
[6] K. Nakayoshi, et al., Nucl. Instr. and Meth. A 600 (2009) 173

H. Ohshita High Energy Accelerator Research Organization, Tsukuba, Ibaraki, 305-0801, Japan

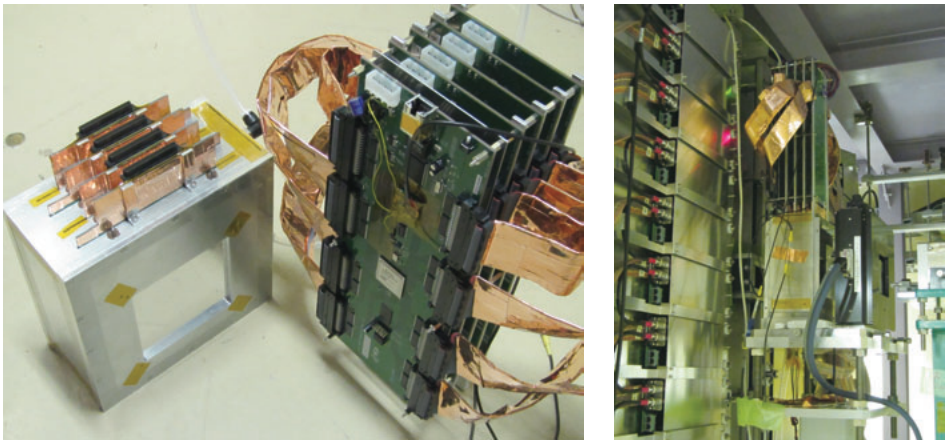

GEM detector system (left) used as neutron beam monitor, installed upstream of the NOVA diffractometer (right).

Readout system of neutron scintillating detector

The NEUNET system [1] for the ^{3}He-PSD readout is widely used for neutron experiments at J-PARC/MLF. This NEUNET system has good performance not only for the high transfer rate but flexibility-use applying to other detectors. Two-dimensional scintillating detector, RPMT system, is the second application using NEUNET system. Because the standard RPMT detector is used with USB2.0 transfer, networking DAQ system is desired for the J-PARC/MLF. The RPMT-NEUNET detector is developed with only a few changes from NEUNET.

Some experimental users desire a detector system which has high counting rate and high efficiency. One of them is a direct-reading two-dimensional detector (Li-TA) system.

RPMT-NEUNET system

The RPMT system consists of a two-dimensional photomultiplier tube (PMT), an amplifier, and a readout module. There are two kinds of PMT, five inches (R3292) and three inches (R2486) tubes which are made by Hamamatsu Photonics company. It becomes two-dimensional neutron-detector system with a neutron scintillator. The effective area and the spatial resolution of the RPMT are about 10 cm in diameter and 0.8mm resolution for the five inches detector. The three inches RPMT detector has about 5 cm in diameter and has 0.5 mm spatial resolution. They are used at BL05 and BL16 at MLF.

Fig. 1 shows a block diagram of the RPMT-NEUNET system. The RPMT-NEUNET module needs only one ADC daughter-board, although the NEUNET module needs four boards. Two-dimensional data are obtained by only two charge-division functions which are X axis and Y axis in this detector. Because the RPMT-NEUNET module equals the NEUNET module, it has SiTCP [2] which makes it possible to use the same program for storing the event data through network. It only needs a program which makes two-dimensional data.

The RPMT-NEUNET module sends X axis data and Y axis data to a computer (PC) as independent event data. Each event data consist of TOF time (24 bits, 25 ns unit), PSD number (8 bits), right-pulse height (12bits), and left-pulse height (12 bits). The PC calculates positions of them from the right-pulse height and the left-pulse height independently by charge division method. The X axis data and the Y axis data correspond with 0 and 1 of the PSD number respectively, and they are always obtained alternately. If they arrive within a few micro-seconds, which time is set by software, they are recognized as neutron data.

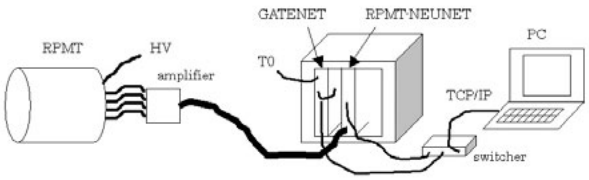

Fig.1 Block diagram of the RPMT-NEUNET system.

It is easy to obtain high detection efficiency because the neutron scintillator is put directly on the detection area of the RPMT. The detection efficiency is obtained almost 100% compared with ^{3}He by ^{6}Li glass which has 1mm in thickness, and is about 30% obtained by ZnS scintillator which has 0.25 mm in thickness. Fig. 2 shows the RPMT-NEUNET data obtained by the ZnS scintillator with shadows of cadmium pieces. It is seen in the two dimension graph and has X axis in the horizontal, Y axis in the vertical, and the neutron number in the light and shade. Many histograms can be produced besides this at offline analysis.

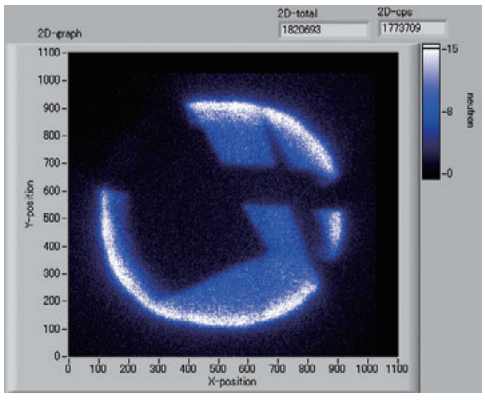

Fig.2 RPMT-NEUNET data.

Li-TA system

Almost of the all neutron-detectors have a low counting rate. Typical detector can count up to only 20 ~ 30 Kcps (count per second) in 80 ~ 1000 cm^2 area. Li-TA system can measure up to several Mcps in 25 cm^2 area. It is sometimes used at BL04 at MLF.

The detector is put on neutron scintillators directly to 256 channel multi-anode PMT (H9500 series) made by Hamamatsu Photonics company (Fig. 3). Each channel is used as an independent PMT to achieve the high count rate.

The detector area of 16ch*16ch matrix is covered at intervals of 3 mm with ^{6}Li glass scintillators. Each scintillator is 2.1 mm square and 1mm thick. The system can measure high count rate because of having 256 channel PMTs.

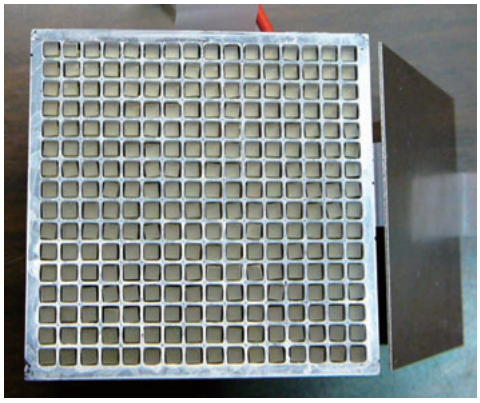

Fig.3 Li-TA256ch detector

Fig. 4 shows a block diagram of the readout system. The outputs of the detector are amplified by 256ch amplifiers, and are digitalized by 256 ADCs which are 50MHz 10bit. They are discriminated neutron signal from noise. The neutron signal of each multi anode PTM is accumulated to a time analysis histogram.

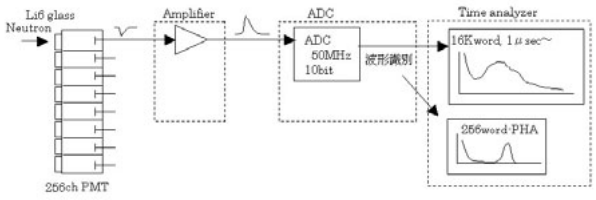

Fig.4 Block diagram of Li-TA256ch detector

The neutron signal is identified from the shape of waves of the digital signal. If the signal exceeds the threshold value, it is recognized as a neutron signal.

Figure 5 shows the Li-TA data obtained by a "K" character mask of cadmium. The upper graph shows the pulse height distribution. The horizontal axis is pulse height (light output) and the vertical axis is neutron counts. Noise of the neutron signals is removed easily, because the signal of ^{6}Li glass neutron scintillator isolates the noise. The lower graph below shows two-dimensional position-data. Although the "K" character needs some rotations and reverses, the system detects neutrons at the exact position. Uniformity of the system is very stable because it uses ^{6}Li glass neutron scintillators.

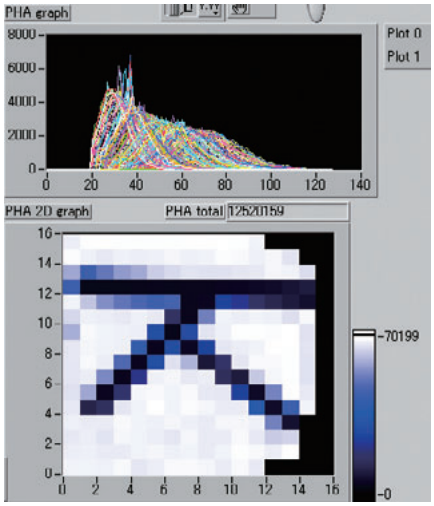

Fig.5 PHA & 2D data

It endures in the high count rate up to several Mcps. It is an indispensable detector system for experiments in which a very high count rate is necessary.

References

1) S. Satoh, S. Muto, N. Kaneko, T. Uchida, M. Tanaka, Y. Yasu, K. Nakayoshi, E. Inoue, H. Sendai, T. Nakatani and T. Otomo: Nucl. Instr. and Meth. A 600 (2009) 103-106.
2) T. Uchida: IEEE Trans. Nucl. Sci. NS-55 (2008) 1631.

S. Satoh, K. Hirota* and S. Muto

Neutron Science Laboratory, Institute of Materials Structure Science, High Energy Accelerator Research Organization, Tsukuba, Ibaraki, 305-0801

*Nishina Center, RIKEN, Wako, Saitama, 351-0198

Computing Environment

In J-PARC/MLF, neutron experimental instruments which have groups of detectors with thousands of pixels measure the neutron signals while changing scanning conditions of the several equipments such as sample environment devices and beamline components. The data size on each scanning condition can be more than GB. Because J-PARC/MLF is a high intensity pulsed neutron source, the measurement at one scanning condition can be performed in very short time (less than 1min). Users need to optimize the condition in a short time by taking account of the result of previous or current data analysis. Thus, the data processing must be scalable. There are 23 neutron instruments in J-PARC/MLF. Various kinds of instruments are in use, being commissioned, constructed and proposed. Each instrument is used in several disciplines with various experimental setups and various types of software. However, the human resources to construct and maintain the computing environment of the instrument are limited. Therefore, we have decided to construct the software on a common and flexible software framework. The whole information of the instruments should be recorded for maintenance. The parameters of the measurement under various scanning conditions and the analysis results associated with the measured raw data are also recorded as experimental meta-data in a database. The results of the simulation such as a first-principle calculation are also recorded in it. The experimental users can make use of this information before their experiments. The number of experimental users who visit J-PARC/MLF is expected to be about 10,000 per year. The majority of the users are not professionals in neutron experiments. Hence, the system of the instrument should be user-friendly. In addition, since the raw data size is enormous (several tens GB), it is very difficult for users to bring the data back to their home laboratories. They often access the MLF computing environment and analyze the acquired raw data from their laboratories.

On the basis of these, we have been constructing the MLF computing environment based on the following policies:

- Users can make instrumental control and data analysis from a unified interface, “Working Desktop”.
- The cost for maintenance and upgrading can be largely reduced by the common software environment.

We have considered four requirements to follow these policies. The first is scalability which is high throughput for the large-scale data of gigabyte order. The second is flexibility which is adaptability of various experimental purposes and reduction of resources for development and maintenance. The third is a database for logging the whole experimental information and practical use of previous experimental results. The last is usability which is user-friendly system for a lot of users considering remote access.

Figure 1 shows the diagram of the MLF computing environment. The computing environment has many software components distributed in the network. The software framework [1] is responsible for the communication between components with XML and input/output to data storage including database.

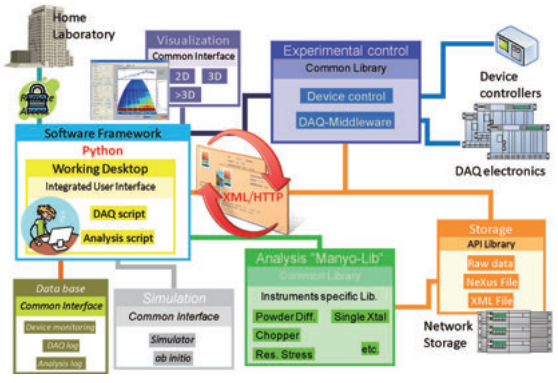

Fig.1 The diagram of MLF computing environment

One of the components, a user interface (UI) component called “Working Desktop” (WD), has been developed based on an object oriented script language, Python. Users can perform their experiment and data analysis by sending Python commands through the component. In another words, users can seamlessly operate experimental controlling, data analysis and visualization with one Python script. So far,

basic commands were implemented. Graphical user interface (GUI) of WD component is under development. We have been constructing several components in WD. The experimental controlling component consists of controlling DAQ hardware and other equipments such as sample environment devices and beamline components. We introduced "DAQ-Middleware" [2] as the standard DAQ software. Since DAQ-Middleware recognizes and absorbs differences between detectors, such as 3He gas position sensitive detectors, scintillation detectors and so on, commands on WD are the same for every kind of detector. The analysis component called "Manyo-Lib" [3] is a C++ library wrapped in Python by SWIG (Simplified Wrapper and Interface Generator). Manyo-Lib provides the standard data structure called "Element Container" based on STL (Standard Template Library). Users can process the data by using built-in functions of Manyo-Lib (for mainly data reduction) on Python command line and also add new functions written in Python or C++ for their own scientific analysis. Manyo-Lib is mainly responsible for heavy tasks like the conversion function of histograms from event data. The core function of histogram is implemented with GSL (GNU Scientific Library). The developed visualization component written by wxPython and matplotlib visualizes the 2D/3D data processed via Many-Lib.

We have grouped the instruments by kinds of detectors and the methods of analysis. Figure 2 shows software development groups of data acquisition (a) and data analysis (b). The software development of data acquisition has been grouped by a detector type such as He-PSD, Scintillator and GEM. That of data analysis has been grouped by the analytical methods such as inelastic, powder and so on. The software developed by each group is flexibly shared because it is developed under the standard software such as DAQ Middleware and Manyo-Lib.

Figure 3 is the actual data production from each MLF instrument after the proton power of J-PARC increased to 120 kW. We will prepare the data storage and high bandwidth network.

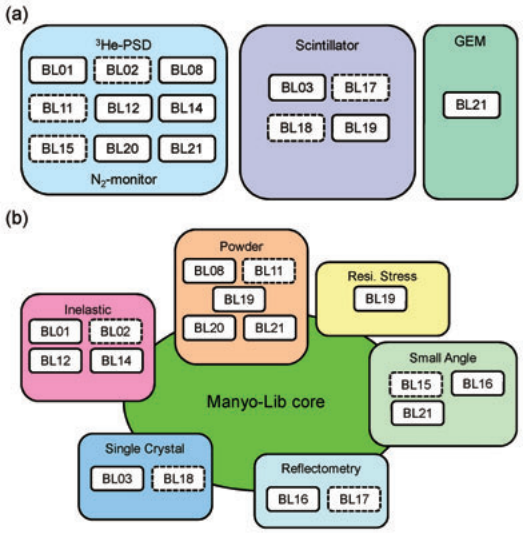

Fig.2 The software development groups: (a) data acquisition, (b) data analysis

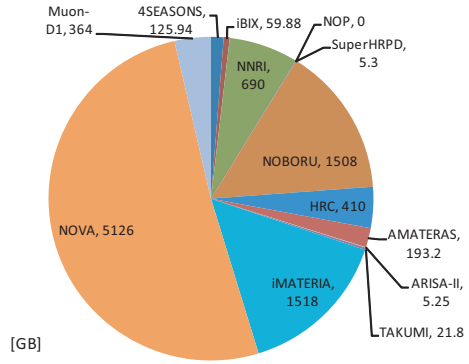

Fig.3 Data production of each instrument from Run #27, #28 and #29, total data size is 10TB.

The MLF computing environment unifies the instrumental control and data analysis under the common software environment. We will continuously develop the software with the aim of the improvement of usability in MLF.

References

1) T. Nakatani, Y. Inamura, T. Ito, S. Harjo, R. Kajimoto, M. Arai, T. Ohhara, H. Nakagawa, T. Aoyagi, T. Otomo, J. Suzuki, T. Morishima, S. Muto, R. Kadono, S. Torii, Y. Yasu, T. Hosoya, M. Yonemura, The proceedings of ICALEPCS 2009, in press.
2) K. Nakayoshi, Y. Yasu, E. Inoue, H. Sendai, M. Tanaka, S. Satoh, S. Muto, N. Kaneko, T. Otomo, T. Nakatani, and T. Uchida, Nucl. Instrum. Methods Phys. Res., Sect. A 600 (2009) 173.
3) J. Suzuki, T. Nakatani, T. Ohhara, Y. Inamura, M. Yonemura, T. Morishima, T. Aoyagi, A. Manabe and T. Otomo, Nucl. Instrum. Methods Phys. Res., Sect. A 600 (2009) 123.

T. NAKATANI, T. OTOMO*
Neutron Science Section, Materials and Life Science Division, J-PARC Center, Japan Atomic Energy Agency, Tokai, Ibaraki, 319-1195
* Institute of Materials Structure Science, High Energy Accelerator Research Organization, Tsukuba, Ibaraki, 305-0801

Disk Choppers at MLF, J-PARC

1. Disk-Choppers in MLF, J-PARC

Neutron disk-choppers are simple but indispensable devices for neutron spectrometers. Therefore most of the neutron instruments at MLF, J-PARC equip disk-choppers. The disk-choppers employed at constructed and planned neutron instruments in MLF, J-PARC are listed in Table 1. At MLF, two types of disk-choppers are used. One is slow disk-chopper, which runs at relatively slowspeed, $f \leq 50$Hz and is used to define the band width or frame or eliminate undesired neutrons. The other one is fast disk-chopper, maximum revolution of which can exceed 300Hz, and is used for a monochromater or shaping the pulse width of the neutron beam coming from source. Pulse shaping is a rather special task of the fast disk-choppers at MLF, since some inelastic instruments are taking a strategy to utilize high intensity from the coupled moderator source by shaping bad pulse shape from this type of source by fast disk-choppers to realize both high-intensity and high-resolution simultaneously. Therefore, many efforts have been devoted in the development works for fast disk-choppers as well as those for slow disk-choppers.

Two different benders, Kobe Steel Co. Ltd. and MEISYO KIKO provide disk-choppers to the instruments at MLF. There we try to unify the menu terms and look and feel and not to confuse in use.

Commissioning of disk-choppers was conducted by MLF chopper task team, which is headed by Dr. K. Shibata. Electronic noise level which can affect other devices in the experimental halls, and performance (phase stability, transmission of the disks, temperature evolution of spindles and housing and etc.) were investigated for all disk-choppers installed to instruments at MLF. The information is shared by all instrumental teams through this task team.

2. Slow Disk-Choppers

The slow-speed disk chopper was developed for the device as a band definition or a flame-overlap suppression chopper.

The prototype slow disk chopper was developed from 2004 with Kobe Steel Co., Ltd. Its main specifications were as follows.

i. For ease of maintenance, the neutron beam is passed under part of disk chopper, and body of chopper disk and motor is mounted on the stand (see Fig.1)
ii. For the reduction of disk weight, disk was made by aluminum alloy applied with {isotope enriched $^{10}B_4C$ powder + epoxy resin} as a neutron absorber.
iii. The transmission of neuron was less than 10^{-6} at Ei = 100 meV

Nowadays many slow disk choppers were produced and installed in many beamlines, which were designed referring to the prototype slow disk chopper even in those produced by MEISYO (see Table 1).

On the slow single disk chopper installed in BL19, we performed some commissioning tests. Fig.2 shows one of the commissioning results. From this phase control test, we determined the operational parameter for this disk chopper.

3. Fast Disk-Choppers

The development of fast disk-choppers was started from 2004 with Kobe Steel Co., Ltd. The cold-neutron disk-chopper spectrometer AMATERAS (BL14) requires the minimum burst time of less than 8 μsec. to realize 1%

Table 1 Disk choppers in MLF.

Beam Line	Type of chopper (No.)	Manufacturers
BL01	SI(2)	KOBELCO
BL02	FII(1),FI(2),SII(2),SI(1)	KOBELCO
BL03	SI(1)	MEISYO
BL04	SII(1)	MEISYO
BL08	SII(1),SI(1)	MEISYO
BL10	SI(1)	MEISYO
BL11	SI(2)	KOBELCO
BL14	FII(2),FI(1),SII(2)	KOBELCO
BL15	SI(3)	KOBELCO
BL16	SI(1)	Vacum Prod.
BL17	SI(3)	KOBELCO
BL18	SI(2)	KOBELCO
BL19	SI(1)	KOBELCO
BL20	SII(1),SI(2)	MEISYO
BL21	SI(1)	MEISYO

*S: slow chopper, F: fast chopper, I; shingle disk, II; double disk, (number of that type chopper in the beamline)

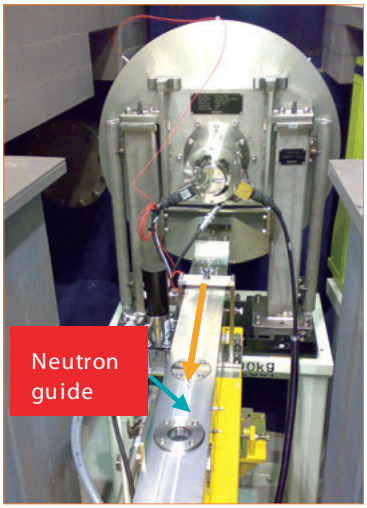

Fig.1 The slow single disk chopper installed in BL19 .

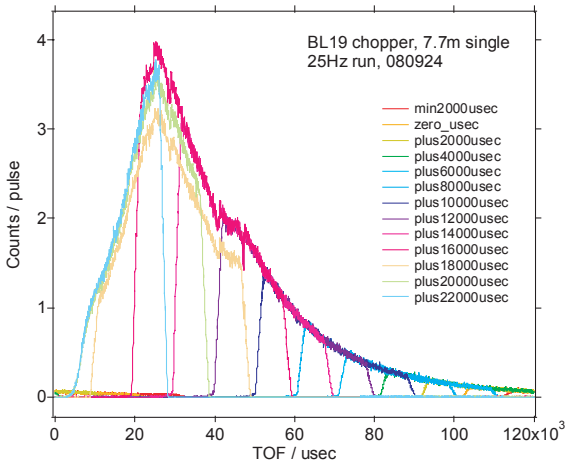

Fig.2 Phase control test on the slow single chopper in BL19. It shows the incident beam TOF spectrum selected by the disk chopper in the several phase delay conditions.

energy resolution. The requirement is that a disk of 600 mm diameter with 1 cm slit should run at 350Hz revolution. In 2004, such disk-choppers were not available in the world, which is the reason why we started the development. There were several technical issues in the development. The most important clue is the disk itself. After experiencing several crashes of disks and sometimes a full chopper system, finally disks can be run at revolution of > 350Hz. (Fig. 3(a)) Special care was taken in optimizing direction of fibers of CFRP and method of placing. Also, we adopted metal ^{10}B, not $^{10}B_4C$ to reduce the mass at the edge of the disk.

At MLF, three sets of fast disk-choppers have been installed at AMATERAS (BL14). Specifications of three choppers of AMATERAS are listed in Table 2. By combination of No. 2 chopper, No. 1 chopper shapes the width of a pulse from the source. No. 2 chopper is the monochromating chopper. No. 3 chopper is used for removing unwilling neutrons coming through No. 1 choppers. Motors and disks of No. 2 chopper are placed one above the other to set two disks as close as possible (Fig. 3 (b)).

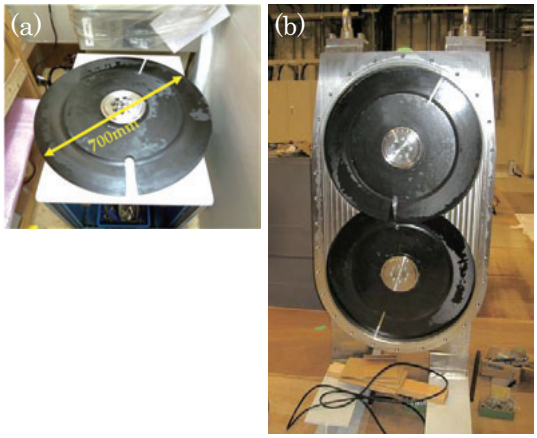

Fig.3 (a) A disk for fast-disk choppers and (b) inside view of No. 2 fast-disk chopper of AMATERAS.

That is essential to perform multi-E_i measurements on AMATERAS. [1] Commissioning of fast disk-choppers has been done in the course of the commissioning of AMATERAS. By using these choppers, we have confirmed $\Delta E/E_i \sim 1\%$ energy resolution in the range of $E_i \leq 3$ meV.

Table 2 Fast disk-choppers installed at AMATERAS.

	No. 1	No. 2	No. 3
$L_{modrator\text{-}chopper}$	7.1 m	28.4 m	14.2 m
Disk Radius	350 mm	350 mm	350 mm
Revolution	≤350 Hz	≤350 Hz	≤350 Hz
No. of Disks	2 (Counter-Rotating)	2 (Counter-Rotating)	1
Slit Width	30 mm	10 & 30 mm	30 mm
Min. Burst Time	22.7 μsec.	7.6 μsec.	45.5 μsec.
Gap between Disks	50 mm	20 mm	-

Drawing on the experience of fast disk-choppers of AMATERAS, now manufacturing of other fast disk-choppers is in progress for the biomolecular dynamics spectrometer DNA (BL02). DNA will use three sets of fast disk-choppers (one of 300 Hz-type and two of 200Hz-type) and these choppers will be delivered in 2011.

References

1) M. Nakamura, K. Nakajima, R. Kajimoto, M. Arai, J. of Neutron Res. **15** (2007) 31-37.

K. Nakajima and K. Shibata Neutron Science Section, MLF Division, J-PARC Center

Development of T0 chopper

At KEK, the T0 chopper has been developed under the collaboration between Neutron Science Division (KENS) and Mechanical Engineering Center (MEC). To utilize eV neutrons, we designed and assembled a T0 chopper rotating at 100 Hz. On BL12 at J-PARC/MLF, the dimension of the chopper blade (shielding part) on the rotor was 78 mm × 78 mm × 300 mm (300 mm is the length along the beam) with the margin of $\Delta w = \pm 1$ mm (the beam cross section is 76 mm × 76 mm). This margin corresponds to the phase control accuracy of ± 5 μs at f = 100 Hz ($\Delta t = \Delta w / 2\pi Rf$), where R = 300 mm is the rotational radius of the rotor. Since this T0 chopper was installed at 8.5 m from the neutron source, high energy neutrons up to 2 eV can be utilized. In our T0 chopper, the rotor made of Inconel X 750 was mounted inside the vacuum, the shaft is supported by ball bearings, and the rotation is transferred through a magnetic seal from the motor located outside the vacuum chamber. A continuous running time of 1000 hours and a total running time of 4000 hours are required without changing components. We confirmed these specifications. We transferred these results of the development to a company and successfully started the production of the actual machines of the T0 choppers for the beam lines, BL04, BL12, BL16, and BL21, at J-PARC.

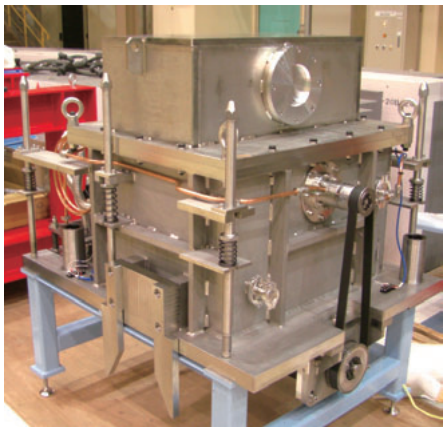

Fig.1 The T0 chopper developed at KEK for BL12.

On the other hand, a more compact type T0 chopper has been developed in collaboration with JAEA/MLF and Kobe Steel, Ltd (KOBELCO). To reduce overall size, we introduce an in-wheel type motor to the T0 chopper. This type motor having an inner stationary portion (the stator), and an outer rotating portion (the outer-rotor) that rotates around the stator and drives a chopper blade (Inconel X 750) attached to the outer-rotor. By attaching the blade directory to the outer surface of the outer-rotor, a compact and stable T0 chopper, rotating 50 Hz, system has been achieved. On BL01 (4-SEASONS), the dimension of the chopper blade (shielding part) on the outer-rotor is 84 mm × 84 mm (cross section) × 300 mm (long along the beam), and the thickness (along the beam) of the whole body is 500 mm. The phase control accuracy is ± 5 μs at f = 50 Hz, where R = 300 mm is the rotational radius.

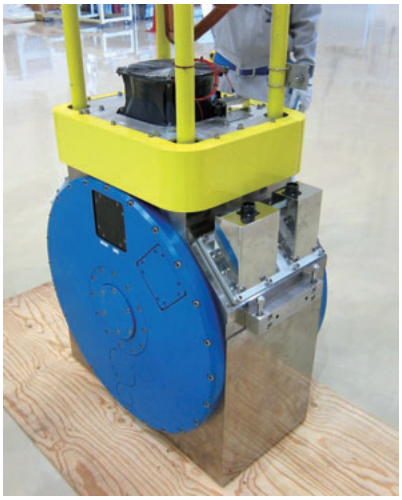

Fig.2 The T0 chopper developed by JAEA/KOBELCO for BL01.

The first T0 chopper of this type installed at BL01 shows powerful effect to suppress the high energy neutrons and to reduce the background dramatically (see Fig. 5 in the report of BL01). The compact type T0 chopper (50 Hz) will be installed on BL11, BL15, and BL18.

S. Itoh, K. Suzuya* and R. Kajimoto*
Neutron Science Laboratory, Institute of Materials Structure Science, High Energy Accelerator Research Organization, Tsukuba, 305-0801
*Materials & Life Science Facility Division, J-PARC Center, Japan Atomic Energy Agency, Tokai, 319-1195

Development of Fermi chopper

At KEK, the Fermi chopper has been developed under the collaboration between the Neutron Science Division (KENS) and Mechanical Engineering Center (MEC). We tried to develop the Fermi chopper by modifying a turbo molecular pump (TMP) with a magnetic bearing system. First, the TMP blade was replaced by the slit package, and we could rotate up to 600 Hz by the TMP controller. Next, we tried to design the phase control system of the Fermi chopper synchronized with the repetition of the accelerator. We could drive the motor of this system by an external power supply and just by using the TMP controller as a magnetic bearing controller. Finally, we successfully developed the phase control system. Based on the developments, we produced the first model of the Fermi chopper made in Japan, as shown in Fig. 1. The commercially available composites made of boron fibers were used for the slit materials. In this actual system, we confirmed the phase control accuracy less than 0.3 μs at 600 Hz against the timing of the external trigger. A shifting mechanism of two Fermi choppers was also developed in order to select one of the choppers or white beam condition. The investigations of the slit materials for high energies are still in progress.

On the other hand, a Fermi chopper developed by SKF Magnetic Bearings is introduced for BL01. It utilizes a magnetic bearing and can rotate the slit package up to 600 Hz with an accuracy of $< \pm 0.05°$. The slit package was developed by SNS and loaned to JAEA by courtesy of SNS. The slits consist of boron absorbers and aluminum spacers. The important feature of the slits is that they have straight shape, which enhances the transmission of neutrons over a wide energy range and enables a measurement with multiple incident energies (multi-E_i measurement). The Fermi chopper is located on a translation table which was designed by a technician of J-PARC. One can switch between the chopper-on/off statuses remotely.

In addition, we are developing a new slit package for low energy measurements and one for the multi-E_i measurements. The former utilizes gadolinium thin films as the absorbers. The latter, which is called 'MAGIC chopper', utilizes supermirror-coated slits. These special slits automatically tune the opening time for a wide neutron energy range by reflections of the mirror. We have already developed a prototype of the slit package of the MAGIC chopper, and performed test measurements for the angular dependence of the transmission at MUSASI in JRR-3 and NOBORU in MLF.

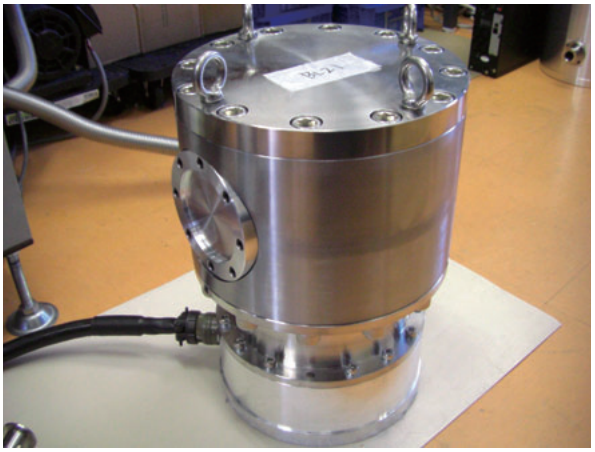

Fig.1 The 1st Fermi chopper made in Japan

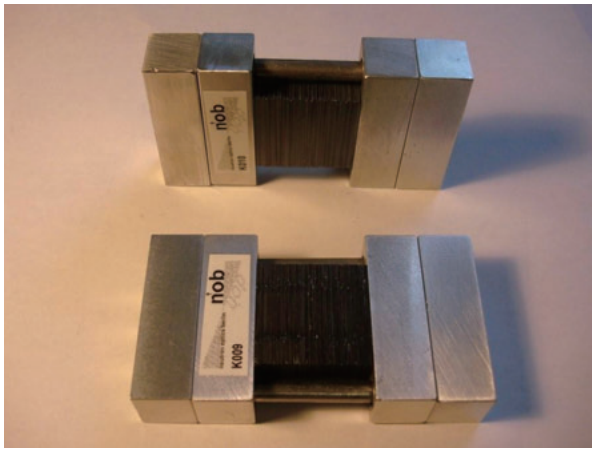

Fig.2 Pieces of prototype slit packages for the MAGIC chopper (collaboration with Th. Krist)

S. Itoh and R. Kajimoto*
Neutron Science Laboratory, Institute of Materials Structure Science, High Energy Accelerator Research Organization, Tsukuba, 305-0801
*Materials & Life Science Facility Division, J-PARC Center, Japan Atomic Energy Agency, Tokai, 319-1195

Neutron Guides

Neutron guide is an important device for neutron instruments that is usually used to avoid intensity loss, to reduce backgrounds and in some cases to increase intensity for small gauge volume. Since J-PARC/MLF is a pulsed neutron source, most neutron instruments apply the time-of-flight (TOF) method. As is well known, many TOF instruments have long primary flight paths (distance from neutron source to sample position) to increase their instrumental resolutions. Therefore, neutron guides are especially essential for neutron instruments having long primary flight paths, and designing neutron guide is very important since it may determine performances of the instruments.

There were seven instruments constructed in MLF at 2008 FY. The instruments and the applications of neutron guides are listed in Table 1.

Table 1. Instruments in MLF at 2008 FY

Instrument	L1 (m)	Neutron guide devices
BL01 4SEASONS	18	Straight, vertical & horizontal elliptically focused
BL03 iBIX	40	Curved, vertical linearly tapered
BL04 NNRI	22, 28, 29	---
BL08 SuperHRPD	94.2	Curved
BL10 NOBORU	14	---
BL19 TAKUMI	40	Curved, vertical elliptically focused (end part)
BL20 iMATERIA	26.5	Straight

Fig.1 Neutron guide system of BL01 4SEASONS

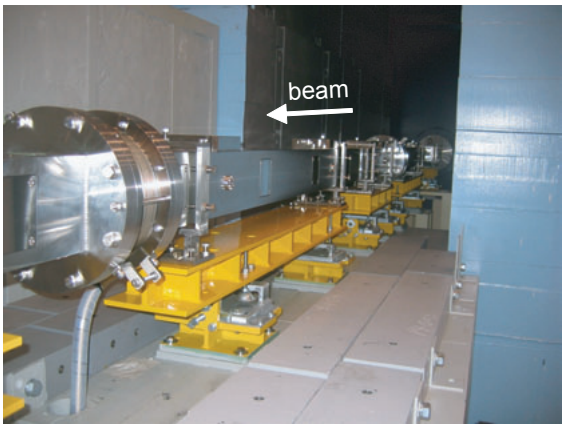

Fig.2 Neutron guide of BL01 after allignment

BL01 4SEASONS

On 4SEASONS [1], the sample position is 18 m downstream of the coupled moderator. The neutron guide tube starts at L (distance from the moderator) = 2.3 m and ends at L = 15.8 m (with gaps for T0 and disk choppers). It is straight and elliptically converged guide with cross-sectional areas of 90x90 mm^2 at the entrance and 43 x 43 mm^2 at the exit. It is equipped with high-critical angle super-mirrors with m = 3.2-4.0, most of which were manufactured in the in-house facility. The mirrors are housed in a thick stainless steel jacket (see Fig.1), and the jacket is evacuated by a scroll pump.

BL03 iBIX

On iBIX [2], the sample position is 40 m downstream of the coupled moderator. The neutron gu-ide starts at L = 13m and ends at L = 38 m with a 17 m curved section followed by 8 m straight and tapered section in the horizontal direction. The whole section is a vertically tapered guide with cross-sectional areas of 17.0 x 68.0 mm^2 at the entrance and 14.3 x 14.3 mm^2 at the exit. The neutron guides are equipped with high-critical angle super-mirrors with m = 1.0~3.0. The mirrors are housed in a steel jacket (see Fig. 3) which is evacuated by a scroll pump. The adjustable stages with stepping motor were

installed on the joints between the steel jackets in order to realign easily the mirrors even after the subsidence of ground (see Fig. 4). A hydrostatic leveling system is set along beamline to watch the floor elevation over the long period.

Fig.3 Neutron guide system of BL03 iBIX

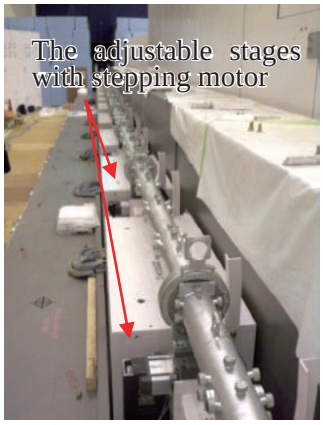

Fig.4 Neutron guide of BL03 after alignment

BL08 SuperHRPD

SuperHRPD sample position is located at 94.2 m from a thin side of a decoupled poisoned moderator. To install such a long flight path instrument, a beamline building with 50 m length and an annex experimental hall are constructed on the east side of MLF experimental hall. Neutron guides start at L = 7.1 m, with a 32 m curved section followed by 50 m straight section (Fig. 5) (with gaps for disk choppers). Cross-sectional areas at the curved section and the straight section are 25 x 75 mm^2 and 25 x 55 mm^2, respectively, to minimize neutron loss at the building junction due to an unequal settlement. They are equipped with high-critical angle super-mirrors with m = 3.0. The mirrors at the curved section are housed in a stainless steel jacket, and the jacket is evacuated by a scroll pump. The mirrors at the straight section have no steel jacket housing, and are evacuated directly from both entrance and exit parts. A hydrostatic leveling system is set along the beamline to watch the floor elevation over the long period.

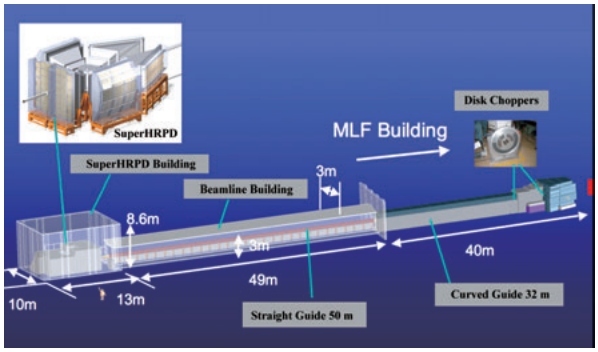

Fig.5 Image view of BL08 SuperHRPD

BL19 TAKUMI

On TAKUMI [3], the sample position is 40 m downstream on the thick side of a decoupled poisoned moderator. The neutron guides starts at L = 7.8 m, with a 20 m curved section followed by a 10 m straight section (with gaps for optional disk chopper and a divergence slit). The cross-sectional area at the curved part is 20.0 x 59.8 mm^2. The straight section is vertical elliptically converged guide with cross-sectional areas of 20.0 x 59.8 mm^2 at the entrance and 20.0 x 40.2 mm^2 at the exit. The neutron guides are equipped with super-mirrors with m = 2.0-3.0. The mirrors are housed in a thick stainless steel jacket (see Fig. 6), and the jacket is evacuated by two scroll pumps. A hydrostatic leveling system (see Fig. 6) is set along beamline to watch the floor elevation over the long period.

Fig.6 Neutron guide system of BL19 TAKUMI

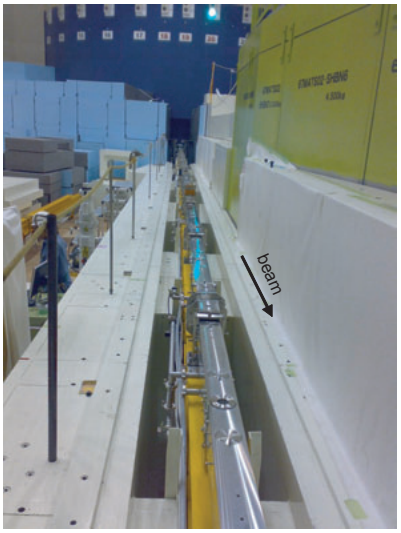

Fig.7 Neutron guide of BL19 after allignment

Fig.8 Neutron guide system of BL20 iMATERIA

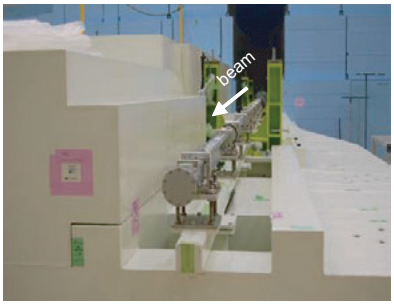

Fig.9 Neutron guide system of BL20 iMATERIA

BL20 iMATERIA

On iMATERIA [4,5], the sample position is 26.5 m downstream on the thick side of a decoupled poisoned moderator. The neutron guides start at L = 7.6 m and end at L = 23, with the total length of 14 m. They are straight with reducing cross-sectional areas step by step; 39.7 x 39.7 mm^2 for the first 2.4 m section, 34.4 x 34.4 mm^2 for the second 7.4 m section, and 34.0 x 34.0 mm^2 for the third 14 m section (there are gaps for disk choppers in between). The neutron guides are equipped with high-critical angle super-mirrors with m = 3.0. The mirrors are housed in a stainless steel jacket (see Fig. 8), and the jacket is evacuated by a scroll pump.

References

1) R. Kajimoto, T. Yokoo, K. Nakajima, M. Nakamura, K. Soyama, T. Ino, S. Shamoto, M. Fujita, K. Ohoyama, H. Hiraka, K. Yamada and M. Arai, J. Neutron Res. **15** (2007) 5-12.
2) I. Tanaka, K. Kusaka, K. Tomoyori, N. Niimura, T. Ohhara, K. Kurihara, T. Hosoya, T. Ozeki; NIMA 600(2009) 161-163.
3) S. Harjo, A. Moriai, S. Torii, H. Suzuki, K. Suzuya, Y. Morii, M. Arai, Y. Tomota, K. Akita and Y. Akiniwa: Mater. Sci. Forum, **524-525** (2006) 199-204.
4) T. Ishigaki et al., Physica B **385-386** (2006) 1022-1024.
5) S. Harjo, T. Kamiyama, S. Torii, T. Ishigaki, M. Yonemura, Physica B **385-386** (2006) 1025-1028.

S. Harjo, R. Kajimoto, S. Torii, T. Ishigaki* and K. Kusaka*
Neutron Science Section, J-PARC Center, Tokai, Naka, Ibaraki
*Frontier Research Center for Applied Atomic Sciences, Ibaraki University, Tokai, Naka, Ibaraki

Sample Environment at MLF

Facility supports on experimental requirements are essentially significant in order to carry out user experiments and maintain facility service. Sample environment (SE) is one of the key items to control the success in neutron researches. Particularly in a large facility, it is necessary to prepare for various demands of experiments. J-PARC/MLF is required to equip many types of SE devices as well.

We started organizing the SE team and establishing a guideline (*SE-protocol*) for standardization of equipments and devices, to begin with. In 2001, SE-task has been organized by several scientists as a forerunner of the current SE team. Now, the team is composed of three technical staffs and two scientists as a sub-group of device safety group, obviously not enough number for supporting full SE at MLF. The SE team and budget should be expanded in the near future. The above mentioned former SE-task members shifted to an advisory SE team in charge of administration of whole SE matters such as requesting budget, investigating, strategic discussion, a liaison with the user community and so forth.

Starting with organized small members, a SE standardization guideline has been settled as *SE-protocol*. It is stated in the *protocol* that flange type (dimension), distance from beam center to the bottom of the flange, recommended cryostat engine, controllers, temperature sensors, a type of couplings, and so on. Since J-PARC/MLF is the aggregate community in viewpoint of operating the facility, funding source, ownership *etc.*, the guideline essentially makes sense with the concept of standardization that saving resources, manpower, costs and time, also sharing the devices. It should be also noted that researchers have taken care of everything by themselves in Japan. Taking into account this historical fact, each beamline prepares its own desired SE devices. However, for the use of large devices such as dilution refrigerator and large high magnetic field devices, standardized design of instrument enables us to share the expensive devices. Table 1 is the list of SE devices currently available for the experiments. Since we just started the user programme, these numbers and the range of supports will be enhanced.

Table 1 List of SE devices used (will be used) in MLF/J-PARC for user program

BL	SE Devices	Options	SE Devices (being installed)
BL01	4K TL Cryo *1	ω-gonio	600K heater option
BL03	Gasflow Cryo		
BL04	ASC *2		
BL05	N/A		
BL08	4K Cryo 10K TL Cryo ASC		
BL10	Goniometer		
BL12	4K TL Cryo	ω-gonio	1K cryo ω-gonio
BL14	4K Cryo	ω-gonio	
BL16	ASC		
BL19	Loading machine Furnace (1000)	In-situ neutron dilatometer	
BL20	ASC		
BL21	ASC		In-situ measurement system *3

*1 "TL" represents "Top Loading"
*2 ASC=Auto Sample Changer
*3 H2/D2 gas 10MPa 50-473K, vanadium foil heater

As a future plan, the following several items are now considered.

1) Expanding budget and manpower, in particular long term plan to achieve similar levels of resourcing over some reasonable timescale.

2) The workshop space in MLF must be maintained for SE devices as well as chopper maintenance area.

3) Thousands of SE devices and tools at former pulse neutron facility KENS are scheduled to be moved and reused in J-PARC.

4) As mentioned above, ordinal devices such as 4K cryostat and goniometer are prepared by each instrument according to users' demands. However, MLF is responsible for some special devices that require particular expertise like huge magnet, dilution refrigerator and so forth.

T. Yokoo, S. Kawamura T. Kambara, K. Nakajima, A. Hoshikawa, R. Kajimoto, S. Torii, Y. Inamura, T. Nakatani and J. Suzuki
Material and Life Science Division, J-PARC Center

Software Development on Chopper Spectrometer for MLF, J-PARC

Introduction

In MLF of J-PARC, several inelastic spectrometers, such as BL01 and BL14, have been constructed and have started their operation. At the same time, the development of software to control instrument devices and to analyze data for users is also our urgent task for running these instruments. The required software for chopper instruments consists of several parts, i.e. the instrument control (data acquisition and devices), support for decisions of experimental conditions, data reduction and visualization. In this development works, we considered some features of computing environments peculiar to MLF. One feature is that software developments should be based on two software frameworks, i.e. MLF software frameworks [1] and Manyo Library [2]. Another feature is the event data recording method. MLF decided to employ this method instead of the traditional histogram recording method. On making histogram from event-recorded data for analysis, users can freely and flexibly decide or remake the binning of both time and position after the measurement.

Each developed program has both the command-based interface on Python interpreter and the graphical user interface (GUI) constructed by wxPython [3]. These programs can be mainly executed on Linux. Some developments, especially in data reduction part, have been progressed under collaboration between J-PARC and HANARO in Korea. The results of this collaboration will also be utilized on a chopper spectrometer for HANARO, which is under construction.

Status of development

Currently, we have already produced a series of software for the instrument control, the informative visualization, the data reduction, the data visualizations and the commands sequence control, as described below.

Instrument control software

An inelastic spectrometer consists of many devices to be controlled by users on their measurements. For example, BL01 has a DAQ system, three choppers, two beam narrowers, sample temperature control and goniomator for a direction of sample. This software has several GUI tabs used as an interface to set parameters of each device.

Informative visualization software

This software, shown in Fig. 1, is a utility to help users in making decisions on the experimental conditions such as chopper frequencies, choice of incident energies, choices of slit packages of Fermi-choppers or slit width of disk-choppers and so on. Before users carry out their measurements, they can consider experimental parameters by referring visual information in the space for momentum transfer (Q) and energy transfer ($\hbar\omega$). Reachable space is determined by certain crystal orientation and instrumental conditions given. This software can display Q-$\hbar\omega$ space, expected flux at sample position and expected resolutions in Q and $\hbar\omega$ at the specific point.

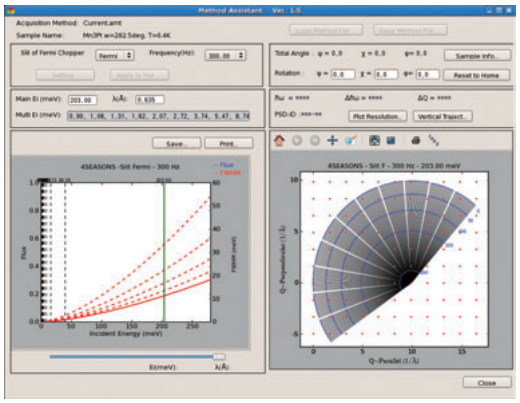

Fig.1 Screen shot of the informative visualization.

Data reduction software

Data reduction means processes to obtain a dynamical structure factor, $S(\vec{Q}, \hbar\omega)$, from raw event data produced by DAQ system. When all neutron events are stored as series of events with their own unique time tags, they will be called into the first step of the data reduction software, “Event to Histogram”. Here, it will be converted to histograms, which will be further checked to discriminate data from bad detectors by so-called masking process. Then time-of-flight (TOF) of the data is converted to the energy transfer by

using detector information embedded in histogram data. After the conversion, the data of individual segments of detectors will be constructed by using information described in a mapping file. For example, circular averaging (averaging on same |Q| value) can be done at this part. After that, background treatments (subtraction of empty can data and constant background correction), normalization by monitor counts, Vanadium correction and detector efficiency correction will be carried out. Then users obtain $S(\phi, \hbar\omega)$ or $S(\vec{Q}, \hbar\omega)$, which will be used in other analysis programs produced by us and other developers. Each part of these processes is produced as an individual module of Python script or C++ functions in Manyo Library. Most of modules have been already utilized in several instruments.

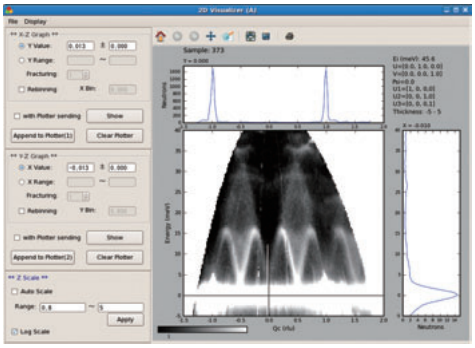

Fig.2 Example of visualization software (2D-plotter)

Visualization software

Visualization software helps users to treat and visualize any data in or after data reduction steps, such as the simple TOF data and the $S(\vec{Q}, \hbar\omega)$ data. $S(\vec{Q}, \hbar\omega)$ data calculated from inelastic neutron scattering have the five dimensions (three axes for Qx, Qy, Qz, one axis for $\hbar\omega$ and the intensity). Visualization software mainly consists of several parts, PSD map visualization, 1D-plotter (X and Y axes), 2D-plotter (X, Y axes and the intensity), shown in Fig.2, and the single crystal data slicing software from a higher dimensional space to a lower dimensional one. These plotters can be controlled by direct commands on Python interpreter or by means of the interface for commands in the other software.

Command sequence control software

This software helps users to make procedures for executing analysis commands (Fig. 3). Users can select necessary command from the Command List placed on left column of the window, which the instrument scientist prepared beforehand, and enter its command to the Sequence List in the middle. A set of arguments for selected command in the Sequence List is shown in a frame on the bottom. The contents in the arguments frame change dynamically by the motion of selecting command. Users can control command sequence step by step by means of buttons to start, stop and resume. Data produced by commands can be sent directly to visualization software. In addition, the command sequence can be saved as a file of python script, which is directly executed on console. Currently, executable commands on this software are limited to the use for analysis. We have a plan to extend the use of this software to control instruments and devices.

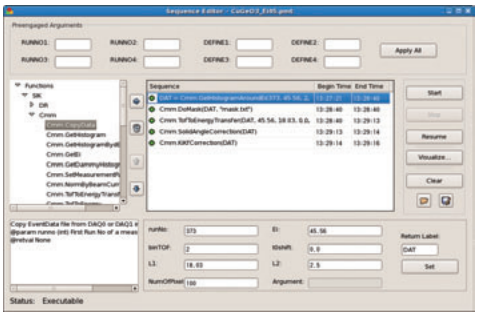

Fig.3 Screen shot of command sequence control.

Summary

A series of software for chopper spectrometers in MLF has been produced. This includes a lot of results of software developments, i.e. MLF software framework, Manyo Library project and the collaboration between J-PARC and HANARO. We have successfully utilized them to control instruments on many experiments and to analyze and visualize actual measured data, as described in other pages about BL01 [4] and BL14 in this report.

References

1) T. Nakatani et al., submitted to Proceedings of ICALEPCS2009 JACoW.M.
2) J. Suzuki et al., Nuclear Instruments and Methods in Physics Research, A 534(2004) 175.
3) http://www.wxpython.org/
4) M. Nakamura et al., *J. Phys. Soc. Jpn. 78(2009) 093002*

Y. Inamura Material and Life Science Division, J-PARC Center

STARGazer, a data processing software for iBIX

For a single crystal diffractometer, data processing software which extracts a HKLF list from raw data of detectors is one of the most important components. We have developed new data processing software, named "STARGazer", for a new TOF single crystal neutron diffractometer, "IBARAKI Biological Crystal Diffractometer (iBIX)", which is constructed at Materials and Life-science Facility (MLF) of J-PARC.

STARGazer has several functional components; 1) making histogram format data from the event format raw data of detectors, 2) peak search from the histogram data, 3) determination of the UB matrix, 4) finding the Bravais lattice, 5) refinement of the UB matrix, 6) calculating the intensities of all Bragg reflections, and 7) data visualization. The procedure of data processing is shown in Fig. 1 and the GUI is shown in Fig. 2. The algorithms of crystallographic fundamental functions of those components referred the algorithms of program ISAW [1], which is a data processing software package developed on Argonne National Laboratory. In addition, STARGazer has some additional functions optimized for the measurement of protein crystals on the iBIX; real-space indexing technique to find UB matrix, refinement of the detector position simultaneously in UB matrix refinement, and finding the Bragg reflections which are overlapping with neighboring reflections. In the near future, a function to de-convolute the overlapping Bragg reflections will be added.

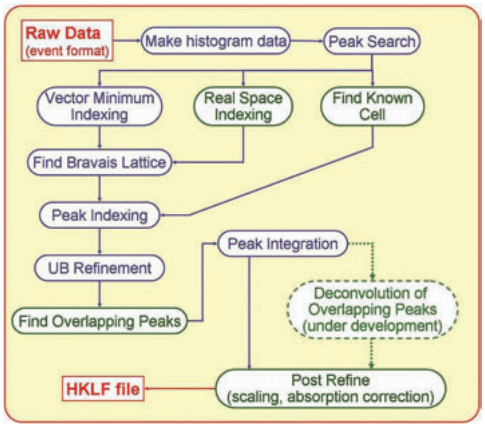

Fig.1 Procedure of data processing by STARGazer.

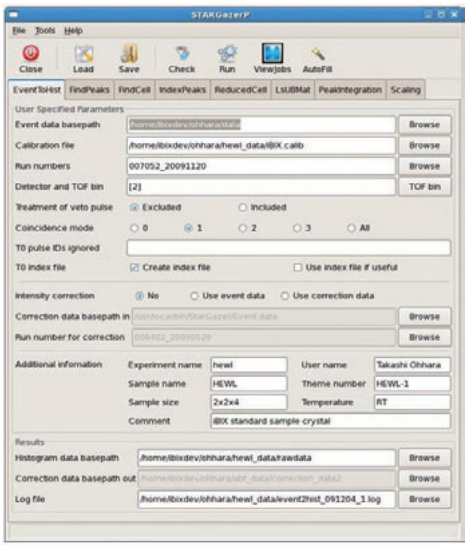

Fig.2 Tab structure GUI for the data processing functions of STARGazer.

STARGazer also has a feature to visualize the histogram data of detectors. In addition, predicted positions of Bragg reflections can be overlapped on the data of detectors as shown in Fig. 3. Therefore, users of iBIX can confirm whether the obtained UB matrix is correct or not by using this feature.

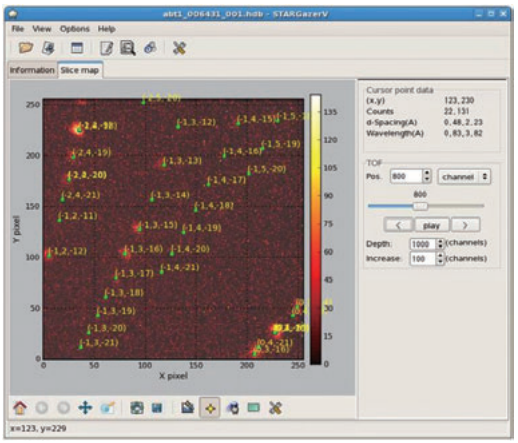

Fig.3 Data visualization by STARGazer. Green points and yellow numbers denote the predicted positions of Bragg reflections and those indexes.

STARGazer was developed based on a software library "Manyo-Lib" [2], which is framework software for data analysis at MLF developed by J. Suzuki and co-workers. Each component of STARGazer works independently as a part of Manyo-Lib, and users of other

instruments in MLF and other pulsed neutron facilities can easily use the components for their data processing.

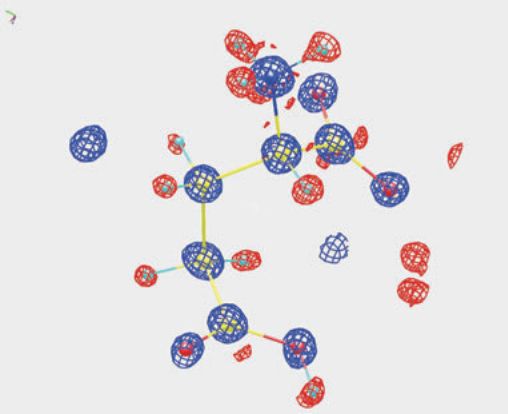

Fig.4 Density map of atomic nuclear scattering length of glutamic acid obtained by iBIX and processed by STARGazer. Blue mesh denotes positive density(+3σ) and red mesh denotes negative (-3σ). Negative density shows the positions of hydrogen atoms (light blue).

We have already collected and processed neutron diffraction dataset of ammonium bitartrate, glutamic acid and some crystals of organic molecules. Fig. 4 shows a density map of atomic nuclear scattering length of glutamic acid obtained by iBIX and processed by STARGazer. As is shown in this figure, hydrogen atoms were observed as negative density and non-hydrogen atoms were positive. The obtained cell parameters agreed with the known values and positions of hydrogen atoms are reasonable.

References

1) http://www.pns.anl.gov/computing/isaw/index.shtml
2) J. Suzuki, K. Murakami, A. Manabe, S. Kawabata, T. Otomo, M. Furusaka, Nuclear Inst. & Meth. Phys. Res., A534, 175 (2004).

T. Ohhara
Quantum Beam Science Directorate/J-PARC Center, Japan Atomic Energy Agency, Shirakata-shirane 2-4, Tokai, Ibaraki 319-1195, Japan.

Dan Neumann (NIAC chair, NIST) smiling with his favorite large buckyball (iBIX detector module).

Data reduction software for TAKUMI

As described in the instrumental chapter, the Engineering Materials Diffractometer "TAKUMI" has been constructed on BL19. In TAKUMI, event data taken by an event recording system have information of time-of-flight (*TOF*) in 1μs units, detecting positions of 3600 pixels and neutron pulse timings in micro second during one measurement for every neutron count. It is necessary to manipulate various types of histograms from event data to achieve experimental purposes, for example, 2θ - *TOF* 2-d histogram for the texture analysis, or *time-TOF* 2-d histogram for *in-situ* time transient measurement. Figure 1 shows a conceptual diagram of data container of histograms. Users can select binning pattern or extraction section of *TOF* (or *d-spacing*), detecting pixel and real time using TAKUMI's software.

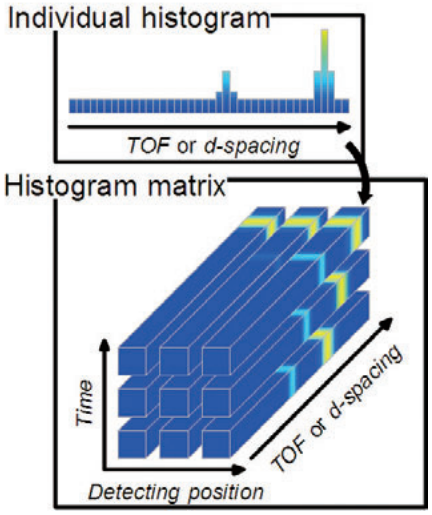

Fig.1 Conceptual diagram of histogram data container. *TOF* (or *d-spacing*) histogram constitutes of detecting position (pixel) and time matrix.

Figure 2 shows an in-situ experiment program with changing temperature and (compressive) load (a), and diffraction pattern (b) obtained during the measurement. In this case, we start diffraction measurement and heating/compression test in synchronized time. We can then slice data in accordance with time, temperature, load or statistics. Event recording system is very useful for such type measurement in that we can manipulate data even after measurement has finished, and this will lead us to take advantages of the diffraction data as much as possible.

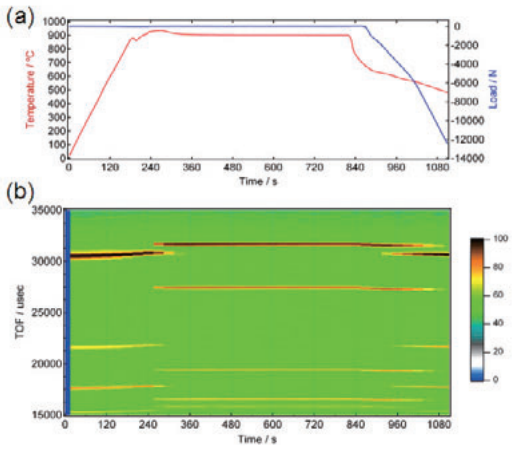

Fig.2 Result of neutron diffraction measurement under high temperature and compression loading. (a) Temperature and compression load profile. (b) *Time-TOF* 2-d diffraction pattern.

Figure 3 shows 2θ-*d-spacing* 2-d histogram of a superconducting composite material. It consists of highly oriented superconductor and less oriented substrates. We can observe preferred orientation of superconductor and extract a histogram in the region of interest using this type histogram creation.

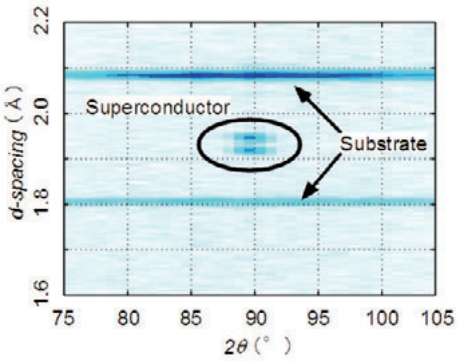

Fig.3 2θ-*d-spacing* 2-d histogram of a superconducting composite material which consists of superconductor and substrate.

In conclusion, event recording system and histogram creation software provide us with various types of histograms to analyze transient phenomena, i.e. heating or tensile loading process, or texture with much greater flexibility than conventional data recording system.

T. Ito and S. Harjo
Neutron Science Section, Materials and Life Science Division, J-PARC Center, Japan Atomic Energy Agency, Tokai, Ibaraki, 319-1195

DAQ System

In MLF/J-PARC, a lot of neutron experimental instruments which have groups of detectors with thousands of pixels are measuring the neutron signals. The types of the detectors are various, such as ^{3}He-position sensitive detector (He-PSD), 1D/2D scintillation detector and the gas electron multiplier (GEM) type detector according to the purpose of the instruments. We have standardized the DAQ system to record the signals detected by these detectors. We have also decided to record the signals in event by event with clock because we want to know the history of each neutron from production to detection. Thus, for example, in the case of the measurement of transient phenomena, we can reconstruct the correlation between the neutron and each phenomena recorded with clock under the various conditions after the measurement.

It is the first priority of our DAQ system that the system records the neutron detection events without fail. The second priority is that the system is scalable according to increasing the neutron intensity of MLF/J-PARC. The third priority is the standardization using commercial products to the utmost. For these purposes, we have introduced the field bus with Ethernet into our standard DAQ system. The user interface (CPU UI), DAQ computers (CPU DAQs) and DAQ electronics are connected via Ethernet as shown in Fig. 1.

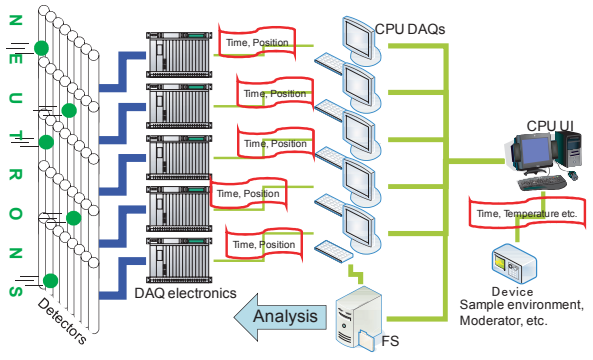

Fig.1 The schematic view of the event mode DAQ system.

In this system, there are two new technologies developed in KEK. One is the specified Ethernet interface which we call "SiTCP" [1]. Another is the flexible and scalable DAQ software which we call "DAQ-Middleware" [2]. The features of the SiTCP are the data transferability with almost 100Mbps full speed, the ability of implementation on one chip, low power and low noise. The SiTCP looks like FIFO memory from electronics and TCP server from computers. We attach the SiTCP on each of our DAQ electronics [3]. The DAQ-Middleware is a software framework specified data acquisition and consists of several DAQ-Components. The DAQ-Middleware is based on Robot Technology Middleware (RTM) developed in Advanced Industrial Science and Technology [4]. The RTM is one of the Object Management Group domain specifications. We have installed the DAQ-Middleware in CPU DAQs. The DAQ-Middleware includes the function of data recording into storage as well as online monitoring. We can measure monitoring the 2D image on the detectors and TOF histogram. We can do run control our DAQ system by exchanging the messages (Begin/End/Pause/Resume) written in XML format via our software framework [5] and a web-browser.

Every neutron event data includes the information of TOF and the position when and where each neutron was detected. The event data format is different depending on the kinds of the detectors. In the past histogram recording, we have recorded the data preselected TOF bin. In the event recording, we can do histogram in arbitrary time bin width after the measurement. As an example, we show the event data formats of He-PSD in Fig. 2. We have developed two types of DAQ electronics, NEUNET and GATENET. The NEUNET processes the neutron event detected by He-PSD and the GATENET controls trigger of the spallation (TOF trigger) and counts the clock. In additional function, the GATENET processes the neutron monitor event and the external trigger event. Each neutron event data processed in the NEUNET includes the values of the pulse height at both ends of the PSDs. Because of this, we can resolve arbitrarily the pixel size by changing the proportional distribution of the PSD. The event data from

GATENET include the pulse ID which shows the number of the spallation and the clock information of the TOF trigger (T_0 data and Instrument clock data shown in Fig. 2). We also measure the status of the devices of the sample environment and the beamline components with the clock. Furthermore, the status of the neutron source is recorded with the clock, such as the proton current in every beam shot, the temperature and the ratio of ortho / para hydrogen of the moderators, and so on. We can recognize the correlation between the neutron detection event and these statuses. For example, we can extract the data set of various conditions in the transient phenomena.

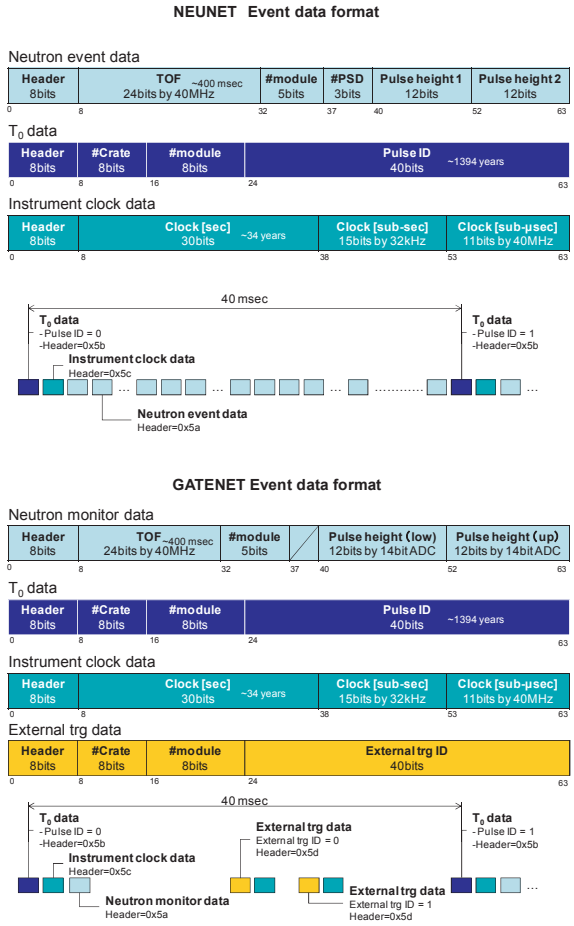

Fig.2 The event data formats in He-PSD DAQ system

There are 23 neutron instruments in MLF/J-PARC. Now 12 instruments are in operation. Our standard DAQ system has been installed in eight instruments shown in Table 1. The number of the He-PSD type is 6, the scintillator is 2 and GEM is 1. We have been grouping the DAQ system by the detector type. These are developed and maintained by each group [6, 7]. The other instruments are the original or old DAQ system in use.

Table 1 The correspondence between the instruments and detectors

BL No.	Instruments	Detector type
01	4SEASONS	He-PSD
03	iBIX	2D Scintillator
08	SuperHRPD	He-PSD
12	HRC	He-PSD
14	AMATERAS	He-PSD
19	TAKUMI	1D Scintillator
20	iMATERIA	He-PSD
21	NOVA	He-PSD, GEM

The event recording is standard on the DAQ system in MLF/J-PARC. We have succeeded in standardizing the DAQ hardware interface and software. The event mode DAQ system has been installed to several instruments and some applications have been done. We will gradually install our DAQ system when the old DAQ system will be replaced or new instruments will be constructed.

References

1) T. Uchida: IEEE Trans. Nucl. Sci. NS-55 (2008) 1631.
2) http://daqmw.kek.jp/
3) S. Satoh, S. Muto, N. Kaneko, T. Uchida, M. Tanaka, Y. Yasu, K. Nakayoshi, E. Inoue, H. Sendai, T. Nakatani and T. Otomo: Nucl. Instr. and Meth. A 600 (2009) 103-106.
4) http://www.openrtm.org/
5) T. Nakatani, Y. Inamura, T. Ito, S. Harjo, R. Kajimoto, M. Arai, T. Ohhara, H. Nakagawa, T. Aoyagi, T. Otomo, J. Suzuki, T. Morishima, S. Muto, R. Kadono, S. Torii, Y. Yasu, T. Hosoya and M. Yonemura: submitted to Proceedings of ICALEPCS2009 JACoW.
6) K. Nakayoshi, Y. Yasu, E. Inoue, H. Sendai, M. Tanaka, S. Satoh, S. Muto, N. Kaneko, T. Otomo, T. Nakatani and T. Uchida: Nucl. Instr. and Meth. A 600 (2009) 173-175.
7) T. Hosoya, T. Nakamura, M. Katagiri, A. Birumachi, M. Ebine and K. Soyama: Nucl. Instr. and Meth. A 600 (2009) 217-219.

T. Nakatani and S. Satoh*
Neutron Science Section, Materials and Life Science Division, J-PARC Center, Japan Atomic Energy Agency, Tokai, Ibaraki, 319-1195
*Institute of Materials Structure Science, High Energy Accelerator Research Organization, Tsukuba, Ibaraki, 305-0801

Neutron Studies of High Boron Carbide Content, Resin Bonded, Neutron Shielding Materials: B_4C-resin

Boron carbide (B_4C) has been used in many forms for neutron shielding because of the large thermal and epithermal neutron capture cross-section of ^{10}B and because it is an inert material. However, since boron carbide is difficult to machine due to the hardness other methods for shaping it for neutron shielding have been used. Boron carbide grit can be poured into a container such as an aluminum can or a thin polyethylene bag, it can be sintered to form sheets, or it can be bonded together with a binder.

Because powder-metallurgically sintered boron carbide (sintered-B_4C) is expensive and the forms of the products are limited, resin bonded boron carbide (B_4C-resin) tiles, have been widely used for neutron shielding. Resins have small neutron capture cross-sections and contain hydrogen which is efficient at thermalizing neutrons, but if the resin content is minimized the composite material has a large neutron capture to scatter ratio for both thermal and epithermal neutrons, Prof. N Watanabe and his co-workers of KENS Japan have developed a recipe and technique for producing a composite with a resin content of 6-10 wt% [1]. In attempting to repeat these results in ISIS, Pugh et al have found two optimal compositions of the B_4C-resin that have good mechanical properties, fairly uniform density and allow for simple fabrication techniques [2].

An aim of this study is to investigate the neutron scattering background from the surface of the B_4C-resin shielding tiles to achieve the highest possible signal-to-noise ratio with the lowest possible cost. For comparison with other B_4C products, the sintered-B_4C tile (EaglePitcher, size 100 mm × 100 mm, and 1 mm thickness) is used as a standard. Neutron diffraction experiments have been performed using RAC spectrometer installed at KENS, Tsukuba, Japan. We set a sample and a 3He detector with the flight paths L_1 = 13 m (moderator-sample), L_2 = 0.35 m (sample-detector) and the scattering angle 2θ = 45 deg. The B_4C sample plate was set at the sample position in symmetric θ -2θ (45°–90°) reflection geometry as shown in Figure 1. We investigate two compositions of B_4C-resin tile. "Crisp-type" tile has the composition of 3 wt% epoxy resin (Grout-type, Sho-Bond) and 97 wt% B_4C grit (Wacker Ceramics). The B_4C grit consists of three particle-sizes: F20 (course) 38 wt%, F40 (medium) 56 wt%, F60 (fine) 3 wt%. Another type of B_4C-resin, "Flexible-type", is composed of 10 wt% epoxy resin and 90 wt% B_4C grit (F20: 35 wt%, F40: 52 wt%, F60: 3 wt%). The mix was cast in an open mold (size 100 mm x 100 mm, and 1 mm thickness) and was oven cured at 120 C° for two hours.

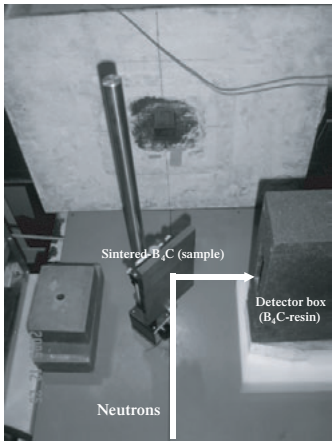

Fig.1 Layout of neutron diffraction measurements of B_4C tiles at RAC spectrometer, KENS.

Figure 2 shows neutron time-of-flight diffraction profiles of the B_4C-resin tiles and the sintered-B_4C tile with background profile. (The background profile was measured by a detector located in the closed B_4C-resin detector box.) In the profiles there are many broad peaks that can

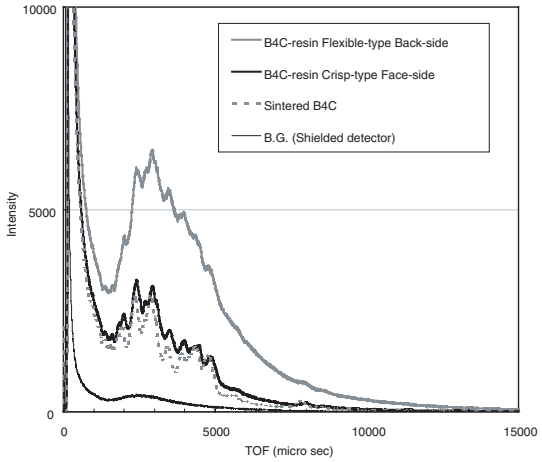

Fig.2 Time-of-flight neutron scattering spectra of two type B_4C-resin materials and a sintered-B_4C.

be assigned to the Bragg peaks of B_4C crystal (R3m, rhombohedral) [3].

The scattering intensity from the back-side (resin-rich side) of the flexible-type B_4C-resin tile is higher than those of other samples because of the large incoherent scattering from hydrogen atoms in the resin-rich surface layer. On the other hand, the scattering intensity from the face-side (B_4C-grit-rich side) of crisp-type B_4C-resin tile is relatively low and is almost identical to that from the surface of the sintered-B_4C tile.

These data show that the crisp-type B_4C-resin is a good candidate for low cost shielding materials covered inside the scattering chamber of neutron scattering instrument instead of costly sintered-B_4C tiles.

Because of its high cost-performance characteristics, the crispy-type B_4C-resin is widely used as shielding tiles on the inside surface of the scattering chambers (Fig. 3) and of the detector boxes of various neutron scattering instruments in J-PARC.

Fig.3 B_4C-resin tiles on the inner surface of the scattering chamber of NOVA diffractometer (BL21).

References

1) N. Watanabe, private communication.
2) V. T. Pugh and B. W. Hendy, ICANS-VIII (1985) proceedings, Report RAL-85-110 (1985) 670.
3) H. L. Yakel, Acta Cryst. **B31** (1975) 1797.

K. Suzuya[1], K. Kusaka[2], S. Torii[3], S. Harjo[1], K. Aizawa[1], S. Satoh[3], T.kaiyama[4] and M. Arai[1]

[1] MLF Division, J-PARC Center, Japan Atomic Energy Agency, Tokai, Ibaraki 319-1195, Japan
[2] Frontier Research Center for Applied Nuclear Sciences, Ibaraki University, Tokai, Ibaraki 319-1106, Japan
[3] Neutron Science Laboratory, High Energy Accelerator Research Organization, Tsukuba, Ibaraki 305-0801, Japan
[4] Division of Quantum Science and Energy Engineering, Hokkaido University, Sapporo 060-0801, Japan

High-pressure group, Asami Sano (JAEA), Kazuki Komatsu and Masashi Arakawa (University of Tokyo), at TAKUMI (BL19) setting up the palm cubic-anvil cell installed in a cryostat to study structure of ice under high-pressure.

Gas Desorption Examination of B_4C Resin

Some neutron instruments, particularly pulsed neutron instruments, require a large volume vacuum chamber (VC) in the neutron flight path. The role of the chamber is not only to avoid air scattering, but also to utilize the chamber as OVC for refrigerator of the sample environment (SE) equipments. The dimension of the VC quite depends on required instrument performance. In the case of direct geometry chopper spectrometer, size of the VC tends to be larger, L2 (sample-detector distance) is almost 3-5 m. Thus, the chamber volume is estimated to be 30-50 m^3. In this chamber, the inner surface covered with neutron absorber as a liner is usually going to be 100-200 m^2, which yields an enormously large amount of out gas. Some instruments may, moreover, need other components such as vanes and SE equipments that also give rise to out gas. In particular, using the chamber as OVC for refrigerator, its vacuum is required relatively high in the order of 10^{-4} to 10^{-5} Pa. Reasonably large vacuum pumps and controlling system are necessary to operate the smooth experiments. We have performed the gas desorption rate measurements for several types of B_4C and resin to figure out the reasonable conditions that *effectively shield neutrons with minimum out gas*. This could also give a guide for selecting the vacuum system.

On various types of mixture of B_4C and resin, we have measured gas desorption rate (GDR). In Fig. 1 the obtained results are summarized with the case of dry-air. Crispy type B_4C and ISIS B_4C shows rather good GDR. Dry-air also much affects reduction of GDR for any types of B_4C except for sintered. Since porous B_4C resin contains much water in it, dry-air can prevent the re-adsorption of water molecules. Also it is found that 27.8% difference in GDR at one hour is observed, which is dominant compared to the 8.5% density difference.

In order to quantitatively check the effects of dry-air on GDR, we conducted pumping tests. The obtained GDR for each pumping time is summarized in Fig. 2. Difference of the pre-pumping time corresponds to the effect of dry-air. Plateau (or dip) regions appear on pre-pumping data, whereas no such behaviour has been observed on data without pre-pumping. Also, plateaus seem to be proportional to pre-pumping time. After plateau region, all the curves recover to the original (no pre-pumping) GDR curvature. Again, this is a quite visible dry-air effect result suggesting that introducing a dry-air system is indispensable for saving time.

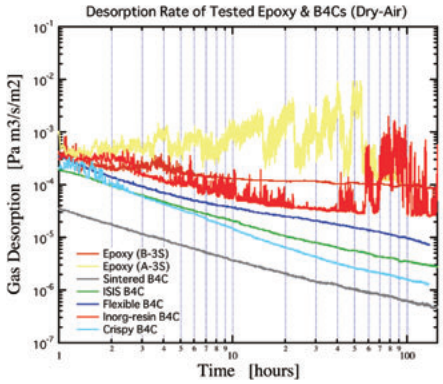

Fig.1 Summary of the GDR results on various types of B_4C resin tested using dry-air.

In conclusion gas desorption rate for several neutron shielding B_4C resins has been investigated. Main contribution of out gas turned out water from B_4C and resin. The resin is particularly undesirable from this point. Also, the difference of B_4C density and effects of dry-air have been tested. We found smaller out gas is released from a larger density sample. Its gain seems to be not so much. However, a large density with small out gas is obviously better for neutron shielding. Purge with dry-air greatly affect the gas desorption, and its installation is worth considering.

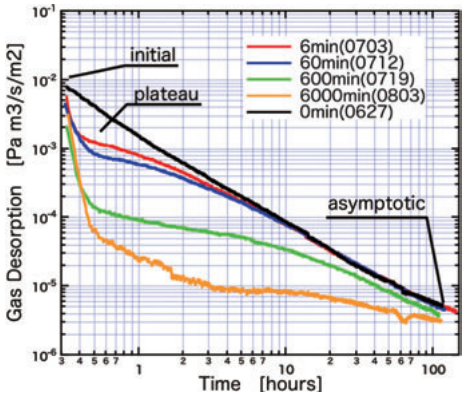

Fig.2 Summary of the pumping test. Each GDR was measured after "pre-pumping" and purged by dry-air.

T. Yokoo, N. Kaneko, S. Itoh, T. Ottomo K. Suzuya, Y. Suetsugu and M. Shirai
Material and Life Science Division, J-PARC Center

Shield Design for Neutron Beam Line

One of the design goals for neutron scattering instruments has been to achieve the highest possible signal-to-background ratio. As the power of the source increases, the MeV and keV neutrons and the initial gamma burst become crucial to achieving low beamrelated backgrounds and, therefore, high instrument performance. The instrument design with the devices becomes a delicate balance between the neutronic efficiency of the devices and the beam-line shielding. However, most designing of neutron scattering instruments and devices has been carried out using several ray-trace Monte Carlo simulation packages, which excluded shielding considerations. Then, we studied the performance of both the neutron optical devices and the beamline shields for neutron scattering instruments at a 1-MW spallation neutron source facility (JSNS) in the High-Intensity Proton Accelerator Project (J-PARC) using simultaneous neutron ray-tracing and transport Monte Carlo (MC) simulation method with the PHITS (Particle and Heavy Ion Transport Code System) code [1, 2].

We have employed multi-purpose particle and heavy ion transport Monte Carlo code system PHITS for a study of neutron beamline and shielding design. As the nuclear data, Japanese Evaluated Nuclear Data Library (JENDL) was used. PHITS can treat not only the neutron scattering processes for ray tracing but also the transport processes for shielding design by simulating neutron interactions with various materials and by production of secondary particles at the same time. For the ray-tracing simulation, calculations were performed with two steps. At first, the neutron and photon flux at the entrance of each beamline starting from a collision between target and incident protons were calculated. Then these calculated flux data for each beamline are stored in a database and used as a source in the second step calculation for each beamline from the moderator to the detectors.

The main subject of shield design is to protect the humans from radiation. The shields were mainly composed of realistic shield materials of iron, concrete and materials containing high levels of hydrogen. The thickness and the arrangement of materials were optimized to reduce the total amount of the shield materials. The reduction of the shield helps to obtain large space inside the beamline and to cut the cost.

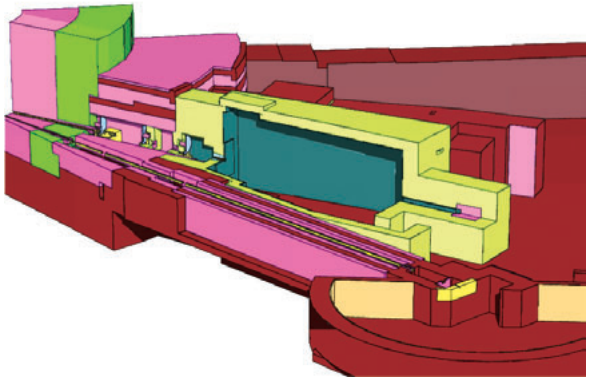

Fig.1 Shield Design of BL15. The yellow part is composed by Boron included concrete.

Another important issue besides the shielding problem is the reduction of the beam-related background of MeV and keV neutrons using the T0 chopper or curved guide. PHITS can simulate some portion of high-energy components of the incident neutron flux that survive after passing of the neutrons through the T0 chopper or curved guide by neutron penetration and scattering with the materials of the devices, which cannot be described by ray-

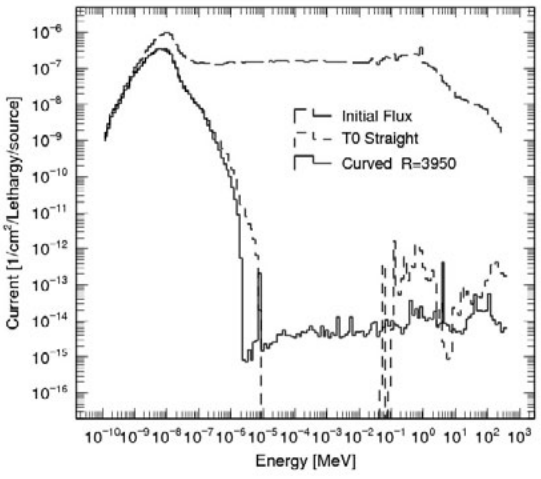

Fig.2 Energy spectra of neutrons inside the guide tube at the entrance and the end of the beamline for the straight T0 chopper system and the curved guide system.

trace MC simulation codes.

The optimization studies to reduce the neutron dose were carried out by changing the material used to build the supermirror guide. We used silica (SiO_2) glass as a material of the supper-mirror guide in the first calculation. We changed the material to a glass including 12 wt % boron oxide (B_2O_3) in the next calculation. This boron containing glass has drastically reduced the neutron dose in the case of the straight guide, but the dose for the curved guide is not changed. This is because a high-energy component of neutron flux is dominant in the dose distribution around the curved guide, but the main component of the dose around the straight guide is from thermal neutrons. The thickness of the shield concrete is roughly 10 cm around the straight guide to satisfy the dose limitation of 0.02 μSv/h in this case.

To reduce the background, the usage of materials including boron with high concentration was effective especially in the scattering area of neutron experiment. Because the scattered neutrons' energy is mainly low, the boron-included materials of appropriate thickness surrounding the scattering area are enough to reduce the neutron background. We have calculated several materials such as resin including boron oxide, mortar including B_4C powder and epoxy with Colemanite powder, and have compared their shielding capabilities. The mortar with B_4C powder is very good to attenuate the low energy neutrons, but the materials using resin and epoxy for their matrix are effective to attenuate relatively high-energy neutrons around eV to keV.

References

1) H. Iwase, K. Niita and T. Nakamura, J. Nucl. Sci. Technol. **34**, 1142 (2002).
2) K. Niita, H. Takada, S. Meigo and Y. Ikeda, Nucl. Instr. and Meth. **B184**, 406 (2001).

T. Shinohara[1], K. Suzuya[1] and K. Niita[2]
[1]J-PARC Center, Japan Atomic Energy Agency, Tokai, Ibaraki 319-1195, Japan
[2]Research Organization for Information Science and Technology, Tokai, Ibaraki 319-1106, Japan

BL15 being under construction.

Development of polarized ^{3}He neutron spin filters

Polarized ^{3}He neutron spin filters use very high spin-dependent neutron capture cross section of ^{3}He gas. Unlike supermirrors, they provide their performances over the full energy range of cold, thermal and hot neutrons. Therefore, the ^{3}He spin filters can be an ideal candidate for broadband polarizers and analyzers covering large solid angle, and there are strong demands to use the ^{3}He neutron spin filters in several beam lines in J-PARC.

Currently, there are mainly two available techniques to polarize ^{3}He gas: spin-exchange optical pumping (SEOP) and metastability exchange optical pumping (MEOP). Our group has developed the ^{3}He neutron spin filters based on the SEOP technique, with which on-line optical pumping is possible.

On NOP beam line at JRR-3, we performed ^{3}He polarization experiment by monitoring the transmission of unpolarized neutrons (λ = 7.6 Å) through ^{3}He gas with on-line optical pumping (Fig. 1) [1]. In the experiment, we used a compact SEOP box with dimensions 60 cm x 60 cm x 30 cm (length x width x height). In the box, all necessary equipments, the optical system for narrow-band laser beam, a coil for homogeneous magnetic field, and a ^{3}He neutron spin filter cell (16.9 bar･cm), are included.

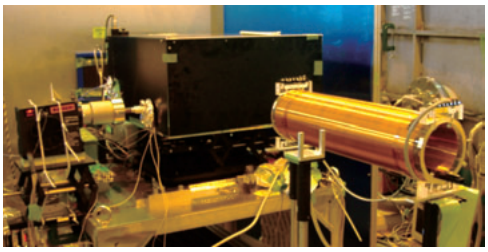

Fig.1 Compact SEOP box, set on NOP at JRR-3

Fig.2 shows the time variation of the transmitted neutron intensity and ^{3}He polarization during optical pumping. The ^{3}He polarization increased with time except laser-off period and it finally reached 72.3 %. Due to the recent development of SEOP technique, the ^{3}He polarization exceeding 70 % can be obtained in several institutions in the world in these days [2]. The result shows that such ^{3}He neutron spin filters are now available in J-PARC.

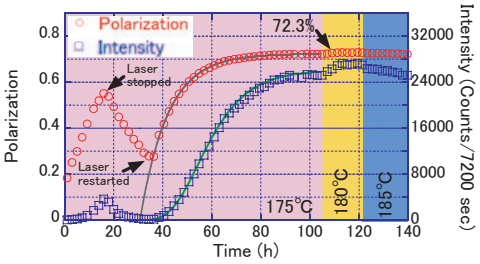

Fig.2 Time variation of the transmitted neutron intensity (blue squares) and ^{3}He polarization (red circles) during optical pumping.

On BL05/NOP at MLF/J-PARC, a ^{3}He neutron spin filter was applied for the accurate determination of neutron polarization in the polarized beam branch and it was used as a neutron spin analyzer. For the measurement, adiabatic fast passage nuclear magnetic resonance (AFP-NMR) system was newly installed and the flipping of the polarized ^{3}He nuclear spins was made by the system (Fig. 3). The ^{3}He gas in the spin filter cell was polarized at our pumping station in KEK and was transported to the beam line. From the measurement, the neutron polarization for the beam branch was estimated to be 0.9562 ± 0.0003 [3].

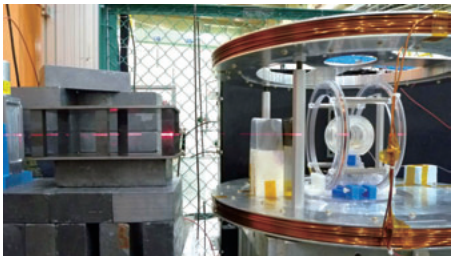

Fig.3 AFP-NMR system with a ^{3}He neutron spin filter, set on BL05

References

1) H. Kira et al., submitted to Physica B and J. Phys.: Conf. Ser.
2) For example, W. C. Chen et al., Nuclear Instrum. Meth. A 404 (2009) 2663.
3) T. Ino et al., Physica B, in press doi:10.1016/j.physb.2011.01.2009.

T. Oku[1], H.kira[1], Y. Sakaguchi[2], J. Suzuki[1], L. J. Chang[2),3),4)], K. Kakurai[2], Y. Arimoto[5], T. Ino[5], H. M. Shimizu[5], H. Hiraka[6], K.Ohoyama[6], K. Aizawa[1] and M. Arai[1]

[1] MLF Division, J-PARC Center, Japan Atomic Energy Agency, Tokai, Ibaraki 319-1195, Japan
[2] Quantum Beam Science Directorate, Japan Atomic Energy Agency, Tokai, Ibaraki 319-1195, Japan
[3] Department of Physics, National Cheng Kung University, Tainan 70101, Taiwan
[4] Nuclear Science and Technology Development Center, National Tsing Hua University, Hsinchu 30013, Taiwan
[5] Nuclear Science Division, High Energy Accelerator Research Organization (KEK), 1-1 Oho, Tsukuba, Ibaraki 305-0801, Japan
[6] Institute for Materials Research, Tohoku University, 2-1-1 Katahira, Aoba-ku, Sendai 980-8577, Japan

Two-dimensional neutron detectors for iBIX instrument

A two-dimensional neutron detector with a high detector efficiency, a high spatial resolution, and a minimized neutron-insensitive area is of great importance for a single-crystal neutron diffractometer for biological and chemical crystallography. We have successfully developed such a two-dimensional detector by using the neutron-sensitive scintillator and wavelength-shifting fiber technology. The detector is dedicated to the "iBIX" instrument in the J-PARC/MLF and the detector components are optimized for his best performance [1].

The neutron-detection head of the detector is comprised of two ZnS/$^{10}B_2O_3$ scintillator screens and ribbons of wavelength shifting (WLS) fibers. The neutrons scattered in the sample are absorbed in the scintillator screens and the generated scintillation light is read out with the crossed WLS fiber arrays. The pixel size of the detector is 0.5×0.5 mm^2, which is well matched with a typical size of the sample crystal.

Photo 1 shows one of the detector modules for the iBIX. The detector has a neutron-sensitive area of 133×133 mm^2 with a successful neutron-sensitive area of 65% over the detector face. The detector exhibits a spatial resolution of 1.2 mm with a detector efficiency of 40% for 2.2-Å neutrons. Thanks to the ^{10}B contained scintillator materials and the scintillator-fiber structure, where the WLS fibers are sandwiched with the two scintillator screens, the detector efficiency is satisfactory.

The detector module is designed to be as compact as possible to fit 64 detectors in the mounting frame of the instrument. The dedicated small-sized amplifier/discriminator and encoder/signal processing electronics that handle 512 channels are developed and are mounted right behind the detector head. The detector system including these electronics is fitted in the space of $165 \times 165 \times 1000$ mm. The compactness of the detector also helps the detector be light at 17 kg and have low power dissipation.

After the successful demonstration of the detector performances [2] the manufacturing technologies were transferred to the industry. 14 detectors were delivered and have been in service (Photo 2). Figure 1 shows one of the examples of the diffraction data measured at the proton beam power of 20 kW. It was confirmed that the instrument can collect similar amount and quality of data to the BIX-3 instrument in the JRR-3 reactor at this limited power, demonstrating a significant impact on the data collection efficiency of the iBIX.

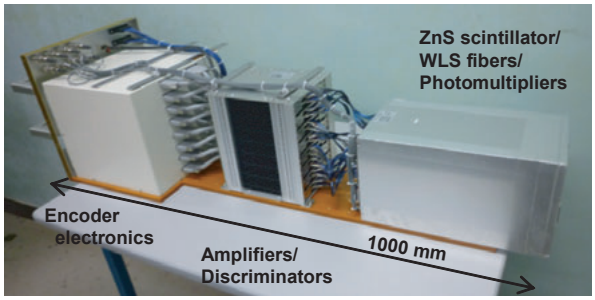

Photo. 1 A photograph of the detector module for the iBIX

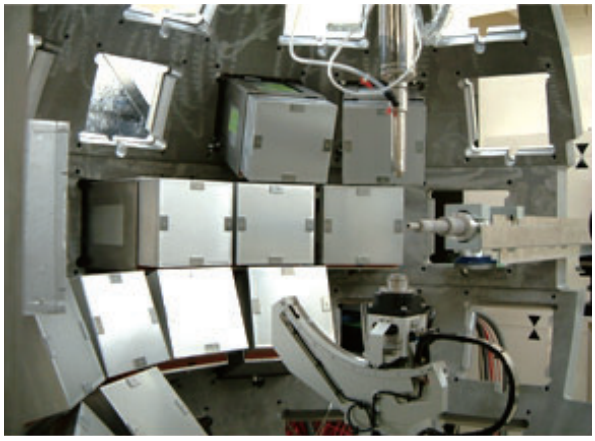

Photo. 2 A close-up view of the iBIX (14 detectors have been implemented in the instrument)

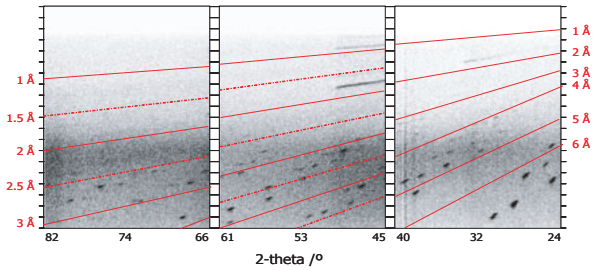

Fig.1 Diffraction data of a RNA sample measured in the iBIX

One-dimensional neutron detectors for TAKUMI

The Engineering Materials Diffractometer, TAKUMI, is one of the neutron instruments

installed in the Materials and Life Science Facility at J-PARC. TAKUMI is expected to be used for industrial application such as residual stress measurement. The detailed information on TAKUMI can be found at the website [3]. The commissioning of TAKUMI was started in September 2008.

The neutron detectors of TAKUMI are required to have a large detection area with a relatively small pixel size and good detection efficiency. The detector requirements are as follows:

- Number of detectors: 10
- Sensitive area: 1000 mm × 196 mm
- Spatial resolution: 3 mm
- 360 channel / detector
- Detection efficiency: >50%@1Å
- Gamma sensitivity: $<10^{-6}$@1.3MeV
- Secondary flight path: 2.0 m

As a result of international cooperation between JAEA and Rutherford Appleton Laboratory (RAL), an ENGIN-X-type linear scintillation neutron detector was developed for TAKUMI after confirmation of performances of a prototype detector [4-5]. The detector head mainly consists of scintillators, reflectors, and optical fibers. The main part of the detector with photomultiplier tubes (PMTs) is shown in Fig.2. The detector has a large sensitive area of about 1000 x 196 mm that consists of 360 pixels with a position resolution of 3 mm.

The incident neutrons are detected on the basis of ZnS:Ag/^{6}LiF scintillation techniques. To determine the incident neutron position and to reduce the number of PMTs, the optical fibers connected with the detector head are pair coded into the PMTs. The electric signals from the PMTs are sent to data acquisition electronics (DAE) and decoders, which were also developed at the same time. The neutron incident channel is determined in the decoders by coincidence of DAE output of any two PMTs.

The detector and the electronics system showed excellent performances such as a neutron detection efficiency of more than 50% at a neutron wavelength of 1 Å and a gamma-ray sensitivity of less than 10^{-6} at a gamma-ray energy of 1.3 MeV.

As an example of commissioning data, Fig. 3 shows the time-of-flight neutron-scattering spectrum by a 10 mmϕ Fe rod. One can see clear peaks that originated from the lattice spacing of Fe. Although only two detectors had been installed by September 2008, the installation of all detectors was completed by the end of March 2009. Figure 4 shows detectors installed in the south bank of TAKUMI.

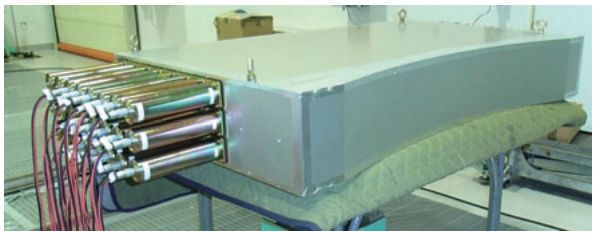

Fig.2 The main part of the detector with photomultiplier tubes

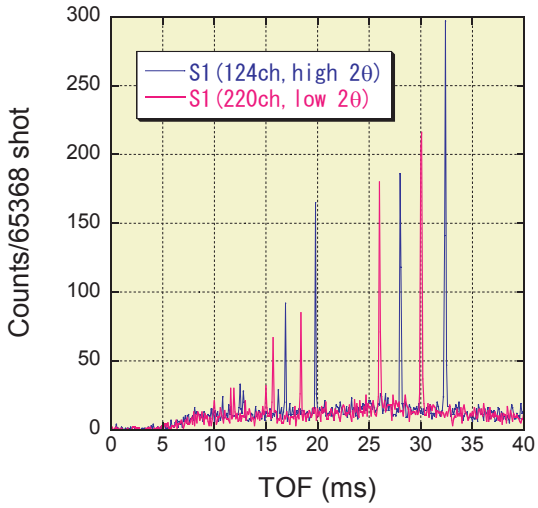

Fig.3 Time-of-flight neutron scattering spectrum by a 10mmϕ Fe rod

Fig.4 Detectors installed at the south bank of TAKUMI

Micro-pixel neutron detectors

A gas-based neutron detection system which reads out individual lines with a micro-pixel

detector element was developed, and preliminary neutron irradiation tests were conducted. The detection system consisted of a micro-pixel detector element, a gas chamber that had feedthroughs for lines of 541 channels, amplifier-shaper-discriminator boards, position encoders with field programmable gate arrays, and a device capable of fast data acquisition.

The micro-pixel detector element comprises pixel anodes in the shape of pins, and these anode pins are in the centers of circular cathode holes. A schematic view of the detector element is shown in Fig. 5. The pitch between anodes and between cathodes is 0.4 mm and the diameters of the anode pin and cathode hole are 65 mm and 250 mm, respectively. The charge signal is induced by gaseous amplification around each anode pin due to the strong electric field between the electrodes. There are 128 channels for anodes and cathodes, and anode lines and cathode lines

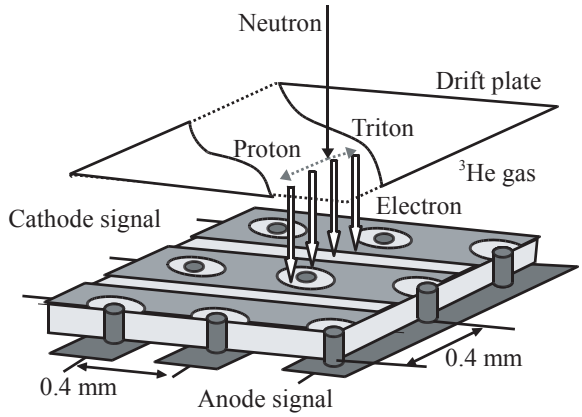

Fig.5 Schematic view of the micro-pixel detector element

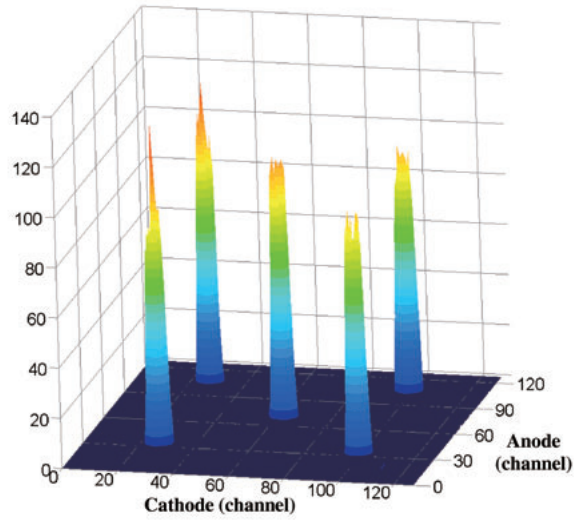

Fig.6 Two-dimensional response obtained using a collimated neutron beam with a size of 0.3 × 0.3 mm^2

are arranged orthogonally. The signal of every channel is read out individually.

The micro-pixel detector element pulses had a short duration, the full width at half maximum of the pulse being 160 ns. Fig. 6 shows a typical two-dimensional image of our detection system irradiated by a neutron beam. The detection system is irradiated with a collimated neutron beam of 0.3 × 0.3 mm^2 cross section by scanning the detection area. Our detection system exhibits similar spatial resolutions, of about 2.5 mm FWHM, in both the anode and cathode directions at gas pressures of 0.45 MPa for He and 0.05 MPa for CF_4. The thermal neutron detection efficiency was estimated to be about 73% at these gas pressures from calculations that considered the nuclear reaction cross section of He-3 gas and the conversion gap of 20 mm.

Supermirror coatings for the new spallation source J-PARC MLF

Neutron supermirrors are increasingly important devices for transporting, bending, and focusing neutron beams. High-performance neutron supermirrors with high reflectivity and large *m*, where *m* is the ratio of the effective critical angle of the supermirror to that of natural nickel, is important in neutron experiments, since they lead to a considerable increase in available neutron intensity. We have developed neutron supermirrors using ion beam sputtering (IBS) since it enables the production of layers with high density and small grain size. An IBS system with an effective deposition area of 2,000 cm^2 has been installed at the JAEA to produce neutron guides, benders, and other optical devices based on supermirrors for the MLF. Ni/Ti supermirrors have been fabricated with large critical angles extending up to m = 3, 4, and 6.7 using the IBS system. The neutron reflectivity of the supermirrors at the critical angle is 0.82, 0.66, and 0.23, respectively [6,7].

Although supermirrors with large critical angle have been fabricated, the realization of higher reflectivity may be more important for neutron experiments. There is a technique of adding carbon atoms to the nickel layer that leads to higher reflectivity that has been demonstrated by several groups to be effective in improving the reflectivity of supermirrors. We have tested this technique and fabricated NiC/Ti

supermirrors with m=3 and 4. The neutron reflectivities of these supermirrors are 0.90 and 0.80, respectively, at the critical angle. We have also demonstrated that a NiC/Ti supermirror with a reflectivity of 0.40 at a critical angle of m=6 can be fabricated (Fig. 7) [8].

High-performance supermirrors also allow the realization of focusing systems. Reflected neutrons from a supermirror are divided into specular and off-specular (diffuse) components. The specular component contributes to the focused intensity, but the diffuse component generates background noise around the focal point. This causes the serious problem of low signal-to-noise ratio in focusing systems for such purposes as small angle neutron scattering measurements, in which the diffuse component from the focusing mirror cannot be removed by slits. The suppression of the diffuse component is, therefore, an important problem along with the realization of higher reflectivity and larger critical angle. The diffuse intensity from a NiC/Ti supermirror was found to be lower than that from a Ni/Ti supermirror by more than one order of magnitude (Fig. 8). This improvement was attributed to the impeded crystal growth of nickel in Ni-C cosputtering process. This result implies that a high performance focusing system with a diffuse intensity down to the order of 10^{-5} of the specular intensity can be realized by using the NiC/Ti supermirror.

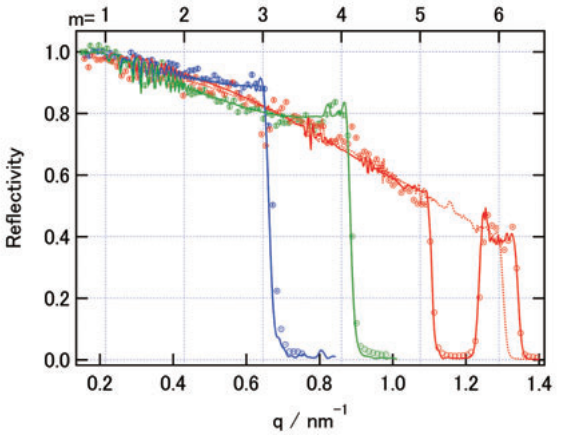

Fig.7 Neutron reflectivity profiles of the NiC/Ti supermirrors with m=3, 4, and 6. Lines indicate the calculated reflectivity profiles.

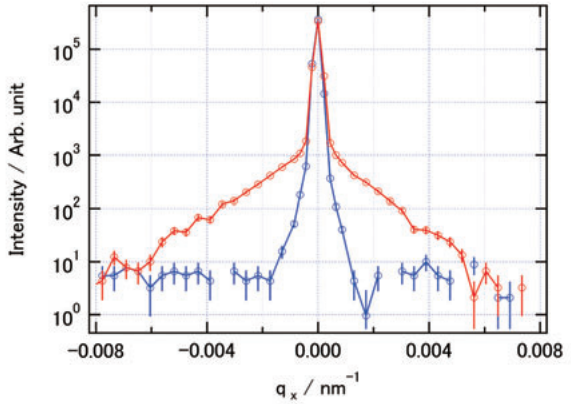

Fig.8 Diffuse intensity profiles of the Ni/Ti (closed circles) and NiC/Ti (open circles) supermirrors with m=3. Rocking scan with q_z=0.62 nm^{-1}.

Wideband beam focusing using an precisely fabricated elliptic supermirror

We have developed a 1-dimensional elliptic mirror combining a supermirror coated with ion-beam sputtering and precise elliptic surface figured with the numerically-controlled local wet etching process. In this study, focusing of wide-band neutron beam was demonstrated.

A mirror substrate was prepared by figuring a surface of synthesized quartz glass into a plano-elliptical shape. The ellipsoid is of $(x/1050.31)^2 + (z/25.66)^2 = 1$, where the units of x and z are mm. The focal length is 1050 mm. The aperture size is 90 mm (elliptic) × 40 mm (straight) and it covers eccentric angle $87.55 < \theta < 92.45$ deg of the ellipsoid.

NiC/Ti supermirror (m = 4) was deposited on the elliptic quartz surface. The elliptic mirror is supposed to accept a neutron beam with nominal glancing angle of 1.40 deg and to reflect and focus wideband neutrons with wavelength $\lambda \geq 3.5$ Å. The acceptance angle, therefore, is 0.12 deg. Details of the fabrication are described elsewhere [9] together with a test result of monochromatic beam focusing. Figure 9 shows a photograph of the fabricated elliptic supermirror.

Fig.9 Elliptic supermirror.

Wideband neutron beam focusing was demonstrated on the CHOP beam port of JRR-3.

CHOP provides a neutron beam of $\lambda \geq 3$ Å which is bent by 20 degrees with a multi-channel cold neutron bender at the end of the C-2 guide tube.

Figure 10 shows a horizontal profile of the focused and unfocused beam. The intensities are expressed in "photo-stimulated luminescence (PSL)" per pixel of an imaging plate (50 × 50 μm^2). Focused beam width was 0.25 mm in full width at half maximum, almost reproducing the initial beam size defined by the slit. This result is adequate because the focusing mirror is based on the elliptic arc with eccentric angle around 90 degree. Focused peak intensity was 6 times the unfocused average intensity. Note that the tail of the focused beam is no more than that of the unfocused beam profile, which suggests that the focusing mirror produces little diffuse scattering.

Figure 11 compares a time-of-flight (TOF) spectrum of the focused beam with that of the unfocused one. (Sharp dips are attributed to Bragg reflections by monochromators of upstream instruments in the C-2 beam line.) One can see that neutrons are reflected and focused over a wide wavelength band. Taking the ratio of the two TOF profiles yields a typical reflectivity profile of a supermirror (reflectivity ≃ 0.6 at a critical Q_z value of 0.084 $Å^{-1}$). This result suggests that most reflected neutrons are transported to the focal spot without significant loss.

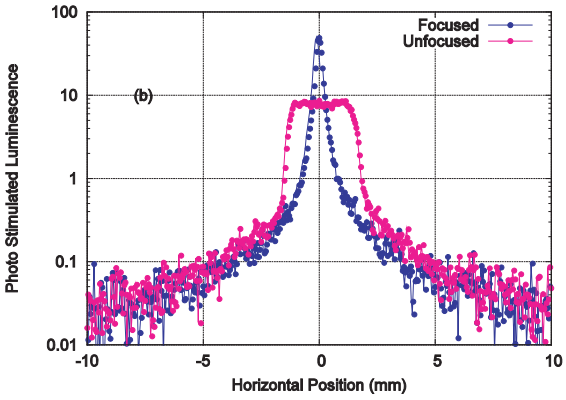

Fig.10 Horizontal profiles of a focused and unfocused beam.

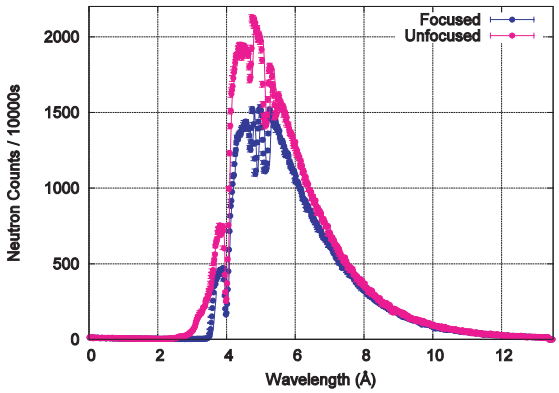

Fig.11 TOF profiles of the focused and unfocused beam.

To summarize, an elliptic NiC/Ti super mirror (m=4) was fabricated using the ion-beam sputtering and the numerically-controlled local wet etching techniques. Wideband neutrons of $\lambda > 3.64$ Å were effectively focused with focal spot size down to 0.25 mm, peak intensity gain up to 6 without significant diffuse scattering. Time-of-flight measurements suggest that wideband neutrons are effectively focused to the focal point. Wideband neutron beam focusing was demonstrated on the CHOP beam port of JRR-3 [10].

References

1) T. Nakamura et al., JAEA-Research 2008-115.
2) T. Hosoya et al., Nucl. Instr. & Meth. A **600** (2009) 217.
3) http://j-parc.jp/MatLife/en/instrumentation/bl19/bl19.html.
4) T. Nakamura et al., JAEA-Research 2007-014.
5) K. Sakasai et al., Nucl. Instr. & Meth. A **600** (2009) 157.
6) R. Maruyama et al., Physica B **385-386** (2006) 1256.
7) R. Maruyama et al., Thin Solid Films **515** (2007) 5704.
8) R. Maruyama et al., Nucl. Instr. & Meth. A **600** (2009) 68.
9) K. Yamamura et al., Opt. Express **17** (2009) 4614.
10) D. Yamazaki et al., J. Phys.: Conf. Series 251 (2010) 012076.

K. Soyama, K. Sakasai, D. Yamazaki, T. Nakamura, K. Toh, R. Maruyama, H. Yamagishi, and K. Katagiri
Material and Life Science Fasility, J-PARC Center

Muon Science

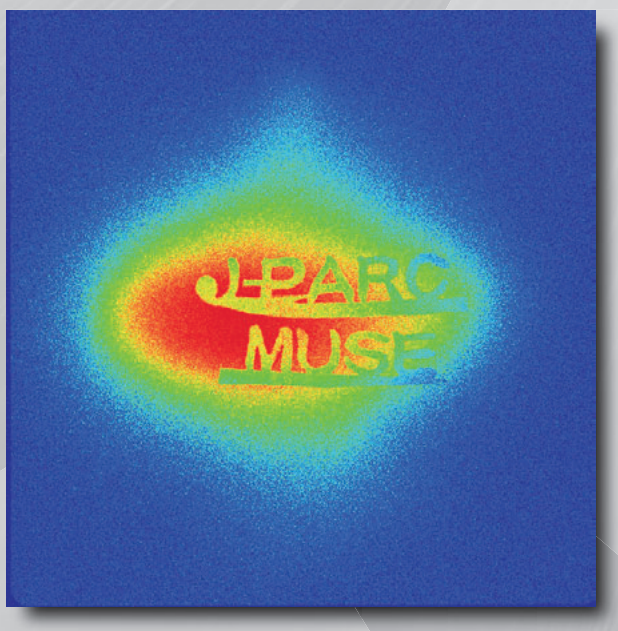

MUSE Status: World strongest pulsed muon beam was obtained at J-PARC MUSE

Y. Miyake[a], K. Shimomura[a], N. Kawamura[a], P. Strasser[a], A. Koda[a], H. Fujimori[a], S. Makimura[a], M. Kato[a], K. Nishiyama[a], Y. Ikedo[a], K.M. Kojima[a], R. Kadono[a], W. Higemoto[b], T. Ito[b], K. Ninomiya[b] and K. Kubo[c]

[a] Meson Science Laboratory, High Energy Accelerator Research Organization, Ibaraki 305-0801, Japan
[b] Japan Atomic Energy Research Center (JAEA), Ibaraki 319-1195, Japan
[c] International Christian University

The muon science facility (MUSE, abbre-viation of MUon Science Establishment) has almost completed the construction of the D-line, one of the four muon beamlines planned at the Materials and Life Science Facil-ity (MLF) of the Japan Proton Accelerator Research Complex (J-PARC). The MLF accommodates both the neutron and muon sci-ence programs, taking about 85% of the current from the 3 GeV Rapid Cycle Syn-chrotron (RCS) to generate intense pulsed neutron and muon beams. On the way to-wards the neutron source at MLF, one graph-ite target [1] with a thickness of 20 mm was installed in the proton beamline, in order to produce both positively (π^+) and negatively (π^-) charged pions through the nuclear reac-tions between the 3 GeV proton beam and the carbon nucleus.

For phase 1 of the construction schedule, the MUSE team managed to install one su-perconducting decay/surface muon channel, so called D-Line, with a modest-acceptance (about 45 mSr) pion injector. With this beamline, either surface muons (from the decay of π^+stopped near the surface of the graphite target) or decay muons (from the in-flight decay of π^+/π^- confined by a strong longitudinal magnetic field of super-conducting solenoid [2]) can be extracted. Figure 1 shows the schematic layout of the MUSE facility as of March 2010.

Practically, the muon beam tuning has been done with the use of a beam profiler, a two dimensional scintillator array (15 × 15), as shown in Figure 2. This beam profiler was found to be very useful for the optimization of the beam size, timing, slits, and back-grounds, as well as the settings of the mag-nets along the secondary beamline [3].

In order to remove positron contamination having the same momentum as the surface muons, a static $\boldsymbol{E} \times \boldsymbol{B}$ filter, so called DC

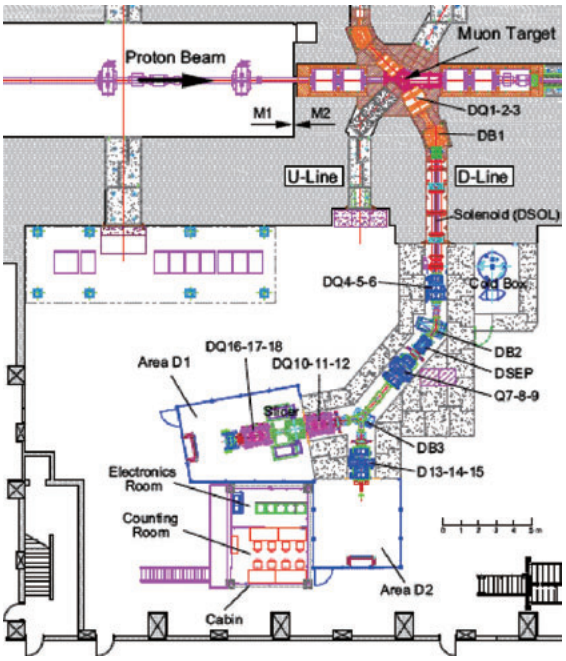

Fig.1 Layout of the decay muon channel in the experimental hall No.2 of the MLF building.

separator, has been installed [4]. By replac-ing the older separator having an electrode gap of 100 mm (±100 kV), with a new sepa-rator having a gap of 200 mm (±150 kV), the muon beam loss by hitting the electrodes or the beam ducts reduced significantly. Figure 3 shows a picture of the new separa-tor.

By replacing the separator and conducting iterative beam tuning, the number of sur-face muons (μ^+) extracted was significantly increased up to 1.8×10^6/s with the use of 120 kW proton beam from the RCS. The achieved intensity is equivalent or even higher than that available at the RIKEN-RAL muon facility [5]. This is the reason why we claim an achievement of the world strongest pulsed muon source at J-PARC/MUSE, al-ready at 120 kW proton beam intensity. This intensity would correspond to 1.5×10^7/s surface muons when the full intensity of the proton beam (1 MW) becomes available in

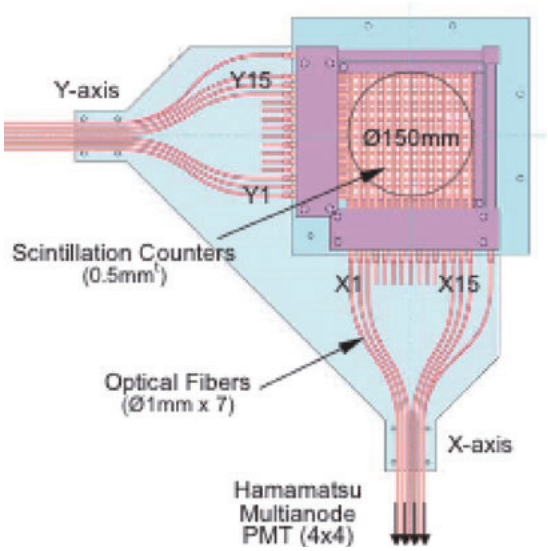

Fig.2 Schematic view of a beam profiler, which consists of a two dimen-sional scintillator array (15 × 15)

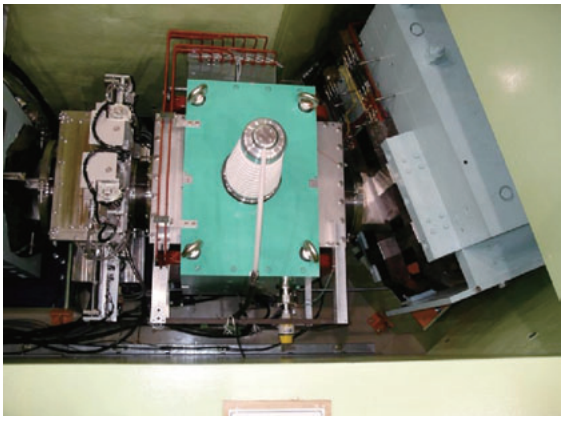

Fig.3 Picture of the new separator which en-abled muon beam to pass through more effi-ciently

the future.

The muon beam available at J-PARC/MUSE is already open for users experiments approved in the experimental proposal evaluation committee. More than 15 user's experiments have been performed already. With the use of the MUSE facility, we have already pub-lished a paper [6] demonstrating the presence of a macroscopic phase separation between the superconducting and magnetic phases in Co-Doped Iron Pnictide $CaFe_{1-x}Co_xAsF$. This is the first scientific paper published among the entire J-PARC facilities.

References:

[1] The current design and performance of the existing muon production target at MUSE may be found at S. Makimura et al., KEK-MSL progress report (2008) and earlier years.

[2] The present status of superconducting solenoid and on-line refrigerator may be found in this MLF annual report: K. Shimomura et al.

[3] P. Strasser et al., Journal of Physics: Conference Series 225 (2010) 012050.

[4] The present status of DC-separator may be found in this MLF annual report: K. Nishiyama et al.

[5] K. Nagamine, et al. Hyperfine Interac-tions 101/102(1996)521

[6] S. Takeshita, et al., PRL 103, 027002 (2009)

Status of Decay and Surface Muon Beamline

N. Kawamura for Muon Science Section

Muon Science Section, Materials and Life Science Division, J-PARC Center, Tokai, Ibaraki 319-1195
High Energy Accelerator Research Organization, Tsukuba, Ibaraki 305-0801
Japan Atomic Energy Agency, Tokai, Ibaraki 319-1195

Muon Science Section decided to construct a beamline which has 6 m long solenoid as a pion-to-muon decay section as the first muon beamline in J-PARC. As is shown in Fig. 1, from the muon target inserted 30m upstream of the neutron target, we have four options for the space of the secondary beamline. The first beamline has been required to provide muons for many users with multi-purpose. On the other hand, after several-years blank of muon beam in Japan, the users' society anticipated quick recovery of beam. Due to these requirements, a decay-muon beamline is a unique option for the first beamline. The decay-muon beamline provides momentum-tunable positive and negative muon beam, as well as surface muon beam, satisfying a variety of experimental needs. The design concept of the decay muon beamline has been established in KEK Muon Facility (BOOM) and the RIKEN-RAL Muon Facility, although the forefront part of the beamline operating under high radiation field requires many R&D works at J-PARC.

The first muon beam was successfully transported to D1 experimental area in September 2008. Since then, beam tuning was performed to increase the muon transmission efficiency and to obtain the small beam spot at the sample position. In December 2009, the beam intensity was confirmed to reach the world-strongest 7.2×10^{4} surface-muons per pulse, 1.8×10^{6} per second, under 120 kW proton beam. This value is about a half of the preliminary evaluation. A recent beam-transport calculation, which took into account the higher order effect due to the fringing field of the quadrupole magnets, reproduces the observed beam intensity and also response of the beam profile to the magnet setting.

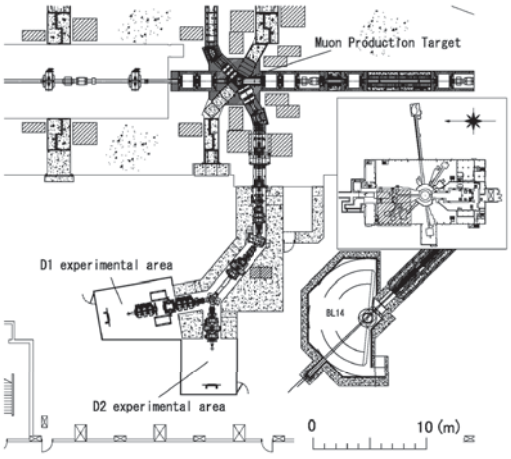

Fig.1 A cut-away view of the muon facility.

In the progress of beamline understanding, *i.e.* beam tuning, we found that some of the beamline components are placing constraint on the beam transmission condition. Most of the decay-muon beamline magnets were made for BOOM and old KEK beamlines, and are reused to save the construction cost. In order to obtain higher muon beam intensity, we replaced the limiting magnets in summer 2010.

In addition to the above mentioned development, works for pioneering uses of muons are promoted. The time width of the muon beam is determined by the proton beam width of ~100ns, intrinsically. For higher timing resolution experiment, a beam slicer device has been installed in D1 area. Details are reported elsewhere in the article [1].

At the branching point of the beamline, a bending magnet is installed at present, and the double peak structure of the beam pulse is both transported either D1 or D2 area, exclusively. For the simultaneous use of both areas, a kicker device, which separates each peak structure, is under fabrication. Installation is planned in this financial year. For the further understanding of the beamline, the beam diagnostic devices, *i.e.* beam profile monitors, are under development for installation in this FY, also.

References

1) W. Higemoto *et al.*, J. Phys.: Conf. Ser. 225 (2010) 012012.

Present Status of the Muon Rotating Target in J-PARC/MUSE

S. Makimura, Y. Kobayashi, M. Kato, R. Shimizu, N. Kawamura, Y. Miyake, K. Nishiyama, K. Shimomura, P. Strasser, A. Koda, H. Fujimori, K. M. Kojima and R. Kadono

Muon Section, MLF division, J-PARC Center, KEK, Toukaimura, Ibaraki, 319-1106

Since the run cycle in November of 2009, the most intensive pulsed muon beam in the world has been continuously produced with a proton beam of 120 kW in J-PARC/MUSE (Muon Science Establishment). At present, the fixed edge-cooling method is adopted for cooling the muon target. The proton beam intensity is going to be upgraded to 1MW operation (3-GeV 333-μA) in near future. The energy deposit by a 1 MW proton beam on a muon target made of 20 mm thick isotropic graphite (IG-430) is estimated to be 3.5 kW by PHITS [1,2]. It is predicted that the graphite will break down in six months due to the radiation damage [3]. To extend the lifetime of the muon target, we are planning to adopt the rotating target method, which can distribute the radiation damage of graphite to a wider area. In the present design, the outer diameter of the rotating target is 336 mm, and the inner diameter is 230 mm. In an evaluation, it is assumed that the emissivity of both the graphite and the inner surface of the chamber with a black coating are 0.8, and the temperature of the chamber is 100 °C. Then the temperature of the graphite is estimated to be 670 °C. When the graphite is rotated at a speed of 5 rpm, the maximum temperature gradient is estimated to be less than 30 °C. In the rotating method, the lifetime of the graphite is prolonged and is estimated to be longer than 30 years.

Though the lifetime of graphite becomes long enough, the lifetime of the bearing is supposed to be the critical issue for the rotating target method. The lifetime of the bearing generally depends on the load, the temperature, the pressure, and the lubricant. The bearings of the rotating target are located in high vacuum (10^{-4} Pa) and at high temperature. In addition, they are under intense radiation. Consequently an inorganic solid lubricant must be used. At present, the candidates as solid lubricants are disulfide molybdenum, disulfide tungsten, and arc ion plated silver. By taking advantage of the solid lubricant, the lifetime is aimed to be 10 years. To measure and compare the respective lifetime of the bearings, a mock-up was fabricated, and heating and rotating tests have been performed.

The rotating body is composed of a graphite disk, a support, and a shaft supported by two bearings. The two bearings are attached to a cooling jacket with a cooling pipe. While in reality the 3.5 kW of heat is deposited on a beam spot size of 25 mm in diameter in the beamline, in the mock-up the 4 kW of heat is on the entire target through a couple of stainless seethe heaters. Figure 1 shows a picture of the rotating target of the mock-up. To decrease the temperature of the bearings, a long path of thermal conduction from the graphite to the shaft was adopted. The rotation speed can be as slow as 5 rpm in the beamline. However, if the heating and rotating tests are to be performed at that speed, it may take several years for the bearings to break down. Therefore, in the tests, the rotating target can be rotated at a speed of 500 rpm. The resistance of the bearings is carefully monitored through the current of the AC servo-motor for rotation to acquire the lifetime of the bearings. When the motor current is beyond an experimentally determined criterion, the rotating target itself is replaced.

Fig.1 Picture of the rotating target

The heating and the rotating tests have been performed since March of 2009. The maximum temperature of the bearings has been experimentally measured to be 140 °C. The current of motor has been successfully monitored. We have not reached the final design of the rotating target, but the research and development is underway.

References

1) H. Iwase, K. Niita, T. Nakamura, J. Nucl. Sci. Technol. 39 (2002) 1142
2) N. Kawamura et al., Nucl. Instruments. Methods A 600(2009)114.
3) S. Makimura et al., Nuclear Instruments and Methods in Physics Research A 600 (2009) 146-149

Status of Superconducting Solenoid and Online Refrigeration System for the Decay /Surface Muon Channel

K. Shimomura, A. Koda, P. Strasser, N. Kawamura, H. Fujimori, S. Makimura, Y. Nemoto, W. Higemoto[1], R. Kadono, K. Nishiyama and Y. Miyake

High Energy Accelerator Research Organization (KEK), Tsukuba
[1]Advanced Science Research Center, Japan Atomic Energy Agency, Tokai

In FY 2008, a conventional superconducting muon channel (D1) was successfully installed at the MLF experimental hall II. Here, the superconducting sole-noid and its online refrigeration system are briefly reported. The superconducting solenoid magnet is 6 m long and consists of twelve units of 0.5 m coil. The magnet coil is forced-indirectly cooled by a su-percritical helium gas (4.8K at 0.80 MPaG) supplied from the on-line helium refrigeration system. The 80 K copper thermal shield, which is cooled by the helium gas taken from the intermediate heat exchanger in the cold box, is positioned between the 6 K shield tube and the warm iron cryostat vessel. There are only two sets of 12.5μm-thick thermal insulating aluminum foils adopted at the entrance and the exit of the 80K shield, and no other foil is used for 6K shield and coils in order to achieve the muon extraction at low mo-mentum as possible. The 80 K and 6 K shields are newly covered with thermal insulators to reduce the radiation heat load from the outside (Fig.1).

The He screw compressor of the on-line refrigerator supplies high-pressure helium gas (0.85 MPaG) to the cold box, which is designed to supply various types of helium requested to the superconducting solenoid. In the initial cooling stage, two transfer tubes going to the superconducting coils run in parallel mode to save the cooling time. In the final stage, they are cooled in series mode to satisfy the supercritical condition of 5 K helium, where at least 0.5 MPaG is required. For these transfer tubes, special care was taken to reduce the heat deposit from the outside. The cooling power of the on-line helium refrigeration system is 35 W at 4.5 K and 200 W at 80 K, and it can also produce 8 l/h of liquid helium. The whole system is monitored, con-trolled and interlocked by a VME-based controller and a dedicated software on LabVIEW (Fig.2). It cools down the system automatically, taking about three days from the room temperature. A long-term (typically one month) operation is now established under quite sta-ble condition.

Once the interlock detects any anomalies of the system, such as solenoid quench and/or refrigerator trip, the electric power supply immediately stops the current supply and the refrigerator changes to self-operation mode. To avoid the rapid increase of the pressure in the solenoid, a newly-made valve unit, which consists of safety valves, rapture disks and pressure gauges, opens the buffer pass returning He gas to the buffer tank. The monitor system records the temperatures and pressures of the superconducting coils, the helium re-frigeration system and the power leads, automatically. All recorded data are broadcasted to the MLF control room, by using MELSEC-NET.

In FY 2008, July, a valve unit installation and all piping, cabling works were finished and the first commission-ing was started. At that time, due to the lack of stabil-ity for the power lead flow, we met some difficulty with the operation to increase the electric power sup-ply current, only 1T (150A) was achieved as a stable condition. Therefore only surface muon beam was extracted at Day One (September 26th 2008). We im-mediately prepared temperature monitors of power lead at upper position etc. Careful operation with these monitors enabled us to achieve 4.1T (600A) stable operations at December for the decay muon. The present magnetic field for normal operation for surface/decay muon extraction is 0.308 T (45A) / 2.33 T (340A), respectively.

Fig.1 80K shield installing with thermal insulators.

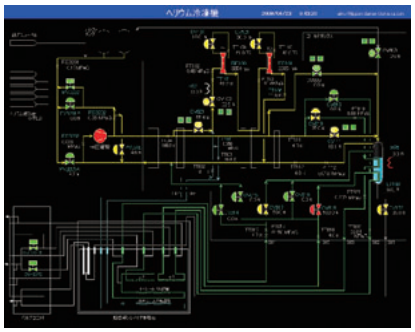

Fig.2 Diagram on the control/monitor software

DC-separator at D-line

K. Nishiyama, H. Fujimori, P. Strasser, A. Koda, Y. Kobayashi, K. Shimomura and Y. Miyake.

Muon Science Laboratory, High Energy Accelerator Research Organization (KEK)

One of the important items of equipment on the muon beamline is the DC-separator. It deflects undesired particles (mainly positrons) and transmits only muons to the experimental areas and reduces the background. At the first construction of muon D-beamline, the old DC-separator, which was disassembled and transported from the old KEK/BOOM facilities in Tsukuba, was installed. During the beam commissioning in FY 2008 the old separator showed its usefulness to im-prove the beam quality. However, the beam trajectory analysis and beam tuning revealed that the small gap of the DC-separator (10 cm) restricted beam intensity, and we decided to upgrade the separator.

A new DC-separator, shown in Fig 1. was manufactured by TOKIN, using the basic design of DC-separator at RIKEN-RAL: rectangular vacuum box, with ceramic isolation terminals up and down (rating voltage 300kV, supplied from the stock of accelerator group KEK), and a gap of 20 cm. To achieve homogeneity in electric field and magnetic field in a larger space, we performed 3-D FEM calculations for designing. The shape of the electrode was changed from parallel plate to bended plate optimized for the 20 cm gap. We could not improve magnetic field homogeneity by shimming or selecting of the pole thickness and positions. Homogenous magnetic field could be realized only using a window frame type of magnet coils, but such design was excluded due to the big electric terminals. In the future separator, the electric feed-through and magnetic winding should be re-designed. The effective field length as shown in Fig.2 is 891 mm measured for magnetic field and 585 mm calculated for electric field.

Fig.1 The photo of test of new DC-separator.

Tab.1 Parameters of DC-separator (dimensions in mm)

	Old separator	New separator
Beam gap / (mm)	100	200
HV-supply (KV/mA)	120 / 1	150 / 1
Electrode (L*W)	560*220 (Al,SUS)	500*300 (Al,Al)
HV-terminal	Cable /Trans oil	Porcelain/Air
Chamber (L*H*W) in	720*400	844*630*560
MagnetPole (L*H/G)	460*300/420	600*590/620
Coils (I,V,B)	100A32V, 30mG	85A32V, 28mG

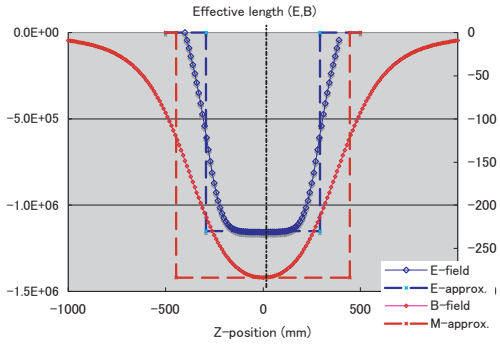

Fig.2 E-calculated and B-measured along z axis

The non-homogeneity for BL and EL value is about 5% in the 200 mm diameter. The deflection angle for positron at surface muon setting with ±150 kV is 5.40 deg (94 mrad) and muon spin is tilted by 7.3 deg. The muon beam trajectory will be affected at most ±6.3mrad in y-direction due to field inhomogeneity. A momentum spread Δp of muon beam will also affect the angle dispersion by $127\,\Delta p/p$ mrad.

The high voltage up to ±150 kV, the maximum output of the present power supply was achieved after several days of conditioning. The muon intensity at the experimental target is doubled due to the wider gap and reversing the polarity of quadrupole triplet mag-net Q7-9. For the surface muon, positron contamination was still visible even at the highest applied voltage when tuning was selected for optimizing the muon rate. Positron contamination can be removed practically by careful tuning of the solenoid and transport magnet while minimizing the e/μ ratio.

To achieve a better performance of e/μ separation, high voltage power supply will be exchanged soon to a 250 keV model.

KICKER and SEPTUM SYSTEM for DECAY MUON LINE

H. Fujimori, P. Strasser, K. Koseki*, Y. Hori*, H. Matsumoto* and Y. Miyake

Muon Science Laboratory, Institute of Materials Structure Science, High Energy Accelerator Research Organization, Tsukuba, Ibaraki, 305-0801
*Accelerator Laboratory, High Energy Accelerator Research Organization, Tsukuba, Ibaraki, 305-0801

The double pulse proton beam from the RCS hits the muon production target in MLF and produces a double pulsed muon beam. The muons are transported through the decay muon line to the two experimental areas (D1 and D2). As the dipole magnet (DB3), which directs the muon beam to the experimental area, has only one direction D.C. field, it is impossible to send the muon beam to both of the areas at the same time. If it becomes possible to divide the double pulsed muon beam and send them to both areas simultaneously, for example the first pulse to the area D1 and the second pulse to the area D2, the experimental efficiency will increase even further. Therefore a kicker and septum system will be installed to replace DB3.

The kicker and septum system is composed of five magnets, that is, two kicker magnets, two switchyard magnets and a septum magnet with two poles. The operation principle is shown in Fig. 1. The double pulse muon beam with 600 ns interval enters the kicker and septum system from the right. The first pulse turns right at 4.5 degrees by the two switchyards, while the second pulse turns left at 4.5 degrees by the two kickers, and each pulse enters the septum. Then, the first and second pulses are bent further by the septum by 35.5 degrees to the right to the area D1, and to the left to the area D2, respectively.

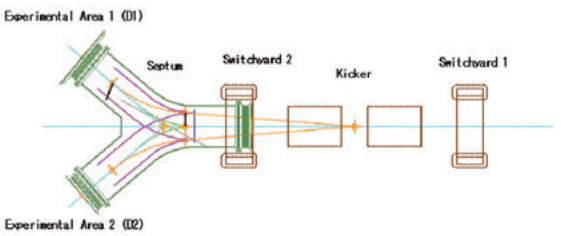

Fig.1 Kicker and septum system

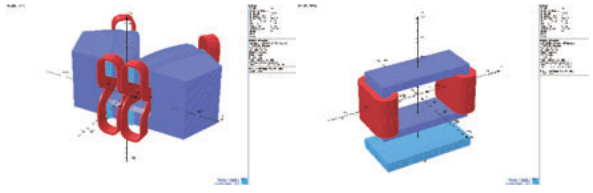

Fig.2 Analysis models of the septum and switchyard

Figure 2 shows the field analysis models of the septum and switchyard.

The septum magnets and the switchyard magnets, which were fabricated by NEC Tokin Corporation, have already been delivered. Figure 3 shows the field measurements of the septum and switchyard. Table1 shows a comparison between the measured and calculated BL integration values, which agree well with each other.

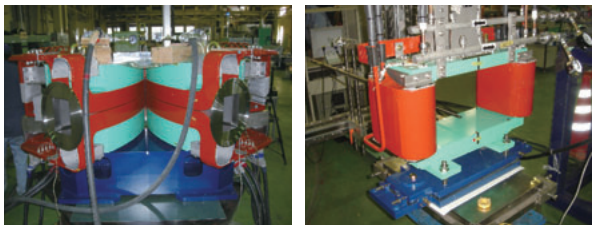

Fig.3 Field measurements of the septum and switchyard

Table1 Comparison between measurement and calculation

	BL integration (T・m)	
Magnet	Measurement	Calculation
Septum (at 1700A)	0.1298	0.1291
Switch yard (at 240A)	0.263	0.276

The bidding for the two kicker magnets and the vacuum chamber, which is called the kicker chamber, was won by Mirapro Corporation. The kicker chamber will be delivered this year. On the other side, the power supply for the kickers, which was fabricated by Nihon Koshuha Corporation, has already been delivered, and an operation test with a dummy load was successfully completed. The bidding for the power supply for the septum will take place this year. The power supply for DB3, which will no longer be needed, will be used for the switchyard magnets connected in series.

When the kicker chamber and the power supply for the septum will be completed, operation tests with the real magnets will be performed. The installation of the kicker and septum system is scheduled in summer 2011.

Design and implementation of the vacuum system of J-PARC MUSE

A. Koda[1,2], S. Makimura[1,2], H. Fujimori[1,2], P. Strasser[1,2], N. Kawamura[1,2], M. Kato[1,2], K. Nakahara[1,2], S. Takeshita[1,2], K. Shimomura[1,2], K. Nishiyama[1,2], Y. Miyake[1,2], N. Sato[3], H. Funahashi[3], K. Ueno[3], W. Higemoto[1,4] and S. Meigo[1]

[1]Materials and life science division, J-PARC Center, Tokai 319-1195
[2]Muon Science Laboratory, High Energy Accelerator Research Organization (KEK), Tokai, Ibaraki 319-1195
[3]Mechanical Engineering Center, High Energy Accelerator Research Organization (KEK), Tsukuba, Ibaraki 305-0801
[4]Advanced Science Research Center, Japan Atomic Energy Agency (JAEA), Tokai, 319-1195

In the M2 primary proton beamline in the Materials and Life Science Experimental Facility (MLF), the use of elastomer seal should be avoided because of the severe radiation due to the intense proton beam. Moreover, the beamline components must be handled remotely due to the residual radiation. Therefore, we developed the so-called KEK Muon Model of pillow-seal for the vacuum connection of the M2 primary beamline ducts [1,2,3]. The pillow installed between opposing flanges is actuated by compressed N_2 gas, achieving a good vacuum in the beamducts by additional differential pumping between the contact gaps. A mockup test of the pillow-seal assembly, which had been performed prior to the installation in the M2 beamline tunnel, revealed that the flatness and the average roughness of the opposing flanges are crucially important. Each of the 30 flanges of the vacuum ducts was individually checked to comply with the specifications; flatness below 100μm and average roughness below 0.2μm. Re-machining and re-polishing were performed if they exceed the limit.

The ducts of the first secondary muon beamline (D-line) constructed in MLF are connected by using tapered flanges (Yokohama Rubber Co., Ltd. YMV15090-K370 and YMV15090-K520), because the radiation problem during the maintenance is less important in the secondary beamline.

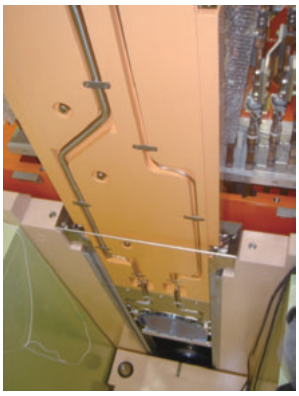

Fig. 1 Pillow-seal assembly installed in M2 beamline

The vacuum system of D-line (Fig.2) is isolated from the primary proton beamline by an all-metal gate valve (DGV1) assembled with a beam window of 50μm Kapton foil. The beam window is essentially important to prevent the tritium produced at the muon production target from defusing into and being absorbed by the cryogenic system of the superconducting solenoid. In the event of a quench of superconducting solenoid, absorbed tritium would be released due to the temperature rise. To prevent contamination by the tritium passed through the Kapton window, the section including the solenoid has a separate pumping station where the exhaust is led to the vent stack without passing through the other pumping stations.

References

[1] Original design of pillow-seal was developed at PSI and we redesigned it to M2 beamline.
[2] A. Koda et al., KEK-MSL report 2006, 11.
[3] A. Koda et al., KEK-MSL report 2008, 13.

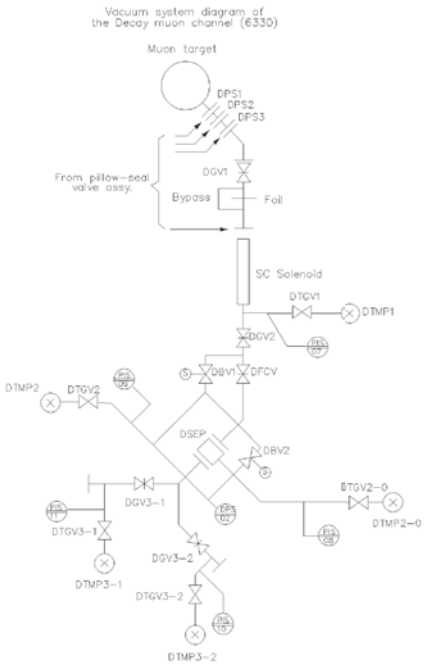

Fig.2 Schematics of the vacuum system of D-line

EPICS-based Remote Control System for D-line Slits

T. U. Ito[1,2], Y. Kobayashi[2,3], K. M. Kojima[2,3] and W. Higemoto[1,2]

[1]Advanced Science Research Center, Japan Atomic Energy Agency, Tokai, Ibaraki, 319-1195
[2]Muon Science Section, Materials and Life Science Division, J-PARC Center, Tokai, Ibaraki, 319-1195
[3]Muon Science Laboratory, High Energy Accelerator Research Organization (KEK), Tsukuba, Ibaraki, 305-0801

The D-line at J-PARC MUSE currently consists of three bending magnets, 18 quadrupole magnets, four slits, a DC separator, a superconducting solenoid and a beam slicer [1]. Among the beam line elements, the bending magnets, the quadrupole magnets, and the slits can be controlled remotely using the Experimental Physics and Industrial Control System (EPICS). In this report, we describe the current status of the EPICS-based remote control system for the D-line slits briefly.

EPICS is a set of Open Source software tools, libraries, and applications to create distributed soft control systems for large scientific experiments [2]. This system is used extensively for real-time and slow control of accelerator devices. At J-PARC MUSE, EPICS is used for the slow control of the beam line devices with own Programmable Logic Controllers (PLCs) via Ethernet. The EPICS software framework was installed in a standard Linux PC, including a Channel Access (CA) client and an Input / Output Controller (IOC) to serve as a server that communicates with the PLCs and publish the information to the CA client using the CA network protocol. A graphical user interface (GUI) was developed using the Motif Editor and Display Manager (MEDM) [3], allowing users easily to access the PLCs via EPICS.

The four slits of the D-line are powered and governed by two control boxes with own PLCs. The control box for three slits, DSL2, DSL3-1, and DSL3-2, is equipped with a PLC with a serial communication port (KV-3000, Keyence Corp.) and an Ethernet interface unit (KV-LE21V) while the other one for DSL4 is controlled by a PLC with an Ethernet port (KV-5000, Keyence Corp.). These are connected to the MLF control system network and communicate with an EPICS-IOC installed on Debian GNU/Linux running on a standard PC. Device supports for the KV-3000 and KV-5000

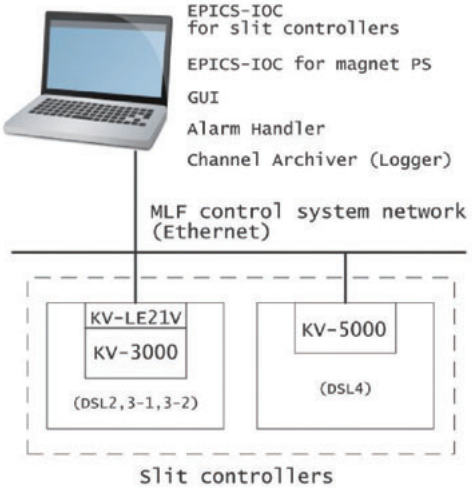

Fig.1 The schematic diagram of the EPICS-based remote control system for the D-line slits.

were developed on asynDriver [4] and netDev [5], respectively. A schematic diagram of the EPICS-based remote control system for the D-line slits is shown in Fig.1. Note that the KV-3000 was initially connected to another Linux PC serving as an EPICS-IOC with a RS-232C cable, which was connected to the MLF control system network [6]. However, this old configuration held a serious problem with the response speed, which is drastically improved with the current configuration.

The GUI for monitoring and changing device status via EPICS was also developed and installed on the same PC. The positions of the slits are displayed on status monitors and updated typically every one second. The users can control the move/stop switch and set point of the slit position from these panels.

References

1) W. Higemoto et al., Nucl. Instr. and Meth. A 600 182-184 (2009)
2) http://www.aps.anl.gov/epics/
3) http://www.aps.anl.gov/epics/extensions/medm/
4) http://www.aps.anl.gov/epics/modules/soft/asyn/
5) http://www-acc.kek.jp/EPICS_Gr/Products/NetDev/netdev-man.html
6) T. U. Ito et al., J. Phys.: Conf. Ser. 225 012022 (2010)

Development of Muon Beam Slicer

W. Higemoto, T. U. Ito, K. Ninomiya, R.H. Heffner, K. Shimomura*, K. Nishiyama* and Y. Miyake*

Advanced Science Research Center, Japan Atomic Energy Agency, Tokai, Naka, Ibaraki 319-1195
* Muon Science Laboratory, Institute of Materials Structure Science, High Energy Accelerator Research Organization, Tsukuba, Ibaraki, 305-0801

For pulsed-beam μSR experiments, the largest observable muon spin precession frequency is restricted by the width of the muon pulse. Since the time structure of the muon pulse is about the same as that of the proton pulse, the width of the muon pulse is going to be longer than 100ns at the 1MW operation. In addition, the proton beam has a two bunch structure, which gives a constraint to the observable muon spin precession frequencies. To overcome the limited time resolution which comes from the time structure of the proton beam, a muon beam slicer is installed into the Decay/Surface beamline. The beam slicer consists of an electric kicker, a pulsed electric power supply which has a fast rise time, and a correction magnet. Figure 1 shows the photograph of the electric pads which are located inside of the slicer. A rise time of the electric field less than 20 ns (10-90%) and a pulse width of about 300 ns have been achieved. This allow a chopped muon pulse width of less than 30 ns[1].

In FY2009, we examined the performance of the muon beam slicer. Figure 2 shows the muon beam observed by a plastic scintillator placed on the muon beam. Without the electric field, the muon beam is bent by the correction magnet at the muon slicer. When the electric field is applied, the muon beam comes back to the original trajectory and can reach to the counter position. In Figure 2, an electric field was applied synchronized to the timing of the second muon pulse, and only the second muon pulse reached to the muon spectrometer position. We have confirmed that muon spin rotation measurement is possible in this "single pulse operation mode".

We have also succeeded in the beam slice operation. When the electric field is applied in the middle of the second muon pulse, only the tail part of the muon beam can reach the spectrometer and a narrow pulse can be obtained. By using such "muon slice mode", we have obtained narrower pulse width of less than 37ns (FWHW) for the muon beam.

In the muon slice mode, much of the muon is lost and high intensity beam is required to obtain reasonable amount of muons available for the experiment. As shown in Fig. 2, the pulse shape of the electric field is not a perfect rectangular shape and development of the pulsed power supply is still underway.

Detail of the performance will be reported elsewhere.

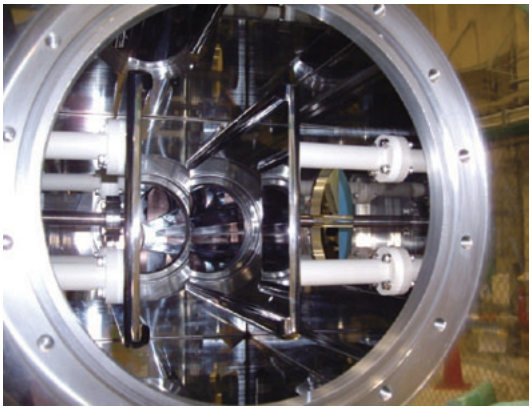

Fig.1 Photograph of the electric pads

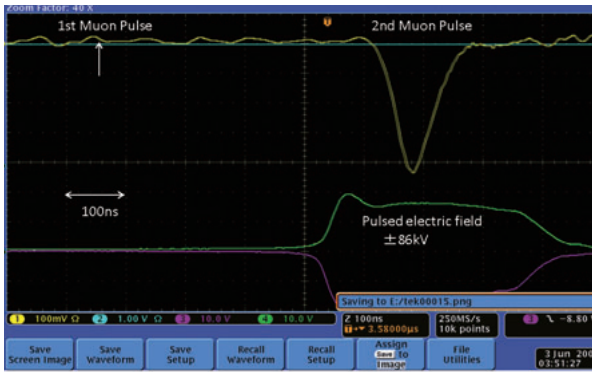

Fig.2 By applying pulse electric field, muon pulse is kicked.

References

1) W. Higemoto et al., Journal of Physics: Conference Series 250 (2010) 012012.

A pulse-height analysis for the tuning of D1 general purpose μSR spectrometer

K.M. Kojima[1,2], M. Hiraishi[2], M. Miyazaki[2], A. Koda[1,2], T. U. Ito[3], N. Kawamura[1], K. Nishiyama[1], K. Shimomura[1], Y. Miyake[1], W. Higemoto[3] and R. Kadono[1,2]

[1] Muon Science Laboratory, Institute of Materials Structure Science, High Energy Accelerator Research Organization(KEK), Tsukuba, Ibaraki, 305-0801
[2] Department of Materials Structure Science, The Graduate University for Advanced Studies (SOKENDAI)
[3] Advanced Science Research Center, Japan Atomic Energy Agency (JAEA), Tokai, Naka, Ibaraki, 319-1195

Since the instantaneous μ-e decay rate becomes enormously large (~10^9cps for 120kW operation) right after the arrival of pulsed muons, μSR spectrometers in pulsed facilities have large number of positron counters. The general-purpose μSR spectrometer at D1 beamline of MUSE (muon science establishment) / MLF has currently 256 positron counters (128 telescope pairs). Adjustment of high-volts (HV's) of the photo-tubes and the threshold levels (Vth's) of the discriminators needs a well-defined guideline for tuning. We employed a charge sensitive analogue to digital converter (QDC) and measured the pulse-height for positron events of all the individual counters of the spectrometer and determined HV's and Vth's of the detector channels. Fig.1 shows the schematic diagram of the pulse height measurement of the photo-tubes. In the current D1 spectrometer, we have one HV connected to a 16-channel photo-tube, each of the channels connected to a lightguide attached to a plastic scintillator. Since one HV controls the 16 counters which may vary in efficiency, we have to choose the HV so that none of the attached 16 counters should be saturated nor poorly gained. Since the QDC we employed (Nikiglass A3200) has 16 channels of analog input and individual gate input, we simultaneously took histograms of the counters belonging to the same HV.

An example of resulting pulse-height spectrum for one counter is shown in Fig.2. The

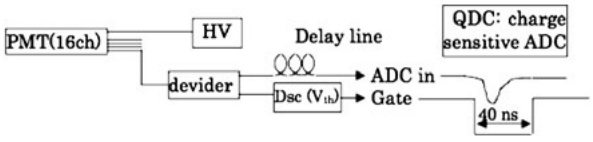

Fig.1 Schematic diagram of pulse-height analysis. The signal from the photo-tube is divided by a passive divider; one is sent to the discriminator which makes the gate pulse. The other is delayed by a cable and goes to the linear input of QDC.

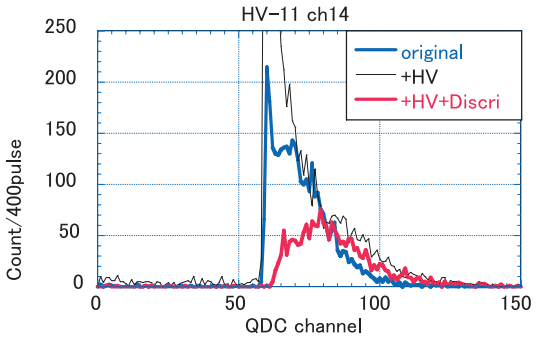

Fig.2 An example of pulse-height distribution of a photo-tube. The original setting (blue) had a noise peak near the threshold level (Vth). We increased HV by 100V (black) and simultaneously increased Vth to cut the noise peak (red).

noise peak, which was apparent in the original setting disappeared after raising the HV and Vth. We have done such adjustments to the parameters for the 256 positron counters.

In Fig. 3, we show the result of the tuning. The shown time spectra (Ag in zero-field) are supposed to be time-independent. Before the tuning, there was a residual relaxation due to the noise peaks in individual counters. After the tuning, the artifact goes away. The tuning was completed in Run #33 (May 2010) and all the measurements of the users enjoy the result.

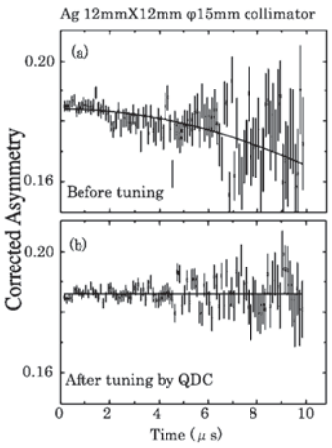

Fig.3 Result of the spectrometer tuning at D1 beamline. After the adjustment of HV and Vth, the spectrum became flat as it should be for Ag.

Development of DAQ system at J-PARC MUSE

A.Koda[1,2], S. Takeshita[1,2], K.M. Kojima[1,2], M. Miyazaki[2], M. Hiraishi[2], R. Kadono[1,2], S. Yamagata-Suzuki[3], Y. Yasu[4], T. Uchida[4], K. Tauchi[4] and M. Tanaka[4]

[1] Materials and Life Science Division, J-PARC Center, Tokai, Ibaraki 319-1195
[2] Muon Science Laboratory, High Energy Accelerator Research Organization (KEK), Tokai, Ibaraki, 319-1195
[3] Computing Research Center, High Energy Accelerator Research Organization (KEK), Tsukuba, Ibaraki 305-0801
[4] Detector Technology Project, High Energy Accelerator Research Organization (KEK), Tsukuba, Ibaraki 305-0801

The data acquisition (DAQ) system for the μSR experiment at J-PARC MUSE (Muon Science Establishment) was entirely renewed from that used at Tsukuba, because of the high event rate expected for the intense primary proton beam which is planned to have power of 1 MW power. To build our DAQ system, we employed the DAQ middleware [1] developed by members of Detector Technology Project of KEK. The DAQ middleware is commonly used in several neutron experiment groups [2,3] in MLF (Materials and Life science experimental Facility), J-PARC. Gigabit Ethernet is used as the data transfer bus connecting the front-end electronics and the DAQ programs. The DAQ middleware, which is based on the Robot Technology middleware, is comprised of components, or small programs, exchanging messages among them. The middleware is suitable for a multi processor hardware environment distributed on the high-speed network; considerably high data-taking rate is cooperatively processed in parallel by the multi processor environment.

Currently, the μSR data acquired at the D1 experimental area in MLF are processed by five middleware components running on three different Linux PCs. The system was examined in the test beam time in December 2009 where the proton beam intensity of 300 kW was delivered for a few minutes, and showed no problem handling the data rate of ~130k counts per pulse, as shown in Fig. 2.

Another benefit of using the commonly used DAQ middleware is that we can employ the user interface currently being developed by the neutron experimental groups of MLF. This will provide users similar *look-and-feel* of the experimental procedures both at the neutron and muon beam lines in MLF. This will promote the usage of the two experimental probes provided at MLF without being bothered by tedious differences in the experimental procedures.

References

[1] **http://daqmw.kek.jp/**
[2] S.Y. Suzuki et al., Nucl. Instr. and Meth. A **600** (2009) 53.
[3] S.Y. Suzuki et al., Physica B **404** (2009) 1002.

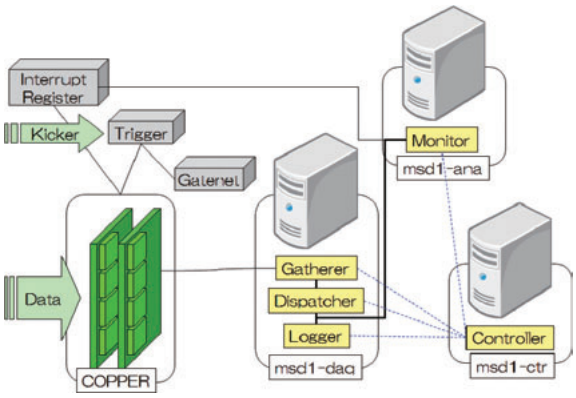

Fig.1 Schematic diagram of the μSR DAQ system at D1 beamline. Five DAQ middleware components are running on three PCs, and the DAQ front-end (COPPER) communicates with them via Gigabit Ethernet.

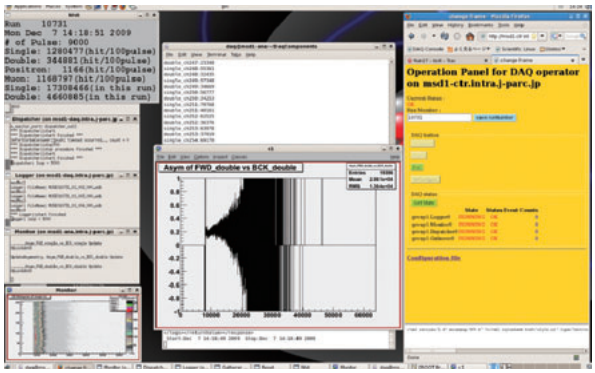

Fig.2 Screen shot of the μSR DAQ software in the beam test with the proton beam intensity of 300 kW.

Auto-run sequence on LabVIEW at D1 general purpose μSR spectrometer

K.M. Kojima, A. Koda, N. Kawamura, T.U. Ito[1] W. Higemoto[1], Y. Miyake and R. Kadono

Muon Science Laboratory, Institute of Materials Structure Science, High Energy Accelerator Research Organization(KEK), Tsukuba, Ibaraki, 305-0801

[1] Advanced Science Research Center, Japan Atomic Energy Agency (JAEA), Tokai, Naka, Ibaraki, 319-1195

Muon beam intensity at the 20 kW operation (upto October 2009) and the 120 kW operation (since November 2009) is qualitatively different: the latter takes only no more than 20 minutes to accumulate necessary event statistics for a standard μSR measurement, In this short measurement time and frequent necessity to change the experimental conditions, automatic run control, including the ability to change and stabilize the temperatures and the magnetic fields becomes essentially important.

The auto-run sequence on LabVIEW, which we introduce here, was originally developed by KMK in 2002 for an infrared spectrometer. NK modified Exp2k (old data acquisition system at KEK-MSL) so that it accepts commands via TCP/IP port 2000 from the auto-run sequence. Up to 2006, AK updated the auto-run sequence to incorporate new equipment.

At MLF Muon Science Establishment (MUSE), the data acquisition system was newly developed based on "data acquisition middleware" (DAQ-MW) [1], which accepts controls via TCP/IP port 80. We have rewritten the run start/stop sub-VIs (subroutines in LabVIEW) of the pre-existing auto-run sequence so that it controls the new DAQ system.

The magnet control is based on EPICS [2] at J-PARC and TUI developed a front-end for the magnetic field at the sample. We have also rewritten the sub-VI so that the sequence can access it.

In Fig.1, the Front Panel of the auto-run sequence is shown. It is made of two parts: one is the command part to run the experiment and the other is the monitor part to record the experimental conditions. These two are independent loops and run parallel in the LabVIEW macro.

The monitor part keeps on logging the temperature and fields, etc., which are saved in a log file. The time evolution of the monitored values also appears on the "Monitor graph" window. The command part executes the commands written in the "Command window" in sequence. The response of DAQ and selected commands appears on "DAQ status" and "Command status" window, respectively.

The standard user interface of MLF (neutron and muon) is currently being developed. The introduced auto-run sequence on LabVIEW is a quick fix before the standard environment is introduced to the muon facility.

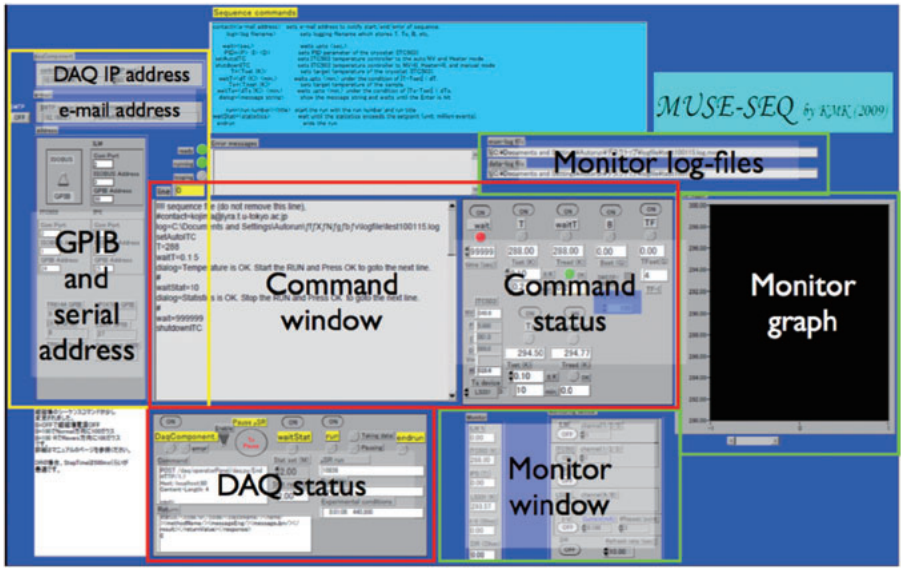

Fig.1 The front panel of the auto-run sequence on LabVIEW

References

[1] http://daqmw.kek.jp/

[2] http://www.aps.anl.gov/epics/

Development of muonic X-ray measurement system

K. Ninomiya[a, b], P. Strasser[b, c], K. M. Kubo[d], N. Kawamura[b, c], K. Shimomura[b, c], T. U. Ito[a, b], W. Higemoto[a, b], T. Nagatomo[d], M. Kita[e], A. Shinohara[e] and Y. Miyake[b, c]

[a] Advanced Science Research Center, Japan Atomic Energy Agency, Ibaraki 319-1195
[b] Muon Science Section, Materials and Life Science Division, J-PARC Center, Ibaraki 319-1195
[c] Muon Science Laboratory, High Energy Accelerator Research Organization, Ibaraki 305-0801,
[d] Division of Natural Sciences, International Christian University, Tokyo, 181-8585
[e] Graduate School of Science, Osaka University, Osaka, 560-0043

In J-PARC MUSE, intense negative muon beam is available due to the high production efficiency for negative muons because of the high energy (3 GeV) of the primary proton beam. The application studies using negative muons are beneficial at J-PARC, as well as those using positive muons. When a negative muon stops in a material, it is captured by the Coulomb field of a nucleus and forms a muonic atom that has one negative muon substituting for an electron. The captured muon exists in highly excited state initially. The muon immediately cascades down to the muonic 1s state while muon characteristic X-rays (muonic X-ray) are emitted on the way. Some experiments using negative muon beam have already been started in J-PARC MUSE. To advance such research, development of muonic X-ray measurement system is necessary. Here we report on the status of the muonic X-ray measurement system.

Figure 1 shows the photo spectrum measured by high purity germanium detector by muon irradiation for nitrogen oxide gas at D1 beamline in MUSE. Muonic X-rays emitted from muonic nitrogen and oxygen atoms are clearly identified. We achieved S/N~10 for muonic nitrogen K_α X-rays by using a coincidence method with the muon beam as described below. In J-PARC MUSE, pulsed muon beam with ~100 ns width is provided. Muonic X-ray emissions occur just after muon stop in the sample. So we can obtain low background muonic X-ray spectra by extracting photo events correlated with muon beam pulse (proton injection signal on muon production target). The electronic diagram in our system is shown in Fig. 2. The signal from germanium detector is divided into two. One is amplified by fast filter amplifier. The signal that has correlation with the muon beam pulse signal is extracted as the gate signal for X-ray detection. Another is amplified and shaped by spectroscopy amplifier. The pulse height is recorded by a CAMAC-based ADC. By using this method, the S/N ratio is improved threefold over the previous measurement [1] without any resolution degradation.

Now we prepare six germanium detectors for muonic X-ray detection at MUSE and effective measurement ranging from 10 to 2000 keV is available. The better S/N ratio will be achieved by improving arrangement of radiation shields.

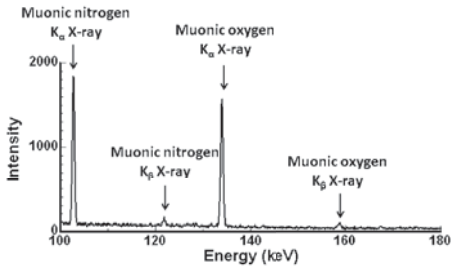

Fig.1 Muonic X-ray spectrum for nitrogen oxide sample. The momentum of incident muon in this measurement is 19 MeV/c.

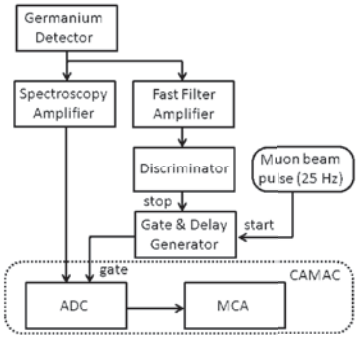

Fig.2 Electronics block diagram for muonic X-ray measuring system

References

1) J-PARC News, vol.48 (2009) and K. Ninomiya et al., J. Phys., Conf. Ser., **225**, (2010) 012040.

Status of Super Omega Channel for the U Beamline of MUSE

Y. Ikedo, Y. Miyake, K. Shimomura, P. Strasser, K. Nishiyama, N. Kawamura,H. Fujimori, S. Makimura, A. Koda T. Ogitsu, Y. Makida, T. Adachi[1], M. Yoshida, A. Yamamoto, T. Nakamoto, K. Sasaki, K. Tanaka, N. Kimura, W. Higemoto[2],Y. Ajima, K. Ishida[3] and Y. Matsuda[1]

High Energy Accelerator Research Organization, Tsukuba, Ibaraki
[1] University of Tokyo, Bunkyo, Tokyo
[2] JAEA, Tokai, Ibaraki
[3] RIKEN, Wako, Saitama

Super Omega muon beamline is currently under construction at the Materials and Life Science Facility (MLF) in the J-PARC. The Super Omega beamline has a large acceptance for muons from the production target and will produce the highest intensity pulsed muon beam in the world. This beamline is designed to capture and transport both surface and cloud muons for simultaneous use in a variety of experiments such as ultra-slow muon generation and the muon transfer reaction experiment. The expected rate is 4×10^8 μ^+/s for surface muons, and 10^7 μ^-/s for cloud muons [1].

Super Omega beamline consists of the normal-conducting capture solenoids, the superconducting curved transport solenoids, and the axial focusing system. At present, the construction of the capture solenoids has been completed and was installed at March 2009. The design work of the transport solenoids has been finished. The calculation of the beamline optics involving the axial focusing system and the positron separator are underway with particular care to ensure their connectivity with the transport solenoids.

The transport solenoids consist of two curved sections and a 6 m straight section. Each curved section is segmented into seven individual solenoids aligned in an eighth of torus with a radius of 1 m in order to bend the captured muons by 45-degree. It is designed to transport both positive and negative muons simultaneously into experimental hall 2. It will be cooled using five 1.5-W Gifford-McMahon (GM) refrigerators.

The optional function of the transport solenoid system is to select the muon polarity for experimental motives. After the muons pass the upstream curved section, the μ^+ and the μ^- drift up and down respectively due to curved flux effect. Then diverting flux line vertically in the long straight section by using a pair of vertical field dipole coils, the one polarity muons can be absorbed by the coil material. The dipole coils are each mounted on the outside of the solenoid symmetrically between a solenoid central plane. At the exit solenoid, both vertical and horizontal dipole fields with axially integration of 0.01 T·m are applied to improve adjustability of the final focusing, which is mainly done by magnets in the experimental area.

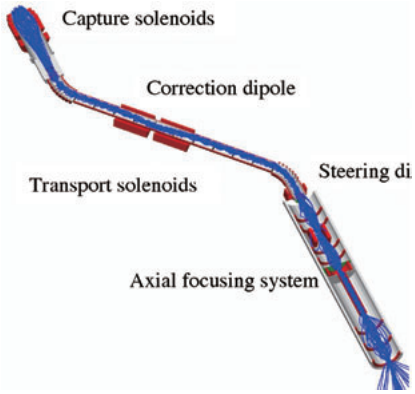

Fig.1 Schematic figure of the Super Omega beamline

The beam transportation and their trajectories of Super Omega beamline were calculated using a GEANT4-based simulation package called G4Beamline [2]. According to the simulated result, the transport rate of the captured surface muons is almost 100% at the end of the curved transport solenoids. Finally, the curved transport solenoids will be installed in the MLF/J-PARC in the summer of 2011 and will be tested until March 2012.

References

1) K. Nakahara et al., Nucl. Inst. and Meth. in Phys. Res., vol. A**600**, pp.132-134, 2009.
2) Muons, Inc. 552 Nm Batavia Avenue, Batavia, IL, available at http://www.muonsinc.com.

Generation of negative slow muon beam in J-PARC Muon Facility

N. Kawamura, T. Matsuda, P. Strasser and Y. Miyake

Muon Science Section, Materials and Life Science Division, J-PARC Center
Muon Science Laboratory, High Energy Accelerator Research Organization

The J-PARC Muon Facility succeeded in transporting the first muon beam to the ex-perimental area in September 2008. In comparison with the proton beam energies of other meson facilities in the world, which are around 500~800 MeV, in J-PARC, 3 GeV is about four times higher. The negative pion production cross section increases steeply above 1GeV, while positive one does not show a big change [1]. Thus, the negative pion yield in J-PARC Muon Facility is higher than the value simply scaled up by the beam current. Therefore, the negative muon characterizes J-PARC Muon Facility.

The other characteristic point in J-PARC Muon Facility is ultra slow muon beam by la-ser resonant-ionization (LRI) method [2,3]. Based upon their developments, in J-PARC Muon Facility, the design work of ultra slow beam line by LRI is in progress for practical use. However, LRI method is available only to positive muon and not to negative muon, be-cause positive muon forms muonium which is dissociated by laser, while a negative muon forms muonic atom. A negative muon has 200-times higher binding energy than a nor-mal atom, in which a negative muon waits for the decay to an electron and two neutrinos or a competitive process of nuclear capture.

In order to generate slow negative muon beam, from the world-intense negative muon beam in J-PARC, we started a fundamental study.

Technically, slowing down of a negative muon is very difficult in comparison with positive one. We cannot use any cooling method applied to positive muons like the degrader method established at PSI or the LRI method. Furthermore, muon has a 2.2-μs lifetime, which is too short to apply any cooling methods for any other particles with infinite life time. Slowing down have to be completed earlier enough than the muon life time to free-decay loss.

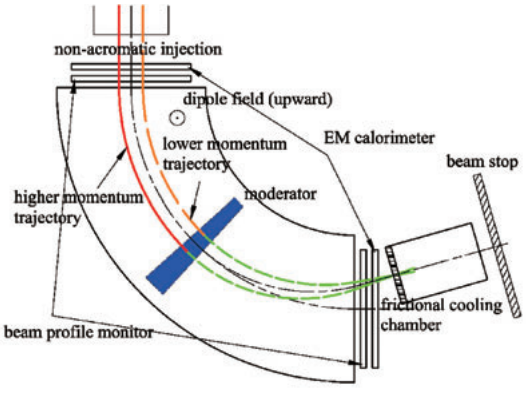

Fig.1 Schematic figure of the test setup.

For the first step of negative slow muon production at J-PARC Muon Facility, we will use a cyclotron to trap a few MeV muons from pion decay. Simons *et al*. succeeded in trapping cloud muons, i.e. 30 MeV/c μ^-, and slowed them down to the range of around 10 keV [4]. Negative muons are injected toward the outer side of the weak-focusing cyclotron field and are bound into the orbit where they lose the ener-gies through moderators placed at the mid-plane of cyclotron. By a pulse kicker de-vice, the accumulated muons are extracted to the axis direction of cyclotron and are injected into a frictional cooling chamber. The frictional cooling method [5], moderation in matter and acceleration in an electric field, is well matched through connecting to the cyclotron trap. The balanced energy is typically a few keV, and could be around 1 keV.

In J-PARC Muon Facility, 30-MeV/c μ^- rate is expected to be above 10^5/s for 1-MW proton beam, and this yields 10^2 keV-muons per second. The optimization of the moderator and cyclotron field is important in the design work. Construction of the setup for the test experi-ment has started in J-PARC, as shown in Fig. 1. The first step is to check the effect of moderators placed in the magnetic field. For this purpose, a dipole magnet will be used, and several moderators containing rare-gases solids will be examined and may be placed in the cyclo-tron trap.

References

1) B.J. VerWest *et al*., Phys. Rev. C, 25 1979 (1982).
2) K. Nagamine *et al*., Phys. Rev. Lett., 74 4811 (1995).
3) Y. Miyake *et al*., J. Nucl. Sci. Technol., 39 287 (2002).
4) L.M. Simons, Hyperfine Interactions 81 253 (1993).
5) Mühlbauer et al., Hyperfine Interactions 119 305 (1999).

A Test of Muon Beam Tracking by GEM

T. Masuda, N. Kawamura, K. Ninomiya[1] and P. Strasser

Muon Science Laboratory, High Energy Accelerator Research Organization(KEK)
1 Advanced Science Research Center, Japan Atomic Energy Agency (JAEA)

Information on muon beam trajectory is important for developing new subjects of beam utilization. In this study, we performed a test of the Gas Electron Multi-plier (GEM) to detect the muon beam. This detector has nine GEMs comprising three segments in length and three segments in width. One drift mesh (cathode), two GEM printed circuit boards (Fig. 1) [1], and one readout pad are set up in one segment as shown in Fig. 2, and it is filled with the Ar-CO_2 gas. When charged particles go into the detector where the bias voltage is applied between the drift mesh and the GEM printed circuit board, the electromagnetic shower is generated. This electromagnetic shower is accelerated and in-creased while passing the hole of the GEM printed circuit board. This is read from the readout pad, and the charged particles are detected.

When the GEM is used, the beam is usually entered vertically from the mesh side of the GEM for detec-tion. However, this experiment aimed to test whether it was possible to determine the trajectory of the muon beam with the GEM. Therefore, the beam was in-jected horizontally, penetrating to the narrow wall of the GEM of approximately 5 mm × 30 mm (Fig.2). There are nine segments in the active area of the GEM as shown in Fig. 3, and the beam trajectory may be identified by the segments. For instance, it can be deduced that the muon beam passes along the A-line when the muon incident signals are detected in the place of 1, 2, and 3 of the detector, and are not de-tected in the places of 4, 5, 6, 7, 8, and 9. In the actual experiments, the number of the incident muons was reduced to several counts per pulse by the slit.

Fig. 4(a) shows the number of complete muon trajec-tory events. There are 1228, 738 and 655 muon beam trajectories detected, respectively for the A-, B- and C-lines. Fig. 4(b) shows the number of the partial tra-jectory events for the B-line. There are 2163, 646 and 738 counts for “6”-only, “6+5”-only and “6+5+4” (i.e. complete B-line) trajectory events. It was found that single segment event is the most in the result of this experiment.

There are a few points for improvement of this ex-periment: estimate of the absolute number of trajecto-ries after correcting efficiency, estimate of the errors, and establishment of accurate positioning of the GEM relative to the beam. However, this is the first confir-mation that muon beam trajectory is detected by using a GEM detector.

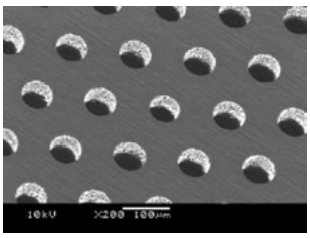

Fig.1 GEM printed circuit board diagram

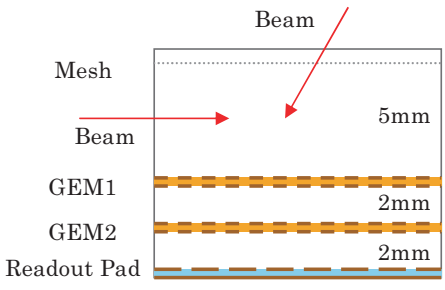

Fig.2 GEM schematic

Reference

[1] F. Sauli, NIMA 386 (1997) 531.

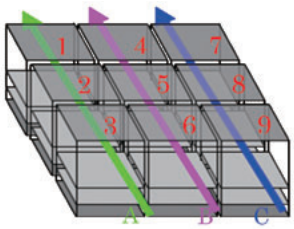

Fig.3 Muon beam tracking

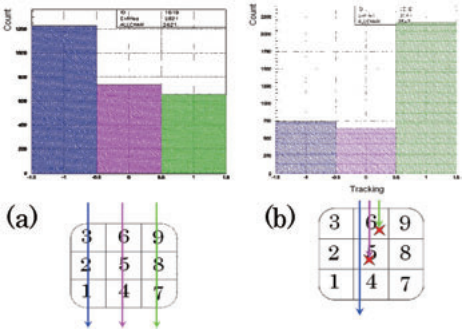

Fig.4 The result of the muon beam tracking. (a) number of A,B,C-line events. (b) number of partial trajectory events.

Facility Status

Beam operation status at MLF

Beam commissioning of the MLF was started on May 30th 2008. On the first day of the beam commissioning, the first neutron beam was observed at BL10 of the JSNS. On September 26, 2008, the first muon beam was observed at the MUSE. Since December 2008, user programs have started with the beam power of 20 kW and continuous 24-hour operation. In the early stage of beam operation, beam was frequently stopped due to the discharge at the RFQ in LINAC accelerator. In order to operate according to schedule as much as possible, we decided to take a short maintenance period to refresh the surface of the RFQ for one day every four days. Although four-hour conditioning in each day was required in the end of Run #22 held in February 2009, the beam availability became better thanks to the surface treatment. After Run #26 in October 2009, the vacuum system at the RFQ was drastically improved. Consequently the availability reached larger than 80%. Run #27 in November 2009, beam operation of 120-kW proton beam was succeeded with extremely high availability larger than 90 %.

During JFY 2008 and 2009, two major failure incidents happened at MLF, leading to long-term of beam stoppage. At the end of Run #22 on February 28th 2009, a pump in the cryogenic system for neutron source was tripped while warming up the liquid hydrogen after terminated Run #22. The cryogenic system was recovered at the end of May 2009 so that Run #23 was canceled. In the beginning of Run #30 on February 13th 2010, the accumulator in the cryogenic system for neutron source leaked hydrogen. Therefore, Runs #30 and 31 were cancelled in JFY2009. In what should be described as a minor trouble, due to failure of door switch for interlock system, the personnel protection system (PPS) was activated on January 31st, 2010, and this turned off the ion source of J-PARC and lead to 10 h beam stop for MLF.

Table 1 Run cycle, scheduled time and availability

Run cycle	Date	Scheduled Time (h)	Availability (%).
20	Dec 2008	66	85.3
21	Jan 2009	257	63.1
22	Feb 2009	427	60.0
23	Apr 2009	Canceled due to pump failure	
24-25	May/June 2009	394	75.1
26	Oct 2009	183	84.3
27	Nov 2009	270	86.3
28	Dec 2009	273	92.6
29	Jan 2009	297	89.7
30	Feb 2009	Canceled due to accumulator failure	
31	Mar 2009	Canceled due to accumulator failure	

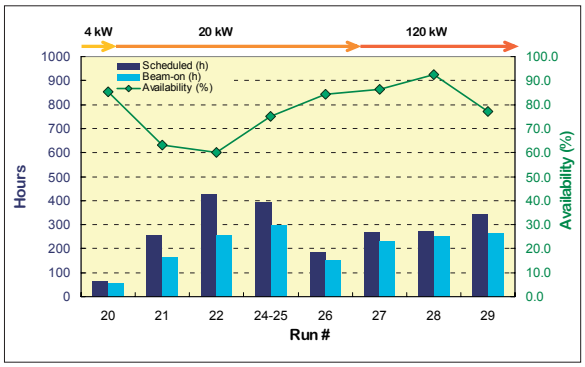

Fig.1 Beam operational time and availability

Users at MLF

At the user office of J-PARC, the cumulative number of users is recorded, excluding the inner house users belonging to J-PARC. Since the beginning of the user program at MLF in December 2008, 1,052 person-days of users came to MLF in JFY 2008, of which 62 person-days were foreigners. In JFY 2009, 3,539 person-days of users came to MLF, where 119 person-days came from foreign countries.

Accepted proposals list for MLF experiments in JFY2008

	Beam Line	Proposal ID	Applicant	Affiliation	Type of Use	Title of Experiment
1	BL-01	2008A0024	Kenji Ohoyama	Tohoku University	General Use	Determination of Wave Function of the 4f Ground States in Quadrupolar Ordering Systems RB_2C_2 by Observation of Crystal Electric Fields
2	BL-01	2008A0070	Seung-Hun Lee	University of Virginia	General Use	Magnetic Excitaions in a Trilpet Superconductor Sr_2RuO_4
3	BL-08	2008A0008	Ryoji Kiyanagi	Tohoku university	General Use	Investigation of Subtle Structural Changes in Impurity Doped $C_{12}A_7$
4	BL-08	2008A0052	Hajime Sagayama	Tohoku University	General Use	Origin of Ferroelectricity in Multiferroic $MnWO_4$
5	BL-08	2008A0059	Yuji Noguchi	University of Tokyo	General Use	Structural Analysis for Materials Design of Bi-based Perovskite Ferroelectric Oxides
6	BL-08	2008A0065	Yasushi Idemoto	Tokyo University of Science	General Use	Crystal Structure Change During Charge-discharge Process in Li(Mn, Ni)O_2 as a Cathode Active Material for Lithium ion Battery
7	BL-08	2008A0069	Yukio Noda	Tohoku University	General Use	Ferroelectric Transition on Breaking Quantum Paraelectricity in $SrTiO_3$
8	BL-10	2008A0018	Hiroyuki Nojiri	Tohoku University	General Use	High Magnetic Field Neutron Diffractions in Frustrated Multi- ferroics
9	BL-10	2008A0028	Masahiro Hino	Kyoto University	General Use	Experimental Test of TOF-MIEZE Spectrometer
10	BL-10	2008A0049	Shigehisa Yamamoto	RENESAS Technology	General Use	Study of Neutron-induced Soft Error in the Advanced Semiconductor Device
11	BL-19	2008A0022	Yo Tomota	Ibaraki University	General Use	Time Slice Structure Analysis for Microstructure Evolution During Processing of Advanced Steels
12	BL-19	2008A0025	Hiroshi Suzuki	Japan Atomic Energy Agency	General Use	Thermal Stress in Bulk Metallic Glasses and Their Accommodation by Annealing

Accepted proposals list for MLF experiments in JFY2009A

	Beam Line	Proposal ID	Applicant	Affiliation	Type of Use	Title of Experiment
1	BL-01	2009A0005	Seung-Hun Lee	University of Virginia	General Use	High Energy Magnetic Excitations in a Triplet Superconductor Sr_2RuO_4
2	BL-01	2009A0093	Ryoichi Kajimoto	Japan Atomic Energy Agency	Instrumental Development Use	Commissioning of the 4SEASONS Spectrometer
3	BL-01	2009A0087	Masatoshi Arai	Japan Atomic Energy Agency	Project use	Neutron Scattering Study of High-Tc Superconductors
4	BL-03	2009A0044	Yoko Sugawara	Kitasato University	General Use	Neutron Diffraction Analysis of Disodium Uridine 5'-Monophosphate Heptahydrate
5	BL-04	2009A0010	Yoshiaki Kiyanagi	Hokkaido University	Project use	Measurements of Nuclear Data of Minor Actinides and Long Lived Fission Products for Advanced Nuclear Systems
6	BL-08	2009A0003	Yuji Noguchi	University of Tokyo	General Use	Structural Determination for Materials Design of Bi-based Perovskite Ferroelectric Oxides
7	BL-08	2009A0004	Je-Geun Park	Sungkyunkwan university KOREA	General Use	To Understand the Multiferroic Mechanism of Pb$(Fe_{0.5}Nb_{0.5})O_3$
8	BL-08	2009A0009	Hiroyuki Kimura	Tohoku University	General Use	Crystal and Magnetic Structure of Multiferroic $BiFeO_3$-$BaTiO_3$ Composite
9	BL-08	2009A0013	Yasushi Idemoto	Tokyo University of Science	General Use	Heat-treatment Effects on Crystal Structures of Li (Mn, Ni, Co) O_2 as Cathode Active Materials for Lithium Ion Battery
10	BL-08	2009A0038	Ryoji Kiyanagi	Tohoku University	General Use	Doping Effect on Crystal Structure in Nanoporous Material $C_{12}A_7$

	Beam Line	Proposal ID	Applicant	Affiliation	Type of Use	Title of Experiment
11	BL-08	2009A0070	Sadamu Takeda	Hokkaido University	General Use	Structures of Hydrogen-Molecule Storage Rh- and Cu- Coordination Complexes
12	BL-08	2009A0090	Takashi Kamiyama	KEK	Project use	Structual Study of Funcutional Materials and Development of Advaned Methodology Using SuperHRPD
13	BL-10	2009A0078	Hiroaki Asai	HIREC Corporation	General Use	Feasibility Estimation of White-Spectrum Neutron for the Single Event Tolerance Examination of Semiconductor Element
14	BL-10	2009A0017	Masahiro Hino	Kyoto University	General Use	Experimental test of TOF-MIEZE spectrometer
15	BL-10	2009A0024	Tetsuro Matsumoto	National Institute of Advanced Industrial Science and Technology	General Use	Experimental study on a calibration method of devices for neutrons from thermal to several 100 MeV using a spallation neutron source
16	BL-10	2009A0027	Hiroyuki Nojiri	Tohoku University	General Use	High Magnetic Field Neutron Diffractions in Frustrated Multi-ferroics
17	BL-10	2009A0046	Tatsuya Nakamura	Japan Atomic Energy Agency	General Use	Development of Neutron Scintillator Monitor Detector
18	BL-10	2009A0065	Dai Yamazaki	Japan Atomic Energy Agency	General Use	Development of Neutron Beam Focusing Devices Using Large-m Supermirror on Precisely Figured Aspheric Surfaces
19	BL-10	2009A0069	Kazuhiko Soyama	Japan Atomic Energy Agency	General Use	Neutron Micrometer-scale Imaging Detector Using Electronic Zooming Tube
20	BL-10	2009A0058	Fujio Maekawa	Japan Atomic Energy Agency	Instrumental development use	Study on Neutronic Performance of JSNS
21	BL-10	2009A0081	Masahito Matsubayashi	Japan Atomic Energy Agency	Project use	Research and Development of Energy Selective Neutron Imaging Technique
22	BL-10	2009A0083	Jun-ichi Suzuki	Japan Atomic Energy Agency	Project use	Development and Application of Neutron Optical and Detection Systems
23	BL-10	2009A0084	Yoshimi Kasugai	Japan Atomic Energy Agency	Project use	Prompt Gamma-ray Analysis on NOBORU
24	BL-14	2009A0080	Jitsuo Sugai	Technology Research Institute of Osaka Prefecture	General Use	Analysis of Dynamic Characteristic of Adsorption Water at Fiber Surface by the Incoherence Neutron Inelastic Scattering Measurement
25	BL-14	2009A0051	Hiroshi Nakagawa	Japan Atomic Energy Agency	General Use	Effect of Hydration on Protein Dynamics by TOF-Elastic Resolution Spectroscopy
26	BL-14	2009A0054	Yukinobu Kawakita	Kyushu University	General Use	Cooperative Dynamics in Noble-metal Halides Superionic Melts
27	BL-14	2009A0092	Kenji Nakajima	Japan Atomic Energy Agency	Instrumental Development Use	Commissioning of AMATERAS
28	BL-14	2009A0073	Kazuhisa Kakurai	Japan Atomic Energy Agency	Project use	Magnetic Excitations in Quantum Spin Systems and Frustrated Magnets
29	BL-14	2009A0089	Masatoshi Arai	Japan Atomic Energy Agency	Project use	Neutron Scattering Study of High-Tc Superconductors
30	BL-19	2009A0076	Hiromitsu Asai	Denso Co.	General Use	Measurement of Axial Force at Bolt in the Structure
31	BL-19	2009A0077	Tatsumi Hirano	Hitachi co	General use	Estimaiton of Residual Strain in Piston of Engine
32	BL-19	2009A0022	Yo Tomota	Ibaraki University	General Use	In-Situ Neutron Diffraction During Tensile Deformation in Nano-TRIP Steels and Advanced Cast Irons
33	BL-19	2009A0026	Kenji Iwase	Ibaraki University	General Use	In-Situ Investigation of Residual Strain by Bragg-edge Transmission Method and Diffraction.
34	BL-19	2009A0034	Satoshi Awaji	Tohoku University	General Use	Three Dimensional Strain Analysis of the Nb_3Sn Superconducting Composite Cables
35	BL-19	2009A0036	Hiroshi Suzuki	Japan Atomic Energy Agency	General Use	Thermal Stress in Bulk Metallic Glasses and Their Accommodation by Annealing

	Beam Line	Proposal ID	Applicant	Affiliation	Type of Use	Title of Experiment
36	BL-19	2009A0079	Kazuyoshi Kagawa	Kanto Auto Works, Ltd.	General Use	Measurement of Residual Strength in Cold Spray Coating
37	BL-19	2009A0053	Kozo Osamura	Research Institute for Applied Sciences	General Use	Flux-pinning-induced Stress and Magnetostriction in Bulk Superconductors
38	BL-19	2009A0094	Kazuya Aizawa	Japan Atomic Energy Agency	Instrumental Development Use	Residual Stress Study on BL19
39	BL-19	2009A0082	Wataru Utsumi	Japan Atomic Energy Agency	Project use	Development of High Pressure Devices for Neutron Powder Diffraction Study
40	BL-19	2009A0085	Harjo Stefanus	Japan Atomic Energy Agency	Project use	Stress/Strain Effects on Industrial Superconducting Composites
41	BL-20	2009A0020	Hiroshi Kageyama	Kyoto University	General Use	Structural Study on Square-planarly Coordinated Iron Oxides
42	BL-20	2009A0030	Ryoji Kanno	Tokyo Institute of Technology	General Use	Crystal Structure Analysis of Li_2MnO_3 Reduced by Metal Hydride - New Cathode Material for Lithium Batteries
43	BL-20	2009A0039	Ryoji Kiyanagi	Tohoku university	General Use	Incorporated Hydride in Nanoporous Material $C_{12}A_7$-H- and its Reaction to UV Irradiation
44	BL-20	2009A0042	Taku Iiyama	Shinshu University	General Use	The determination of Hydorogen Bonding Structure of Water Molecular Assemblies in Hydrophobic Small Spaces
45	D1	2009A0007	Ryosuke Kadono	High Energy Accelerator Research Organization	General Use	Correlation between Magnetism and Superconductivity in Iron-Oxypnictide Superconductors
46	D1	2009A0016	Masaki Azuma	Kyoto University	General Use	Magnetic Ground State of a Frustrated S=3/2 Honeycomb Antiferromagnet $Bi_3Mn_4O_{12}(NO_3)$
47	D1	2009A0023	Masaharu Aoki	Osaka University	General Use	Measurements of an Extinction Ratio and a Muonic Atom Formation Rate
48	D1	2009A0031	Jun Sugiyama	Toyota Central R&D Labs. Inc	General Use	Lithium Diffusion in Lithium-Transition-Metal-Oxides
49	D1	2009A0055	Kenya Kubo	International Christian University	General Use	Development of Non-destructive Multi-elemental Analysis System by Muonic X-Ray
50	D1	2009A0060	Kazuyasu Tokiwa	Tokyo University of Science	General Use	mSR Study of Magnetic Properties of $CaFe_2O_4$-type $NaMn_2O_4$ and $LiMn_2O_4$
51	D1	2009A0075	Koichiro Shimomura	High Energy Accelerator Research Organization	General Use	mSR Study on Isolated Hydrogen Charge State in Oxygen Deficient $SrTiO_3$
52	D1	2009A0091	Yasuhiro Miyake	KEK	Instrumental Development Use	Muon Beam Commissioning I for the Decay-Surface Muon Channel
53	D1	2009A0086	Wataru Higemoto	Japan Atomic Energy Agency	Project use	Microscopic Study of Novel Properties of f-electron Systems by means of mSR

Accepted proposals list for MLF experiments in JFY2009B

	Beam Line	Proposal ID	Applicant	Affiliation	Type of Use	Title of Experiment
1	BL-03	2009B0049	Kiyoaki Tanaka	Nagoya University	General use	Disordered crystal structure and intrinsic temperature factors of an electride by TOF neutron diffraction
2	BL-08	2009B0013	Yasushi Idemoto	Tokyo University of Science	General use	Crystal Structure of xLi_2MnO_3-(1x)$LiMn_{1/3}Ni_{1/3}Co_{1/3}O_2$ as a Cathode Active Material for Lithium Ion Battery
3	BL-08	2009B0015	Yuji Noguchi	University of Tokyo	General use	Materials Design Based on Ferroelectric Crystal Structure for Bi-based Perovskite Ferroelectric Oxides
4	BL-08	2009B0033	Donald Brown	Los Alamos National Laboratory	General use	Line Profile Study of the Evolution of the Microstructure of Magnesium Alloys during Deformation.

	Beam Line	Proposal ID	Applicant	Affiliation	Type of Use	Title of Experiment
5	BL-08	2009B0039	Ryoji Kanno	Tokyo Institute of Technology	General use	Crystal Structure Analysis of Thio-LISICONs - Super Ionic Conductor for Lithium Batteries
6	BL-08	2009B0043	Sadamu Takeda	Hokkaido University	General use	Precise Structure Determination of Newly Synthesized Cu(II) (S=1/2) Equilateral Triangular Lattice Compound above and below the Second Order Structural Phase Transition Temperature of 18 K
7	BL-10	2009B0008	Hiroaki Asai	HIREC Corporation	General use	Feasibility Estimation of White-Spectrum Neutron for the Single Event Tolerance Examination of Semiconductor Element (Part 2)
8	BL-10	2009B0019	Hiroyuki Nojiri	Tohoku University	General use	High Magnetic Field Neutron Diffractions in Frustrated Multi-ferroics
9	BL-10	2009B0022	Masahiro Hino	Kyoto University	General use	Experimental Test of TOF-MIEZE Spectrometer
10	BL-10	2009B0029	Je-Geun Park	Sungkyunkwan University KOREA	General use	High Field Magnetic Structure of Single Crystal Multiferroic $BiFeO_3$
11	BL-10	2009B0031	Tetsuro Matsumoto	National Institute of Advanced Industrial Science and Technology	General use	Experimental Study on a Calibration Method of Devices for Neutrons from Thermal to Several 100 MeV using a Spallation Neutron Source
12	BL-14	2009B0003	Kazuaki Iwasa	Tohoku University	General use	Actual Ground State of Higher-Rank Multipolar Ordered State in Pr-filled Skutterudite
13	BL-14	2009B0012	Kenji Maruyama	Niigata University	General use	Measurement of the Slow Dynamics of Water Molecules in Lower Alcohol Solutions and its Relation to the Hydrophobic Hydration.
14	BL-14	2009B0024	Kazuya Kamazawa	TOYOTA CENTRAL R&D LABS., INC.	General use	Investigation of Li Diffusion by Quasielastic Neutron Scattering for High Li Ionic Conductor, Garnet-related $Li_6La_3Nb_2O_{12}$
15	BL-14	2009B0044	Sadamu Takeda	Hokkaido University	General use	Observation of Magnetic Ordering and Excitation in Triangular Antiferromagnetic Copper Compound
16	BL-16	2009B0007	Masashi Harada	Toyota Central R&D Labs. Inc	General use	Structure Analisys Water in Thin-Nafion film
17	BL-16	2009B0011	Kazuhide Ozeki	Ibaraki University	General use	Measurement of Deuterium and Hydrogen Content of DLC Film by Neutron Reflectivity.
18	BL-16	2009B0052	Hideki Seto	High Energy Accelerator Research Organization (KEK)	Instrumental development use/Project use	Structural Properties of Soft-interfaces / Commissioning and Development of High-Performance Neutron Reflectometer ARISA-II
20	BL-19	2009B0004	Hiroyuki Yasuda	Osaka University	General use	In-Situ Neutron Diffraction Study for Fe-based Shape Memory Materials
21	BL-19	2009B0006	Pingguang Xu	Japan Atomic Energy Agency	General use	Competition Behavior among Static Recovery, Recrystallization of Martensite and Precipitation of Austenite during Annealing in Cold Rolled Martensite 17Ni-0.2C Steel
22	BL-19	2009B0009	Yo Tomota	Ibaraki University	General use	SCC Crack Propagation Characteristics from Inconel Weld Metal to Low-Alloyed Steel
23	BL-19	2009B0010	Tatsumi Hirano	Hitachi	General use	Estimaiton of Residual Strain in Piston of Engine (2)
24	BL-19	2009B0017	Satoshi Morooka	Yokohama National University	General use	Heterogeneous Deformation Behavior of Ti Alloys Studied by In-Situ Neutron Diffraction During Tensile Deformation
26	BL-19	2009B0021	Jun Kubo	Nissan Motor Coorporation	General use	Measurement of Internal Residual Stress of Aluminum-Casting Parts for Automobile
27	BL-19	2009B0025	Hiroshi Suzuki	Japan Atomic Energy Agency	General use	Development of In-situ Material Evaluation Technique using TAKUMI Diffractometer
28	BL-19	2009B0042	Yoshinori Shiota	Japan Atomic Energy Agency	General use	Local Crystal Rotation and Misfit Strain after High Temperature Creep in a Single-Crystal Nickel-base Superalloy
30	BL-20	2009B0016	Shinichi Komaba	Tokyo University of Science	General use	Structural Analyses of New $LoCoO_2$ for Lithium-Ion Batteries

	Beam Line	Proposal ID	Applicant	Affiliation	Type of Use	Title of Experiment
31	BL-20	2009B0027	Takashi Kamiyama	Hokkaido University	General use	Study on Preferred Orientation Analysis with the Comparison of the Diffraction and Transmission Measurements
32	BL-20	2009B0028	Hidetoshi Oguro	Ibaraki University	General use	Residual Strain Measurement for Practical Nb_3Sn Wire by Neutron Diffraction
34	BL-20	2009B0040	Taku Iiyama	Shinshu University	General use	The Determination of Mixture State of Hydrophobic Molecule and Water in Hydrophobic Small Spaces
35	BL-20	2009B0051	Takashi Kamiyama	High Energy Accelerator Research Organization (KEK)	General use	Preliminary Studies on Jomon Pottery (Cord Impressed Ware between 0 - B.C.13000)
36	D1	2009B0005	Jun Sugiyama	Toyota Central R&D Labs. Inc	General use	Li Diffusion in LiCrO (2)
37	D1	2009B0014	Mototsugu Mihara	Osaka University	General use	Pre-martensitic Phenomena of Thermoelastic Martensitic Transformation in NiTi Alloys Studied by Muon
38	D1	2009B0020	Masao Doyama	Teikyo University of Science and Technology	General use	Applications of Imaging Plates to the Research on Muon Science
39	D1	2009B0023	Akihiro Koda	High Energy Accelerator Research Organization (KEK)	General use	Spin Dynamics in Multiferroic Perovskite $TbMnO_3$ Probed by Muon Spin Relaxation
40	D1	2009B0032	Masaharu Aoki	Osaka University	General use	Measurement of an Extinction Ratio of MLF Proton Beam
41	D1	2009B0034	Shinsaku Kambe	Japan Atomic Energy Agency	General use	Internal Magnetic Field in SDW State of $EuFe_2As_2$ (Mother Compound for Punictide Superconductivity)
42	D1	2009B0035	Kazuhiko NINOMIYA	Japan Atomic Energy Agency	General use	Study on the Relation Between Molecular Structure and Muon State of the First Step of Muon Capture Phenomena for Nitrogen and Oxygen Compounds
43	D1	2009B0036	Masashi Kosaka	Saitama University	General use	mSR Study of Magnetic Frustration in $Ce_2Ni_5C_3$ with the Shastry-Sutherland Lattice Just Above Tc
44	D1	2009B0037	Hirotaka Okabe	Aoyama Gakuin University	General use	μSR Study on a Mott State in the Iridium Oxides
45	D1	2009B0050	Khashayar Ghandi	Faculty member	General use	Studies of Muonium Formation in Liquids
46	D1	2009B0054	Hiroyuki Sugai	Japan Atomic Energy Agency	General use	Hydrogen Diffusion in NaTl-type Intermetallic Compound LiAl

Proposals Approved

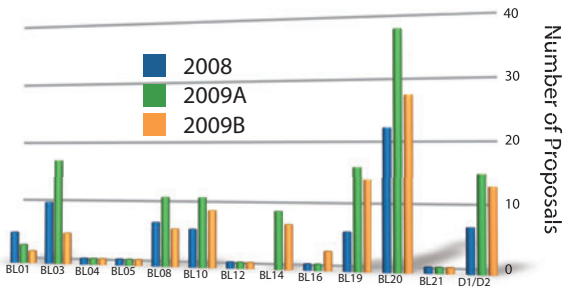

Affiliation of Proposals

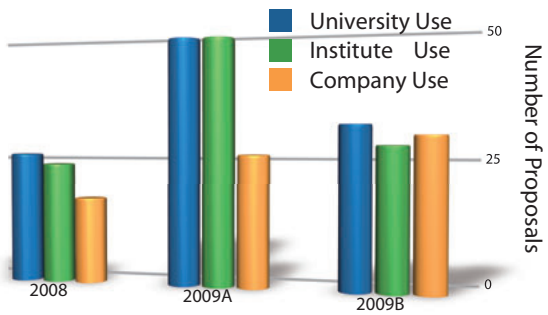

Staff 2007~2009

MLF Division Staff since 2007~2009

Director

Yujiro Ikeda

Vice Director

Masatoshi Arai

Susumu Ikeda

Neutron Source Section Staff since 2007 (JAEA)

JAEA			JAEA		
Junichi	Adachi	(2007)	Chisato	Mutoh	(2007)
Bucheeri	Ahmed	(2008)	Masakazu	Nakamura	
Hideyuki	Aizawa	(2007)	Takashi	Naoe	
Jun	Akimoto	(2007)	Hiroaki	Natsume	(2007)
Atsushi	Akutsu		Erkan	Nedjet	(2008)
Tomokazu	Aso		Kiyotaka	Nemoto	
Takayuki	Awatani	(2007)	Koji	Niita	(2007)
Shigenori	Azuma	(2007)	Akira	Ogawa	
Ahmed	Bucheeri	(2007)	Hironori	Ohhashi	(2007)
Eiji	Dantsuji	(2007)	Motoki	Ohi	
Akihiro	Fukuda	(2007)	Satoshi	Ohi	(2007)
Miho	Funabashi	(to 2008)	Ryuji	Ohsone	(2007)
Michihiro	Furusaka	(2007)	Hidenori	Ohtake	(2007)
Masatoshi	Futakawa		Kiichi	Ohtsu	
Katsuhiro	Haga		Kenichi	Oikawa	
Kohei	Hanano		Yoshinao	Okamoto	(2007)
Masahide	Harada		Takehiro	Ono	(2007)
Tetsuya	Haraguchi		Ryuji	Ozone	(2008)
Shoichi	Hasegawa		Akio	Sakai	(2007)
Chieko	Higuchi		Kenji	Sakai	
Ryutaro	Hino	(2007)	Shinichi	Sakamoto	
Shiro	Honmura	(2007)	Hisashi	Sakurayama	
Yoshihiro	Hoshino	(2007)	Shinobu	Sasaki	(2007)
Masato	Ida		Hiroshi	Sato	(2007)
Naruhiro	Iizumi		Masakazu	Seki	
Yujiro	Ikeda	(2007)	Daisuke	Shigaki	(2007)
Kiyomi	Ikezaki		Naoko	Shimizu	(2007)
Syuichi	Ishikura	(2007)	Kenji	Shinomiya	(2007)
Manabu	Ito		Toru	Suzuki	
Toshimitsu	Ito		Hiroshi	Takada	
Eiichi	Iwamoto		Katsunori	Takagiwa	(2007)
Tetsuya	Kai		Toshio	Takahashi	(2007)
Akimoto	Kajiyama	(2007)	Shunichi	Takatama	(2007)
Masanori	Kaminaga	(to 2009)	Toshio	Takayasu	(2007)
Syuji	Kanechika	(2007)	Masaya	Tamura	(2007)
Yoshimi	Kasugai		Sachiko	Tanaka	(2007)
Masao	Kato	(2007)	Shigeto	Tanaka	
Takashi	Kato	(2007)	Hideki	Tatsumoto	
Yoshihiko	Kawakami		Atsuhiko	Terada	(2007)
Susumu	Kawasaki	(2007)	Hiroshi	Teraoku	(2007)
Tomoyuki	Kawasaki		Makoto	Teshigawara	
Katsuya	Kimura	(2007)	Hiroshi	Tomita	
Hidetaka	Kinoshita		Yoshikatsu	Torii	(2007)
Kaoru	Kobayashi	(2007)	Takashi	Uchiyama	
Hiroyuki	Kogawa		Kazuaki	Ueda	(2007)
Chikara	Konno	(2007)	Toshiaki	Uehara	
Tomonori	Koyama	(2007)	Shinichi	Urai	
Teruo	Kuboki		Isamu	Ushijima	(2007)
Atsushi	Kurosawa		Takashi	Wakui	
Takashi	Kurosawa		Hatsue	Watahiki	(2007)
Fujio	Maekawa		Kentaro	Watanabe	
Kaoru	Matsumura		Noboru	Watanabe	(2007)
Shin-ichiro	Meigo		Yoshihito	Yamaguchi	(2007)
Yuya	Miyamoto		Katsuyoshi	Yamazaki	(2007)
Takuya	Miyo		Shizuka	Yoshinari	

Neutron Science Section Staff since 2007 (KEK and JAEA)

KEK			JAEA		
Susumu	Ikeda		Kazuya	Aizawa	
Takashi	Ino		Ryoko	Aoyama	
Shinichi	Ito		Masatoshi	Arai	(to 2008)
Takashi	Kamiyama		Hiroshi	Arima	
Nokatsu	Kaneko		Shino	Hagiwara	(2007)
Yasuo	Kobayashi	(to 2008)	Stefanus	Harjo	
Suguru	Muto		Takanori	Hattori	
Toshiya	Otomo		Akinori	Hosokawa	(2007)
Hidenori	Sagehashi		Takaaki	Hosoya	(2007)
Setsuo	Sato		Yasuhiro	Inamura	
Hirohiko	Shimizu		Toru	Ishigaki	(2007)
Shuki	Torii		Takayoshi	Ito	
Naoya	Torikai	(to 2008)	Yukihiro	Ito	
Norifumi	Yamada		Takaaki	Iwahashi	
Tetsuya	Yokoo		Ryouichi	Kajimoto	
Junrong	Zhang		Wataru	Kanbara	
			Seiko	Kawamura	
			Hiroshi	Kira	
			Kazuo	Kurihara	
			Katsuhiro	Kusaka	(2007)
			Atsushi	Moriai	
			Kenji	Nakajima	
			Mitsutaka	Nakamura	
			Takeshi	Nakatani	
			Takashi	Ohhara	
			Takayuki	Oku	
			Toyotaka	Osakabe	
			Makiko	Sakai	(2007)
			Ayako	Sato	(2008)
			Kaoru	Shibata	
			Takenao	Shinohara	
			Yukari	Sugikawa	
			Jun-ichi	Suzuki	
			Kentaro	Suzuya	
			Nobuaki	Takahashi	
			Shin-ichi	Takata	
			Masayasu	Takeda	
			Michihiro	Tanaka	
			Chiho	Tobe	
			Wataru	Utsumi	
			Shuichi	Wakimoto	
			Noboru	Yoshida	

Neutron Instrumentation Section Staff since 2007 (JAEA)

JAEA		
Ryoko	Aoyama	(2007)
Masaki	Katagiri	
Ryuji	Maruyama	
Tatsuya	Nakamura	
Kaoru	Sakasai	
Kazuhiko	Soyama	
Chiho	Tobe	
Kentaro	Toh	
Hideshi	Yamagishi	
Dai	Yamazaki	

Muson Science Section Staff since 2007 (KEK and JAEA)

KEK			JAEA		
Hiroshi	Fujimori		Robert H.	Heffner	(2007)
Yutaka	Ikedo		Wataru	Higemoto	
Ryosuke	Kadono		Takashi	Itoh	
Mineo	Kato		Kazuhiko	Ninomiya	
Naritoshi	Kawamura		Kazuki	Ohishi	(2007)
Yasuo	Kobayashi				
Akihiro	Koda				
Kenji M.	Kojima				
Shunsuke	Makimura				
Tetsuya	Masuda				
Yasuhiro	Miyake				
Kazutaka	Nakahara	(2007)			
Yasuhisa	Nemoto				
Kusuo	Nishiyama				
Koichiro	Shimomura				
Patrick	Strasser				
Soshi	Takeshita	(2007)			

Jack Carpenter (Argonne) presents the Motoharu Kimura Award to Noboru Watanabe (JAEA), in recognition of his outstanding contributions over many years in the field of pulsed spallation neutron source, at IPS08.

International Symposium on Pulsed Neutron and Muon Science at J-PARC (IPS-08)
Chair: Yujiro Ikeda, Susumu Ikeda
March 5-7, 2008 at Shichouson-Kaikan of Ibaraki prefecture, Mito, with 255 participants.
Oral presentations: 71
Poster presentations: 121

Group photo of IPS-08

1st MLF symposium (MLF users meeting)
Chair: Yujiro Ikeda, Susumu Ikeda (KEK)
March 29-31, 2010 at Ibaraki Quantum Beam Center (IQBRC), Tokai, with 220 participants.
Oral presentations: 25 (17 for neutron science and 8 for muon science).
Poster presentations: 44 (38 for neutron science and 6 for muon science).

Group photo of 1st MLF symposium

Committees and Meetings for the MLF

J-PARC Materials and Life Science Facility Technical Advisory Committee (N-TAC)

N-TAC1 (October 28-30, 2002 at Japan Atomic Energy Research Institute (JAERI))
N-TAC2 (September 24-26, 2003 at KEK)
N-TAC3 (October 26-28, 2004 at JAERI)
N-TAC4 (November 14-16, 2005 at Japan Atomic Energy Agency (JAEA))
N-TAC5 (November 20-22, 2006 at JAEA)
N-TAC6 (February 27-29, 2008 at JAEA)

Members of committee from N-TAC1 to N-TAC6
Dr. Günter S. Bauer
ex Forschungszentrum Juelich GmbH, Germany
Dr. Timothy A. Broome
Rutherford Appleton Laboratory, UK
Dr. John M. Carpenter
Argonne National Laboratory, USA
Dr. Hajo Heyck
Paul Scherrer Institute, Switzerland
Prof. Hiroaki Kurishita
Tohoku University, Japan
Dr. Thomas J. McManamy
Oak Ridge National Laboratory, USA

Poster of N-TAC1 meeting room


A photo of meeting room at N-TAC1

Neutron Technical Advisory Committee (N-TAC7)

N-TAC7 (March 5-6, 2009 at Techno Community Square RICOTTI)

Members of committee of N-TAC7

Dr. Günter S. Bauer
ex Forschungszentrum Juelich GmbH, Germany
Dr. Dan A. Neumann
National Institute of Standards and Technology, USA
Dr. John R. Haines
Oak Ridge National Laboratory, USA
Prof. Kurt N. Clausen
Paul Scherrer Institute, Switzerland
Prof. Robert Robinson
Australian Nuclear Science and Technology Organization, Australia
Prof. Stephen M. Bennington
Rutherford Appleton Laboratory, UK
Prof. Yoshiaki Kiyanagi
Hokkaido University, Japan
Prof. Kazuyoshi Yamada
Tohoku University, Japan
Prof. Toshiji Kanaya
Kyoto University, Japan

Group photo of N-TAC7

The Japan Spallation Neutron Source (JSNS) International Advisory Committee (NIAC-1)

NIAC-1 (February 24-26, 2010 at Ibaraki Quantum Beam Research Center)

Member of committee of NIAC-1

Dr. Günter S. Bauer
ex Forschungszentrum Juelich GmbH, Germany
Dr. Dan A. Neumann
National Institute of Standards and Technology, USA
Dr. John R. Haines
Oak Ridge National Laboratory, USA
Prof. Kurt N. Clausen
Paul Scherrer Institute, Switzerland
Prof. Robert Robinson
Australian Nuclear Science and Technology Organization, Australia
Prof. Stephen M. Bennington
Rutherford Appleton Laboratory, UK
Prof. Yoshiaki Kiyanagi
Hokkaido University, Japan
Prof. Kazuyoshi Yamada
Tohoku University, Japan
Prof. Toshiji Kanaya
Kyoto University, Japan

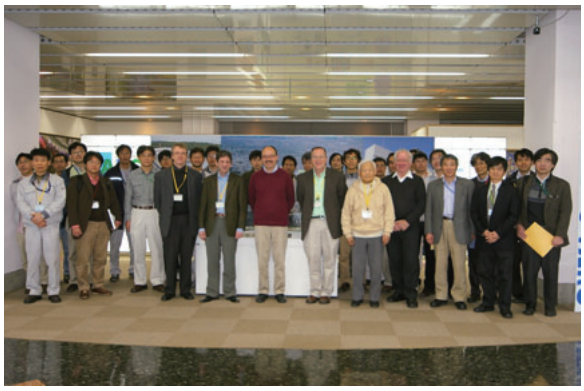

Group photo of NIAC-1

Workshops/ Advisory committees for neutron instrumentations (~2010.3)

2004. 12.2-12.3
BL01, BL12, BL14: Workshop on Inelastic Neutron Spectrometers 2004 (WINS2004)
JAERI, Tokai, Ibaraki, Japan
R. E. Lechner (HMI), R. Bewley (RAL, ISIS), P. E. Sokol (Indiana Univ.), I. Zaliznyak (BNL), F. Mezei (HMI), S. Itoh (KEK), M. Arai (JAEA), K. Nakajima (JAEA) K. Shibata (JAERI) Y. Kawabata (Kyoto Univ.), D. Yamazaki, T. Ebisawa (JAERI) S. Muto (KEK), T. Otomo (KEK), J. Suzuki (KEK), J.-G. Park (SungKyunKwan Univ.)

2005.3.4-3.5
BL03 iBIX: International Meeting on Data Acquisition and Reduction for TOF Neutron Biological Diffractometer at J-PARC
P. Langan (LANSCE, LANL), N. Niimura (Ibaraki Univ.), I. Tanaka (Ibaraki Univ.)

2005.3.10-3.11
BL20 iMATERIA: Neutron Powder Diffraction Instrumentation Meeting 2005
T. C. Hansen (ILL), A. Studer (Bragg Institute), J. P. Attfield (Univ. Edinburgh), J. Hodges (SNS, ORNL), T. Ishigaki (Ibaraki Univ.), T. Kamiyama (KEK)

2005.11.1-11.2
BL01 4SEASONS workshop
Izura. Kitaibaraki, Ibaraki, Japan
K. Yamada (Tohoku Univ.), Y. Koike (Tohoku Univ.), M. Fujita (Tohoku Univ.), M. Ogata (Univ. Tokyo), T. Tohyama (Tohoku Univ.), H. Aoki (Univ. Tokyo), A. Fujimori (Univ. Tokyo), N. Nagaosa (Univ. Tokyo), M. Tachiki (NIMS), Y. Fujii (JAEA), M. Arai (JAEA), S. Shamoto (JAEA), R. Kajimoto (JAEA), T. Fukuda (JAEA), K. Ishii (JAEA)

2006.1.23
Workshop on Neutron Total Scattering instrument for Hydrogenous Materials
JAEA, Tokai, Ibaraki, Japan
A. K. Soper (RAL, ISIS), A. C. Hannon (RAL, ISIS), Y. Kameda (Yamagata Univ.), T. Otomo (KEK), K. Suzuya (JAEA), T. Yamaguchi (Fukuoka Univ.), K. Itoh (Kyoto Univ.), T. Ishigaki (JAEA), S. Shamoto (JAEA), M. Arai (JAEA)

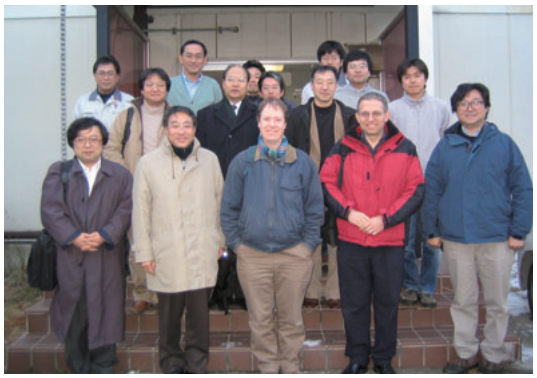

2006.1.24
BL21 NOVA: Workshop on Neutron Total Scattering instruments
KEK, Tsukuba, Ibaraki, Japan
A. K. Soper (RAL, ISIS), A. C. Hannon (RAL, ISIS), T. Egami (Unv. Tennessee), S. Ikeda (KEK), T. Otomo (KEK), H. M. Shimizu (KEK), T. Kamiyama, K. Suzuya (JAEA), K. Soyama (JAEA), T. Ishigaki (JAEA), M. Arai (JAEA)

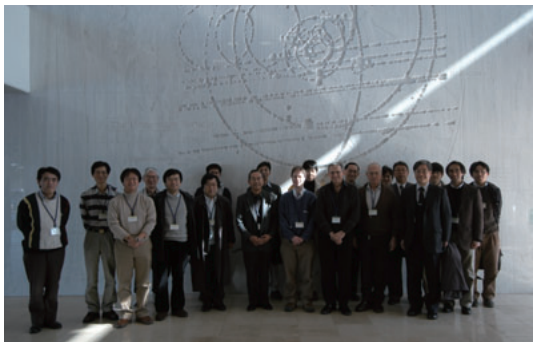

2006.1.25
BL15 HI-SANS (TAIKAN): International Workshop on SANS Instruments at Pulsed Neutron Sources for Nanoscience
JAEA, Tokai, Ibaraki, Japan
D. F. R. Mildner (NIST), J. Zhao (SNS, ORNL), K. C. Littrell (IPNS, ANL), J. Suzuki (JAEA), T. Oku (JAEA), Y. Morii (JAEA), M. Arai (JAEA), Masaaki Sugiyama (KURRI)

2006.1.27
BL16 HREF (ARISA-II): International Workshop on Interfacial Nanoscience
KEK, Tsukuba, Ibaraki, Japan
J. Penfold (ISIS), J. Ankner (SNS, ORNL), G. Felcher (IPNS, ANL), Tsang-Lang Lin(National Tsing Hua Univ., Taiwan)Fangwei Wang(Institute of Physics, CAS), N. Torikai (KEK), S. Ikeda (KEK), D. Yamazaki (JAEA)

2006.1.30-1.31
BL03 iBIX: International Meeting for Construction and Utilization of IBARAKI Biological Crystal Diffractometer at J-PARC
R. Bau (Univ. Southern California), M. J. Gutmann (RAL, ISIS), C. Hoffmann (SNS, ORNL), F. Meileur (ILL), S. Arai (JAEA), Y. Ohashi (JASRI), Y. Ohnishi (Ibaraki Univ.), M. Sato (Yokohama City Univ.), N. Niimura (Ibaraki Univ.), I. Tanaka (Ibaraki Univ.)

2006.3.9-3.10
BL16 ARISA-II: Workshop on Interfacial Nanoscience
KEK, Tsukuba, Ibaraki, Japan
K. Iimura (Utsunomiya Univ.), Y. Ouchi (Nagoya Univ.), T. Kanaya (Kyoto Univ.), K. Sakurai (NIMS), M. Takeda (JAEA), Y. Tsujii (Kyoto Univ.), K. Fukao (Kyoto Inst. Tech.), H. Matsushita (Kyoto Univ.)H. Matsushita (Nagoya Univ.), D. Yamazaki (JAEA), H. Yokoyama (AIST), N. Torikai (KEK)

2007.3.7-3.9
BL03 iBIX: International Workshop on New Neutron Diffractometer for Biological and Chemical Crystallography
M. Blabber (Florida State Univ.), J. Cooper (Univ. Southampton), H. Xu (SUNY), A. J. Schultz (ANL), P. Thiyagarajan (ANL), N. Niimura (Ibaraki Univ.), I. Tanaka (Ibaraki Univ.)

2007.7.24
1st KJ-Collaboration meeting on Chopper Software Development
JAEA, Toaki, Ibaraki, Japan
M. Moon (KAERI), K. C. Jin (KAERI), S-Y. So (KAERI), J-G. Park(SungKyunKwan Univ.), M. Arai (JAEA), K. Nakajima (JAEA), Y. Inamura (JAEA), T. Nakatani (JAEA), T. Otomo (KEK), J. Suzuki (KEK), S. Itoh (KEK), T. Yokoo (KEK)

2007.9.10-9.14
2nd KJ-Collaboration meeting on Chopper Software Development
JAEA, Toaki, Ibaraki, Japan
S-Y. So (KAERI), J-G. Park(SungKyunKwan Univ.), M. Arai (JAEA), K. Nakajima (JAEA), Y. Inamura (JAEA), T. Nakatani (JAEA), T. Otomo (KEK), J. Suzuki (KEK), K. Tomiyasu (Tohoku Univ.)

2007.10.11-10.12
BL19 TAKUMI, International Advisory Committee on Engineering Diffractometer with Pulsed Neutron Source
Xun-Li Wang (SNS, ORNL), M. Daymond (Queen's University), J. Hodges (SNS, ORNL), S. C. Vogel (LANSCE, LANL), S. Harjo (JAEA), K. Suzuya (JAEA), K. Aizawa (JAEA), M. Arai (JAEA)

2007.12.10-12.13
1st International mini Workshop on Chopper Software Development
JAEA, Toaki, Ibaraki, Japan
S-Y. So (KAERI), J-G. Park(SungKyunKwan Univ.), M. Arai (JAEA), K. Nakajima (JAEA), Y. Inamura (JAEA), T. Nakatani (JAEA), T. Otomo (KEK), J. Suzuki (KEK), K. Tomiyasu (Tohoku Univ.), M. Takahashi (Tsukuba Univ.), T. G. Perring (RAL, ISIS), G. E. Granroth (SNS, ORNL)

2007.12.14-12.15
BL01 4SEASONS workshop
Izura. Kitaibaraki, Ibaraki, Japan
K. Yamada (Tohoku Univ.), S. Uchida (Univ. Tokyo), Y. Ando (Osaka Univ.), M. Ogata (Univ. Tokyo), T. Tohyama (Tohoku Univ.), A. Fujimori (Univ. Tokyo), S. Tajima (Osaka Univ.), J. Akimitsu (Aoyama Gakuin Univ.), H. Fukuyama (Tokyo Univ. Sci.), Y. Fujii (JAEA), M. Arai (JAEA), S. Shamoto (JAEA), S. Iikubo (JAEA), M. Nakamura (JAEA)

2007.12.20-12.21
BL14 AMATERAS workshop
JAEA, Toaki, Ibaraki, Japan
K. Nakayama (Hokkaido Univ.), T. Kanaya (Kyoto Univ.), T. Atake (Tokyo Inst. Tec.), J. Sugiyama (Toyota Central Res.), H. Nakagawa (JAEA), Y. Kawakita (Kyusyu Univ.), H. Kadowaki (Tokyo Met. Univ.), O. Yamamuro (Univ. Tokyo), H. Fukazawa (JAEA), M. Hase (NIMS), K. Hirota (Univ. Tokyo), N. Metoki (JAEA)

2008.2.27-2.29
BL02 DNA; International Advisory Committee on "Biomolecular Dynamics Instrument DNA"
(J-PARC, Tokai, Ibaraki, Japan)
D. Neumann (NIST, USA), F. Mezei (ISSPO, Hungary), H. Mutka (ILL, France), P. Tregenna-Piggott (PSI, Switzerland), M. Arai (JAEA), K. Shibata (JAEA), K. Nakajima (JAEA), N. Takahashi (JAEA)

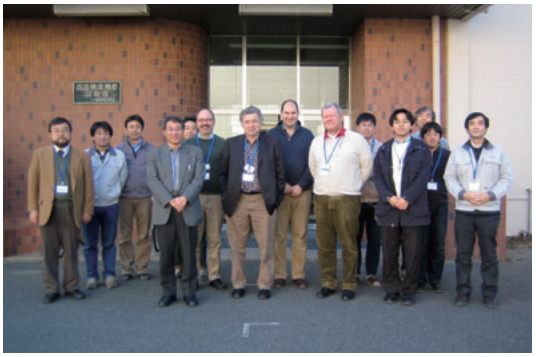

2008.4.5
3rd KJ-Collaboration meeting on Chopper Software Development
JAEA, Tokyo, Japan
S-Y. So (KAERI), J-G. Park(SungKyunKwan Univ.), M. Arai (JAEA), K. Nakajima (JAEA), Y. Inamura (JAEA), T. Nakatani (JAEA), R. Kajimoto (JAEA)

2008.5.26-5.27
2nd International mini Workshop on Chopper Software Development
JAEA, Tokai, Ibaraki, Japan
S-Y. So (KAERI), J-G. Park(SungKyunKwan Univ.), M. Arai (JAEA), K. Nakajima (JAEA), Y. Inamura (JAEA), T. Nakatani (JAEA), R. Kajimoto (JAEA), K. Shibata (JAEA), T. Otomo (KEK), N. Takahashi (JAEA), T. Aoyagi (JAEA), T. G. Perring (RAL, ISIS), G. E. Granroth (SNS, ORNL)

2008.6.18
BL12 HRC workshop
KEK, Tsukuba, Japan
O. Yamamuro (Univ. Tokyo), T. Kamiyama (Hokkaido Univ.), K. Nasu (KEK), K. Iwasa (Tohoku Univ.), S. Kuroda (Univ. Tsukuba), K. Sato (Osaka Univ.), Y. Endo (KEK), K. Ohyama (Tohoku Univ.), S. Ikeda (KEK), S. Itoh (KEK), T. Yokoo (KEK)

2008.9.19
BL16 ARISA-II; Workshop on Interfacial Nanoscience with J-PARC reflectometer
KEK, Tsukuba, Ibaraki, Japan
K. Okuda (Kyoto Univ.), T. Takigami (Kyushu Univ.), M. Mizukami (Tohoku Univ.), M. Yonemura (Ibaraki Univ.), T. Kondo (Univ. Tsukuba), M. Otani (AIST), H. Matsushita (Nagoya Univ.), H. Takahashi (Gunma Univ.), K. Tanaka (D. Yamazaki (Kyushu Univ.), H. Seto (KEK), N. Torikai (KEK)

2008.9.25
BL12 HRC workshop
KEK, Tsukuba, Ibaraki, Japan
O. Yamamuro (Univ. Tokyo), T. Sato (Univ. Tokyo), K. Kuwabara (Ibaraki Univ.), S. Yano (Aoyama Gakuin Univ.), K. Iwano (KEK), S. Kuroda (Univ. Tsukuba), K. Ohyama (Tohoku Univ.), K. Nasu (KEK), K. Iwasa (Tohoku Univ.), Y. Endo (KEK), H. Seto (KEK), S. Itoh (KEK), T. Yokoo (KEK)

2008.11.12-11.13
BL02 DNA; The 2nd International Advisory Committee on Biomolecular Dynamics Instrument DNA J-PARC, Tokai, Ibaraki, Japan
D. Neumann (NIST, USA), F. Mezei (ISSPO, Hungary), H. Mutka (ILL, France), P. Tregenna-Piggott (PSI, Switzerland), M. Arai (JAEA), K. Shibata (JAEA), K. Nakajima (JAEA), N. Takahashi (JAEA)

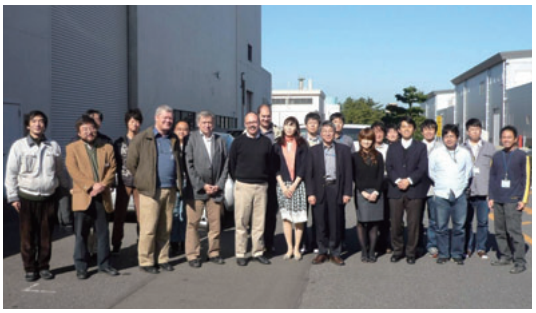

2008.12.8-12.9
3rd International mini Workshop on Chopper Software Development
Fukuroda, Ibaraki, Japan
S-Y. So (KAERI), J-G. Park(SungKyunKwan Univ.), M. Arai (JAEA), K. Nakajima (JAEA), Y. Inamura (JAEA), T. Nakatani (JAEA), R. Kajimoto (JAEA), T. Otomo (KEK), Y. Kawakita (Kyusyu Univ.), T. G. Perring (RAL, ISIS), G. E. Granroth (SNS, ORNL)

2009.1.27
BL15 TAIKAN: Workshop on Nanostructural Analysis with Wide-q Data
JAEA, Tokai, Ibaraki, Japan
H. Mertens (EMBL), A.K. Soper (ISIS), M. Hirai (Gunma Univ.), M. Misawa (KEK), A. Wiedenmann (ILL), M. Sugiyama (KUR, Kyoto. Univ.), M. Arai (JAEA), J. Suzuki (JAEA), S. Takata (JAEA)

2009.1.28-1.29
BL15 TAIKAN: International Advisory Committee on the Smaller-angle Neutron Scattering Instrument of J-PARC
JAEA, Tokai, Ibaraki, Japan
A.K. Soper (ISIS), M. Hirai (Gunma Univ.), A. Wiedenmann (ILL), M. Sugiyama (KUR, Kyoto. Univ.), M. Furusaka (Hokkaido Univ.), M. Arai (JAEA), J. Suzuki (JAEA), S. Takata (JAEA), T. Shinohara (JAEA), T. Oku (JAEA)

2009.2.24
BL12 HRC workshop
J-PARC, Tokai, Ibaraki, Japan
O. Yamamuro (Univ. Tokyo), T. Sato (Univ. Tokyo), T. Kamiyama (Hokkaido Univ.), S. Kuroda (Univ. Tsukuba), K. Ohyama (Tohoku Univ.), Y. Ohara (Univ. Tokyo), M. Kubota (KEK), K. Iwasa (Tohoku Univ.), Y. Endo (KEK), S. Itoh (KEK), T. Yokoo (KEK)

2009.7.8-7.9
Workshop on Possible Scientific View from New Neutron Spectroscopy Opportunities in J-PARC
Ibaraki Quantum Beam Research Center, Tokai, Ibaraki, Japan
Ruep E. Lechner, M. Russina (Helmholtz Zentrum Berlin), Tsuneyoshi Nakayama (Toyota Phys. Chem. Res. Inst., Hitoshi Endo (Univ. Tokyo), Zenji Hiroi (Univ. Tokyo), Yutaka Ikedo (KEK), S. Takeda (Hokkaido Univ.), H. Fukui (RIKEN), T. Arima (Tohoku Univ.), M. Fujita (Tohoku Univ.), S. Wakimoto (JAEA), M. Matsuda (JAEA), M. Sato (Yokohama City Univ.), M. Arai (JAEA), K. Nakajima (JAEA), Y. Inamura (JAEA), R. Kajimoto (JAEA), K. Shibata (JAEA), S. Itoh (KEK), M. Kohgi (IPAP), S. Kawamura (JAEA), T. Oku (JAEA), K. Aizawa (JAEA)

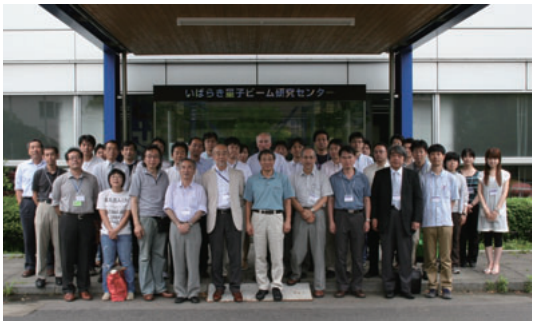

2009.7.25-7.26
BL11 PLANET: International Advisory Committee for High-Pressure Neutron Diffractometer
Mito, Ibaraki, Japan
J. B. Parise (SUNY, Stony Brook), J. S. Loveday (Univ. Edinburgh), S. Klotz (Univ. P. & M. Curie, Paris), C. T. Tulk (SNS, ORNL), Y. Zhao (LANSCE, LANL), M. Guthrie (APS, ANL), C. L. Bull (Univ. Edinburgh), T. Yagi (Univ. Tokyo), T. Hattori (JAEA), H. Arima (JAEA), H. Kagi (Univ. Tokyo), K. Komatsu (Univ. Tokyo),

2009.8.5
BL04 ANRRI workshop
JAEA, Ueno, Tokyo, Japan
Y. Kiyanagi (Hokkaido Univ.), Y. Nagai (JAEA), T. Nakanishi (Univ. Tokyo), M. Igashira (Tokyo Inst. Tech.), T. Katabuchi (Tokyo Inst. Tech.), M. Oshima (JAEA), H. Harada (JAEA), T. Otsuki (Tohoku Univ.), H. Utsunomiya (Konan Univ.), T. Shima (Osaka Univ.), M. Ebihara (Tokyo Metro. Univ.), M. Matsuo (Univ. Tokyo), Y. Oura (Tokyo Metro. Univ.), M. Furusaka (Hokkaido Univ.), T. Hayakawa (JAEA), H. Matsue (JAEA), H. M. Shimizu (KEK)

2010.1.19
BL16 ARISA-II: Workshop on Horizontal-type Neutron Reflectometer at J-PARC
KEK, Tsukuba, Ibaraki, Japan
K. Mitamura (Kyushu Univ./JST), T. Takahashi (Univ. Tokyo), M. Kobayashi (Kyushu Univ./JST),), H. Yokoyama (Univ. Tokyo), N. Torikai (Mie Univ.), A. Takahara (Kyushu Univ.), N. Torikai (Mie University), N. Yamada (KEK)

Member lists of the Advisory Committees organized for MLF/J-PARC (as of March, 2010)

Neutron Instrument Proposal Review Committee FY2002 - FY2009
中性子実験装置計画検討委員会 FY2002 - FY2006
中性子実験装置部会 FY2007 - FY2009

Committee members

Yuji Ohashi	Tokyo Institute of Technology, Japan (2002~2004)
Kenji Suzuki	Research Institute for Special Inorganic Materials, Japan (2002~2004)
Yasuo Endo	Tohoku University, Japan (2002~2004)
Kazuyoshi Yamada	Tohoku University, Japan (2002~)
Michihiro Furusaka	Hokkaido University, Japan (2002~)
Toshiharu Fukunaga	Kyoto University, Japan (2004~)
Toshiji Kanaya	Kyoto University, Japan (2002~)
Mamoru Sato	Yokohama City University, Japan (2004~)
Masaru Tanokura	University of Tokyo, Japan (2002~2004)
Hideki Yoshizawa	University of Tokyo, Japan (2007~)
Mitsuhiro Shibayama	University of Tokyo, Japan (2007~)
Yukio Noda	Tohoku University, Japan (2007~)
Yuichiro Maeda	RIKEN, Japan (2004)
Yasuki Nagai	Osaka University, Japan (2002~)
Kazuma Hirota	Osaka University, Japan (2008~2009)
Makoto Hayashi	Ibaraki Prefecture, Japan (2004~2007)
Etsuo Akiba	AIST, Japan (2004~2007)
Tatsumi Hirano	Hitachi, Ltd., Japan (2007~)
Toshio Akai	Mitsubishi Chemical Co., Japan (2007~)
Chang-Hee Lee	Korea Atomic Energy Research Institute, Korea (2004~2006)
Yukio Oyama	Japan Atomic Energy Agency, Japan (2002~2004)
Yujiro Ikeda	Japan Atomic Energy Agency, Japan (2002~)
Yasuhiko Fujii	Japan Atomic Energy Agency, Japan (2002~2007)
Yukio Morii	Japan Atomic Energy Agency, Japan (2002~)
Nobuo Niimura	Japan Atomic Energy Agency, Japan (2002~2004)
Kazuhisa Kakurai	Japan Atomic Energy Agency, Japan (2004~)
Masatoshi Arai	Japan Atomic Energy Agency, Japan (2002~)
Susumu Ikeda	High Energy Accelerator Research Organization, Japan (2002~)
Masayoshi Kawai	High Energy Accelerator Research Organization, Japan (2002~2006)
Hirohiko Shimizu	High Energy Accelerator Research Organization, Japan (2007~)
Takashi Kamiyama	High Energy Accelerator Research Organization, Japan (2007~)
Toshiya Otomo	High Energy Accelerator Research Organization, Japan (2007~)
Naoya Torikai	High Energy Accelerator Research Organization, Japan (2007~)

Working group members

Masaike Akira	Japan Society of the Promotion of Science, Japan (2002~2007)
Koichiro Asahi	Tokyo Institute of Technology, Japan (2002~)
Isao Tanihata	RIKEN, Japan (2002~2004)
Tokushi Shibata	Japan Atomic Energy Agency, Japan (2002~)
Yoshiaki Kiyanagi	Hokkaido University, Japan (2004~)
Hirohiko Shimizu	High Energy Accelerator Research Organization, Japan (2004~2006)
Hiroshi Ikezoe	Japan Atomic Energy Agency, Japan (2004~)
Yuji Ohashi	Tokyo Institute of Technology, Japan (2004~)
Makoto Sakata	Nagoya University, Japan (2002~)
Yukio Noda	Tohoku University, Japan (2002~2006)
Kenji Ohoyama	Tohoku University, Japan (2004~)
Takashi Kamiyama	High Energy Accelerator Research Organization, Japan (2004~2006)
Junichi Suzuki	Japan Atomic Energy Agency, Japan (2004~)
Ysuo Endo	International Institute for Advanced Studies, Japan (2004~)

Tsuneyoshi Nakayama	Hokkaido University, Japan (2002~)
Hideki Yoshizawa	University of Tokyo, Japan (2002~2006)
Shojiro Takeyama	University of Tokyo, Japan (2004~2007)
Takao Ohta	Hiroshima University, Japan (2002~)
Akira Inaba	Osaka University, Japan (2004~)
Shinichi Itoh	High Energy Accelerator Research Organization, Japan (2004~)
Masahumi Kohgi	Tokyo Metropolitan University, Japan (2004~)
Hiroyuki Takahashi	University of Tokyo, Japan (2004~)
Masaki Katagiri	Japan Atomic Energy Agency, Japan (2004~)
Masakatsu Misawa	Niigata University, Japan (2002~)
Yushu Matsushita	Nagoya University, Japan (2004~)
Mitsuhiro Shibayama	University of Tokyo, Japan (2002~2006)
Takashi Odagaki	Kyushu University, Japan (2002~)
Toshiharu Fukunaga	Kyoto University, Japan (2002~2004)
Takeji Hashimoto	Kyoto University, Japan (2002~2004)
Toshiya Otomo	High Energy Accelerator Research Organization, Japan (2004~2006)
Makoto Yao	Kyoto University, Japan (2004~2007)
Mikio kataoka	Nara Institute of Science and Technology, Japan (2002~)
Nobuhiro Go	Japan Atomic Energy Agency, Japan (2002~)
Mitsuhiro Hirai	Gunma University, Japan (2002~)
Yoko Sugawara	Kitasato University, Japan (2002~)
Yukio Morimoto	Kyoto University, Japan (2002~)
Nobuo Niimura	Ibaraki University, Japan (2004~)
Ryota Kuroki	Japan Atomic Energy Agency, Japan (2004~)

Materials and Life Science Facility Advisory Board FY2007 - FY2009
物質・生命科学実験施設利用委員会 FY2007 - FY2009

Etsuo Akiba	AIST, Japan (~2008)
Kazuyoshi Yamada	Tohoku University, Japan
Toshiji Kanaya	Kyoto University, Japan
Toshiharu Fukunaga	Kyoto University, Japan
Hideki Yoshizawa	University of Tokyo, Japan (~2008)
Nobuo Niimura	Ibaraki University, Japan (~2008)
Jun Akimitsu	Aoyama Gakuin University, Japan (~2008)
Mikio kataoka	Nara Institute of Science and Technology, Japan (~2008)
Mamoru Sato	Yokohama City University, Japan (2009~)
Mitsuhiro Shibayama	University of Tokyo, Japan (2009~)
Makoto Hayashi	Ibaraki Prefecture, Japan
Shinichi Kamei	Mitsubishi Research Institute, Japan
Nobuhiko Nishida	Tokyo Institute of Technology, Japan
Eiko Torikai	Yamanashi University, Japan (~2008)
Masahiko Iwasaki	RIKEN, Japan (~2008)
Teiichiro Matsuzaki	RIKEN, Japan (2009~)
Sugiyama Jun	Toyota Central R&D Labs., Japan (2009~)
Yukio Noda	Tohoku University, Japan (2009~)
Yoji Koike	Tohoku University, Japan (2009~)
Yujiro Ikeda	Japan Atomic Energy Agency, Japan
Yasuhiko Fujii	Japan Atomic Energy Agency, Japan
Yukio Morii	Japan Atomic Energy Agency, Japan (~2007)
Masatoshi Arai	Japan Atomic Energy Agency, Japan
Junichiro Mizuki	Japan Atomic Energy Agency, Japan
Junichi Suzuki	Japan Atomic Energy Agency, Japan (2009~)
Kazuhisa Kakurai	Japan Atomic Energy Agency, Japan (2008~)
Susumu Ikeda	High Energy Accelerator Research Organization, Japan
Hirohiko Shimizu	High Energy Accelerator Research Organization, Japan
Takashi Kamiyama	High Energy Accelerator Research Organization, Japan
Kusuo Nishiyama	High Energy Accelerator Research Organization, Japan

Ryosuke Kadono	High Energy Accelerator Research Organization, Japan
Hideki Seto	High Energy Accelerator Research Organization, Japan (2009~)
Yasuhiro Miyake	High Energy Accelerator Research Organization, Japan (2009~)
Yoshishige Yamazaki	J-PARC Center, Japan (~2008)

MLF Neutron Proposal Review Committee FY2008 -FY 2009
MLF中性子課題審査部会 FY2008 - FY2009

Kazuyoshi Yamada	Tohoku University, Japan
Toshiji Kanaya	Kyoto University, Japan
Toshiharu Fukunaga	Kyoto University, Japan
Hideki Yoshizawa	University of Tokyo, Japan
Mamoru Sato	Yokohama City University, Japan
Mitsuhiro Shibayama	University of Tokyo, Japan
Masao Ogata	University of Tokyo, Japan
Makoto Hayashi	Ibaraki Prefecture, Japan
Shinichi Kamei	Mitsubishi Research Institute, Japan
Masaki Takata	RIKEN, Japan
Yukio Noda	Tohoku University, Japan
Yukio Morimoto	Kyoto University, Japan
Yo Tomota	Ibaraki University, Japan
Toshio Yamaguchi	Fukuoka University, Japan
Hideto En'yo	RIKEN, Japan
Brendan Kennedy	University of Sydney, Australia
Sung-Min Choi	Korea Advanced Institute of Science and Technology, Korea
Pete Timmins	Institut Laue-Langevin, France
Je-Geun Park	SungKyunKwan University, Korea
Yujiro Ikeda	Japan Atomic Energy Agency, Japan
Yasuhiko Fujii	Japan Atomic Energy Agency, Japan
Masatoshi Arai	Japan Atomic Energy Agency, Japan
Kazuhisa Kakurai	Japan Atomic Energy Agency, Japan
Susumu Ikeda	High Energy Accelerator Research Organization, Japan
Takashi Kamiyama	High Energy Accelerator Research Organization, Japan (2009~)
Kusuo Nishiyama	High Energy Accelerator Research Organization, Japan (~2008)
Yasuhiro Miyake	High Energy Accelerator Research Organization, Japan (2009~)
Yukio Morii	Hitachinaka Techno Center, Japan

Muon Science Advisory Committee (MuSAC)

MuSAC-1 (February 7, 2003 at KEK)
MuSAC-2 (February 19-20, 2004 at KEK)
MuSAC-3 (February 25-26, 2005 at KEK)
MuSAC-4 (February 25-26, 2006 at KEK)
MuSAC-5 (January 11-13, 2007 at KEK)
MuSAC-6 (January 15-16, 2008 at JAEA)
MuSAC-7 (March 6-7, 2009 at JAEA)
MuSAC-8 (March 11-12, 2010 at JAEA)

Members of committee from MuSAC-1 to MuSAC-5

Chair: J.-M. Pouttisou	TRIUMF
J. Akimitsu	Aoyama-Gakuin University
S. Ikeda	KEK
Y. Ikeda	JAEA
M. Iwasaki	RIKEN
K. Nagamine	KEK
N. Nishida	Tokyo Inst. Technology
Y. Miyake	KEK
Y. Yamazaki	JAEA
H. Yasuoka	JAEA
R.H. Heffner	Los Alamos National Lab.
C. Petitjean	Paul Scherrer Institute
L.I. Ponomarev	Kurchatov Inst.

Members of committee from MuSAC-6 and MuSAC-7

Chair: J.-M. Pouttisou	TRIUMF
J. Akimitsu	Aoyama-Gakuin University
S. Ikeda	KEK
Y. Ikeda	JAEA
M. Iwasaki	RIKEN
K. Nishiyama	KEK
N. Nishida	Tokyo Inst. Technology
Y. Miyake	KEK
Y. Yamazaki	JAEA
Y. Hatano	JAEA
R.H. Heffner	Los Alamos National Laboratory
C. Petitjean	Paul Scherrer Institute
L.I. Ponomarev	Kurchatov Inst.

Members of committee of MuSAC-8

Chair: E. Morenzoni	Paul Scherrer Institute
J.Akimitsu	Aoyama-Gakuin University
H. Amitsuka	Hokkaido University
R. Cywinski	University Huddersfield
J.-M. Poutissou	TRIUMF
A. Shinohara	Osaka University
J. E. Sonier	Simon Fraser University
E. Torikai	Yamanashi University

Y. Miyake presenting at MuSAC-7: members at the round table. Observers at the right.

Muon Science Establishment (MUSE) Future Planning Committee

1st meeting (September 30, 2009 at KEK)
2nd meeting (January 13, 2010 at Tokyo)

Members of committee for MUSE Future Planning Committee

E. Torikai	Yamanashi University
N. Nishida	Tokyo Institute of Technology
Y. Koike	Tohoku University
T. Matsuzaki	RIKEN
Y. Kuno	Osaka University
R. Kadono	KEK
Y. Miyake	KEK
K. Shimomura	KEK
W. Higemoto	JAEA

11th International Conference on Muon Spin Rotation, Relaxation and Resonance (mSR2008)

Chair: K. Nishiyama KEK

July 21-25, 2008 at Epochal Tsukuba with 141 participants.

Proceedings were published in a special issue of Physica B 404 (2009).

Group photo of μSR2008 conference

Muon Proposal Approval Committee (MLF muon-PAC) Members & venue

1st muon-PAC September 17, 2004, KEK tsukuba
2nd muon-PAC February 28, 2005, KEK tsukuba
External members
Masahiko Iwasaki (RIKEN)
Masao Ogata (U. Tokyo)
Shinsaku Kambe (JAEA)
Yoshitaka Kuno (Osaka U.)
Yoji Koike (Tohoku U.)
Atsushi Shinohara (Osaka U.)
Isao Shimamura (RIKEN)
Hiroyuki Nojiri (Tohoku U.)
Kazuyoshi Yamada (Tohoku U.)
Isao Watanabe (RIKEN)
Internal members
Tadashi Matsushita (KEK)
Susumu Ikeda (KEK)
Kusuo Nishiyama (KEK)
Masaharu Nomura (KEK)
Yoshiharu Mori (KEK)
Ryosuke Kadono (KEK)
Takashi Kamiyama (KEK)
Tokushi Shibata (KEK)
Kei-ichiro Nasu (KEK)
Kanetada Nagamine (KEK)

3rd muon-PAC October 4, 2005, KEK tsukuba
4th muon-PAC May 22, 2006, KEK tsukuba
5th muon-PAC July 26, 2006, in e-mails
6th muon-PAC August 31, 2006, in e-mails
7th muon-PAC September 21, 2006, in e-mails
8th muon-PAC November 2, 2006, in e-mails
9th muon-PAC February 23, 2007, KEK tsukuba
10th muon-PAC May 28, 2007, in e-mails
11th muon-PAC July 27, 2007, KEK tsukuba
12th muon-PAC November 13, 2007, in e-mails
13th muon-PAC February 26, 2008, KEK tsukuba
14th muon-PAC August 6, 2008, in e-mails
15th muon-PAC November 19, 2008, in e-mails
16th muon-PAC February 6, 2009, in e-mails
17th muon-PAC March 5, 2009, in e-mails
External members
Hiroshi Amitsuka (Hokkaido U.)
Masahiko Iwasaki (RIKEN)
Masao Ogata (U. Tokyo)
Shinsaku Kambe (JAEA)
Yoshitaka Kuno (Osaka U.)
Yoji Koike (Tohoku U.)
Atsushi Shinohara (Osaka U.)
Masashi Takigawa (U. Tokyo)
Shinji Tsuneyuki (U. Tokyo)
Hiroyuki Nojiri (Tohoku U.)
Katsuyuki Fukutani (U. Tokyo)
Isao Watanabe (RIKEN)
Internal members
Susumu Ikeda (KEK)
Kusuo Nishiyama (KEK)
Masaharu Nomura (KEK)
Koutaro Sato (KEK)
Ryosuke Kadono (KEK)
Takashi Kamiyama (KEK)
Kei-ichiro Nasu (KEK)
Tadashi Matsushita (KEK) ~2007
Kanta Ono (KEK) 2007~2008

18th muon-PAC September 9, 2009, in e-mails
External members
Hiroshi Amitsuka (Hokkaido U.)
Eimoku Yuichiro (JAEA)
Masahiko Iwasaki (RIKEN)
Masao Ogata (U. Tokyo)
Shinsaku Kambe (JAEA)
Yoshitaka Kuno (Osaka U.)
Yoji Koike (Tohoku U.)
Atsushi Shinohara (Osaka U.)
Suzuya Kentaro (JAEA)
Masashi Takigawa (U. Tokyo)
Shinji Tsuneyuki (U. Tokyo)
Hiroyuki Nojiri (Tohoku U.)
Katsuyuki Fukutani (U. Tokyo)
Isao Watanabe (RIKEN)
Internal members
Susumu Ikeda (KEK)
Hideki Seto (KEK)
Ryosuke Kadono (KEK)
Kenji Ito (KEK)
Hitoshi Kobayashi (KEK)
Takashi Kamiyama (KEK)
Kanta Ono (KEK) 2007~2008
Kei-ichiro Nasu (KEK)
Yasuhiro Miyake (KEK)

Award List

(**Award name/** *Theme* / Personal or group name / Organization / Date)

The Japanese Society for Experimental Mechanics, Paper Award, *"球接触多層モデルを用いた逆解析"*, Masatoshi Futakawa, Hiroyuki Kogawa, March 2006

The Japanese Society for Neutron Science, Poster Award, *"大面積イオンビームスパッタ装置による高性能中性子スーパーミラーの開発"*, Ryuji Maruyama, December 2006

Atomic Energy Sciety of Japan, Presentation Award, *"イオンビームスパッタ法による高性能スーパーミラーの開発"*, Ryuji Maruyama, September 2007

The Japanese Society for Neutron Science, Technology Award, *"大強度パルス中性子実験装置用高分解能２次元検出器の開発"*, Masaki Katagiri, December 2007

Cryogenic Association of Japan, Young Scientist Award, *"若手研究者として低温工学の活発な研究開発活動"*, Hideki Tatsumoto, May 2008

Japan Atomic Energy Agency, Creativity Achievement Award, *"冷中性子ビーム利用を飛躍的に向上させる小型高性能分岐装置の考案"*, Ryuji Maruyama, Dai Yamazaki, Kazuhiko Soyama, Kazuya Aizawa, October 2008

The Japanese Society for Neutron Science, Technology Award, *"パルス中性子光学システムの開発と中性子分光法の研究－超高偏極中性子の発生と集光型超高偏極中性子小角散乱システムの完成－"*, Takayuki Oku, December 2008

The Japanese Society for Neutron Science, Young Scientist Award, *"パルス中性子非弾性散乱装置の性能向上を目的とした装置仕様の最適化"*, Nobuaki Takahashi, December 2008

Journal of the Physical Society of Japan, JPSJ Papers of Editors' Choice, *"Dimensional Crossover of Low-Energy Magnetic Excitation for Delafossite Oxide* $Cu_{1-x}Ag_xCrO_2$ *with a Spin-3/2 Antiferromagnetic Triangular Sublattice"*, Ryoichi Kajimoto, January 2009

The KEK Technology Prize 2008, *"Optimized design of J-PARC 3NBT beamline magnets and M1, M2 magnets under....high....radiation....fields,....using....detailed....three dimensional calculations."*, Hiroshi Fujimori, High Energy Accelerator Research Organization, March 2009

Journal of the Physical Society of Japan, JPSJ Papers of Editors' Choice, *"First Demonstration of Novel Method for Inelastic Neutron Scattering Measurement Utilizing Multiple....Incident....Energies"*, Mitsutaka Nakamura, Yasuhiro Inamura, Fumio Mizuno, Ryoichi Kajimoto, September 2009

Japan Atomic Energy Agency, President's Award, *"J-PARC・MLFの初パルス中性子発生及び関連施設の建設完遂"*, Yujiro Ikeda, Takashi Kato, Masatoshi Futakawa, Kenichi Oikawa, Shinichi Sakamoto, Masahide Harada, Tetsuya Kai, Fujio Maekawa, Hiroshi Takada, Kenji Sakai, Yoshimi Kasugai, Katsuhiro Haga, Motoki Ohi, Hideki Tatsumoto, Makoto Teshigawara, Hiroyuki Kogawa, Tomokazu Aso, Shin-ichiro Meigo, Hidetaka Kinoshita, Takashi Wakui, Hiroyuki Kogawa, October 2009

Creativity Achievement Award, *"J-PARC中性子非弾性散乱実験装置「四季」における新たな高効率測定手法の開発"*, Mitsutaka Nakamura, Yasuhiro Inamura, Wataru Kambara, Ryoichi Kajimoto, Japan Atomic Energy Agency, March 2010

The KEK Technology Prize 2010, *"Development of muon production target at J-PARC"*, Shunsuke Makimura, High Energy Accelerator Research Organization, March 2010

Foundation for High Energy Accelerator Science, Special Prize, Yasuhiro Miyake, Koichiro Shimomura, Naritoshi Kawamura, Patrick Strasser, Akihiro Koda, Shunsuke Makimura, Hiroshi Fujimori, Wataru Higemoto, Kusuo Nishiyama, March 2010

Publication List

Neutron Sections

1: Kazuya Aizawa, Masatoshi Arai
Inelastic scattering measurement option of TOF-USANS instrument at J-PARC
Physica B 385-386 1114 (2006)

2: M. Arai, H. Iwase, M. Nakamura, T. Otomo, E. Kartini, K. Itoh, S.J. Levett and S.M. Bennington
Relation between High Ionic Conductivity and Boson Peak in Superionic Glass
AIP Conference Proceedings 832 299 (2006)

3: 新井正敏
Ｊ-ＰＡＲＣの先端的中性子実験装置群
月刊エネルギー 39 52 (2006)

4: 新井正敏・安藤陽一・大柳宏之・上村 洸・高重正明・前野悦輝
会議だより 高温超伝導発見20周年記念シンポジウムに出席しての印象記
固体物理 41 537 (2006)

5: M. Arai, K. Aizawa, K. Nakajima, K. Shibata, N. Takahashi
Proceedings of the International Advisory Committee on Biomolecular Dynamics Instrument DNA and the Workshop on Biomolecular Dynamics Backscattering Spectrometers
JAEA-Review 2008-036 (2008)

6: 新井正敏
J-PARC実現への道と更なる将来に向かって
日本中性子科学会誌「波紋」 18 44 (2008)

7: M. Arai, K. Aizawa, K. Nakajima, K. Shibata, N. Takahashi
Proceedings of the 2nd International Advisory Committee on Biomolecular Dynamics Instrument DNA in MLF at J-PARC
JAEA-Review 2009-014 (2009)

8: Masatoshi Arai and Kent Crawford
Neutron Sources and Facilities
Neutron Imaging and Applications, Neutron Scattering Applications and Techniques 13 (2009)

9: M. Arai, F. Maekawa
Japan Spallation Neutron Source (JSNS) of J-PARC
Nuclear Physics News 19 34 (2009)

10: 新井正敏
世界最強パルス中性子施設J-PARCの稼動開始
高圧力の科学と技術 19 4 (2009)

11: 新井正敏
大強度陽子加速器施設"J-PARCと磁性研究への期待"
日本磁気学会誌「まぐね」 4 4 (2009)

12: Hrioshi Arima, Kazuki Komatsu, Kazuaki Ikeda, Katsuya Hirota, Hiroyuki Kagi
Designing an elliptical supermirror guide for the high-pressure material science beamline of J-PARC
Nucl. Instrum. Methods Phys. Res. A 600 71 (2009)

13: T. Aso, M. Monde, H. Sato, H. Tatsumoto, T. Kato, Y. Ikeda
Estimation of JSNS Moderator Flowing Condition Based on Impinging Jet Heat Transfer
Proc. of the 17th Meeting of the Int. Collaboration on Advanced Neutron Sources, Los Alamos Report LA-UR-06-3904 385 (2006)

14: A. Bucheeri, Y. Kurishita, T. Kato, T. Naoe, H. Kogawa, M. Futakawa
Fabrication of a bubbler nozzle for micro-bubble injection in liquid mervury
International Conference on Porous Metals and Metallic Foams (MetFoam 2007) 189 (2007)

15: A. Bucheeri, H. Kogawa, T. Naoe, M. Futakawa
Wettability effect on bubble formation at orifice type nozzle
日本実験力学会 7 331 (2007)

16: A. Bucheeri, H. Kogawa, T. Naoe, M. Futakawa, K. Haga
Microbubble Formation at a Nozzle in Liquid Mercury
J. Nucl. Sci. Technol. 45 525 (2008)

17: Toru Ebisawa, Kazuhiko Soyama, Dai Yamazaki, Ryuji Maruyama, Seiji Tasaki, Yutaka Abe, Hiroyuki Hayashida, Masahiro Hino, Masaaki Kitaguchi, Yuji Kawabata, and Koji Niita
Shield evaluation of cold neutron curved guide tubes for J-PARC neutron resonance spin echo spectrometers
Nucl. Instrum. Methods Phys. Res. A 600 126 (2009)

18: 藤井保彦，新井正敏，門野良典，金谷利治，神山 崇，新村信雄，野尻浩之，野田幸男，八木健彦，山田和芳
J-PARCの拓く凝縮系科学
固体物理 43 441 (2008)

19: K. Fujita, H. Takahashi, P. Siritiprussamee, H. Niko, M. Kai, M. Nakazawa, T. Ino, S. Sato, T. Yokoo, M. Furusaka and M. Kanazawa
Neutron Beam Test of Multi-Grid-type Microstrip Gas Chamber
Physica B 385-386 1290 (2006)

20: K. Fujita, H. Takahashi, P. Siritiprussamee, H. Niko, M. Kai, M. Nakazawa, T. Ino, S. Sato, T. Yokoo, M. Furusaka and M. Kanazawa
A High-resolution Two-dimensional He-3 Neutron MSGC with Pads for Neutron Scattering Experiments
Nucl. Instrum. Methods Phys. Res. A 580 1027 (2007)

21: A. Fujiwara, K. Okita, Y. Matsumoto, M. Futakawa, S. Hasegawa, H. Kogawa, Y. Ikeda
Strategy to Mitigate Pitting Damage in JSNS Mercury Target
Proc. of the 17th Meeting of the Int. Collaboration on Advanced Neutron Sources, Los Alamos Report LA-UR-06-3904 552 (2006)

22: M. Futakawa, T. Naoe, H. Kogawa, M. Teshigawara, Y. Ikeda
Effects of pitting damage on fatigue limit and lifetime in mercury target
J. Nucl. Mater. 356 168 (2006)

23: M. Futakawa, T. Naoe, H. Kogawa, Y. Ikeda
Mercury Target Life Estimation Under Impulsive Proton Beam Injection
Proc. of the 17th Meeting of the Int. Collaboration on Advanced Neutron Sources Los Alamos Report LA-UR-06-3904 562 (2006)

24: M. Futakawa, H. Kogawa, S. Hasegawa, Y. Ikeda, Riemer, Wendel., Haines, Bauer, T. Naoe, K. Okita, A, Fujiwara, Y. Matsumoto, N. Tanaka
Cavitation damage prediction for spallation target vessels by assessment of acoustic vibration
J. Nucl. Mater. 377 182 (2008)

25: M. Futakawa, H. Kogawa, S. Hasegawa, T. Naoe, M. Ida, K. Haga, T. Wakui, N. Tanaka, Y. Matsumoto, Y. Ikeda
Mitigation technologies for damege induced by pressure waves on high-power mercury spallation neutron sources (II) - bubbling effect to reduce pressure wave -
J. Nucl. Sci. Technol. 45 1041 (2008)

26: M. Futakawa, H. Kogawa, S. Hasegawa, M. Ida, K. Haga, T. Wakui, T. Naoe, N. Tanaka, Y. Matsumoto, Y. Ikeda
R&D on Pressure-wave Mitigation Technology in Mercury Targets.
Proc. of the 18th Meeting of the Int. Collaboration on Advanced Neutron Sources, Chinsese Academy of Science Progress Report 547 (2008)

27: M. Futakawa, K. Haga, T. Wakui, H. Kogawa
Development of the Hg target in the J-PARC neutron source
Nucl. Instrum. Methods Phys. Res. A 600 18 (2009)

28: K. Haga, H. Kogawa, H. Sato, S. Ishikura, H. Kinoshita, M. Futakawa, M. Kaminaga
Present Status of JSNS Mercury Target
Proc. of the 17th Meeting of the Int. Collaboration on Advanced Neutron Sources, Los Alamos Report LA-UR-06-3904 315 (2006)

29: K. Haga, T. Wakui, H. Kogawa, M. Harada, M. Futakawa, K. Hayashi, K. Nakamura
Thermal hydraulic design of the mercury target vessel
JAEA-Technology 2008-033 (2008)

30: K. Haga, H. Kogawa, T. Wakui, Y. Okamoto, M. Futakawa, M. Kaminaga, T. Kato
Present Status of JSNS Mercury Target
Proc. of the 18th Meeting of the Int. Collaboration on Advanced Neutron Sources, Chinsese Academy of Science Progress Report 577 (2008)

31: K. Haga, T. Naoe, H. Kogawa, T. Wakui, M. Futakawa
Mockup Experiments to Investigate the Leak Rate Correlation between Mercury and Helium for the Mercury Target System of J-PARC
J. Nucl. Sci. Technol. 46 1145 (2009)

32: K. Haga, H. Kogawa, T. Wakui, T. Naoe, M. Futakawa, S. Yamazaki, N. Tanaka
Bubble flow simulations in target vessel
Nucl. Instrum. Methods Phys. Res. A 600 64 (2009)

33: M. Harada, N. Watanabe, M. Teshigawara, T. Kai, F. Maekawa, T. Kato, Y. Ikeda
Deterioration of Pulse Characteristics and Burn-up Effects with an Engineering Model in Japanese Spallation Neutron Source
Proc. of the 17th Meeting of the Int. Collaboration on Advanced Neutron Sources, Los Alamos Report LA-UR-06-3904 700 (2006)

34: M. Harada, N. Watanabe, M. Teshigawara, T. Kai, T. Kato, Y. Ikeda
Neutronics of a poisoned para-hydrogen moderator for a pulsed spallation neutron source
Nucl. Instrum. Methods Phys. Res. A 574 407 (2007)

35: M. Harada, N. Watanabe, F. Maekawa, M. Futakawa
Pulse characteristics of epithermal neutrons from a spallation source
Nucl. Instrum. Methods Phys. Res. A 597 242 (2008)

36: M. Harada, F. Maekawa, M. Teshigawara, N. Watanabe, T. Kato, Y. Ikeda
Nuclear Heating Calculation for JSNS
Proc. of the 18th Meeting of the Int. Collaboration on Advanced Neutron Sources, Chinsese Academy of Science Progress Report 616 (2008)

37: Stefanus Harjo, Atsushi Moriai, Shuki Torii, Hiroshi Suzuki, Kentaro, Suzuya, Yukio Morii, Masatoshi Arai, Yo Tomota, Koichi Akita and Yoshiaki Akiniwa
Design of Engineering Diffractometer at J-PARC
Materials Science Forum 524-525 199 (2006)

38: Stefanus Harjo, Takashi Kamiyama, Shuki Torii, Toru Ishigaki, Masao Yonemura
The Ibaraki prefecture materials design diffractometer for J-PARC-Designing neutron guide
Physica B 385-386 1025 (2006)

39: ステファヌス ハルヨ，神山崇
中性子ビーム利用の基礎とJ-PARC
日本鉄鋼協会会報誌「ふぇらむ」 11 567 (2006)

40: S. Hasegawa, T. Kato, T. Aso, I. Ushijima, H. Tatsumoto, K. Otsu, Y. Ikeda
Numeral Analysis for the Emergency Discharge of the Hydrogen Loop of JSNS
Proc. of the 17th Meeting of the Int. Collaboration on Advanced Neutron Sources, Los Alamos Report LA-UR-06-3904 402 (2006)

41: S. Hasegawa, T. Aso, H. Tatsumoto, K. Otsu, T. Uehara, F. Maekawa, T. Kato, Y. Ikeda
Estimation of Pressure Change Based on Hybrid Control System in JSNS Hydrogen Loop.
Proc. of the 18th Meeting of the Int. Collaboration on Advanced Neutron Sources, Chinsese Academy of Science Progress Report 497 (2008)

42: S. Hasegawa, T. Aso, H. Tatsumoto, K. Otsu, T. Uehara, F. Maekawa, T. Kato, Y. Ikeda
Effect of hydrogen loop fluctuation on cold neutron performance with hybrid control system in JSNS
Nucl. Instrum. Methods Phys. Res. A 600 81 (2009)

43: Makoto Hayashi, Toru Ishigaki, Takashi Kamiyama,

Ichiro Tanaka
Construction of Ibaraki Prefectural Neutron Spectrometers
Nucl. Instrum. Methods Phys. Res. A 600 14 (2009)

44: Hayashida, Masaaki Kitaguchi, Masahiro Hino, Yuji Kawabata, Ryuji Maruyama, and Toru Ebisawa
Development of a resonance spin flipper for NRSE/MIEZE on a pulsed neutron beam with an oscillating frequency of 500 kHz
Nucl. Instrum. Methods Phys. Res. A 574 292 (2007)

45: Masahiro Hino, Hirotoshi Hayashida, Masaaki Kitaguchi, Yuji Kawabata, Masayasu Takeda, Ryuji Maruyama, Toru Ebisawa, Naoya Torikai, Tetsuya Kume, and Seiji Tasaki
Development of large-m polarizing neutron supermirror fabricated by using ion beam sputtering instrument at KURRI
Physica B 385-386 1187 (2006)

46: Masahiro Hino, Masaaki Kitaguchi, Hirotoshi Hayashida, Yuji Kawabata, Seiji Tasaki, Toru Ebisawa, Dai Yamazaki, Ryuji Maruyama, Keiji Tanaka, Naoya Torikai, Rintaro Inoue, and Toshiji Kanaya
A test of MIEZE-reflectometer for study of surface and interface
Physica B 385-386 1125 (2006)

47: Masahiro Hino, Masaaki Kitaguchi, Hirotoshi Hayashida, Seiji Tasaki, Toru Ebisawa, Ryuji Maruyama, Norio Achiwa, Yuji Kawabata
A study on reflectivity limit of neutron supermirror
Nucl. Instrum. Methods Phys. Res. A 600 207 (2009)

48: A. Hoshikawa, T. Ishigaki, M. Nagai, Y. Kobayashi, H. Sagehashi, T. Kamiyama, M. Yonemura, K. Aizawa, T. Sakuma, Y. Tomota
Development of an automatic sample chnger for iMATERIA
Nucl. Instrum. Methods Phys. Res. A 600 203 (2009)

49: T. Hosoya, T. Nakamura, M. Katagiri, A. Birumachi, M. Ebine, and K. Soyama
Development of a new detector and DAQ systems for iBIX
Nucl. Instrum. Methods Phys. Res. A 600 217 (2009)

50: M. Ida, T. Naoe, M. Futakawa
Direct observation and theoretical study of cavitation bubbles in liquid mercury
Phys. Rev. E 75 46304 (2007)

51: M. Ida, T. Naoe, M. Futakawa
Suppression of cavitation inception by gas bubble injection; A Numericalstudy focusing on bubble-bubble interaction
Phys. Rev. E 76 46309 (2007)

52: M. Ida, T. Naoe, M. Futakawa
Numerical study of gas and cavitation bubble dynamics in liquid mercury under negative pressure
Proc. of 5th Joint ASME/JSME Fluids Engineering Conf. 1 (2007)

53: M. Ida, T. Naoe, M. Futakawa
On the effect of microbubble injection on cavitation bubble dynamics in liquid mercury
Nucl. Instrum. Methods Phys. Res. A 600 367 (2009)

54: M. Ida
Multibubble cavitation inception
Phys. Fluids 21 113302 (2009)

55: Y. Ikeda
Status of J-PARC Project and JSNS Construction
Proc. of the 17th Meeting of the Int. Collaboration on Advanced Neutron Sources, Los Alamos Report LA-UR-06-3904 58 (2006)

56: Takashi Ino and Suguru Muto
A tiny neutron spin filter
Physica B 385-386 1138 (2006)

57: Takashi Ino and Suguru Muto
Measurements of the ^{3}He spin relaxation below room temperature
Physica B 397 182 (2007)

58: Takashi Ino, Mitsutaka Nakamura, Takayuki Oku, Takenao Shinohara, Jun-ichi Suzuki, Kenji Ohoyama, Haruhiro Hiraka
Development of a compact on-beam SEOP neutron spin filter
Physica B 404 2667 (2009)

59: Toru Ishigaki, Stefanus Harjo, Masao Yonemura, Takashi Kamaiyama, Kazuya Aizawa, Kenichi Oikawa, Takashi Sakuma, Yukio Morii, Masatoshi Arai, Kazuhiro Ebata, Yoshiki Takano, Takuro Kasao
IBARAKI Materials Design Diffractometer for J-PARC
Physica B 385-386 1022 (2006)

60: 石垣　徹，星川晃範，米村雅雄，神山　崇，鳥居周輝，森嶋隆裕，大石亮子
粉末回折装置の概要と構造科学・材料開発に与えるインパクト
日本結晶学会誌 50 18 (2008)

61: T. Ishigaki, A. Hoshikawa, M. Yonemura, T. Morishima, T. Kamiyama, R. Oishi, K. Aizawa, T. Sakuma, Y. Tomota and M. Arai
IBARAKI materials design diffractometer (iMATERIA)-Versatile neutron diffractometer at J-PARC
Nucl. Instrum. Methods Phys. Res. A 600 189 (2009)

62: M. Ishikado, R. Kajimoto, S. Shamoto, M. Arai, A. Iyo, K. Miyazawa, P. M. Shirage, H. Kito, H. Eisaki, S. Kim, H. Hosono, T. Guidi, R. Bewley, and S. M. Bennington
Two-dimensional Spin Density Wave State in LaFeAsO
J. Phys. Soc. Jpn. 78 43705 (2009)

63: S. Itoh, K. Ueno, R. Ohkubo, H. Sagehashi, Y. Funahashi, S. Koike, M. Kawai, M. Ishihama and N. Hitomi
Development of 100Hz T0 Chopper
KEK Progress Report 2006-4 M 371 (2006)

64: S. Itoh, J. Suzuki, K. Ueno, S. Takata, K. Tomiyasu and T. Otomo
Engineering on windows on vacuum scattering chamber of neutron instruments
Proc. of the 17th Meeting of the Int. Collaboration on Advanced Neutron Sources, Los Alamos Report LA-UR-06-3904 994 (2006)

65: S. Itoh, K. Ohoyama, T. Kamiyama, T. Otomo, K. Nakajima, R. Kajimoto, T. Yokoo, K. Kuwahara, K. Tomiyasu, O. Yamamuro, S. Muto, H. Sagehashi, J. Suzuki, K. Ueno and T. Ino
High Resolution Chopper Spectrometer at J-PARC
Proc. of the 17th Meeting of the Int. Collaboration on Advanced Neutron Sources, Los Alamos Report LA-UR-06-3904 1019 (2006)

66: S. Itoh, K.Ueno, R. Ohkubo, H. Sagehashi, Y. Funahashi, N. Sato, M. Kawai, N. Hitomi and M. Ishihama
Development of 100 Hz T0 chopper
Proc. of the 17th Meeting of the Int. Collaboration on Advanced Neutron Sources, Los Alamos Report LA-UR-06-3904 1038 (2006)

67: S. Itoh, T. Yokoo, K. Ohoyama, T. Kamiyama, O. Yamamuro, K. Kuwahara, T. J. Sato, T. Otomo, K. Nakajima, R. Kajimoto, K. Ueno, J. Suzuki, R. Ohkubo, H. Sagehashi, Y. Funahashi, S. Koike, M. Kawai
Recent Progress in Development and Construction of High Resolution Chopper Spectrometer at J-PARC
Proc. of the 18th Meeting of the Int. Collaboration on Advanced Neutron Sources, Chinsese Academy of Science Progress Report 362 (2007)

68: 伊藤晋一
チョッパー分光器概要と構造科学にもたらす新展開
日本結晶学会誌 50 51 (2008)

69: S. Itoh, T. Nakayama, R. Kajimoto, and M. A. Adams,
Single-length-scaling analysis for antiferromagnetic fractons in dilute heisenberg system $RbMn_{0.4}Mg_{0.6}F_3$
J. Phys. Soc. Jpn. 78 13707 (2009)

70: 伊藤晋一，横尾哲也
小特集 次世代新中性子源 J-PARCにより広がる新しい材料科学「何ができる？どこがすごい？」 高分解能チョッパー分光器 (High Resolution Chopper Spectrometer) HRC
日本金属学会報「まてりあ」 48 363 (2009)

71: 伊藤晋一，上野健治，横尾哲也
フェルミチョッパーの開発
日本中性子科学会誌「波紋」 19 224 (2009)

72: H. Iwashita, H. Iwasa, F. Hiraga, T. Kamiyama, Y. Kiyanagi, J. Suzuki, T. Shinohara, T. Oku and H. M. Shimizu
Simulation Study of a Pulsed Neutron Focusing using a Pulsed Electromagnetic Lens Coupled with a Permanent Magnet
Nucl. Instrum. Methods Phys. Res. A 600 129 (2009)

73: Isao Kagomiya, Yoshiaki Hata, Daisuke Eto, Hideto Yanagihara, Eiji Kita, Kenji Nakajima, Kazuhisa Kakurai, Masakazu Nishi, Kenji Ohoyama
On the magnetic symmetry of the low temperature phase of $ZnCr_2O_4$
J. Phys. Soc. Jpn. 76 64710 (2007)

74: T. Kai, Y. Kasugai, F. Maekawa, S. Meigo, H. Takada, Y. Ikeda
Analysis of Induced-Radioactivity Using DCHAIN-SP for Iron at a Mercury Target Irradiated by 2.8 or 24 GeV protons
Proc. of the 17th Meeting of the Int. Collaboration on Advanced Neutron Sources, Los Alamos Report LA-UR-06-3904 484 (2006)

75: T. Kai, Y. Kasugai, F. Maekawa, S. Meigo, H. Takada, Y. Ikeda
"Analysis of Induced-radioactivity using DCHAIN-SP for Iron, Copper and Niobium at a Mercury Target Irradiated by 2.83 and 24GeV Protons"
"Proc. of the 2005 Symp. on Nuclear Data, JAEA-Conf "2006-009 130 (2006)

76: T. Kai, T. Kamiyama, F. Hiraga, T. Kato, Y. Kiyanagi
Measurements of spatial distribution of intensity and energy spectrum of neutrons from coupled hydrogen moderators by using a position sensitive detector (Cooperative research)
JAEA-Research 2006-090 (2007)

77: T. Kai, T. Kamiyama, F. Hiraga, K. Hirota, M. Ooi, F. Maekawa, T. Kato, Y. Kiyanagi
Measurements of Spatial Distribution and Pulse Shapes of Neutrons from a Cylindrical Coupled Para-hydrogen Moderator.
Proc. of the 18th Meeting of the Int. Collaboration on Advanced Neutron Sources, Chinsese Academy of Science Progress Report 482 (2008)

78: T. Kai, K. Sakai, K. Nakatani, H. Takada, K. Oikawa, K. Shimomura, W. Higemoto, H. Kinoshita, M. Ooi, M. Kaminaga
Users' beam interlock system at the Materials and Life Science Experimental Facility of J-PARC
Nucl. Instrum. Methods Phys. Res. A 600 176 (2009)

79: R. Kajimoto, M. Nakamura, T. Osakabe, T. J. Sato, K. Nakajima, M. Arai
Study of converging neutron guides for the cold neutron double-chopper spectrometer at J-PARC
Physica B 385-386 1236 (2006)

80: R. Kajimoto, T. Yokoo, K. Nakajima, M. Nakamura, K. Soyama, T. Ino, S. Shamoto, M. Fujita, K. Ohoyama, H. Hiraka, K. Yamada, and M. Arai
High intensity chopper spectrometer 4SEASONS at J-PARC
J. Neutron Research 15 5 (2007)

81: R. Kajimoto, T. Yokoo, M. Kofu, K. Noda, K. Kuwahara,
Ferroelectric polarization and magnetic structure in $Eu_{0.595}Y_{0.405}MnO_3$
J. Phys. Chem. Solids 68 2087 (2007)

82: R. Kajimoto, K. Nakajima, M. Nakamura, T. Osakabe, T. J. Sato, and M. Arai

Curved neutron guide of the cold neutron disk-chopper spectrometer at J-PARC
J. Neutron Research 16 81 (2008)

83: R. Kajimoto, K. Nakajima, M. Nakamura, K. Soyama, T. Yokoo, K. Oikawa, and M. Arai
Study of the Neutron Guide Design of the 4SEASONS Spectrometer at J-PARC
Nucl. Instrum. Methods Phys. Res. A 600 185 (2009)

84: R. Kajimoto, H. Sagayama, K. Sasai, T. Fukuda, S. Tsutsui, T. Arima, K. Hirota, Y. Mitsui, H. Yoshizawa, A.Q.R. Baron, Y. Yamasaki, and Y. Tokura
Unconventional ferroelectric transition in the multiferroic compound $TbMnO_3$ revealed by the absence of an anomaly in c-polarized phonon dispersion
Phys. Rev. Lett. 102 247602 (2009)

85: 加倉井和久
偏極中性子による磁性研究－定常およびパルス中性子源の相補利用による新展開－
固体物理 44 (2009)

86: 加倉井和久・奥 隆之
偏極中性子を活用した磁性研究
日本磁気学会誌「まぐね」 4 10 (2009)

87: M. Kaminaga, C. Konno, H. Kinoshita, T. Kato,M. Futakawa, Y. Ikeda
J-PARC Materials and Life Science Facility Building Design Policy and Design Results
Proc. of the 17th Meeting of the Int. Collaboration on Advanced Neutron Sources, Los Alamos Report LA-UR-06-3904 119 (2006)

88: M. Kaminaga, H. Kinoshita, K. Sakai, M. Ooi, Y. Kasugai, H. Aizawa, S. Kawasaki, F. Maekawa, M. Futakawa, T. Kato, Y. Ikeda
Present Status of Materials and Life Science Experimental Facility (MLF) and Spallation Neutron Source Related Comoponents.
Proc. of the 18th Meeting of the Int. Collaboration on Advanced Neutron Sources, Chinsese Academy of Science Progress Report 5 (2008)

89: 神山崇，池田裕二郎
MLF利用者支援体制について
日本結晶学会誌 50 61 (2008)

90: 神山崇，鳥居周輝
J-PARC/MLFの超高分解能粉末構造解析装置「Super HRPD」
中性子産業利用促進協議会季報「四季」 2 2 (2009)

91: 神山崇，鳥居周輝
超高分解能粉末中性子回折装置 SuperHRPD
日本金属学会報「まてりあ」 48 353 (2009)

92: T. Kanaya, N. Takahashi, K. Nishida, H. Seto, M. Nagao and Y. Takeda
Dynamic and static fluctuations in polymer gels studied by neutron spin-echo
Physica B 385-386 676 (2006)

93: E. Kartini, M. Arai, F. Mezei, M. Nakamura, and M. Russina
Structure and Dynamics on Superionic Conducting Phosphate Glasses by Neutron Scattering
Physica B 385-386 236 (2006)

94: Y. Kasugai, T. Kai, F. Maekawa, S. Meigo, H. Takada, Y. Ikeda
Analysis of Induced-radioactivity using DCHAIN-SP for Pb and Hg at a Mercury Target Irradiated by 2.8 and 24 GeV Protons
Proc. of the 2005 Symp. on Nuclear Data, JAEA-Conf 2006-009 136 (2006)

95: Y. Kasugai, T. Kai
Risk assessment of the mercury leak at Materials & Life Science Experimental Facility of J-PARC
JAEA-Technology 2009-010 (2009)

96: M. Katagiri, T. Nakamura, M. Ebine, A. Birumachi, S. Sotoh, E. M. Schooneveld, N. J. Rhodes
High-position-resolution neutron imaging detector with crossed wavelength shifting fiber read-out using two ZnS/^{6}LiF scintillator sheets
Nucl. Instrum. Methods Phys. Res. A 573 149 (2007)

97: 加藤崇，麻生智一，達本衡輝，長谷川勝一，大都起一
J-PARC 中性子源と低温水素システム
低温工学 42 244 (2007)

98: 加藤崇，麻生智一，達本衡輝，長谷川勝一，大都起一
J-PARC中性子源用低温水素システムの安全設計
低温工学 42 255 (2007)

99: 加藤崇，達本衡輝，麻生智一，長谷川勝一，大都起一
J-PARC中性子源用極低温水素システム
低温工学 43 409 (2008)

100: M. Kawai, M. Teshigawara, M. Harada, M. Saito, F. Maekawa, K. Kikuchi, N. Watanabe, Y. Ikeda, Y. Kurishita, S. Chiba
R&D of Fabricating Ag-In-Cd Decoupler and Cd Poison Plate for Decoupled Moderators of JSNS
Proc. of the 17th Meeting of the Int. Collaboration on Advanced Neutron Sources, Los Alamos Report LA-UR-06-3904 333 (2006)

101: 木村健一，金野正晴，中村 充孝，中島健次，相澤一也，鈴谷賢太郎，
反射中性子を低減する「高濃度ボロンモルタル」
原子力eye 55 50 (2009)

102: H. Kinoshita, M. Teshigawara, M. Ito, K. Takagiwa, S. Meigo, F. Maekawa, M. Kaminaga, M. Futakawa
Remote handling devices in MLF
Nucl. Instrum. Methods Phys. Res. A 600 78 (2009)

103: Eiji Kita, Ayumu Hatanaka, Hideto Yanagihara, Kenji Nakajima, Isao Kagomiya, Masakazu Nishi, Kazuhisa Kakurai, Kilti Siratori, Kay Kohn
Effect of uniaxial stress cooling on the neutron magnetic scattering in a $ZnCr_2O_4$ single crystal
J. Phys. Chem. Solids 68 2166 (2007)

104: Masaaki Kitaguchi, Masahiro Hino, Yuji Kawabata, Hirotoshi Hayashida, Seiji Tasaki, Ryuji Maruyama, Dai Yamazaki, Toru Ebisawa, and Naoya Torikai

Development of neutron resonance spin flipper for high resolution NRSE spectrometer
Physica B 385-386 1128 (2006)

105: Masaaki Kitaguchi, Masahiro Hino, Yuji Kawabata, Hirotoshi Hayashida, Seiji Tasaki, Ryuji Maruyama, Toru Ebisawa
Development of devices for beam divergence correction in the high-resolution NRSE spectrometer
Nucl. Instrum. Methods Phys. Res. A 600 117 (2009)

106: Y. Kiyanagi, T. Ono, M. Ooi, S. Onuma, T. Kamiyama, H. Iwasa, F. Hiraga
Measurements of Neutronic Characteristics of a Mesitylene Moderator
Proc. of the 17th Meeting of the Int. Collaboration on Advanced Neutron Sources, Los Alamos Report LA-UR-06-3904 506 (2006)

107: H. Kogawa, S. Hasegawa, M. Futakawa, Y. Ikeda, B. Riemer, M. Wendel, J. Haines
Damage Potential Measurements in WNR Proton Beam Tests
Proc. of the 17th Meeting of the Int. Collaboration on Advanced Neutron Sources, Los Alamos Report LA-UR-06-3904 572 (2006)

108: H. Kogawa, M. Futakawa, S. Ishikura
Dynamic Response of Mercury Subjected to Pressure Wave
J. Nucl. Sci. Technol. 44 523 (2007)

109: H. Kogawa, S. Hasegawa, M. Futakawa, B. Riemer, M. Wendel, J. Haines
Numerical study on pressure wave propagation in a mercury loop
J. Nucl. Mater. 377 195 (2008)

110: H. Kogawa, T. Shobu, M. Futakawa, Ahmed, K. Haga, T. Naoe
Effect of wettability on bubble formation at gas nozzle under stagnantcondition
J. Nucl. Mater. 377 189 (2008)

111: H. Kogawa, A. Bucheeri, T. Shobu, T. Naoe, K. Haga, M. Futakawa
Development on Controlled Micro-Gas Bubble Formation in Mercury Targets
Proc. of the 18th Meeting of the Int. Collaboration on Advanced Neutron Sources, Chinsese Academy of Science Progress Report 566 (2008)

112: H. Kogawa, K. Haga, T. Wakui, M. Futakawa
Development on mercury pump for JSNS
Nucl. Instrum. Methods Phys. Res. A 600 97 (2009)

113: J. Kubo, N. Rahman, N. Takahashi, T. Kawai, G. Matsuba, K. Nishida, T. Kanaya, M. Yamamoto
Improvement of Poly(vinyl alcohol) Properties by the Addition of Magnesium Nitrate
Journal of Applied Polymer Science 112 1647 (2009)

114: Y. Kurata, M. Futakawa
Corrosion of CrN-coated steels for nuclear reactors in liquid Pb-Bi
J. Jpn. Inst. Met. 72 470 (2008)

115: Y. Kurata, M. Futakawa, S. Saito
Corrosion behavior of steels in liquid lead-bismuth with low oxygen concentrations, J Nucl. Mater. 373 (2008) 164-178
Corrosion behavior of steels in liquid lead-bismuth with low oxygen concentrations
J. Nucl. Mater. 373 164 (2008)

116: Katsuhiro Kusaka, Takashi Ohhara, Ichiro Tanaka, Nobuo Niimura, Tomoji Ozeki, Kazuo Kurihara, Kazuya Aizawa, Yukio Morii, Masatoshi Arai, Kazuhiro Ebata, Yoshiki Takano
Peak overlapping and its de-convolution in TOF diffraction data from neutron biological diffractometer in J-PARC
Physica B 385-386 1062 (2006)

117: F. Maekawa, K. Oikawa, M. Tamura, M. Harada, Y. Ikeda, N. Watanabe
Design of "Neutron Beam-line for Observation & Research Use (NOBORU)" for JSNS of J-PARC
Proc. of the 17th Meeting of the Int. Collaboration on Advanced Neutron Sources, Los Alamos Report LA-UR-06-3904 129 (2006)

118: 前川藤夫，及川健一
中性子源特性試験装置
日本中性子科学会誌「波紋」 17 187 (2007)

119: F. Maekawa, K. Oikawa, M. Harada, T. Kai, S. Meigo, Y. Kasugai, M. Ooi, K. Sakai, M. Teshigawara, S. Hasegawa, T. Kato, Y. Ikeda, N. Watanabe
Experimental Program at a Neutron Beam Line NOBORU in JSNS.
Proc. of the 18th Meeting of the Int. Collaboration on Advanced Neutron Sources, Chinsese Academy of Science Progress Report 118 (2008)

120: F. Maekawa, K. Oikawa, M. Harada, T. Kai, S. Meigo, Y. Kasugai, M. Ooi, K. Sakai, M. Teshigawara, S. Hasegawa, Y. Ikeda, N. Watanabe
NOBORU: J-PARC BL10 for facility diagnostics and its possible extension to innovative instruments
Nucl. Instrum. Methods Phys. Res. A 600 335 (2009)

121: R. Maruama, D. Yamazaki, T. Ebisawa, M. Hino, and K. Soyama
Supermirror coatings for the new spallation source J-PAR
Proc. of the 18th Meeting of the Int. Collaboration on Advanced Neutron Sources, Chinsese Academy of Science Progress Report 197 (2007)

122: R. Maruyama, D. Yamazaki, T. Ebisawa, M. Hino, K. Soyama
Development of neutron supermirror with large-scale ion-beam sputtering instrument
Physica B 385-386 1256 (2006)

123: R. Maruyama, D. Yamazaki, T. Ebisawa, M. Hino, K. Soyama
Development of neutron supermirrors with large critical angle
Thin Solid Films 515 5704 (2007)

124: R. Maruyama, D. Yamazaki, T. Ebisawa, and K.

Soyama
Effect of interfacial roughness correlation on diffuse scattering intensity in a neutron supermirror
J. Appl. Phys. 105 83527 (2009)

125: R. Maruyama, D. Yamazaki, T. Ebisawa, and K. Soyama
Development of high-reflectivity neutron supermirrors using an ion beam sputtering technique
Nucl. Instrum. Methods Phys. Res. A 600 68 (2009)

126: R. Maruyama, M. Hino, H. Hayashida, M. Kitaguchi, N. Achiwa, D. Yamazaki, T. Ebisawa, and K. Soyama,
A beam divergence correction mirror for neutron resonance spin echo
Physica B 404 2594 (2009)

127: 丸山 龍治,
スーパーミラーからの散漫散乱メカニズムの解明
日本中性子科学会誌「波紋」 19 9 (2009)

128: M. Matsuda, M. Takeda, M. Nakamura, K. Kakurai, A. Oosawa, E. Lelievre-Berna, J.-H. Chung, H. Ueda, H. Takagi and S.-H. Lee
Spiral spin structure in a Heisenberg pyrochlore magnet $CdCr_2O_4$
Phys. Rev. B 75 104415 (2007)

129: N. Matsuda, Y. Iwamoto, M. Harada, M. Teshigawara, S. Meigo, F. Maekawa, T. Oguri, H. Nakano, N. Nakao, Y. Nakane, H. Nakashima
Analyses of benchmark problems for the shielding design of high intensity proton accelerator facilities
JAEA-Technology 2008-030 (2008)

130: S. Meigo, F. Noda, S. Ishikura, M. Futakawa, S. Sakamoto, Y. Ikeda
Evaluation of the 3-GeV Proton Beam Profile at the Spallation Target of the JSNS
Nucl. Instrum. Methods Phys. Res. A 562 569 (2006)

131: S. Meigo, F. Noda, S. Ishikura, M. Futakawa, Y. Ikeda
Evaluation of the 3-GeV Proton Beam Profile at the Spallation Target of the JSNS
Proc. of the 17th Meeting of the Int. Collaboration on Advanced Neutron Sources, Los Alamos Report LA-UR-06-3904 447 (2006)

132: S. Meigo, M. Ooi, T. Kai, Y. Ikeda,H. Fujimori, S. Muto
JSNS Proton Beam Profile Monitor Using Silicon Carbide Wire
Proc. of the 17th Meeting of the Int. Collaboration on Advanced Neutron Sources, Los Alamos Report LA-UR-06-3904 455 (2006)

133: S. Meigo
Beam Commissioning of the J-PARC MLF
J. Part. Accel. Soc. Jpn. 5 327 (2008)

134: 明午伸一郎
J-PARC MLFのビームコミッショニング
日本加速器学会誌「加速器」 5 327 (2008)

135: S. Meigo, M. Ooi, T. Kai, T. Ono, k. Ikezaki, T. Haraguchi, H. Fujimori, S. Sakamoto
Beam commissioning for neutron and muon facility at J-PARC
Nucl. Instrum. Methods Phys. Res. A 600 41 (2009)

136: S. Meigo, M. Ooi, T. Kai, S. Sakamoto, M. Futakawa, H. Fujimori, F. Noda
Beam Commissioning for Spallation Neutron and Muon Source at J-PARC
Proc. of the 23rd Particle Accelerator Conf. TU6PFP066 (2009)

137: Kenji Mishima, Satoru Yamada, Hiromi Sato, Katsuya Hirota, Takenao Shinohara, Takahiro Morishima, Jun-ichi Suzuki, Takayuki Oku, Hirohiko M. Shimizu,
Development of measurement system of neutron β decay
Physica B 385-386 1219 (2006)

138: K. Mishima, T. Ino, K. Sakai, T. Shinohara, K. Hirota, K. Ikeda, H. Sato, Y. Otake, H. Ohmori, S. Muto, N. Higashi, T. Morishima, M. Kitaguchi, M. Hino, H. Funahashi, T. Shima, J.-i. Suzuki, K. Niita, K. Taketani, Y. Seki and H. M. Shimizu
Design of Neutron Beamline for Fundamental Physics at J-PARC BL05
Nucl. Instrum. Methods Phys. Res. A 600 342 (2009)

139: Atsushi Moriai, Shuki Torii, Hiroshi Suzuki, Stefanus Harjo, Yukio Morii, Masatoshi Arai, Yo Tomota, Tetsuya Suzuki, Yoshiaki Akiniwa, Hidehiko Kimura, Koichi Akita
Development of engineering diffractometer at J-PARC
Physica B 385-386 1043 (2006)

140: 永井隆哉，有馬寛，奥地拓生，鍵裕之，八木健彦
J-PARCでの高温高圧専用ビームラインの実現に向けて
高圧力の科学と技術 19 15 (2009)

141: Chiyoko Nagoshi, Ryunosuke Yamamoto, Keitaro Kuwahara, Hajime Sagayama, Daich Kawana, Masahumi Kohgi, Hitoshi, Sugawara, Yuji Aoki, Hideyuki Sato,Tetsuya Yokoo, Masatoshi Arai
Magnetic and Transport Properties of $Gd_3Ir_4Sn_{13}$ with Unique Crystal Structure
J. Phys. Soc. Jpn. 75 44710 (2006)

142: K. Nakajima, M. Nakamura, R. Kajimoto, T. Osakabe, K. Kakurai, M. Matsuda, M. Metoki, S. Wakimoto, T. J. Sato, S. Itoh, M. Arai, K. Yoshida, and K. Niita
Cold-Neutron Disk-Chopper Spectrometer at J-PARC
J. Neutron Research 15 13 (2007)

143: M. Nakamura, M. Arai, E. Kartini, K. Itoh, J.W. Taylor and M. Russina
Unique Vibrational Excitations in Superionic Conducting Glass
AIP Conference Proceedings 832 504 (2006)

144: M. Nakamura, H. Iwase, M. Arai, E. Kartini, M. Russina. T. Yokoo, J.W. Taylor
Low energy vibrational excitations characteristic of superionic glass
Physica B 385-386 552 (2006)

145: 中村 充孝
超イオン伝導性ガラスにおける高いイオン伝導と低エネ

ルギーダイナミクスの関係
日本中性子科学会誌「波紋」 16 209 (2006)

146: M. Nakamura, K. Nakajima, R. Kajimoto, M. Arai
Utilization of multiple incident energies on Cold-Neutron Disk-Chopper Spectrometer at J-PARC
J. Neutron Research 15 31 (2007)

147: M. Nakamura, M. Arai and E. Kartini, in Quasi-Elastic Neutron Scattering Conference 2006 (QENS2006), edited by Paul E. Sokol, Helmut Kaiser, David Baxter, Roger Pynn, Dobrin Bossev, Mark Leuschner,
Low-energy dynamics of superionic glass: Evidence for a direct relation with ionic conductivity
Proc. of the 8th International Conference on Quasi-Elastic Neutron Scattering 169 (2007)

148: M. Nakamura, M. Arai, R. Kajimoto, T. Yokoo, K. Nakajima, and Th. Krist
Conceptual design of MAGIC chopper used for 4 SEASONS at J-PARC
J. Neutron Research 16 87 (2008)

149: 中村龍也，坂佐井馨，片桐政樹，美留町厚，細谷孝明，曽山和彦，佐藤節夫，E. Schooneveld, N. Rhodes
ENGIN-X型1次元シンチレータ中性子検出器の製作と性能試験
JAEA-Research 2007-014 (2007)

150: T. Nakamura, H. Tanaka, H. Yamagishi, K. Soyama, K. Aizawa, K. Ochi, and T. Tanimori
A gas-based neutron imaging detector with individual read-outs
Nucl. Instrum. Methods Phys. Res. A 573 187 (2007)

151: T. Nakamura, E. M. Schooneveld, N. J. Rhodes, M. Katagiri, N. Tsutsui, K. Toh, K. Sakasai, and K. Soyama
High detection efficiency ZnS scintillator for a fibercoded linear neutron detector for thermal neutron scattering instruments
IEEE Nucl. Sci. Symp. Conf. Record 2008 1215 (2008)

152: 中村龍也，片桐政樹，美留町厚，海老根守澄，筒井紀彰，曽山和彦，E. M. Schooneveld, N. J. Rhodes
ENGIN-X型1次元シンチレータ中性子検出器の検出器性能向上に関する技術開発
JAEA-Research 2008-116 (2008)

153: 中村龍也，片桐政樹；細谷孝明，美留町厚，海老根守澄，曽山和彦，E. M. Schooneveld, N. J. Rhodes
波長シフトファイバを用いた高検出効率,高位置分解能型２次元シンチレータ中性子検出器の開発研究
JAEA-Research 2008-115 (2008)

154: T. Nakamura, R. Yasuda, M. Katagiri, K. Toh, K. Sakasai, A. Birumachi, M. Ebine, and K. Soyama
High-Spatial-Resolution Neutron Image Detector Based on Wavelength-Shifting Fiber Read Out for Time-of-Flight Measurements
IEEE Nucl. Sci. Symp. Conf. Record 2009 1271 (2009)

155: T. Nakamura, E. Schooneveld, N. Rhodes, M. Katagiri, K. Sakasai, and K. Soyama
Evaluation of the performance of a fibre-coded neutron detector with a ZnS/$^{10}B_2O_3$ ceramic scintillator
Nucl. Instrum. Methods Phys. Res. A 600 164 (2009)

156: T. Nakamura, E.M. Schooneveld, N.J. Rhodes, M. Katagiri, K. Toh, K. Sakasai, and K. Soyama
A half-millimetre spatial resolution fibre-coded linear position-sensitive scintillator detector with wavelength-shifting fibre read out for neutron detection
Nucl. Instrum. Methods Phys. Res. A 606 675 (2009)

157: T. Nakamura, M. Katagiri, K. Toh, K. Sakasai, M. Ebine, A. Birumachi, and K. Soyama
Wavelength-shifting-fibre-based neutron image detector with a fibre-optic taper to increase the spatial resolution
Nucl. Instrum. Methods Phys. Res. A 604 158 (2009)

158: Takeshi Nakatani, Kenji Nakajima, Shuki Torii, Bharoto, Wataru Higemoto, Setsuo Sato, Toshiya Otomo and Masatoshi Arai
Prototype of network distributed control system for MLF/J-PARC
Physica B 385-386 1327 (2006)

159: T. Nakatani, Y. Inamura, T. Ito, S. Harjo, R. Kajimoto, M. Arai, T. Ohhara, H. Nakagawa, T. Aoyagi, T. Otomo, J. Suzuki, T. Morishima, S. Muto, R., Kadono, S. Torii, Y. Yasu, T. Hosoya, M. Yonemura
The implementation of the software framework in J-PARC/MLF
Proceedings of ICALEPCS2009 673 (2009)

160: K. Nakayoshi, Y. Yasu, E. Inoue, H. Sendai, M. Tanaka, S. Satoh, S. Muto, N. Kaneko, T. Otomo, T. Nakatani, T. Uchida
Development of a data acquisition sub-system using DAQ-Middleware
Nucl. Instrum. Methods Phys. Res. A 600 173 (2009)

161: T. Naoe, M. Futakawa, T. Oi, T. Wakui, Y. Motohashi
Fatigue strength degradation by pitting damage
J. Soc. Mater. Sci. Jpn. 55 944 (2006)

162: 直江 崇，二川 正敏，小山 智史，粉川 広行
水銀キャビテーションにおける気泡挙動
日本実験力学会 6 301 (2006)

163: T. Naoe, M. Futakawa, T. Shobu, T. Wakui, H. Kogawa, H. Takeuchi, M. Kawai
Mitigation Technologies for Damage Induced by Pressure Waves in High-Power Mercury Spallation Neutron Sources (I) -Material Surface Improvement-
J. Nucl. Sci. Technol. 45 698 (2008)

164: T. Naoe, S. Hasegawa, A. Bucheeri, M. Futakawa
Lifetime Estimation of Microbubble in Mercury
J. Nucl. Sci. Technol. 45 1233 (2008)

165: T. Naoe, H. Kogawa, T. Wakui, M. Futakawa, H. Takeuchi
Bending fatigue strength of surface modified stainless steel with pitting damage
J. Soc. Mater. Sci. Jpn. 57 576 (2008)

166: T. Naoe, M. Ooi, H. Kogawa, T. Wakui, M. Futakawa

Pitting damage morphology of surface modified material - Damage suppression by surface hardening treatment -
J. Soc. Mater. Sci. Jpn. 57 159 (2008)

167: T. Naoe, M. Ida, M. Futakawa
Cavitation damage reduction by microbubble injection
Nucl. Instrum. Methods Phys. Res. A 586 382 (2008)

168: K. Niita, K. Suzuya, H. Nakajima, R. Kajimoto, M. Nakamura, K. Shibata, K. Soyama, K. Torii, S. Harjo, H. Aizawa, M. Kawai, T. Kamiyama, S. Ito, N. Torikai, F. Maekawa, K. Oikawa, M. Tamura, M. Harada, M. Arai
Neutron Beam-line and Shield Design for Neutron Scattering Instruments at JSNS J-PARC Project
Proc. of the 17th Meeting of the Int. Collaboration on Advanced Neutron Sources, Los Alamos Report LA-UR-06-3904 640 (2006)

169: Y. Oba, T. Sato, and T.Shinohara
Gas adsorption on the surface of ferromagnetic Pd nanoparticles, e-J. Surf. Sci. Nanotechnol. 4, 439-442 (2006)
Gas adsorption on the surface of ferromagnetic Pd nanoparticles
Surf. Sci. Nanotechnol. 4 439 (2006)

170: Y. Oba, T. Shinohara, T. Oku, J. Suzuki, M. Ohnuma, T. Sato
Magnetic Intraparticle Structure in Ferromagnetic Pd Nanoparticle
J. Phys. Soc. Jpn. 78 44711 (2009)

171: Y. Ogino, H. Fukushima, N. Takahashi, G. Matsuba, K. Nishida, T. Kanaya
Crystallization of isotactic polypropylene under shear flow observed in a wide spatial scale
Macromolecules 39 7617 (2006)

172: Y. Ogino, H. Fukushima, G. Matsuba, N. Takahashi, K. Nishida, T. Kanaya
Effects of high molecular weight component on crystallization of polyethylene under shear flow
Polymer 47 5669 (2006)

173: T. Ohhara, K. Kusaka, T. Hosoya, K. Kurihara, K. Tomoyori, N. Niimura, I. Tanaka, J. Suzuki, T. Nakatani, T. Otomo, S. Matsuoka, K. Tomita, Y. Nishimaki, T. Ajima, S. Ryufuku
Development of data processing software for a new TOF single crystal neutron diffractometer at J-PARC
Nucl. Instrum. Methods Phys. Res. A 600 195 (2009)

174: K. Oikawa, F. Maekawa, M. Tamura, M. Harada,T. Kato, Y. Ikeda, K. Niita
A Preliminary Investigation on the Satellite Building of MLF: Beamline Shielding Analysis
Proc. of the 17th Meeting of the Int. Collaboration on Advanced Neutron Sources, Los Alamos Report LA-UR-06-3904 139 (2006)

175: K. Oikawa, F. Maekawa, M. Harada, T. Kai, S. Meigo, Y. Kasugai, M. Ooi, K. Sakai, M. Teshigawara, S. Hasegawa, M. Futakawa, Y. Ikeda, N. Watanabe
Design and application of NOBORU; NeutrOn Beam line for Observation and Research Use at J-PARC
Nucl. Instrum. Methods Phys. Res. A 589 310 (2008)

176: K. Oikawa, H. Takada, F. Maekawa, M. Harada, T. Kato, Y. Ikeda
Construction of the JSNS Shutter System
Proc. of the 18th Meeting of the Int. Collaboration on Advanced Neutron Sources, Chinsese Academy of Science Progress Report 591 (2008)

177: K. Oikawa, H. Takada, F. Maekawa, M. Harada, M. Futakawa, Y. Ikeda
Engineering design of JSNS shutter system
Nucl. Instrum. Methods Phys. Res. A 600 84 (2009)

178: R. Oishi, M. Yonemura, Y. Nishimaki, S. Torii, A. Hoshikawa, T. Ishigaki, T. Morishima, K. Mori, and T. Kamiyama
Riertveld analysis software for J-PARC
Nucl. Instrum. Methods Phys. Res. A 600 94 (2009)

179: Takayuki Oku, Satoru Yamada, Hajime Sasao, Jun-ichi Suzuki, Takenao Shinohara, Katsuya Hirota, Kazuaki Ikeda, Tsuyosi Tsuzaki, Yoshiaki Kiyanagi, Michihiro Furusaka, Hirohiko M. Shimizu
A magnetic neutron lens based on an extended Halbach-type permanent sextupole magnet
Physica B 385-386 1225 (2006)

180: Takayuki Oku, Satoru Yamada, Takenao Shinohara, Jun-ichi Suzuki, Kenji Mishima, Katsuya Hirota, Hiromi Sato, Hirohiko M. Shimizu
Highly polarized cold neutron beam obtained by using a quadrupole magnet
Physica B 397 188 (2007)

181: Takayuki Oku, Takenao Shinohara, Jun-ichi Suzuki, Roger Pynn, Hirohiko M. Shimizu
Pulsed neutron beam control using a magnetic multiplet lens
Nucl. Instrum. Methods Phys. Res. A 600 100 (2009)

182: Takayuki Oku, Takayuki Kikuchi, Takenao Shinohara, Jun-ichi Suzuki, Yuya Ishii, Masayasu Takeda, Kazuhisa Kakurai, Yuji Sasaki, Mikio Kishimoto, Makoto Yokoyama, Yoshikazu Nishihara
Small-angle polarized neutron scattering study of spherical $Fe_{16}N_2$ nano-particles for magnetic recording tape
Physica B 404 2575 (2009)

183: T. Okuda, T. Kishimoto, K. Uto, T. Hokazono, Y. Onose, Y. Tokura, R. Kajimoto, and M. Matsuda
Dimensional crossover of low-energy magnetic excitation for delafossite oxide $Cu_{1-x}Ag_xCrO_2$ with a spin-3/2 antiferromagnetic triangular sublattice
J. Phys. Soc. Jpn. 78 13604 (2009)

184: M. Ooi, H. Iwasa, F. Hiraga, T. Kamiyama, Y. Kiyanagi
Experimental Study of Neutronic Performance of Para Hydrogen Moderator Depending on the Moderator Temperature
Proc. of the 17th Meeting of the Int. Collaboration on Advanced Neutron Sources, Los Alamos Report LA-UR-06-3904 473 (2006)

185: M. Ooi, T. Kai, S. Meigo, H. Kinoshita, K. Sakai, S. Sakamoto, M. Kaminaga
Present Status of EPICS System Development for Control of 3GeV Proton Beam Transport Line in J-PARC
Proc. of the 17th Meeting of the Int. Collaboration on Advanced Neutron Sources, Los Alamos Report LA-UR-06-3904 1152 (2006)

186: M. Ooi, T. Kai, H. Kinoshita, K. Sakai, M. Kaminaga, M. Futakawa
Developmental status of a server system for the MLF general control system
Nucl. Instrum. Methods Phys. Res. A 600 120 (2009)

187: 大友季哉，鈴谷賢太郎
高強度全散乱装置の概要と水素貯蔵材料研究
日本結晶学会誌 50 29 (2008)

188: 大友季哉
非晶質・液体の静的および動的構造研究
固体物理 44 93 (2009)

189: 大友季哉
高強度全散乱装置 NOVA
日本金属学会報「まてりあ」 48 349 (2009)

190: M. Russina, M. Arai, E. Kartini, F. Mezei and M. Nakamura
Mobile cation motion in superionic glasses
Physica B 385-386 240 (2006)

191: 下ヶ橋秀典
T0チョッパーの開発(制御)
KEK Progress Report 2009-11 38 (2009)

192: K. Sakai, H. Kinoshita, T. Kai, M. Ooi, M. Kaminaga, T. Kato, M. Furusaka
Development status of the general control system of the Material and Life Science Experimental Facility (MLF) of J-PARC
Physica B 385-386 1324 (2006)

193: K. Sakai, M. Ooi, T. Kai, N. Watanabe, K. Nakatani, W. Higemoto, K. Shimomura, H. Kinoshita, M. Kaminaga
J-PARC/MLF全体制御システム(MLF-GCS)の設計・構築・運用
JAEA-Technology 2009-042 (2009)

194: K. Sakai, M. Ooi, T. Kai, H. Kinoshita, S. Kawasaki, N. Watanabe, M. Kaminaga, M. Futakawa
Construction status of a general control system for the Materials and Lif Science Experimental Facility (MLF) at J-PARC
Nucl. Instrum. Methods Phys. Res. A 600 75 (2009)

195: K. Sakasai, Y. Iwamoto, and K. Soyama
Fast neutron detection by storage phosphors with low gamma-ray sensitivity
IEEE Nucl. Sci. Symp. Conf. Record 2007 1404 (2007)

196: K. Sakasai, Y. Iwamoto, and K. Soyama
Storage characteristics of $SrBPO_5$:Eu^{2+} phosphors by fast neutron irradiation
IEEE Nucl. Sci. Symp. Conf. Record 2008 1149 (2008)

197: K. Sakasai, Y. Iwamoto, and K. Soyama
Detection of Fast Neutron by Storage Phosphors With Low Gamma-Ray Sensitivity
IEEE Trans. Nucl. Sci. 55 2352 (2008)

198: K. Sakasai, Y. Iwamoto, T. Nakamura, K. Toh, K. Takakura, and C. Konno
Storage characteristics of KCL:Eu^{2+} phosphors with radiators by irradiation of fast neutrons
IEEE Nucl. Sci. Symp. Conf. Record 2009 1422 (2009)

199: K. Sakasai, T. Nakamura, M. Katagiri, K. Soyama, A. Birumachi, S. Satoh, N. Rhodes, and E. Schooneveld
Development of neutron detector for engineering materials diffractometer at J-PARC
Nucl. Instrum. Methods Phys. Res. A 600 157 (2009)

200: T.J. Sato, O. Yamamuro, K. Hirota, M. Shibayama, H. Yoshizawa, S. Itoh, S. Watanabe, T. Asami, K. Kindo, Y. Uwatoko, T. Kanaya, N. Higashi, K. Ueno
Versatile inelastic neutron spectrometer (VINS) project for J-PARC
Nucl. Instrum. Methods Phys. Res. A 600 143 (2009)

201: 佐藤徹哉，大場洋次郎，篠原武尚
フリースタンディングなPd ナノ粒子に発現する強磁性
日本磁気学会誌「まぐね」 1 601 (2006)

202: S. Satoh, S. Muto, N. Kaneko, T. Uchida, M. Tanaka, Y. Yasu, K. Nakayoshi, E. Inoue, H. Sendai, T. Nakatani, T. Otomo
Development of a readout system employing high-speed network for J-PARC
Nucl. Instrum. Methods Phys. Res. A 600 103 (2009)

203: 佐藤 卓
中性子磁気散乱を用いた磁性研究におけるデータ解析手法の現状と課題
日本磁気学会誌「まぐね」 4 (2009)

204: 社本真一，鈴谷賢太郎，神山崇，樹神克明，大友季哉，福永俊晴
パルス中性子を用いた構造解析の最前線
プラズマ・核融合学会誌 84 323 (2008)

205: 柴田薫，高橋伸明，中川洋，藤原悟，片岡幹雄，佐藤卓，川北至信，筑紫格
ダイナミクス解析装置 (DNA) の概要と研究の展開
日本結晶学会誌 50 46 (2008)

206: Takenao Shinohara, Katsuya Hirota, Tomohiro Adachi, Kazuaki Ikeda, Hirohiko M. Shimizu, Jun-ichi Suzuki, Takayuki Oku
Thermal neutron refraction by material prism
Physica B 385-386 1232 (2006)

207: Takenao Shinohara, Shin-ichi Takata, Jun-ichi Suzuki, Takayuki Oku, Kentaro Suzuya, Kazuya Aizawa, Masatoshi Arai, Toshiya Otomo, Masaaki Sugiyama
Design and performance analyses of the new time-of-flight smaller-angle neutron scattering instrument at J-PARC
Nucl. Instrum. Methods Phys. Res. A 600 111 (2009)

208: Takenao Shinohara, Jun-ichi Suzuki, Takayuki Oku,

Shin-ichi Takata, Hiroshi Kira, Kentaro Suzuya, Kazuya Aizawa, Masatoshi Arai, Toshiya Otomo, Masaaki Sugiyama
Design of a neutron polarizer using polarizing super mirrors for the TOF-SANS instrument at the J-PARC
Physica B 404 2640 (2009)

209: H. Soyama, M. Futakawa, T. Naoe
A prediction method of incubation period on cavitation erosion
Turbomachinery 34 336 (2006)

210: 曽山和彦，坂佐井馨，中村龍也，山岸秀志，片桐政樹
J-PARC大強度パルス中性子実験用検出器開発の現状
放射線 32 223 (2006)

211: 曽山和彦，清水裕彦，大友季哉
1. J-PARCで展開される中性子科学 中性子基盤研究開発
日本結晶学会誌 50 66 (2008)

212: 曽山和彦
中性子検出器への入門
日本中性子科学会誌「波紋」 19 242 (2009)

213: J. Suzuki, T. Nakatani, T. Ohhara, Y. Inamura, M. Yonemura, T. Morishima, T. Aoyagi, A. Manabe, T. Otomo
Object-oriented data analysis framework for neutron scattering experiments
Nucl. Instrum. Methods Phys. Res. A 600 123 (2009)

214: H. Takada, K. Oikawa, H. Ohashi, Y. Hoshino,H. Natsume, F. Maekawa, S. Meigo, M. Harada, Y. Kasugai, T. Kato, Y. Ikeda, N. Watanabe
Heavy Construction Component Design and Installation at the JSNS
Proc. of the 17th Meeting of the Int. Collaboration on Advanced Neutron Sources Los Alamos Report LA-UR-06-3904 346 (2006)

215: H. Takada,T. Kato,M. Kaminaga, H. Natsume, Y. Hoshino
Planning and implementation on transportation of large and heavy components of 1-MW spallation neutron source for Japan Proton Accelerator Research Complex (J-PARC)
JAEA-Technology 2006-060 (2007)

216: H. Takada, T. Kai, K. Oikawa, K. Sakai
Design of control system of neutron beam shutters for 1MW spallation neutron source at Japan Proton Accelerator Research Complex (J-PARC)
JAEA-Technology 2008-027 (2008)

217: H. Takada
Accelerator based facility design in association with nuclear data.
Proc. of the Int. Conf. on Nucl. Data for Sci. and Technol. 23 (2008)

218: H. Takada, K. Kosako, T. Fukahori
Validation of JENDL high-energy file through analyses of spallation experiments at incident proton energies from 0.5 to 2.83 GeV
J. Nucl. Sci. Technol. 46 589 (2009)

219: N. Takahashi, K. Shibata, T. J. Sato and M. Arai
High-Efficiency Improvement for High Energy Resolution Experimental Mode of DIANA Spectrometer at Materials and Life Science Facility (MLF) of J-PARC
JAEA Research 2006-062 (2006)

220: N. Takahashi, T. Kanaya, K. Nishida, Y. Takahashi, M. Arai
Rheo-SANS study on gelation of poly(vinyl alcohol)
Physica B 385-386 810 (2006)

221: N. Takahashi, K. Shibata, T. J. Sato, and M. Arai
Repetition rate multiplication capability for a high energy resolution mode of DIANA at J-PARC
J. Neutron Research 15 61 (2007)

222: N. Takahashi, K. Shibata, T. J. Sato, I. Tamura, R. Kajimoto, S. Harjo, K. Oikawa, M. Arai, and F. Mezei
Instrumental design and expected performance of coupled-source near-backscattering spectrometer at J-PARC
J. Phys. Chem. Solids 68 2199 (2007)

223: N. Takahashi, K. Shibata, T.J. Sato, K. Nakajima, R. Kajimoto, K. Oikawa, M. Arai, C. Schanzer
Advanced neutron guide geometry for the near-backscattering spectrometer, DIANA at J-PARC
Proc. of the 18th Meeting of the Int. Collaboration on Advanced Neutron Sources, Chinsese Academy of Science Progress Report 373 (2007)

224: N. Takahashi, K. Shibata, T.J. Sato, M. Arai, F. Mezei
A Novel Time-Spatial-Focusing Momentum-Correction Analyzer for the Near-Backscattering Spectrometer DIANA at J-PARC
Nucl. Instrum. Methods Phys. Res. A 587 350 (2008)

225: N. Takahashi, K. Shibata, H. Sato, K. Nakajima, R. Kajimoto, K. Oikawa, M. Arai, C.Shanzer
Advanced Neutron Guide Geometry for the Near-backscattering Spectrometer at J-PARC.
Proc. of the 18th Meeting of the Int. Collaboration on Advanced Neutron Sources Chinsese Academy of Science Progress Report 376 (2008)

226: N. Takahashi, K. Shibata, T. J. Sato, Y. Kawakita, I. Tsukushi, N. Metoki, K. Nakajima, M. Arai
Study of the Analyzer Crystals for the Near-Backscattering Spectrometer DNA at J-PARC
Nucl. Instrum. Methods Phys. Res. A 600 91 (2009)

227: M. Takeda, D. Yamazaki, K. Soyama, R. Maruyama, M. Hino, T. Hirano
Magnetic structural analysis of magnetic multilayers by complementary use of X-ray and neutrons
J. Phys. Conf. Ser. 83 12010 (2007)

228: M. Takeda, M. Nakamura, Y. Shimojo and K. Kakurai
Double focusing Heusler monochromator and analyzer systems for the polarized neutron triple-axis spectrometer
Nucl. Instrum. Methods Phys. Res. A 586 229 (2008)

229: H. Tanaka, T. Nakamura, H. Yamagishi, K. Soyama, K. Aizawa, A. Ochi, and T. Tanimori

Development of Two-Dimensional Micro-Strip Gas Detector With Individual Readouts for Neutron Scattering Experiments
IEEE Trans. Nucl. Sci. 53 2264 (2006)

230: T. Takeda, N. L. Yamada, K. Katou, M. Nagao, H. Seto, Y. Kawabata, M. Takeda, and N. Torikai
Development of pi and pi/2 flippers for a neutron spin echo spectrometer
J. Neutron Research 15 83 (2007)

231: 田中浩基，中村龍也，山岸秀志，曽山和彦，相澤一也
個別読み出し型中性子ガス検出器の位置分解能に関する研究
JAEA-Research 2006-014 (2006)

232: H. Tanaka, T. Nakamura, H. Yamagishi, K. Soyama, K. Aizawa, T. Tanimori, and A. Ochi
Testing the performance of a two-dimensional microstrip gas chamber by measuring ranges of secondary particles in the ^{3}He(n,p)t reaction
Physica B 385-386 1293 (2006)

233: H. Tanaka, T. Nakamura, K. Toh, H. Yamagishi, K. Soyama, K. Ochiai, C. Konno, K. Aizawa, A. Maruhashi
Charged particle identification using difference in track length detected by two-dimensional multi-wire proportional counter
IEEE Nucl. Sci. Symp. Conf. Record 2007 590 (2007)

234: H. Tanaka, A. Maruhashi, H. Yamagishi, T. Nakamura, K. Soyama and K. Aizawa
Coincidence measurement of range and energy of charged particles using multi-wire detector with individual readouts
KEK Progress Report 2007-12 169 (2007)

235: H. Tatsumoto, T. Kato, T. Aso, S. Hasegawa, I. Ushijima, K. Otsu, Y. Ikeda
Numeral Analysis for Heat Transfer from a Cd Poison in Cryogenic Hydrogen
Proc. of the 17th Meeting of the Int. Collaboration on Advanced Neutron Sources Los Alamos Report LA-UR-06-3904 426 (2006)

236: H. Tatsumoto, M. Teshigawara, T. Aso, K. Otsu, F. Maekawa, T. Kato
Thermal stress analysis for a transfer line of hydrogen moderator in J-PARC
AIP Conference Proceedings 985 1225 (2008)

237: H. Tatsumoto, Y. Shirai, K. Hata, T. Kato, M. Shiotsu
Forced convection heat transfer of subcooled liquid nitrogen in horizontal tube
AIP Conference Proceedings 985 665 (2008)

238: H. Tatsumoto, Y. Shirai, K. Hata, T. Kato, T. Aso, K. Otsu, M. Shiotsu
Numerical analysis of forced convection heat transfer of subcooled liquid nitrogen
IEEE Trans. Appl. Supercond. 18 1483 (2008)

239: H. Tatsumoto, T. Aso, T. Kato, K. Otsu, S. Hasegawa, F. Maekawa, M. Futakawa
Design of hydrogen vent line for the cryogenic hydrogen system in J-PARC
Nucl. Instrum. Methods Phys. Res. A 600 269 (2009)

240: 達本衡輝
J-PARC核破砕中性子源用低温水素システムの開発を通じて
日本中性子科学会誌「波紋」 19 4 (2009)

241: M. Teshigawara, M. Harada, S. Saito, K. Oikawa, F. Maekawa, M. Futakawa, K. Kikuchi, T. Kato, Y. Ikeda, T. Naoe, T. Koyama, M. Ooi, Zherebtosov, M. Kawai, Y. Kurishita, K. Konashi
Development of aluminum (Al5083)-clad ternary Ag-In-Cd alloy for JSNS decoupled moderator
J. Nucl. Mater. 356 300 (2006)

242: M. Teshigawara, K. Oikawa, H. Aizawa, H. Kinoshita, M. Harada, M. Kaminaga, F. Maekawa, T. Kato, N. Watanabe, Y. Ikeda, H. Ino
Development Status of JSNS Moderator-Reflector Remote Handling Devices
Proc. of the 17th Meeting of the Int. Collaboration on Advanced Neutron Sources, Los Alamos Report LA-UR-06-3904 355 (2006)

243: M. Teshigawara, K. Oikawa, M. Harada, F. Maekawa, T. Kato, N. Watanabe, Y. Ikeda, K. Kikuchi, Y. Oda, T. Hirota
JSNS Moderator Design Update
Proc. of the 17th Meeting of the Int. Collaboration on Advanced Neutron Sources, Los Alamos Report LA-UR-06-3904 365 (2006)

244: M. Teshigawara, M. Harada, H. Tatsumoto, T. Aso, F. Maekawa, T. Kato
Fabrication Status of Moderator-reflector in JSNS.
Proc. of the 18th Meeting of the Int. Collaboration on Advanced Neutron Sources, Chinsese Academy of Science Progress Report 469 (2008)

245: K. Toh, H. Yamagishi, K. Sakasai, T. Nakamura, K. Soyama, A. Ochi, and T. Tanimori
Observation of Neutron-Induced Signals Using Two-Dimensional Micro-Pixel Gas Chamber
IEEE Nucl. Sci. Symp. Conf. Record 2008 2358 (2008)

246: K. Toh, H. Yamagishi, K. Sakasai, T. Nakamura, K. Soyama
Development of two-dimensional micro-pixel gas chamber capable of individual line readout for neutron measurement
IEEE Nucl. Sci. Symp. Conf. Record 2009 678 (2009)

247: K. Toh, H. Yamagishi, K. Sakasai, T. Nakamura, K. Soyama, A. Ochi, and T. Tanimori
Observation of Neutron-Induced Signals Using Two-Dimensional Micro-Pixel Gas Chamber
IEEE Trans. Nucl. Sci. 56 2410 (2009)

248: K. Tomiyasu and S. Itoh
Resolution matching between energy and momentum in position sensitive detector on chopper spectrometer
Physica B 385-386 1110 (2006)

249: Y. Tomota, K. Ikeda, M. Ojima, J. Suzuki, T. Kamiyama

A neutron scattering study on microstructure and deformation behavior in nitrogen bearing austenitic steels
Materials Science Forum 539-543 234 (2007)

250: 鳥飼直也，山田悟史，下ヶ橋秀典，瀬戸秀紀
小特集 次世代新中性子源 J-PARCにより広がる新しい材料科学「何ができる？どこがすごい？」 高分解能チョッパー分光器 (High Resolution Chopper Spectrometer)
HRC
日本金属学会報「まてりあ」 48 360 (2009)

251: K. Ueno, S. Itoh, R. Ohkubo, H. Sagehashi, S. Koike, Y. Funahashi, M. Kawai, T. Yokoo and J. Suzuki
Chopper for T0 Chopper with Magnetic Bearings
KEK Progress Report 2006-4 M 373 (2006)

252: Wataru Utsumi, Hiroyuki Kagi, Kazuki Komatsu, Hiroshi Arima, Takaya Nagai, Takuo Okuchi, Takashi Kamiyama, Yoshiya Uwatoko, Kazuyuki Matsubayashi, Takehiko Yagi
Neutron powder diffraction under high pressure at J-PARC
Nucl. Instrum. Methods Phys. Res. A 600 50 (2009)

253: T. Wakui, M. Futakawa, H. Kogawa, S. Ishikura
Failure Probability Estimation of Multi-walled Vessels for Mercury Target
J. Nucl. Sci. Technol. 44 530 (2007)

254: T. Wakui, H. Kogawa, K. Haga, M. Futakawa, K. Hayashi, N. Uchiyama, Y. Okamoto, K. Nakamura
Fabrication of mercury target vessel
JAEA-Technology 2009-040 (2009)

255: T. Wakui, H. Kogawa, K. Haga, M. Futakawa, N. Uchiyama, K. Nakamura
Structural design on mercury target vessel
JAEA-Technology 2009-041 (2009)

256: T. Wakui, T. Naoe, H. Kogawa, M. Futakawa
Effects of pitting damage and repeated stresses on lifetime of mercury target
Nucl. Instrum. Methods Phys. Res. A 600 150 (2009)

257: Satoru Yamada, Takenao Shinohara, Hajime Sasao, Takayuki Oku, Jun-ichi Suzuki, Hideaki Matsue, Hirohiko M. Shimizu
Development of a multichannel parabolic guide for thermal neutron beam focusing
Physica B 385-386 1243 (2006)

258: M. Yamada, Y. Iwashita, M. Ichikawa, T. Sugimoto, H. Tongu, H. Fujisawa, H. M. Shimizu, T. Ino, K. Mishima, K. Taketani, T. Yoshioka, S. Muto, T. Morishima, T. Oku, J.-i.Suzuki, T. Shinohara, K. Sakai, H. Sato, K. Hirota, Y. Otake, Y. Seki, S. Kawasaki, S. Komamiya, Y. Kamiya, H. Otono, S. Yamashita and P. Geltenbort
Development of modulating permanent magnet sextupole lens for focusing of pulsed cold neutrons
Physica B 404 2646 (2009)

259: 山田和芳，富安啓輔，藤田全基
中性子散乱分光による磁性体研究の現状と将来
固体物理 44 (2009)

260: 山岸秀志
高速二次元ガス中性子検出器用の特定用途向け集積回路(ASIC)の設計
JAEA-Technology 2007-004 (2007)

261: K. Yamamura, M. Nagano, H. Takai, N. Zettsu, D. Yamazaki, R. Maruyama, K. Soyama, and S. Shimada
Figuring of plano-elliptical neutron focusing mirror by local wet etching
Opt. Express 17 6414 (2009)

262: D. Yamazaki, M. Takeda, I. Tamura, R. Maruyama, A. Moriai, M. Hino, and K. Soyama
Polarized neutron reflectometer SUIREN at JRR-3
Physica B 404 2557 (2009)

263: 横尾哲也（編集）
中性子散乱実験試料環境研究会
KEK Progress Report 2005-16 (2006)

264: 横尾哲也
HRC研究会 第1回研究会 低次元磁性体における
KEK Progress Report 2008-6 (2008)

265: T. Yokoo and S. Itoh
学術創成研究「パルス中性子源を活用した量子機能発現機構に関する融合研究」第8回研究会
KEK Progress Report 2009-3 41 (2009)

266: 横尾哲也，その他
物構研シンポジウム '09
KEK Progress Report 2009-10 142 (2009)

267: 横尾哲也，伊藤晋一
東大・KEKパルスチョッパー分光器計画とそのサイエンス
KEK Progress Report 2009-2 34 (2009)

268: 横尾哲也，金子直勝，伊藤晋一，大友季哉，末次祐介，白井満，鈴谷賢太郎
B_4Cレジンのアウトガス測定
KEK Progress Report 2009-4 J-PARC 09-1 (2009)

269: 横尾哲也，伊藤晋一
BL12高分解能チョッパー分光器 (HRC)
日本中性子科学会誌「波紋」 19 118 (2009)

270: S. Zherebtsov, T. Naoe, M. Futakawa, F. Maekawa
Erosion damage of laser alloyed stainless steels in mercury
Surf. Coat. Tech. 201 6035 (2007)

271:
非弾性中性子散乱新手法で実証実験
科学新聞 2009年10月2日記事 (2009)

Muon Section

1: P. Bakule, Y. Matsuda, M. Iwasaki, Y. Miyake, K. Nagamine, Y. Ikedo, K. Shimomura, and P. Strasser
Pulsed source of ultra low-energy muons at RIKEN-RAL
Physica B 374-375 456 (2006)

2: P. Bakule, Y. Matsuda, Y. Miyake, K. Nagamine, M. Iwasaki, Y. Ikedo, K. Shimomura, P. Strasser, and S. Makimura
Pulsed source of ultra low energy positive muons for near-surface μSR studies
Nucl. Instrum. Methods Phys. Res. B 266 335 (2008)

3: P. Bakule, Y. Matsuda, Y. Miyake, K. Nagamine, K. Shimomura, P. Strasser, S. Makimura, and M. Iwasaki
Prospects for ultra-low-energy muon beam at J-PARC
Nucl. Instrum. Methods Phys. Res. A 600 35 (2009)

4: H. Fujimori, N. Kawamura, S. Meigo, P. Strasser, K. Nakahara, and Y. Miyake
Radiation resistant magnets for the J-PARC muon facility
Nucl. Instrum. Methods Phys. Res. A 600 170 (2009)

5: M. Harada, S. Meigo, M. Ito, E. Dantsuji, K. Takigawa, H. Takada, F. Maekawa, M. Futakawa, M. Nakamura, Y. Miyake, Y. Ikeda
Settlement of Materials and Life Science Experimental Facility at J-PARC
Nucl. Instrum. Methods Phys. Res. A 600 87 (2009)

6: W. Higemoto, Y. Haga, T.D. Matsuda, Y. Onuki, K. Ohishi, T.U. Ito, A. Koda, S.R. Saha, and R. Kadono
Possible Unconventional Superconductivity and Magnetism in $CePt_3Si$ Probed by Muon Spin Rotation and Relaxation
J. Phys. Soc. Jpn. 75 124713 (2006)

7: W. Higemoto, K. Ohishi, A. Koda, R. Kadono, H. Sakurai, K. Takada, E. Takayama-Muromachi, and T. Sasaki
Possible unconventional superconductivity and weak magnetism in $Na_xCoO_2 \cdot yH_2O$ probed by μSR
Physica B 374-375 274 (2006)

8: W. Higemoto, Y. Aoki, K. Ohishi, T.U. Ito, R.H. Heffner, S.R. Saha, A. Koda, K.H. Satoh, R. Kadono, D. Kikuchi, H. Sugawara, and H. Sato
Knight shift measurements in the superconducting state of $Pr_{1-x}La_xOs_4Sb_{12}$ (x = 0.4) probed by μSR
J. Magn. Magn. Mater. 310 620 (2007)

9: W. Higemoto, S.R. Saha, A. Koda, K. Ohishi, R. Kadono, Y. Aoki, H. Sugawara, and H. Sato
Spin-triplet superconductivity in $PrOs_4Sb_{12}$ probed by muon Knight shift
Phys. Rev. B 75 20510 (2007)

10: W. Higemoto, K. Shimomura, Y. Kobayashi, S. Makimura, Y. Miyake, Y. Kai, K. Sakai
J-PARC muon control system
Nucl. Instrum. Methods Phys. Res. A 600 179 (2009)

11: W. Higemoto, R.H. Heffner, K. Shimomura, K. Nishiyama, Y. Miyake
JAEA-ASRC μSR project at J-PARC
Nucl. Instrum. Methods Phys. Res. A 600 182 (2009)

12: M. Hiraishi, R. Kadono, S. Takeshita, M. Miyazaki, A. Koda, H. Okabe, and J. Akimitsu
Full Gap Superconductivity in $Ba_{0.6}K_{0.4}Fe_2As_2$ Probed by Muon Spin Rotation
J. Phys. Soc. Jpn. 78 23710 (2009)

13: Y. Ikedo, J. Sugiyama, H. Nozaki, H. Itahara, J. H. Brewer, E. J. Ansaldo, G. D. Morris, D. Andreica, and A. Amato
Spatial inhomogeneity of magnetic moments in the cobalt oxide spinel Co_3O_4
Phys. Rev. B 75 54424 (2007)

14: Y. Ikedo, H. Nozaki, M. Harada, J. Sugiyama, T.J. Sato, Y. Matsuo, K. Nishiyama, and J.D. Copley
Study of hydrogen diffusion in superprotonic ionic conductors, MH_xO_4 by μSR and QNS
Nucl. Instrum. Methods Phys. Res. A 600 316 (2009)

15: Y. Ikedo, J. Sugiyama, H. Nozaki, P.L. Russo, D. Andreica, A. Amato, M. M_nsson, M. Shizuya, M. Isobe, and E. Takayama-Muromachi
Paramagnetic nature of the layered cobalt dioxide with adouble rocksalt-type block
Physica B 404 607 (2009)

16: Y. Ikedo, J. Sugiyama, H. Nozaki, K. Mukai, P.L. Russo, D. Andreica, A. Amato, Y. Ono, and T. Kajitani
μSR study on delafossite $CuCr_{1-x}Mg_xO_2$
Physica B 404 645 (2009)

17: Y. Ikedo, J. Sugiyama, H. Nozaki, K. Mukai, H. Itahara, P.L. Russo, D. Andreica, and A. Amato
High pressure μSR Study on cobalt oxide spinel
Physica B 404 652 (2009)

18: Y. Ikedo, J. Sugiyama, H. Nozaki, K. Nishiyama, Y. Matsuo, and J.H. Lord
Moun dynamics in super protpnic conductors
Physica B 404 798 (2009)

19: H. Imao, N. Kawamura, K. Ishida, T. Matsuzaki, Y. Matsuda, A. Toyoda, and K. Nagamine
Dependence of muon-catalyzed d-d fusion on the ortho-para ratio in solid and liquid deuterium
Phys. Lett. B 632 192 (2006)

20: H. Imao, K. Ishida, N. Kawamura, T. Matsuzaki, Y. Matsuda, A. Toyoda, P. Strasser, M. Iwasaki, and K. Nagamine
Density effect in d-d muon-catalyzed fusion with ortho- and para-enriched D_2
Phys. Lett. B 658 120 (2008)

21: H. Imao, K. Ishida, N. Kawamura, T. Matsuzaki, Y. Matsuda, A. Toyoda, P. Strasser, M. Iwasaki, and K. Nagamine
Preparation of ortho-para ratio controlled D_2 gas for muon-catalyzed fusion
Review of Scientific Instruments 79 53502 (2008)

22: H. Imao, K. Ishida, N. Kawamura, T. Matsuzaki, Y. Matsuda, A. Toyoda, P. Strasser, M. Iwasaki and K. Nagamine
Density effect in d-d catalyzed fusion with ortho- and para-enriched deuterium
Hyperfine Interactions 193 159 (2009)

23: T. Ishiwatari, G. Beer, A.M. Bragadireanu, M. Cargnelli, C. Curceanu (Petrascu), J.-P. Egger, H. Fuhrmann, C. Guaraldo, M. Iliescu, K. Itahashi, M. Iwasaki, P. Kienle, B. Lauss, V. Lucherini, L. Ludhova, J. Marton, F. Mulhauser, T. Ponta, L.A. Schaller, D.L. Sirghi, D.F. Sirghi, P. Strasser, and J. Zmeskal
New analysis method for CCD X-ray data
Nucl. Instrum. Methods Phys. Res. A 556 509 (2006)

24: T.U. Ito, W. Higemoto, K. Ohishi, R.H. Heffner, N. Nishida, Y. Aoki, T. Onimaru, and H.S. Suzuki
Muon Knight shift measurements on $PrPb_3$ in paraquadrupolar state
J. Magn. Magn. Mater. 310 743 (2007)

25: T.U. Ito, W. Higemoto, K. Ohishi, T. Fujimoto, R.H. Heffner, N. Nishida, K. Satoh, H. Sugawara, Y. Aoki, D. Kikuchi, and H. Sato
Evolution of Local Magnetic State in SmRu4P12 Probed by Muon Spin Relaxation
J. Phys. Soc. Jpn. 76 53707 (2007)

26: T. U. Ito, W. Higemoto, K. Ohishi, R. H. Heffner, N. Nishida, K. Satoh, H. Sugawara, Y. Aoki, D. Kikuchi, and H. Sato
Possible low-energy excitations in SmRu4P12 probed by muon spin relaxation
Physica B 404 761 (2009)

27: R. Kadono, K.H. Satoh, A. Koda, T. Nagata, H. Kawano-Furukawa, J. Suzuki, M. Matsuda, K. Ohishi, W. Higemoto, S. Kuroiwa, H. Takagiwa, and J. Akimitsu
Magnetic field-induced quasiparticle excitation in Nb_3Sn: Evidence for anisotropic s-wave pairing
Phys. Rev. B 74 24513 (2006)

28: R. Kadono
Future perspectives of μSR studies in condensed matter physics
J. Phys. Chem. Solids 68 2052 (2007)

29: R. Kadono, S. Kuroiwa, J. Akimitsu, A. Koda, K. Ohishi, W. Higemoto, and S. Otani
Microscopic properties of vortex state in YB6 probed by muon spin rotation
Phys. Rev. B 76 94501 (2007)

30: R. Kadono, K. Shimomura, K. H. Satoh, S. Takeshita, A. Koda, K. Nishiyama, E. Akiba, R. M. Ayabe, M. Kuba, and C. M. Jensen
Hydrogen Bonding in Sodium Alanate: A Muon Spin Rotation Study
Phys. Rev. Lett. 100 26401 (2008)

31: R. Kadono, M. Hiraishi, M. Miyazaki, K. H. Satoh, S. Takeshita, S. Kuroiwa, S. Saura, and J. Akimitsu
Magnetic response of noncentrosymmetric superconductor La2C3：Effect of double-gap and spin-orbit interaction
Physica B 404 737 (2009)

32: R. Kadono, K. H. Satoh, A. Koda, K. Nishiyama, and M. Mihara
High transverse field μSR with π/2-RF pulse spin control technique
Physica B 404 996 (2009)

33: 門野良典，下村浩一郎，髭本亘
ミュオンスピン回転・緩和法で見る固体物理
固体物理 44 (2009)

34: N. Kawamura, S. Makimura, K. Shimomura, P. Strasser, A. Koda, H. Fujimori, K. Nakahara, M. Kato, S. Takeshita, R. Kadono, K. Nishiyama and Y. Miyake
Muon Science Facility in J-PARC
Hyperfine Interactions 194 213 (2009)

35: N. Kawamura, S. Makimura, P. Strasser, A. Koda, H. Fujimori, K. Nishiyama, Y. Miyake, and M.L.F Muon section
Design strategy for devices under high radiation field in J-PARC muon facility
Nucl. Instrum. Methods Phys. Res. A 600 114 (2009)

36: A. Koda, R. Kadono, K. Ohishi, S.R. Saha, W. Higemoto, S. Yonezawa, Y. Muraoka, and Z. Hiroi
Anomalous magnetic phase in an undistorted pyrochlore oxide $Cd_2Os_2O_7$ induced by geometrical frustration
J. Phys. Soc. Jpn. 76 63703 (2007)

37: K.M. Kojima, K. Kawashima, M. Fujita, K. Yamada, M. Azuma, M. Takano, A. Koda, K. Ohishi, W. Higemoto, R. Kadono, and Y.J. Uemura
Magnetism and superconductivity of an electron-doped superconductor $(Sr_{1-x}La_x)CuO2$
Physica B 374-375 207 (2006)

38: M. K. Kubo, H. Moriyama, Y. Tsuruoka, S. Sakamoto, E. Koseto, T. Saito, and K. Nishiyama
Non-destructive elemental depth-profiling with muonic X-rays
J. Radioanal. Nucl. Chem. 278 (2008)

39: S Makimura, H. Ozaki, H. Okamura, M. Futakawa, T. Naoe, Y. Miyake, N. Kawamura, K. Nishiyama, and M. Kawai
The present status of R&D for the muon target at J-PARC: The development of silver-brazing method for graphite
J. Nucl. Mater. 377 28 (2008)

40: S. Makimura, Y. Miyake, N. Kawamura, P. Strasser, A. Koda, K. Shimomura, H. Fujimori, K. Nishiyama, M. Kato, K. Nakahara, R. Kadono, Y. Kobayashi, J. Sagawa, T. Nakamura, M. Kaneko, H. Ozaki, H. Okamura, T. Suzuki, K. Fujimoto and K. Kira
Present status of construction for the muon target in J-PARC
Nucl. Instrum. Methods Phys. Res. A 600 146 (2009)

41: Y. Matsuda, P. Bakule, M. Iwasaki, T. Matsuzaki, Y.

Miyake, Y. Ikedo, P. Strasser, K. Shimomura, S. Makimura, and K. Nagamine
Generation of low-energy muons with laser resonant ionization
Nuclear Physics B (Proc. Suppl.) 155 346 (2006)

42: Y. Matsuda, P. Bakule, Y. Ikedo, K. Ishida, M. Iwasaki, S. Makimura, T. Matsuzaki, Y. Miyake, K. Nagamine, K. Shimomura, and P. Strasser
Development of low-energy beam line at the RIKEN-RAL muon facility
RIKEN Accel. Prog. Rep. 39 149 (2006)

43: H. Miyadera, K. Nagamine, K. Shimomura, K. Nishiyama, K. Fukuchi, and K. Ishida
Design, construction and performance of Dai Omega, a large solid-angle axial-focusing superconducting surface-muon channel
Nucl. Instrum. Methods Phys. Res. A 569 713 (2006)

44: Y. Miyake, K. Nishiyama, N. Kawamura, S. Makimura, P. Strasser, K. Shimomura, J.L. Beveridge, R. Kadono, K. Fukuchi, N. Sato, K. Ueno, W. Higemoto, K. Ishida, T. Matsuzaki, I. Watanabe, Y. Matsuda, M. Iwasaki, S.N. Nakamura, J. Doornbos, and K. Nagamine
Status of J-PARC muon science facility at the year of 2005
Physica B 374-375 484 (2006)

45: Y. Miyake, K. Nakahara, K. Shimomura, P. Strasser, N. Kawamura, A. Koda, S. Makimura, H. Fujimori,K. Nishiyama, Y. Matsuda, P. Bakule, T. Adachi, and T. Ogitsu
Ultra Slow Muon Project at J-PARC, MUSE
AIP Conference Proceedings 1104 47 (2009)

46: Y. Miyake, K. Nishiyama, N. Kawamura, P. Strasser, S. Makimura, A. Koda, K. Shimomura, H. Fujimori, K. Nakahara, R. Kadono, M. Kato, S. Takeshita, W. Higemoto, K. Ishida, T. Matsuzaki, Y. Matsuda and K. Nagamine
J-PARC muon source, MUSE
Nucl. Instrum. Methods Phys. Res. A 600 22 (2009)

47: Y. Miyake, K. Shimomura, N. Kawamura, P. Strasser, S. Makimura, A. Koda, H. Fujimori, K. Nakahara, R. Kadono, M. Kato, S. Takeshita, K. Nishiyama, W. Higemoto, K. Ishida, T. Matsuzaki, Y. Matsuda, K. Nagamine
Birth of an intense pulsed muon source, J-PARC MUSE
Physica B 404 957 (2009)

48: 三宅康博，松田恭幸，西田信彦
超低速ミュオンビームによるナノメーターミュオンスピン回転・緩和法への展開
固体物理 44 (2009)

49: M. Miyazaki, K. Yamaji, T. Yanagisawa, and R. Kadono
Checkerboard States in the Two-Dimensional Hubbard Model with the Bi2212-Type Band
J. Phys. Soc. Jpn. 78 43706 (2009)

50: K. Nakahara, Y. Miyake, K. Shimomura, P. Strasser, K. Nishiyama, N. Kawamura, H. Fujimori, S. Makimura, A. Koda, K. Nagamine, T. Ogitsu, A. Yamamoto, T. Adachi, K. Sasaki, K. Tanaka, N. Kimura, Y. Makida, Y. Ajima, K.Ishida, and Y. Matsuda
Design of the Large Acceptance Muon Beamline at J-PARC
AIP Conference Proceedings 981 312 (2008)

51: K. Nakahara, Y. Miyake, K. Shimomura, P. Strasser, K. Nishiyama, N. Kawamura, H. Fujimori, S. Makimura, A. Koda, K. Nagamine, T. Ogitsu, A. Yamamoto, T. Adachi, K. Sasaki, K. Tanaka, N. Kimura, Y. Makida, Y. Ajima, K. Ishida and Y. Matsuda
The super omega muon beamline at J-PARC
Nucl. Instrum. Methods Phys. Res. A 600 132 (2009)

52: K. Ninomiya, H. Sugiura, T. Nakatsuka, Y. Kasamatsu, H. Kikunaga, W. Sato, T. Yoshimura, H. Matsumura, K. Takamiya, M.K. Kubo, K. Sueki, A. Yokoyama, Y. Hamajima, T. Miura, K. Nishiyama, and A. Shinohara
Study of electronic X-rays emitted from pionic and muonic atoms
J. Radioanal. Nucl. Chem. 272 661 (2007)

53: K. Shimomura, K. Ishida, J. Doornbos, P. Strasser, N. Kawamura, Y. Miyake, K. Nishiyama, S. Makimura, H. Miyadera, and K. Magamine
Design Study of Muon Beam from J-PARC 3 GeV Rapid Synchrotron
Nuclear Physics B (Proc. Suppl.) 155 343 (2006)

54: K. Shimomura, R. Kadono, K. Nishiyama, I. Watanabe, T. Suzuki, F. Pratt, K. Ohishi, M. Mizuta, M. Saito, K. H. Chow, B. Hitti, and R.L. Lichti
Origin of n type conductivity in wide gap semiconductors studied by μSR
Nuclear Physics B (Proc. Suppl.) 155 378 (2006)

55: K. Shimomura, H. Miyadera, Y. Ikedo, H. Tanaka, K. Nishiyama, and K. Nagamine
Shallow Muonium hunting as an acceptor
Physica B 374-375 405 (2006)

56: K. Shimomura, R. Kadono, K. Nishiyama, I. Watanabe, T. Suzuki, F. Pratt K. Ohishi, M. Mizuta, M. Saito, K. H. Chow, B. Hitti, R.L. Lichti, H. Miyadera, Y. Ikedo, H. Tanaka, and K. Nagamine
Isolated hydrogen center in wide gap semiconductors studied by μSR
Physica B 376-377 444 (2006)

57: 下村浩一郎，門野良典，西山樟生
μSR法で探る半導体中水素の電子状態
固体物理 41 773 (2006)

58: K. Shimomura, Y. Miyake, P. Strasser, A. Koda, N. Kawamura, S. Makimura, H. Fujimori, K. Nakahara, R. Kadono, K. Ishida, J. Doornbos, W. Higemoto, K. Nishiyama, and K. Nagamine
Status of Decay/Surface Muon Channel for the Muon Science in J-PARC
AIP Conference Proceedings 981 381 (2008)

59: K. Shimomura, A. Koda, P. Strasser, N. Kawamura, H. Fujimori, S. Makimura, W. Higemoto, K. Nakahara, K. Ishida, K. Nishiyama, K. Nagamine and Y. Miyake
Superconducting muon channel at J-PARC
Nucl. Instrum. Methods Phys. Res. A 600 192 (2009)

60: P. Strasser, A. Taniguchi, T. Matsuzaki, K. Ishida , Y. Matsuda , S. Ohya, M. Iwasaki and K. Nagamine
Muon Spectroscopy with Trace Alkaline-Earth and Rare-Earth Isotopes Implanted in Solid D_2
Hyperfine Interactions 193 121 (2009)

61: P. Strasser, Y. Miyake, N. Kawamura, S. Makimura and K. Nishiyama
Alignment and shields in the M2 primary proton beamline at J-PARC
Nucl. Instrum. Methods Phys. Res. A 600 154 (2009)

62: 杉山　純
μ^+SRで見る電池材料
固体物理 44 (2009)

63: S. Takeshita, R. Kadono, M. Hiraishi, M. Miyazaki, A. Koda, Y. Kamihara, and H. Hosono
Coexistence of Supercondcutivity and Magnetism in LaFeAs(0.94F0.06) Probed by Muon Spin Relaxation
J. Phys. Soc. Jpn. 77 103703 (2008)

64: S. Takeshita and R. Kadono
Competition/coexisitence of magnetism and superconductivity in iron pnictides probed by muon spin rotation
New J. of Phys. 11 35006 (2009)

65: S. Takeshita, M. Hiraishi, M. Miyazaki, A. Koda, R. Kadono, S. Y. Suzuki, Y. Yasu, M. Tanaka, Y. Matsuda, K. Ishida, and T. Matsuzaki
Developmentofpositrondetectorfor μSR basedonmulti-pixel photoncounter
Nucl. Instrum. Methods Phys. Res. A 600 139 (2009)

66: S. Takeshita, R. Kadono, M. Hiraishi, M. Miyazaki, A. Koda, S. Matsuishi, and H. Hosono
Insular Superconductivity in a Co-Doped Iron Pnictide $CaFe_{1-x}Co_xAsF$
Phys. Rev. Lett. 103 27002 (2009)

Editorial Board of MLF Annual Report 2009

From left to right

Kentaro Suzuya	Neutron Science Section
Takayuki Oku	Neutron Science Section
Tetsuya Yokoo	Neutron Science Section
Kaoru Sakasai	Neutron Instrumentaion Section
Shin-ichiro Meigo(managing editor)	Neutron Source Section
Katsuhiro Haga	Neutron Source Section
Kenji M. Kojima	Muon Science Section

Material and Life Science Division
J-PARC Center
Tokai, Naka-gun, Ibaraki 319-1195, Japan
URL: http://j-parc.jp/MatLife/en/index.html

2011 February